



Hashemite Kingdom of Jordan



# Jordan Journal of



# Biological Sciences

*An International Peer-Reviewed Scientific Journal*

*Financed by the Scientific Research and Innovation Support Fund*



<http://jjbs.hu.edu.jo/>

المجلة الأردنية للعلوم الحياتية  
**Jordan Journal of Biological Sciences (JJBS)**  
<http://jjbs.hu.edu.jo>

**Jordan Journal of Biological Sciences (JJBS)** (ISSN: 1995–6673 (Print); 2307-7166 (Online)):

An International Peer- Reviewed Open Access Research Journal financed by the Scientific Research and Innovation Support Fund, Ministry of Higher Education and Scientific Research, Jordan and published quarterly by the Deanship of Scientific Research , The Hashemite University, Jordan.

**Editor-in-Chief**

**Professor Abu-Elteen, Khaled H.**  
Medical Mycology ,  
The Hashemite University

**Assistant Editor**

**Dr. Tahtamouni, Lubna H.**  
Developmental Biology,  
The Hashemite University

**Editorial Board (Arranged alphabetically)**

**Professor Amr, Zuhair S.**  
Animal Ecology and Biodiversity  
Jordan University of Science and Technology

**Professor Elkarmi, Ali Z.**  
Bioengineering  
The Hashemite University

**Professor Hunaiti, Abdulrahim A.**  
Biochemistry  
The University of Jordan

**Professor Khleifat, Khaled M.**  
Microbiology and Biotechnology  
Mutah University

**Professor Lahham, Jamil N.**  
Plant Taxonomy  
Yarmouk University

**Professor Malkawi, Hanan I.**  
Microbiology and Molecular Biology  
Yarmouk University

**Associate Editorial Board**

**Professor Al-Hindi, Adnan I.**  
Parasitology  
The Islamic University of Gaza, Faculty of Health  
Sciences, Palestine

**Dr Gammoh, Noor**  
Tumor Virology  
Cancer Research UK Edinburgh Centre, University of  
Edinburgh, U.K.

**Professor Kasperek, Max**  
Natural Sciences  
Editor-in-Chief, Journal Zoology in the Middle East,  
Germany

**Professor Krystufek, Boris**  
Conservation Biology  
Slovenian Museum of Natural History,  
Slovenia

**Dr Rabei, Sami H.**  
Plant Ecology and Taxonomy  
Botany and Microbiology Department,  
Faculty of Science, Damietta University, Egypt

**Professor Simerly, Calvin R.**  
Reproductive Biology  
Department of Obstetrics/Gynecology and  
Reproductive Sciences, University of  
Pittsburgh, USA

**Editorial Board Support Team**

**Language Editor**  
**Dr. Hala Shureteh**

**Publishing Layout**  
**Eng. Mohannad Oqdeh**

**Submission Address**

**Professor Abu-Elteen, Khaled H**  
The Hashemite University  
P.O. Box 330127, Zarqa, 13115, Jordan  
Phone: +962-5-3903333 ext. 4357  
E-Mail: [jjbs@hu.edu.jo](mailto:jjbs@hu.edu.jo)

International Advisory Board

**Prof. Abdel-Hafez, Sami K.**

Yarmouk University, Jordan

**Prof. Abuharfeil, Nizar M**

Jordan University of science and Technology, Jordan

**Prof. El Makawy, Aida, I**

National Research Center ,Giza, Egypt

**Prof. Ghannoum, Mahmoud A.**

University Hospital of Cleveland and Case  
Western Reserve University, U.S.A.

**Prof. Hamad, Mawieh,**

University of Sharjah, U.A.E

**Prof. Hassanali, Ahmed**

Kenya University, Nairobi, Kenya

**Prof. Ismail, Naim**

The Hashemite University, Jordan

**Prof. Kilbane, John J**

Intertek, Houston, Texas, U.S.A.

**Prof. Martens, Jochen**

Institute Fur Zoologie, Germany

**Prof. Na'was, Tarek E**

Lebanese American University, Lebanon

**Prof. Sadiq, May Fouad George**

Yarmouk University, Jordan

**Prof. Shakhanbeh, Jumah Mutie**

Mutah University ,Jordan

**Prof. Tamimi, Samih Mohammad**

University of Jordan, Jordan

**Prof. Wan Yusoff, Wan Mohtar**

University Kebangsaan Malaysia, Malaysia

**Prof. Abdul-Haque, Allah Hafiz**

National Institute for Biotechnology and  
Genetic Engineering, Pakistan

**Prof. Al-Najjar, Tariq Hasan Ahmad**

The University of Jordan, Jordan

**Prof. Bamburg, James**

Colorado State University, U.S.A.

**Prof. Garrick, Michael D**

State University of New York at Buffalo,  
U.S.A.

**Prof. Gurib-Fakim, Ameenah F**

Center for Phytotherapy and  
Research, Ebene, Mauritius.

**Prof. Hanawalt, Philip C**

Stanford University Stanford , U.S.A

**Prof. Kaviraj, Anilava**

India University of Kalyani, India

**Prof. Matar, Ghassan M**

American University of Beirut, Lebanon

**Prof. Nasher, Abdul Karim**

Sanna' University, Yemen

**Prof. Qoronfleh, Mohammad Walid**

Director of Biotechnology Biomedical Research  
Institute .Qatar

**Prof. Schatten, Gerald**

University of Pittsburgh School of  
Medicine, U.S.A

**Prof. Stanway, Glyn**

University of Essex, England

**Prof. Waitzbauer, Wolfgang**

University of Vienna, Austria

## Instructions to Authors

### Scopes

Study areas include cell biology, genomics, microbiology, immunology, molecular biology, biochemistry, embryology, immunogenetics, cell and tissue culture, molecular ecology, genetic engineering and biological engineering, bioremediation and biodegradation, bioinformatics, biotechnology regulations, gene therapy, organismal biology, microbial and environmental biotechnology, marine sciences. The JJBS welcomes the submission of manuscript that meets the general criteria of significance and academic excellence. All articles published in JJBS are peer-reviewed. Papers will be published approximately one to two months after acceptance.

### Type of Papers

The journal publishes high-quality original scientific papers, short communications, correspondence and case studies. Review articles are usually by invitation only. However, Review articles of current interest and high standard will be considered.

### Submission of Manuscript

Manuscript, or the essence of their content, must be previously unpublished and should not be under simultaneous consideration by another journal. The authors should also declare if any similar work has been submitted to or published by another journal. They should also declare that it has not been submitted/ published elsewhere in the same form, in English or in any other language, without the written consent of the Publisher. The authors should also declare that the paper is the original work of the author(s) and not copied (in whole or in part) from any other work. All papers will be automatically checked for duplicate publication and plagiarism. If detected, appropriate action will be taken in accordance with International Ethical Guideline. By virtue of the submitted manuscript, the corresponding author acknowledges that all the co-authors have seen and approved the final version of the manuscript. The corresponding author should provide all co-authors with information regarding the manuscript, and obtain their approval before submitting any revisions. Electronic submission of manuscripts is strongly recommended, provided that the text, tables and figures are included in a single Microsoft Word file. Submit manuscript as e-mail attachment to the Editorial Office at: [JJBS@hu.edu.jo](mailto:JJBS@hu.edu.jo). After submission, a manuscript number will be communicated to the corresponding author within 48 hours.

### Peer-review Process

It is requested to submit, with the manuscript, the names, addresses and e-mail addresses of at least 4 potential reviewers. It is the sole right of the editor to decide whether or not the suggested reviewers to be used. The reviewers' comments will be sent to authors within 6-8 weeks after submission.

Manuscripts and figures for review will not be returned to authors whether the editorial decision is to accept, revise, or reject. All Case Reports and Short Communication must include at least one table and/ or one figure.

### Preparation of Manuscript

The manuscript should be written in English with simple lay out. The text should be prepared in single column format. Bold face, italics, subscripts, superscripts etc. can be used. Pages should be numbered consecutively, beginning with the title page and continuing through the last page of typewritten material.

The text can be divided into numbered sections with brief headings. Starting from introduction with section 1. Subsections should be numbered (for example 2.1 (then 2.1.1, 2.1.2, 2.2, etc.), up to three levels. Manuscripts in general should be organized in the following manner:

### Title Page

The title page should contain a brief title, correct first name, middle initial and family name of each author and name and address of the department(s) and institution(s) from where the research was carried out for each author. The title should be without any abbreviations and it should enlighten the contents of the paper. All affiliations should be provided with a lower-case superscript number just after the author's name and in front of the appropriate address.

The name of the corresponding author should be indicated along with telephone and fax numbers (with country and area code) along with full postal address and e-mail address.

## **Abstract**

The abstract should be concise and informative. It should not exceed **350 words** in length for full manuscript and Review article and **150 words** in case of Case Report and/ or Short Communication. It should briefly describe the purpose of the work, techniques and methods used, major findings with important data and conclusions. No references should be cited in this part. Generally non-standard abbreviations should not be used, if necessary they should be clearly defined in the abstract, at first use.

## **Keywords**

Immediately after the abstract, **about 4-8 keywords** should be given. Use of abbreviations should be avoided, only standard abbreviations, well known in the established area may be used, if appropriate. These keywords will be used for indexing.

## **Abbreviations**

Non-standard abbreviations should be listed and full form of each abbreviation should be given in parentheses at first use in the text.

## **Introduction**

Provide a factual background, clearly defined problem, proposed solution, a brief literature survey and the scope and justification of the work done.

## **Materials and Methods**

Give adequate information to allow the experiment to be reproduced. Already published methods should be mentioned with references. Significant modifications of published methods and new methods should be described in detail. Capitalize trade names and include the manufacturer's name and address. Subheading should be used.

## **Results**

Results should be clearly described in a concise manner. Results for different parameters should be described under subheadings or in separate paragraph. Results should be explained, but largely without referring to the literature. Table or figure numbers should be mentioned in parentheses for better understanding.

## **Discussion**

The discussion should not repeat the results, but provide detailed interpretation of data. This should interpret the significance of the findings of the work. Citations should be given in support of the findings. The results and discussion part can also be described as separate, if appropriate. The Results and Discussion sections can include subheadings, and when appropriate, both sections can be combined

## **Conclusions**

This should briefly state the major findings of the study.

## **Acknowledgment**

A brief acknowledgment section may be given after the conclusion section just before the references. The acknowledgment of people who provided assistance in manuscript preparation, funding for research, etc. should be listed in this section.

## **Tables and Figures**

Tables and figures should be presented as per their appearance in the text. It is suggested that the discussion about the tables and figures should appear in the text before the appearance of the respective tables and figures. No tables or figures should be given without discussion or reference inside the text.

Tables should be explanatory enough to be understandable without any text reference. Double spacing should be maintained throughout the table, including table headings and footnotes. Table headings should be placed above the table. Footnotes should be placed below the table with superscript lowercase letters. Each table should be on a separate page, numbered consecutively in Arabic numerals. Each figure should have a caption. The caption should be concise and typed separately, not on the figure area. Figures should be self-explanatory. Information presented in the figure should not be repeated in the table. All symbols and abbreviations used in the illustrations should be defined clearly. Figure legends should be given below the figures.

## References

References should be listed alphabetically at the end of the manuscript. Every reference referred in the text must be also present in the reference list and vice versa. In the text, a reference identified by means of an author's name should be followed by the year of publication in parentheses ( e.g.( Brown,2009)). For two authors, both authors' names followed by the year of publication (e.g.( Nelson and Brown, 2007)). When there are more than two authors, only the first author's name followed by "*et al.*" and the year of publication ( e.g. ( Abu-Elteen *et al.*, 2010)). When two or more works of an author has been published during the same year, the reference should be identified by the letters "a", "b", "c", etc., placed after the year of publication. This should be followed both in the text and reference list. e.g., Hilly, (2002a, 2002b); Hilly, and Nelson, (2004). Articles in preparation or submitted for publication, unpublished observations, personal communications, etc. should not be included in the reference list but should only be mentioned in the article text ( e.g., Shtyawy,A., University of Jordan, personal communication). Journal titles should be abbreviated according to the system adopted in Biological Abstract and Index Medicus, if not included in Biological Abstract or Index Medicus journal title should be given in full. The author is responsible for the accuracy and completeness of the references and for their correct textual citation. Failure to do so may result in the paper being withdraw from the evaluation process. Example of correct reference form is given as follows:-

### Reference to a journal publication:

Bloch BK. 2002. Econazole nitrate in the treatment of *Candida vaginitis*. *S Afr Med J* , **58**:314-323.

Ogunseitan OA and Ndoeye IL. 2006. Protein method for investigating mercuric reductase gene expression in aquatic environments. *Appl Environ Microbiol.*, **64**: 695-702.

Hilly MO, Adams MN and Nelson SC. 2009. Potential fly-ash utilization in agriculture. *Progress in Natural Sci.*, **19**: 1173-1186.

### Reference to a book:

Brown WY and White SR.1985. **The Elements of Style**, third ed. MacMillan, New York.

### Reference to a chapter in an edited book:

Mettam GR and Adams LB. 2010. How to prepare an electronic version of your article. In: Jones BS and Smith RZ (Eds.), **Introduction to the Electronic Age**. Kluwer Academic Publishers, Netherlands, pp. 281–304.

### Conferences and Meetings:

Embabi NS. 1990. Environmental aspects of distribution of mangrove in the United Arab Emirates. Proceedings of the First ASWAS Conference. University of the United Arab Emirates. Al-Ain, United Arab Emirates.

### Theses and Dissertations:

El-Labadi SN. 2002. Intestinal digenetic trematodes of some marine fishes from the Gulf of Aqaba. MSc dissertation, The Hashemite University, Zarqa, Jordan.

## Nomenclature and Units

Internationally accepted rules and the international system of units (SI) should be used. If other units are mentioned, please give their equivalent in SI.

For biological nomenclature, the conventions of the *International Code of Botanical Nomenclature*, the *International Code of Nomenclature of Bacteria*, and the *International Code of Zoological Nomenclature* should be followed.

Scientific names of all biological creatures (crops, plants, insects, birds, mammals, etc.) should be mentioned in parentheses at first use of their English term.

Chemical nomenclature, as laid down in the *International Union of Pure and Applied Chemistry* and the official recommendations of the *IUPAC-IUB Combined Commission on Biochemical Nomenclature* should be followed. All biocides and other organic compounds must be identified by their Geneva names when first used in the text. Active ingredients of all formulations should be likewise identified.

### **Math formulae**

All equations referred to in the text should be numbered serially at the right-hand side in parentheses. Meaning of all symbols should be given immediately after the equation at first use. Instead of root signs fractional powers should be used. Subscripts and superscripts should be presented clearly. Variables should be presented in italics. Greek letters and non-Roman symbols should be described in the margin at their first use.

To avoid any misunderstanding zero (0) and the letter O, and one (1) and the letter l should be clearly differentiated. For simple fractions use of the solidus (/) instead of a horizontal line is recommended. Levels of statistical significance such as: \* $P < 0.05$ , \*\* $P < 0.01$  and \*\*\* $P < 0.001$  do not require any further explanation.

### **Copyright**

Submission of a manuscript clearly indicates that: the study has not been published before or is not under consideration for publication elsewhere (except as an abstract or as part of a published lecture or academic thesis); its publication is permitted by all authors and after accepted for publication it will not be submitted for publication anywhere else, in English or in any other language, without the written approval of the copyright-holder. The journal may consider manuscripts that are translations of articles originally published in another language. In this case, the consent of the journal in which the article was originally published must be obtained and the fact that the article has already been published must be made clear on submission and stated in the abstract. It is compulsory for the authors to ensure that no material submitted as part of a manuscript infringes existing copyrights, or the rights of a third party.

### **Ethical Consent**

All manuscripts reporting the results of experimental investigation involving human subjects should include a statement confirming that each subject or subject's guardian obtains an informed consent, after the approval of the experimental protocol by a local human ethics committee or IRB. When reporting experiments on animals, authors should indicate whether the institutional and national guide for the care and use of laboratory animals was followed.

### **Plagiarism**

The JJBS hold no responsibility for plagiarism. If a published paper is found later to be extensively plagiarized and is found to be a duplicate or redundant publication, a note of retraction will be published, and copies of the correspondence will be sent to the authors' head of institute.

### **Galley Proofs**

The Editorial Office will send proofs of the manuscript to the corresponding author as an e-mail attachment for final proof reading and it will be the responsibility of the corresponding author to return the galley proof materials appropriately corrected within the stipulated time. Authors will be asked to check any typographical or minor clerical errors in the manuscript at this stage. No other major alteration in the manuscript is allowed. After publication authors can freely access the full text of the article as well as can download and print the PDF file.

### **Publication Charges**

There are no page charges for publication in Jordan Journal of Biological Sciences, except for color illustrations,

### **Reprints**

Ten (10) reprints are provided to corresponding author free of charge within two weeks after the printed journal date. For orders of more reprints, a reprint order form and prices will be sent with article proofs, which should be returned directly to the Editor for processing.

### **Disclaimer**

Articles, communication, or editorials published by JJBS represent the sole opinions of the authors. The publisher shoulders no responsibility or liability what so ever for the use or misuse of the information published by JJBS.

## **Indexing**

JJBS is indexed and abstracted by:

DOAJ ( Directory of Open Access Journals)	CABI
Google Scholar	EBSCO
Journal Seek	CAS ( Chemical Abstract Service)
HINARI	ETH- Citations
Index Copernicus	Open J-Gat
NDL Japanese Periodicals Index	SCImago
SCIRUS	Clarivate Analytics ( Zoological Abstract)
OAJSE	Scopus
ISC (Islamic World Science Citation Center)	AGORA (United Nation's FAO database)
Directory of Research Journal Indexing (DRJI)	SHERPA/RoMEO (UK)
Ulrich's	



**المجلة الأردنية للعلوم الحياتية**  
**Jordan Journal of Biological Sciences (JJBS)**  
**ISSN 1995- 6673 (Print), 2307- 7166 (Online)**

<http://jjbs.hu.edu.jo>

**The Hashemite University**  
**Deanship of Scientific Research**  
**TRANSFER OF COPYRIGHT AGREEMENT**

Journal publishers and authors share a common interest in the protection of copyright: authors principally because they want their creative works to be protected from plagiarism and other unlawful uses, publishers because they need to protect their work and investment in the production, marketing and distribution of the published version of the article. In order to do so effectively, publishers request a formal written transfer of copyright from the author(s) for each article published. Publishers and authors are also concerned that the integrity of the official record of publication of an article (once refereed and published) be maintained, and in order to protect that reference value and validation process, we ask that authors recognize that distribution (including through the Internet/WWW or other on-line means) of the authoritative version of the article as published is best administered by the Publisher.

To avoid any delay in the publication of your article, please read the terms of this agreement, sign in the space provided and return the complete form to us at the address below as quickly as possible.

Article entitled:-----

Corresponding author: -----

To be published in the journal: Jordan Journal of Biological Sciences (JJBS)

I hereby assign to the Hashemite University the copyright in the manuscript identified above and any supplemental tables, illustrations or other information submitted therewith (the "article") in all forms and media (whether now known or hereafter developed), throughout the world, in all languages, for the full term of copyright and all extensions and renewals thereof, effective when and if the article is accepted for publication. This transfer includes the right to adapt the presentation of the article for use in conjunction with computer systems and programs, including reproduction or publication in machine-readable form and incorporation in electronic retrieval systems.

Authors retain or are hereby granted (without the need to obtain further permission) rights to use the article for traditional scholarship communications, for teaching, and for distribution within their institution.

- ☐ I am the sole author of the manuscript
- ☐ I am signing on behalf of all co-authors of the manuscript
- ☐ The article is a 'work made for hire' and I am signing as an authorized representative of the employing company/institution

Please mark one or more of the above boxes (as appropriate) and then sign and date the document in black ink.

Signed: \_\_\_\_\_ Name printed: \_\_\_\_\_

Title and Company (if employer representative) : \_\_\_\_\_

Date: \_\_\_\_\_

Data Protection: By submitting this form you are consenting that the personal information provided herein may be used by the Hashemite University and its affiliated institutions worldwide to contact you concerning the publishing of your article.

Please return the completed and signed original of this form by mail or fax, or a scanned copy of the signed original by e-mail, retaining a copy for your files, to:

Hashemite University  
Jordan Journal of Biological Sciences  
Zarqa 13115 Jordan  
Fax: +962 5 3903338  
Email: [jjbs@hu.edu.jo](mailto:jjbs@hu.edu.jo)



## EDITORIAL PREFACE

Jordan Journal of Biological Sciences (JJBS) is a refereed, quarterly international journal financed by the Scientific Research and Innovation Support Fund, Ministry of Higher Education and Scientific Research in cooperation with the Hashemite University, Jordan. JJBS celebrated its 11<sup>th</sup> commencement this past January, 2019. JJBS was founded in 2008 to create a peer-reviewed journal that publishes high-quality research articles, reviews and short communications on novel and innovative aspects of a wide variety of biological sciences such as cell biology, developmental biology, structural biology, microbiology, entomology, molecular biology, biochemistry, medical biotechnology, biodiversity, ecology, marine biology, plant and animal biology, plant and animal physiology, genomics and bioinformatics.

We have watched the growth and success of JJBS over the years. JJBS has published 11 volumes, 45 issues and 479 articles. JJBS has been indexed by SCOPUS, CABI's Full-Text Repository, EBSCO, Clarivate Analytics- Zoological Record and recently has been included in the UGC India approved journals. JJBS Cite Score has improved from 0.18 in 2015 to 0.60 in 2018.

A group of highly valuable scholars have agreed to serve on the editorial board and this places JJBS in a position of most authoritative on biological sciences. I am honored to have six eminent associate editors from various countries. I am also delighted with our group of international advisory board members coming from 15 countries worldwide for their continuous support of JJBS. With our editorial board's cumulative experience in various fields of biological sciences, this journal brings a substantial representation of biological sciences in different disciplines. Without the service and dedication of our editorial; associate editorial and international advisory board members, JJBS would have never existed.

In the coming year, we hope that JJBS will be indexed in Clarivate Analytics and MEDLINE (the U.S. National Library of Medicine database) and others. As you read throughout this volume of JJBS, I would like to remind you that the success of our journal depends on the number of quality articles submitted for review. Accordingly, I would like to request your participation and colleagues by submitting quality manuscripts for review. One of the great benefits we can provide to our prospective authors, regardless of acceptance of their manuscripts or not, is the feedback of our review process. JJBS provides authors with high quality, helpful reviews to improve their manuscripts.

Finally, JJBS would not have succeeded without the collaboration of authors and referees. Their work is greatly appreciated. Furthermore, my thanks are also extended to The Hashemite University and the Scientific Research and Innovation Support Fund, Ministry of Higher Education and Scientific Research for their continuous financial and administrative support to JJBS.

Professor Khaled H. Abu-Elteen  
March, 2019



## CONTENTS

## Original Articles

- 123 - 133 A Comparison between CAPS and SCAR Markers in the Detection of Resistance Genes in some Tomato Genotypes against *Tomato Yellow Leaf Curl Virus* and Whitefly  
*Sherin A. Mahfouze and Heba A. Mahfouze*
- 135 - 140 Determination of the Immunogenic and Hematologic Effects of Titanium Nanoparticles Manufactured from *Aspergillus flavus* in Vivo  
*Mohammed N. Maaroof and Asmaa E. Mahmood*
- 141 - 145 Isolation of Blood Group Non-specific Lectin from *Calotropis gigantean* Seeds  
*Vishwanath B. Chachadi*
- 147 - 153 A Morphological Study of the Pharmacological Effects of the *Nigella sativa* on the Reproductive System in Experimental Rats  
*Raith A. S. Al-Saffar and Mohammad K. M. Al-Wiswasy*
- 155 - 159 First Record of the Cochineal Scale Insect, *Dactylopius opuntiae* (Cockerell) (Hemiptera: Dactylopiidae), in Jordan  
*Ahmad M. Katbeh Bader and Asem H. Abu-Alloush*
- 161 - 165 The Genotoxic Potential of Alugbati Leaf Extracts on MCF-7 Cells  
*Darcy L. Garza, Rechel G. Arcilla, Ma. Luisa D. Enriquez, Maria Carmen S. Tan and Marissa G. Noel*
- 167 - 173 The Importance of Zinc-Mobilizing Rhizosphere Bacteria to the Enhancement of Physiology and Growth Parameters for Paddy under Salt-Stress Conditions  
*Yachana Jha*
- 175 - 182 Life-History Traits of the Climbing perch *Anabas testudineus* (Bloch, 1792) in a Wetland Ecosystem  
*Dalia Khatun, Md. Yeamin Hossain, Md. Ataur Rahman, Md. Akhtarul Islam, Obaidur Rahman, Md. Abul Kalam Azad, Most. Shakila Sarmin, Most. Farida Parvin, Ahnaf Tausif Ul Haque, Zannatul Mawa and Md. Akhtar Hossain and Olufemi S. Salami*
- 183 - 189 Virtual Screening for Inhibitors Targeting the Rod Shape- Determining Protein in *Escherichia coli*  
*Mohammed Z. Al-Khayyat, Ammar Gh. Ameen and Yousra A. Abdulla*
- 191 - 196 Antibiotic Resistance and Type III Exotoxin Encoding Genes of *Pseudomonas aeruginosa* Isolates from Environmental and Clinical Sources in Northern West Bank in Palestine  
*Ghaleb M. Adwan, Awni A. Abu-Hijleh and Ne'ma M. Bsharat*
- 197 - 202 Estimation of Biometric Indices for Snakehead *Channa punctata* (Bloch, 1793) through Multi-model Inferences  
*Md. Alomgir Hossen, Alok Kumar Paul, Md. Yeamin Hossain, Jun Ohtomi, Wasim Sabbir, Obaidur Rahman, Julia Jasmin, Md. Nuruzzaman Khan, Md. Akhtarul Islam, Md. Ataur Rahman, Dalia Khatun and Sk. Kamruzzaman*
- 203 - 207 Differential Expression for Genes in Response to Drought and Salinity in *Ruta graveolens* Plantlets  
*Sabah M. Hadi, Kadhim M. Ibrahim and Shatha I. Yousif*
- 209 - 217 A Thermodynamic Study of Partially-Purified *Penicillium humicola*  $\beta$ -mannanase Produced by Statistical Optimization  
*Siham A. Ismail, Om Kalthoum H. Khattab, Shaimaa A. Nour , Ghada E. A. Awad, Amany A. Abo-Elnasr and Amal M. Hashem*
- 219 - 227 Biological Control of *Macrophomina phaseolina* in *Vigna mungo* L. by Endophytic *Klebsiella pneumoniae* HR1  
*Sampad Dey, Prajesh Dutta and Sukanta Majumdar*

- 229 - 235 Effect of Temperature Constraints on Morphological and Cytogenetical Attributes in Cluster bean [*Cyamopsis tetragonoloba* (L.) Taub.]  
*Girjesh Kumar and Shefali Singh*
- 237 - 241 Delta-Aminolevulinic Acid Dehydratase Inhibition and RBC Abnormalities in Relation to Blood Lead among Selected Jordanian Workers.  
*Ziad A. Shraideh, Darwish H. Badran , Abdelrahim A. Hunaiti and Abdelkader Battah*
- 243 - 249 Analysis and Characterization of Purified Levan from *Leuconostoc mesenteroides* ssp. *cremoris* and its Effects on *Candida albicans* Virulence Factors  
*Jehan A.S. Salman, Hamzia A. Ajah and Adnan Y. Khudair*

# A Comparison between CAPS and SCAR Markers in the Detection of Resistance Genes in some Tomato Genotypes against *Tomato Yellow Leaf Curl Virus* and Whitefly

Sherin A. Mahfouze\* and Heba A. Mahfouze

National Research Centre, Genetic Engineering and Biotechnology Research Division, Genetics and Cytology Department, Dokki, 12622, Egypt.

Received June 4, 2018; Revised July 31, 2018; Accepted August 24, 2018

## Abstract

The *Tomato yellow leaf curl virus* (TYLCV) is transmitted by the whitefly vector (*Bemisia tabaci*) and can cause big losses in tomato yields in Egypt and worldwide. Several genes linked to resistance to TYLCV (*Ty-1*, *Ty-2* and *Ty-3*) and whitefly (*Mi-1.2*) in wild species and cultivated tomatoes were detected. Cleaved amplified Polymorphic Sequence (CAPS) and Sequence Characterized Amplified Region (SCAR) markers are used as tools in tomato lines carrying different combinations of *Ty-1*, *Ty-2*, *Ty-3* and *Mi-1.2* alleles. In this study, a total of nineteen tomato genotypes have been selected for the existence of resistance alleles, using five CAPS and three SCAR markers. Resistant allele-specific fragments for TYLCV and whitefly have been identified in some of the genotypes used in the current research. Thus, CAPS markers closely linked to *Ty-1* and *Mi-1.2* discriminated homozygous and heterozygous tomato genotypes. In addition, Sequence Characterized Amplified Region (SCAR) markers linked to *Ty-2* and *Ty-3* genes separated both dominant and recessive alleles in tomato plant materials. On the contrary, CAPS (*Ty-2* and *Ty-3*) and SCAR (*Mi-1.2*) markers gave false positive results. These molecular markers are considered advantageous tools for pyramiding resistance genes of several genotypes into a single line, improving the resistance to *begomoviruses*.

**Keywords:** *Solanum lycopersicon*, Wild tomato, *Ty-1*, *Ty-2*, *Ty-3*, *Mi-1.2*, Disease resistance.

## 1. Introduction

Tomatoes (*Solanum lycopersicum*) are economically important horticultural crops which belong to the *Solanaceae* family, and are used as food for humans (Peralta *et al.*, 2008). Tomato yields are often infected by the *Tomato yellow leaf curl virus* (TYLCV) which causes 100% significant losses in tomato crops in the tropical and subtropical regions around the world (Czosnek, 2007; Mahfouze *et al.*, 2015). TYLCV belongs to the genus *Begomovirus* (family *Geminiviridae*) (Belabess *et al.*, 2016). The virus is transmitted by the sweetpotato whitefly vector (*Bemisia tabaci*) in a persistent and circulative manner (Mahfouze *et al.*, 2017; Geng *et al.*, 2018). Although, the use of insecticides for the sake of whitefly insect control can reduce the spread of the virus, epidemics can appear and resistance of whitefly to insecticides has been reported (Feng *et al.*, 2010; Schuster *et al.*, 2010). The breeding of tomatoes resistant or tolerant to TYLCV is one of the most effective strategies to reduce the yield losses. No resistance has been recorded to date in the *S. lycopersicum* genotype, though some tomato lines have been found to be less susceptible than others. Fortunately, new sources of resistance to TYLCV have been found in several wild tomato species (Ji *et al.*, 2007a; Scott, 2007). Several resistance genes to TYLCV have been identified

(Ji *et al.*, 2007a, 2009; Anbinder *et al.*, 2009). The TYLCV resistance gene *Ty-1* originated from *S. chilense* line LA1969 and is located on chromosome 6 of tomato (Zamir *et al.*, 1994). The *Ty-2* locus (Hanson *et al.*, 2000), was identified in *S. habrochaites* B6013 (Kalloo and Banerjee, 1990), mapped on the long arm of chromosome 11 (Hanson *et al.*, 2006). The third TYLCV resistance gene *Ty-3* was identified in resistant tomato genotypes derived from accessions LA2779 and LA1932 of *S. chilense* and is located on the long arm of chromosome 6, 15 cM away from *Ty-1* locus (Ji *et al.*, 2007a). The dominant whitefly or root-knot nematode resistance gene *Mi-1* was introgressed from *S. peruvianum* into cultivated tomato (Messeguer *et al.*, 1991; Chen *et al.*, 2015). The introgressed DNA region carries many genes and pseudogenes, among which only *Mi-1.2* was proven to give resistance to whiteflies (Nombela *et al.*, 2003), nematodes (Milligan *et al.*, 1998) and aphids (Rossi *et al.*, 1998).

A significant advance has been made in the development of molecular markers associated with disease resistance genes (Ji *et al.*, 2007b; Pérez de Castro *et al.*, 2007; Anbinder *et al.*, 2009). The markers associated with resistance genes can be used to select novel resistant sources at early stages without inoculation with the pathogen, hence shortening the length in breeding programs. In addition, molecular markers are powerful

\* Corresponding author e-mail: sherinmahfouze@yahoo.com.

tools in pyramiding programs, in which different resistance gene alleles are introgressed in a single tomato line to increase the effectiveness and durability of resistance against diseases, also reducing the cost of breeding resistant plants (Vidavski *et al.*, 2008; Slater *et al.*, 2013).

The objective of this study is to identify and compare two functional molecular markers, namely CAPS and SCAR linked to resistance genes for TYLCV (*Ty-1*, *Ty-2* and *Ty-3*) and whitefly resistance locus (*Mi-1.2*) in wild and cultivated tomato genotypes, which can be used as marker-assisted selection (MAS) in breeding programs.

## 2. Materials and Methods

### 2.1. Plant Materials

A total of nineteen tomato genotypes, including commercial cultivars and accessions were used in this research. Fifteen tomato accessions were provided by the Tomato Genetics Resource Center (TGRC), Department of Plant Sciences, University of California, Davis, CA 95616 (<http://tgrc.ucdavis.edu>) and two accessions supported by the Centre for Genetic Resources (CGN), Netherlands (<http://www.wur.nl>). In addition, two commercial cultivars were obtained from the Egyptian Company for Seeds, Oils and Chemicals, Egypt to be used in this study (Table 1). Twenty tomato seeds of each genotype were germinated in a greenhouse until true leaves developed at a temperature regime of 27°C:16°C (Light: Dark), a photoperiod of L16:D8 h, and a relative humidity of 68-75%. The seedlings were planted in peatmoss: sand (2:1) in pots irrigated with a nutritive complex N: P: K (20:20:20).

**Table 1.** Tomato genotypes used in this study.

No.	Genotype	Source	No.	Genotype	Source
1	<i>Solanum hirsutum</i> 24036	CGN	11	<i>S. chilense</i> 56139	CGN
2	<i>S. galapagense</i> 0317	TGRC	12	<i>S. lycopersicon</i> cv. Super Marmande	Egypt
3	<i>S. neoricki</i> 0247	TGRC	13	<i>S. lycopersicon</i> cv. Strain B F1	Egypt
4	<i>S. arcanum</i> 1346	TGRC	14	<i>S. corneliomulleri</i> 1283	TGRC
5	<i>S. corneliomulleri</i> 1274	TGRC	15	<i>S. habrochaites</i> 1739	TGRC
6	<i>S. pennellii</i> 1733	TGRC	16	<i>S. pimpinellifolium</i> 1279	TGRC
7	<i>S. huaylasense</i> 1358	TGRC	17	<i>S. pimpinellifolium</i> 1332	TGRC
8	<i>S. pimpinellifolium</i> 1342	TGRC	18	<i>S. pennellii</i> 2963	TGRC
9	<i>S. peruvianum</i> 1333	TGRC	19	<i>S. pennellii</i> 1942	TGRC
10	<i>S. habrochaites</i> 1352	TGRC			

CGN= Centre for Genetic Resources, The Netherlands; TGRC= Tomato Genetics Resource Center (TGRC), Department of Plant Sciences, University of California, Davis.

### 2.2. Virus Resistance Tests

#### 2.2.1. Source of TYLCV Isolate

The Tomato yellow leaf curl virus (TYLCV) isolate was obtained from the Virology Laboratory, Department of Agricultural Microbiology, Faculty of Agriculture, University of Ain Shams, and was previously isolated and identified from systemically infected tomato plants. The

isolate was maintained on tomato plants cv. Super Marmande. Systemically, the infected leaves were used as sources of inoculum in all experiments.

#### 2.2.2. TYLCV Inoculation

One-month age tomato genotypes (15 plants/genotype) grown in the greenhouse were inoculated by syringes using TYLCV infected tomato sap according to Allam *et al.*, (1994). Inoculated plants were observed for the development of TYLCV symptoms for eight weeks post-inoculation. All of the TYLCV inoculated tomato plants were tested for the presence of viral DNA by PCR using the TYLCV specific primer sets. These materials were evaluated in two seasons during 2015/16 and 2016/17 in the greenhouse.

#### 2.2.3. Extraction of DNA

DNA was extracted from healthy and TYLCV-inoculated fresh tomato leaves, after two months of inoculation. Around 30 mg of tissue was ground in liquid nitrogen and extracted with the DNA purification Kit (Bio Basic, Inc., Markham, Canada) following the manufacturer's instructions. DNA quality and quantity were determined by agarose gel electrophoresis and Spectrophotometer. DNA concentrations were adjusted to 50 ng/μL and the extracts were frozen at -20°C.

#### 2.2.4. Detection of TYLCV by PCR

TYLCV-specific primer sets were designed based on the sequence of TYLCV isolate (KP725055.1) from the GenBank database using the primer3 software program (Rozen and Skaletsky, 2000). The primers set TYLCVF/ TYLCVR were designed to amplify the AVI gene (encodes a coat protein) of the TYLCV isolate (manufactured by Bio Basic, Canada) (Table 2). PCR reaction mixtures of 25 μL contained: 2.5 μL of 2.5 mM dNTPs; 2.5 μL 10X PCR buffer; 2.5 μL 25 mM MgCl<sub>2</sub>; 1 μL 2 U Taq DNA polymerase; 2.5 μL each forward and reverse-sense primer at 10 μM; 1 μL sample DNA and 11.5 μL dsH<sub>2</sub>O. The PCR was carried out in Thermocycler ((Biometra, biomedizinische Analytik, Germany GmbH). The PCR was carried out by denaturing DNA template at 94°C for four minutes, followed by thirty-five cycles of denaturing at 94°C for one minute, primer annealing at 55°C for one minute and DNA extension at 72°C for one minute. Then, it was followed by a final DNA extension at 72°C for seven minute.

### 2.3. PCR Amplification of Alleles Resistant to TYLCV (*Ty-1*, *Ty-2* and *Ty-3*) and Whitefly (*Mi-1.2*)

#### 2.3.1. Cleaved Amplified Polymorphic Sequence (CAPS) Markers

Five markers TY-1CAPS-TG178, JB1, TY-2CAPS-TG105A, TY-3CAPS-FER-G8 and MI-REXCAPS (manufactured by Bio Basic, Canada) and the sequence of primers are shown in Table 2. PCRs were performed in 25 μL reaction volumes containing 1 μL of 50 ng/μL genomic DNA, 1X buffer, 0.5 μM of each primer, 0.6 mM dNTPs, 1.4 mM MgCl<sub>2</sub> and 1 unit of Taq polymerase (Promega, USA). The following conditions were used: an initial denaturation step at 95°C for two minutes, followed by thirty-five cycles of 95°C for forty seconds, annealing temperature (Table 2) for forty seconds, 72°C for sixty seconds and a final extension at 72°C for five minutes.



**Table 2.** Primer sequences used in this study.

Primer and markers	R-gene*	Chromosome No	Single nucleotide sequence (5'-3')	Annealing temperature (AT)°C	Restriction enzyme	Molecular size of band (bp)	Molecular size after digestion with <i>TaqI</i> (bp)	References
TYLCV AV1 F	-	-	TGACAAAGACATGCGGACCA	55	-	335	-	Present study
TYLCV AV1R	-	-	TGGGCTGTCTGAAGTTGAGAC					
TY-1CAPS-TG178F	<i>Ty1</i>	6	GGTACTCCTGGAAGGGTTAAGG	56	<i>TaqI</i>	1000	>200	Barbieri <i>et al.</i> , (2010)
TY-1CAPS-TG178R			CACGCTGGTTCTGTGTATCTC				200	
JB1CAPSF	<i>Ty1</i>	6	AACCATTATCCGGTTCCTC	53	<i>TaqI</i>	950	450	Pérez <i>et al.</i> , (2007)
JB1CAPSR			TTTCATTCTCTGTTTCTCTG				500	
TY-2CAPS-TG105A F			CTTCAGAAATCCTGTTTTAGTCAGTTGAACC	62	<i>TaqI</i>	500	330	Maxwell <i>et al.</i> , (2006)
TY-2CAPS-TG105AR	<i>Ty2</i>	11	ATGTCACATTGTTGCTTGACCATCC				220	
TY-3CAPS-FER-G8F			CATCCC GTGCATCATCCAAAGTGAC				50	
							200	
TY-3CAPS-FER-G8R	<i>Ty3</i>	6	CTAAGGGTGTACCCCAAGGGAAC	55	<i>TaqI</i>	500	250	Jensen <i>et al.</i> , (2007)
							300	
							500	
MI-REX CAPS F	<i>Mi1.2</i>	6	TCGGAGCCTTGGTCTGAATT	55	<i>TaqI</i>	750	180	Michelson <i>et al.</i> , (1994)
MI-REX CAPSR			GCCAGAGATGATTCGTGAGA				570	
							750	
Ty-2SCAR T0302F	<i>Ty2</i>	11	TGGCTCATCCTGAAGCTGATAGCGC	55	-	900	-	Yang <i>et al.</i> , (2014)
Ty-2SCAR T0302R			AGTGTACATCCTTGCCATTGACT			800		
Ty-3SCAR P6-25F	<i>Ty3</i>	6	GGTAGTGGAATGATGCTGCTC	53	-	450	-	Ji <i>et al.</i> , (2008)
Ty-3SCAR P6-25R			GCTCTGCCTATTGTCCCATATATAACC			660		
Mi-1.2SCARMi23F	<i>Mi1.2</i>	6	TGGAAAAATGTTGAATTTCTTTTG	57	-	380	-	Seah <i>et al.</i> , (2007)
Mi-1.2SCARMi23R			GCATACTATATGGCTTGTTTACCC			430		

\*Tomato yellow leaf curl virus (TYLCV) resistance genes.

### 2.3.1.1. Restriction Digestion and Analysis

CAPS-based markers were digested by the restriction enzymes *TaqI* (Table 2). 20 µL reaction mixture containing 16.3 µL dsH<sub>2</sub>O, 2 µL restriction enzyme 10X buffer, 0.2 µL BSA (Bovine serum albumin), 0.5 µL *TaqI* restriction enzyme 10 U/µL (Promega Corp.) and 1 µL DNA. The reaction mixture was placed in a 65°C water bath for about two hours according to the manufacturer's instructions.

### 2.3.2. Sequence Characterized Amplified Region (SCAR) Markers

Three markers Ty-2SCART0302, Ty-3SCARP6-25 and Mi-1.2SCARMi23 (manufactured by Bio Basic, Canada) and the sequence of primers are shown in Table 2. PCR parameters were for 25 µL reactions containing 2.5 µL 2.5

mM dNTPs, 5 µL 5X buffer, 2.5 µL 2.5 mM MgCl<sub>2</sub>, 0.1 µL (0.5 units) *Taq* DNA polymerase (Promega Corp., Madison, WI), 2.5 µL each forward and reverse primers at 10 µM, 1 µL of DNA extract and 8.9 µL dsH<sub>2</sub>O. PCR cycles were 94°C for four minutes, thirty-five cycles of 94°C for thirty seconds, annealing temperature (Table 2) for one minute and 72°C for 1.5 minute. These cycles were followed by 72°C for ten minutes and then the reaction was held at 4°C. PCR reactions were performed in the Thermocycler.

All of the PCR and restriction-digested products were analyzed with 1.5% agarose gel electrophoresis in 1X TBE buffer (89 mM Tris-HCl, 89 mM boric acid, 2.5 mM EDTA, pH 8.3), and were stained with ethidium bromide, and visualized with UV light.

### 3. Results

#### 3.1. Evaluation of TYLCV Resistance in the Tomato Genotypes

TYLCV inoculation tests were performed on nineteen tomato genotypes which showed different responses to the TYLCV infection (Table 3). Resistant tomato line *S. corneliomulleri* 1274 has not shown TYLCV symptoms eight weeks after inoculation. However, ten tomato genotypes were tolerant to TYLCV which showed mild to no-symptoms including leaf cup shape and necrosis. On

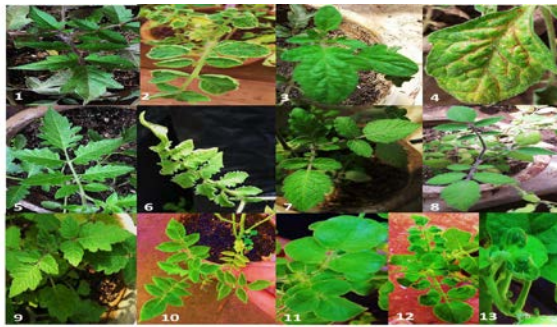
the contrary, eight susceptible tomato accessions displayed moderate to severe symptoms involved leaf curling, crinkle, epinasty, vein clearing, small leaf size, yellowing, veinal necrosis and deformation (Figure 1 and Table 3).

The researchers have designed AV1 primer specific of the TYLCV coat protein gene (*AV1*), in order to detect TYLCV in the nineteen tomato genotypes. The results showed that all tested tomato lines recorded of one amplicon of 335 bp except *S. corneliomulleri* 1274 have not recorded any product, which displayed resistance to the TYLCV isolate.

**Table 3.** Tomato genotypes used to evaluate gene-based markers for resistances to TYLCV.

No.	Genotype	Tomato yellow leaf curl virus (TYLCV) resistance genes and DNA markers								Result of infection test	Detection of TYLCV by PCR
		Ty-1	Ty-2	Ty-3	Mi-1.2						
		JB1-CAPS	CAPS-TG178	CAPS-TG105	SCAR-T0302	CAPS-FER-G8	SCAR-P6-25	MI-REX CAPS	SCAR-Mi23		
1	<i>Solanum hirsutum</i> 24036	H(Ty1/ty1)	S(ty1/ty1)	R(Ty2/Ty2)	H(Ty2/ty2)	H(Ty3/ty3)	R(Ty3/Ty3)	Mi/mi	-	LC, Y, C (Susceptible)	+
2	<i>S. galapagense</i> 0317	S(ty1/ty1)	S(ty1/ty1)	H(Ty2/ty2)	S(ty2/ty2)	H(Ty3a/ty3)	S(ty3/ty3)	mi/mi	mi/mi	LC, C (Susceptible)	+
3	<i>S. neoricki</i> 0247	S(ty1/ty1)	S(ty1/ty1)	R(Ty2/Ty2)	S(ty2/ty2)	S(ty3/ty3)	S(ty3/ty3)	mi/mi	-	LC, Y, C (Susceptible)	+
4	<i>S. arcanum</i> 1346	S(ty1/ty1)	H(Ty1/ty1)	R(Ty2/Ty2)	S(ty2/ty2)	H(Ty3a/ty3)	H(Ty3b/ty3)	Mi/mi	Mi/mi	LCS (Tolerant)	+
5	<i>S. corneliomulleri</i> 1274	S(ty1/ty1)	H(Ty1/ty1)	H(Ty2/ty2)	H(Ty2/ty2)	H(Ty3a/ty3)	R(Ty3/Ty3)	Mi/mi	-	NS (Resistant)	-
6	<i>S. pennellii</i> 1733	S(ty1/ty1)	S(ty1/ty1)	H(Ty2/ty2)	R(Ty2/Ty2)	H(Ty3/ty3)	R(Ty3/Ty3)	Mi/mi	Mi/mi	SL, D (Susceptible)	+
7	<i>S. huaylasense</i> 1358	S(ty1/ty1)	R(Ty1/Ty1)	H(Ty2/ty2)	R(Ty2/Ty2)	H(Ty3a/ty3)	H(Ty3/ty3)	Mi/mi	-	LCS (Tolerant)	+
8	<i>S. pimpinellifolium</i> 1342	S(ty1/ty1)	S(ty1/ty1)	R(Ty2/Ty2)	S(ty2/ty2)	H(Ty3a/ty3)	S(ty3/ty3)	mi/mi	mi/mi	LC, SL, D (Susceptible)	+
9	<i>S. peruvianum</i> 1333	H(Ty1/ty1)	R(Ty1/Ty1)	H(Ty2/ty2)	S(ty2/ty2)	H(Ty3a/ty3)	H(Ty3b/ty3)	Mi/mi	mi/mi	NS (Tolerant)	+
10	<i>S. habrochaites</i> 1352	H(Ty1/ty1)	S(ty1/ty1)	R(Ty2/Ty2)	R(Ty2/Ty2)	H(Ty3a/ty3)	R(Ty3/Ty3)	Mi/mi	mi/mi	NS (Tolerant)	+
11	<i>S. chilense</i> 56139	H(Ty1/ty1)	S(ty1/ty1)	H(Ty2/ty2)	S(ty2/ty2)	H(Ty3a/ty3)	H(Ty3/ty3)	Mi/mi	-	NS (Tolerant)	+
12	<i>S. lycopersicon</i> cv. Super Marmande	H(Ty1/ty1)	S(ty1/ty1)	H(Ty2/ty2)	S(ty2/ty2)	H(Ty3a/ty3)	S(ty3/ty3)	mi/mi	mi/mi	LC, C, SL, VN (Susceptible)	+
13	<i>S. lycopersicon</i> cv. Strain B F1	H(Ty1/ty1)	S(ty1/ty1)	R(Ty2/Ty2)	S(ty2/ty2)	H(Ty3a/ty3)	S(ty3/ty3)	Mi/mi	Mi/mi	LC, C (Susceptible)	+
14	<i>S. corneliomulleri</i> 1283	H(Ty1/ty1)	R(Ty1/Ty1)	H(Ty2/ty2)	R(Ty2/Ty2)	H(Ty3a/ty3)	R(Ty3/Ty3)	Mi/mi	-	LCS, N (Tolerant)	+
15	<i>S. habrochaites</i> 1739	S(ty1/ty1)	S(ty1/ty1)	H(Ty2/ty2)	R(Ty2/Ty2)	H(Ty3a/ty3)	H(Ty3/ty3)	Mi/mi	-	NS (Tolerant)	+
16	<i>S. pimpinellifolium</i> 1279	S(ty1/ty1)	S(ty1/ty1)	R(Ty2/Ty2)	S(ty2/ty2)	H(Ty3a/ty3)	S(ty3/ty3)	mi/mi	mi/mi	E, VC (Susceptible)	+
17	<i>S. pimpinellifolium</i> 1332	S(ty1/ty1)	S(ty1/ty1)	R(Ty2/Ty2)	S(ty2/ty2)	H(Ty3a/ty3)	S(ty3/ty3)	mi/mi	mi/mi	NS (Tolerant)	+
18	<i>S. pennellii</i> 2963	S(ty1/ty1)	S(ty1/ty1)	H(Ty2/ty2)	H(Ty2/ty2)	H(Ty3a/ty3)	R(Ty3/Ty3)	mi/mi	Mi/mi	NS (Tolerant)	+
19	<i>S. pennellii</i> 1942	S(ty1/ty1)	H(Ty1/ty1)	H(Ty2/ty2)	H(Ty2/ty2)	H(Ty3a/ty3)	R(Ty3/Ty3)	mi/mi	Mi/mi	NS (Tolerant)	+

R: Resistance allele, homozygote (Ty/Ty), S: Susceptibility allele, homozygote (ty/ty), H: Heterozygote (Ty/ty), PCR= Polymerase chain reaction, CAPS= Cleaved amplified polymorphic sequence, SCAR= Sequence characterized amplified region, (+)= Positive result, (-)= Negative result, C= Crinkle, D= deformation, E= Epinasty, LC= Leaf curl, LCS= Leaf cup shape, NS= No symptoms, SL= Small leaf size, Y= Yellowing, VC= Vein clearing, VN= Veinal necrosis.



**Figure 1.** TYLCV symptoms in different tomato genotypes compared with the healthy control.

1-The healthy control of *S. lycopersicon* cv. Super Marmande; 2- *S. lycopersicon* cv. Super Marmande infected with TYLCV, showing leaf curl and small leaf size; 3-The healthy control of *S. lycopersicon* cv. Super Marmande; 4- *S. lycopersicon* cv. Super Marmande diseased with TYLCV, showing veinal necrosis; 5- The healthy control of *S. corneliomulleri* 1283; 6- *S. corneliomulleri* 1283 inoculated with TYLCV, showing leaf cup shape; 7- The healthy control of *S. habrochaites* 1739; 8- *S. habrochaites* 1739 inoculated with TYLCV, showing no symptoms; 9- The healthy control of *S. hirsutum* 24036; 10- *S. hirsutum* 24036 diseased with TYLCV, showing leaf curl, crinkle and yellowing; 11- The healthy control of *S. pennellii* 1733; 12- *S. pennellii* 1733 infected with TYLCV showing small leaf size; 13- *S. pennellii* 1733 infected with TYLCV, showing deformation.

### 3.2. Screening Markers Linked to *Ty-1*, *Ty-2*, *Ty-3* and *Mi-1.2* Resistance Loci

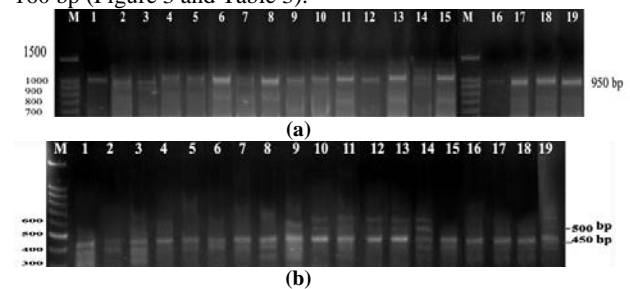
Validation of PCR-based markers is linked to the three TYLCV resistance loci (*Ty-1*, *Ty-2* and *Ty-3*) and one whitefly resistance gene (*Mi-1.2*) in nineteen tomato genotypes (Table 3).

#### 3.2.1. *Ty-1* Locus

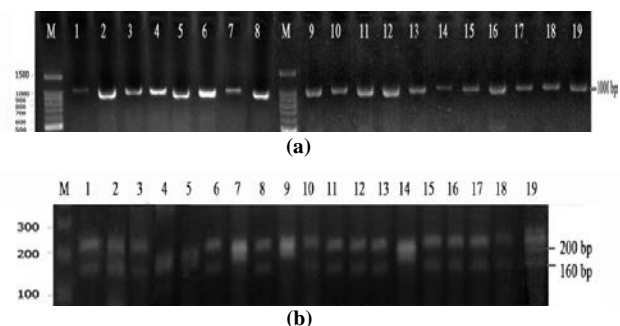
PCR amplification of DNA from the tomato genotypes and subsequent digestion by *TaqI* were performed using JB-1 CAPS marker, and scored a unique band of 950 bp with nineteen lines tested before restriction (Figure 2 and Table 3). After restriction with *TaqI*, twelve tomato lines revealed a susceptible allele (*ty-1*) size of 450 bp, which confirms the gene absence *Ty-1* such as *S. galapagense* 0317, *S. neoricki* 0247, *S. arcanum* 1346, *S. corneliomulleri* 1274, *S. huaylasense* 1358, *S. pimpinellifolium* 1342, 1279 and 1332, *S. habrochaites* 1739 and *S. pennellii* 1733, 2963 and 1942. On the other hand, seven accessions exhibited heterozygous alleles (*Ty1/ty1*) of 450 and 500 bp which confer the presence of the *Ty-1* gene i.e., *S. hirsutum* 24036, *S. peruvianum* 1333, *S. habrochaites* 1352, *S. chilense* 56139, Super Marmande, Strain B F1 and *S. corneliomulleri* 1283 (Figure 2 and Table 3). None of the tomato lines recorded dominant homozygous for *Ty1* (*Ty1/Ty1*). JB-1 CAPS has not discriminated between resistant and susceptible genotypes.

The TY-1CAPS-TG178 primer pair gave one amplicon of 1000 bp with all of the tomato genotypes (Figure 3). Its nucleotide sequence was 500 bp longer than the sequence deduced from unigene because of the presence of four intron sequences in the genomic DNA. PCR products were distinguishable after digestion with restriction enzyme *TaqI*. Three lines which were homozygous plants for *Ty1* (*Ty1/Ty1*) exhibited two alleles (200 and band slightly larger than 200 bp) viz., *S. huaylasense* 1358, *S. peruvianum* 1333 and *S. corneliomulleri* 1283. Three tomato genotypes had three different alleles of 160, 200

and band slightly larger than 200 bp which were heterozygous (*Ty1/ty1*) e.g., *S. arcanum* 1346, *S. corneliomulleri* 1274 and *S. pennellii* 1942. Besides, the other thirteen genotypes were homozygous plants for *ty-1* (*ty1/ty1*) showed two alleles with molecular sizes 200 and 160 bp (Figure 3 and Table 3).



**Figure 2.** (a) PCR profiles of *Ty-1* locus amplified by JB-1CAPS primer from 19 tomato genotypes, lane M= 100 bp DNA ladder. (b) *TaqI* digestion of PCR products amplified by JB1CAPS primer. Lane 1: *Solanum hirsutum* 24036 (resistant, heterozygous); lane 2: *S. galapagense* 0317 (susceptible, homozygous); lane 3: *S. neoricki* 0247 (susceptible, homozygous); lane 4: *S. arcanum* 1346 (susceptible, homozygous); lane 5: *S. corneliomulleri* 1274 (susceptible, homozygous); lane 6: *S. pennellii* 1733 (susceptible, homozygous); lane 7: *S. huaylasense* 1358 (susceptible, homozygous); lane 8: *S. pimpinellifolium* 1342 (susceptible, homozygous); lane 9: *S. peruvianum* 1333(resistant, heterozygous); lane 10: *S. habrochaites* 1352 (resistant, heterozygous); lane 11: *S. chilense* 56139 (resistant, heterozygous); lane 12: *S. lycopersicon* cv. Super Marmande (resistant, heterozygous); lane 13: *S. lycopersicon* cv. Strain B F1 (resistant, heterozygous); lane 14: *S. corneliomulleri* 1283(resistant, heterozygous); lane 15: *S. habrochaites* 1739 (susceptible, homozygous); lane 16: *S. pimpinellifolium* 1279 (susceptible, homozygous); lane 17: *S. pimpinellifolium* 1332 (susceptible, homozygous); lane 18: *S. pennellii* 2963 (susceptible, homozygous) and lane 19: *S. pennellii* 1942 (susceptible, homozygous).



**Figure 3.** (a) PCR profiles of *Ty-1* locus amplified by TY-1CAPS-TG178 primer from 19 tomato genotypes, lane M= 100 bp DNA ladder. (b) *TaqI* digestion of PCR products amplified by TY-1CAPS-TG178 primer. Lane 1: *Solanum hirsutum* 24036 (susceptible, homozygous); lane 2: *S. galapagense* 0317 (susceptible, homozygous); lane 3: *S. neoricki* 0247 (susceptible, homozygous); lane 4: *S. arcanum* 1346 (resistant, heterozygous); lane 5: *S. corneliomulleri* 1274 (resistant, heterozygous); lane 6: *S. pennellii* 1733 (susceptible, homozygous); lane 7: *S. huaylasense* 1358 (resistant, homozygous); lane 8: *S. pimpinellifolium* 1342 (susceptible, homozygous); lane 9: *S. peruvianum* 1333(resistant, homozygous); lane 10: *S. habrochaites* 1352 (susceptible, homozygous); lane 11: *S. chilense* 56139 (susceptible, homozygous); lane 12: *S. lycopersicon* cv. Super Marmande (susceptible, homozygous); lane 13: *S. lycopersicon* cv. Strain B F1 (susceptible, homozygous); lane 14: *S. corneliomulleri* 1283(resistant, homozygous); lane 15: *S. habrochaites* 1739 (susceptible, homozygous); lane 16: *S. pimpinellifolium* 1279 (susceptible, homozygous); lane 17: *S. pimpinellifolium* 1332 (susceptible, homozygous); lane 18: *S. pennellii* 2963 (susceptible, homozygous) and lane 19: *S. pennellii* 1942 (resistant, heterozygous).

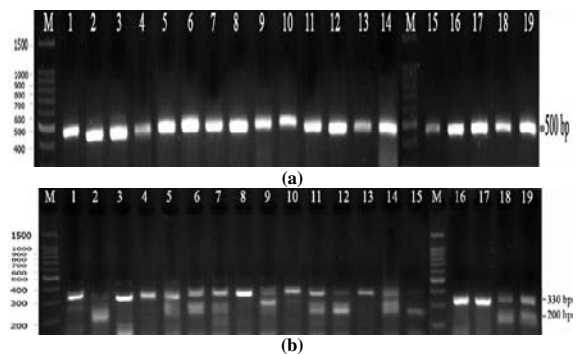
### 3.2.2. Ty-2 Locus

TY-2CAPS-TG105A marker was used to select the tomato lines carrying the *Ty-2* gene. One amplicon of 500 bp was obtained from all of the tested tomato genotypes. The PCR products were distinguishable after the cleavage with restriction enzyme *TaqI* (Figure 4). Two different alleles appeared in tomato plant materials; resistant allele 1 consisted of a fragment of 330 bp and appeared in homozygous eight tomato genotypes for *Ty2* (*Ty2/Ty2*) i.e., *S. hirsutum* 24036, *S. neoricki* 0247, *S. arcanum* 1346, *S. pimpinellifolium* 1342, *S. habrochaites* 1352, Strain B F1, and *S. pimpinellifolium* 1279 and 1332. Both alleles 330 and 200 bp appeared in heterozygous 11 tomato lines (*Ty2/ty2*) as shown in Table (3). On the other hand, there is not any homozygous susceptible accessions carry allele 2 of 200 bp (*ty2/ty2*) (Figure 4 and Table 3). This marker did not discriminate between homozygous and heterozygous accessions from each other.

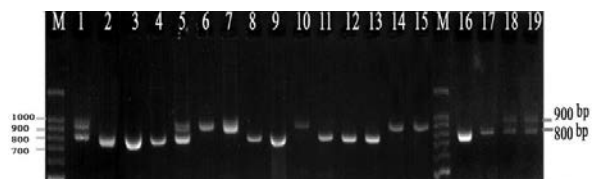
The two co-dominant TY-2CAPS-TG105A marker scored false positive results for the presence of the *Ty-2* locus. This marker did not separate resistant and susceptible alleles. On the contrary, the PCR products of Ty-2SCAR T0302 marker were well separated from each susceptible or resistance allele at each locus. The PCR results successfully amplified DNA fragments for the *Ty-2* locus from all homozygous and heterozygous tomato lines. The five resistant lines (*Ty2/Ty2*) viz., *S. pennellii* 1733, *S. huaylasense* 1358, *S. habrochaites* 1352 and 1739 and *S. corneliomulleri* 1283 scored one allele of 900 bp (Figure 5). Moreover, ten susceptible accessions (*ty2/ty2*) gave PCR fragments of 800 bp e.g., *S. galapagense* 0317, *S. neoricki* 0247, *S. arcanum* 1346, *S. peruvianum* 1333, *S. chilense* 56139, Super Marmande, Strain B F1 and *S. pimpinellifolium* 1342, 1279 and 1332. The four heterozygous tomato genotypes scored two alleles 800 and 900 bp, for example, *Solanum hirsutum* 24036, *S. corneliomulleri* 1274, and *S. pennellii* 2963 and 1942 (Figure 5 and Table 3).

### 3.2.3. Ty-3 Locus

PCR amplification of DNA from the tomato genotypes using primer TY-3CAPS-FER-G8, gave one fragment with a molecular size of 500 bp in all of the homozygous and heterozygous tomato genotypes as shown in Figure (6). A subsequent digestion, when possible, was performed using *TaqI* restriction enzyme. Two accessions *S. hirsutum* 24036 and *S. pennellii* 1733 which were heterozygous for *Ty-3* showed three different alleles of 50, 250 and 300 bp in the presence of two *TaqI* sites. On the other hand, *S. neoricki* 0247 which was homozygous of *ty-3* had one fragment of 500 bp without being digested due to lack of a *TaqI* site in this fragment. However, the rest of the sixteen tomato lines which were heterozygous for *Ty-3a* exhibited two different bands with molecular sizes 200 and 300 bp, in the result of these accessions having one *TaqI* site (Figure 6 and Table 3). TY-3CAPS-FER-G8 marker gave false positive results for the presence of the *Ty-3* locus. In addition, it has not distinguished between *Ty-3*, *Ty-3a*, *Ty3-b* and *ty-3* alleles of resistant and susceptible tomato lines.



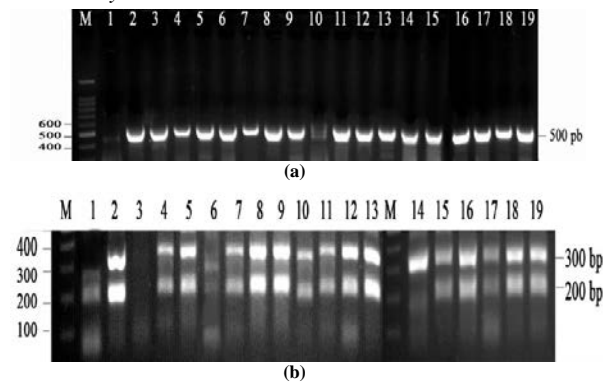
**Figure 4.** (a) PCR products of *Ty-2* locus amplified by TY-2CAPS-TG105A primer from 19 tomato genotypes, lane M= 100 bp DNA ladder. (b) *TaqI* digestion of PCR products amplified by TY-2CAPS-TG105A primer. Lane 1: *Solanum hirsutum* 24036 (resistant, homozygous); lane 2: *S. galapagense* 0317 (resistant, heterozygous); lane 3: *S. neoricki* 0247 (resistant, homozygous); lane 4: *S. arcanum* 1346 (resistant, homozygous); lane 5: *S. corneliomulleri* 1274 (resistant, heterozygous); lane 6: *S. pennellii* 1733 (resistant, heterozygous); lane 7: *S. huaylasense* 1358 (resistant, heterozygous); lane 8: *S. pimpinellifolium* 1342 (resistant, homozygous); lane 9: *S. peruvianum* 1333 (resistant, heterozygous); lane 10: *S. habrochaites* 1352 (resistant, homozygous); lane 11: *S. chilense* 56139 (resistant, heterozygous); lane 12: *S. lycopersicon* cv. Super Marmande (resistant, heterozygous); lane 13: *S. lycopersicon* cv. Strain B F1 (resistant, homozygous); lane 14: *S. corneliomulleri* 1283 (resistant, heterozygous); lane 15: *S. habrochaites* 1739 (resistant, heterozygous); lane 16: *S. pimpinellifolium* 1279 (resistant, homozygous); lane 17: *S. pimpinellifolium* 1332 (resistant, homozygous); lane 18: *S. pennellii* 2963 (resistant, heterozygous) and lane 19: *S. pennellii* 1942 (resistant, heterozygous).



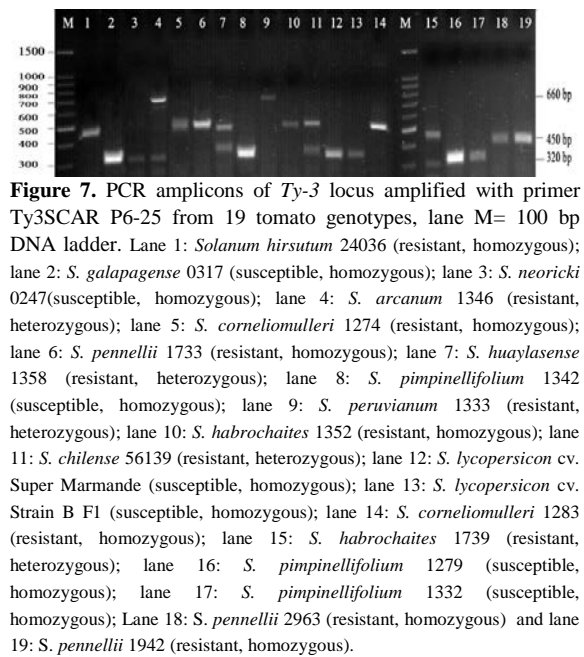
**Figure 5.** PCR amplicons of *Ty-2* locus amplified by primer Ty-2SCAR T0302 from 19 tomato genotypes, lane M= 100 bp DNA ladder. Lane 1: *Solanum hirsutum* 24036 (resistant, heterozygous); lane 2: *S. galapagense* 0317 (susceptible, homozygous); lane 3: *S. neoricki* 0247 (susceptible, homozygous); lane 4: *S. arcanum* 1346 (susceptible, homozygous); lane 5: *S. corneliomulleri* 1274 (resistant, heterozygous); lane 6: *S. pennellii* 1733 (resistant, homozygous); lane 7: *S. huaylasense* 1358 (resistant, homozygous); lane 8: *S. pimpinellifolium* 1342 (susceptible, homozygous); lane 9: *S. peruvianum* 1333 (susceptible, homozygous); lane 10: *S. habrochaites* 1352 (resistant, homozygous); lane 11: *S. chilense* 56139 (susceptible, homozygous); lane 12: *S. lycopersicon* cv. Super Marmande (susceptible, homozygous); lane 13: *S. lycopersicon* cv. Strain B F1 (susceptible, homozygous); lane 14: *S. corneliomulleri* 1283 (resistant, homozygous); lane 15: *S. habrochaites* 1739 (resistant, homozygous); lane 16: *S. pimpinellifolium* 1279 (susceptible, homozygous); lane 17: *S. pimpinellifolium* 1332 (susceptible, homozygous); lane 18: *S. pennellii* 2963 (resistant, heterozygous) and lane 19: *S. pennellii* 1942 (resistant, heterozygous).

Ty3SCAR P6-25 gave one amplified fragment with a molecular size of 450 bp in seven resistant tomato genotypes which were homozygous (*Ty3/Ty3*) e.g., *S. hirsutum* 24036, *S. corneliomulleri* 1274 and 1283, *S. pennellii* 1733, 2963 and 1942 and *S. habrochaites* 1352. Besides, *S. peruvianum* 1333 and *S. arcanum* 1346 which were heterozygous (*Ty3b/ty3*) recorded two amplicons of 320 and 660 bp (Figure 7 and Table 3). On the other hand, three heterozygous tomato lines (*Ty3/ty3*) scored two alleles 320 and 450 bp such as *S. huaylasense* 1358, *S. chilense* 56139 and *S. habrochaites* 1739. The other seven susceptible accessions which were recessive homozygous

(*ty3/ty3*) gave PCR fragments of 320 bp (Figure 7 and Table 3). Furthermore, there are no tomato genotypes that have the *Ty3a* locus.



**Figure 6. (a)** PCR products of *Ty-3* locus amplified by TY-3CAPS-FER-G8 primer from 19 tomato genotypes, lane M= 100 bp DNA ladder. **(b)** *TaqI* digestion of PCR products amplified by TY-3CAPS-FER-G8 primer. Lane 1: *Solanum hirsutum* 24036 (resistant, heterozygous); lane 2: *S. galapagense* 0317 (resistant, heterozygous); lane 3: *S. neoricki* 0247 (susceptible, homozygous); lane 4: *S. arcanum* 1346 (resistant, heterozygous); lane 5: *S. corneliomulleri* 1274 (resistant, heterozygous); lane 6: *S. pennellii* 1733 (resistant, heterozygous); lane 7: *S. huaylasense* 1358 (resistant, heterozygous); lane 8: *S. pimpinellifolium* 1342 (resistant, heterozygous); lane 9: *S. peruvianum* 1333 (resistant, heterozygous); lane 10: *S. habrochaites* 1352 (resistant, heterozygous); lane 11: *S. chilense* 56139 (resistant, heterozygous); lane 12: *S. lycopersicon* cv. Super Marmande (resistant, heterozygous); lane 13: *S. lycopersicon* cv. Strain B F1 (resistant, heterozygous); lane 14: *S. corneliomulleri* 1283 (resistant, heterozygous); lane 15: *S. habrochaites* 1739 (resistant, heterozygous); lane 16: *S. pimpinellifolium* 1279 (resistant, heterozygous); lane 17: *S. pimpinellifolium* 1332 (resistant, heterozygous); lane 18: *S. pennellii* 2963 (resistant, heterozygous) and lane 19: *S. pennellii* 1942 (resistant, heterozygous).

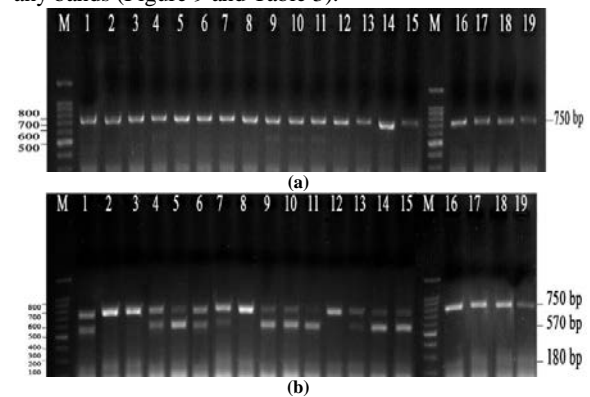


### 3.2.4. *Mi-1.2* Locus

The PCR using MI-REXCAPS primer pairs yielded a 750 bp DNA fragment in all of the studied genotypes,

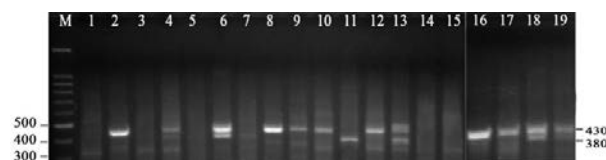
before digestion with *TaqI* (Figure 8). After digestion, a single 750 bp fragment for recessive homozygous eight genotypes (*mi/mi*) was observed. For instance, *S. galapagense* 0317, *S. neoricki* 0247, *S. pimpinellifolium* 1342, 1279 and 1332, Super Marmande and *S. pennellii* 2963 and 1942. However, the remaining eleven genotypes had three loci of 750, 570 and 180 bp which were heterozygous (*Mi/mi*) such as *S. hirsutum* 24036, *S. arcanum* 1346, *S. corneliomulleri* 1274 and 1283, *S. pennellii* 1733, *S. huaylasense* 1358, *peruvianum* 1333, *S. habrochaites* 1352 and 1739, *S. chilense* 56139, and Strain B F1 (Figure 8 and Table 3). The MI-REXCAPS marker distinguished between susceptibility and resistance alleles at *Mi-1.2* locus of the homozygous and heterozygous genotypes.

The *Mi-1.2SCARMi23* gave different results from the MI-REXCAPS primer in the genotypes carrying *Mi-1.2* or not carrying *Mi-1.2*. The PCR with *Mi-1.2SCARMi23* primer pairs yielded 430 band with homozygous seven susceptible lines (*mi/mi*) such as *S. galapagense* 0317, *S. pimpinellifolium* 1342, 1279 and 1332, *S. peruvianum* 1333, *S. habrochaites* 1352 and Super Marmande. Heteroduplex five genotypes (*Mi/mi*) exhibited two amplified fragments of 430 and 380 bp viz., *S. arcanum* 1346, Strain B F1 and *S. pennellii* 1733, 2963 and 1942. Furthermore, the other seven accessions have not scored any bands (Figure 9 and Table 3).



**Figure 8. (a)** PCR products of *Mi-1.2* locus amplified by MI-REXCAPS primer from 19 tomato genotypes, lane M= 100 bp DNA ladder. **(b)** *TaqI* digestion of PCR products amplified by MI-REXCAPS primer. Lane 1: *Solanum hirsutum* 24036 (resistant, heterozygous); lane 2: *S. galapagense* 0317 (susceptible, homozygous); lane 3: *S. neoricki* 0247 (susceptible, homozygous); lane 4: *S. arcanum* 1346 (resistant, heterozygous); lane 5: *S. corneliomulleri* 1274 (resistant, heterozygous); lane 6: *S. pennellii* 1733 (resistant, heterozygous); lane 7: *S. huaylasense* 1358 (resistant, heterozygous); lane 8: *S. pimpinellifolium* 1342 (susceptible, homozygous); lane 9: *S. peruvianum* 1333 (resistant, heterozygous); lane 10: *S. habrochaites* 1352 (resistant, heterozygous); lane 11: *S. chilense* 56139 (resistant, heterozygous); lane 12: *S. lycopersicon* cv. Super Marmande (susceptible, homozygous); lane 13: *S. lycopersicon* cv. Strain B F1 (resistant, heterozygous); lane 14: *S. corneliomulleri* 1283 (resistant, heterozygous); lane 15: *S. habrochaites* 1739 (resistant, heterozygous); lane 16: *S. pimpinellifolium* 1279 (susceptible, homozygous); lane 17: *S. pimpinellifolium* 1332 (susceptible, homozygous); lane 18: *S. pennellii* 2963 (susceptible, homozygous) and lane 19: *S. pennellii* 1942 (susceptible, homozygous).





**Figure 9.** PCR amplicons of *Mi-1,2* locus amplified with primer *Mi-1.2SCARMi23* from 19 tomato genotypes, lane M= 100 bp DNA ladder. Lane 1: *Solanum hirsutum* 24036 (no alleles); lane 2: *S. galapagense* 0317 (susceptible, homozygous); lane 3: *S. neoricki* 0247 (no alleles); lane 4: *S. arcanum* 1346 (resistant, heterozygous); lane 5: *S. corneliomulleri* 1274 (no alleles); lane 6: *S. pennellii* 1733 (resistant, heterozygous); lane 7: *S. huaylasense* 1358 (no alleles); lane 8: *S. pimpinellifolium* 1342 (susceptible, homozygous); lane 9: *S. peruvianum* 1333 (susceptible, homozygous); lane 10: *S. habrochaites* 1352 (susceptible, homozygous); lane 11: *S. chilense* 56139 (no alleles); lane 12: *S. lycopersicon* cv. Super Marmande (susceptible, homozygous); lane 13: *S. lycopersicon* cv. Strain B F1 (resistant, heterozygous); lane 14: *S. corneliomulleri* 1283 (no alleles); lane 15: *S. habrochaites* 1739 (no alleles); lane 16: *S. pimpinellifolium* 1279 (susceptible, homozygous); Lane 17: *S. pimpinellifolium* 1332 (susceptible, homozygous); lane 18: *S. pennellii* 2963 (resistant, heterozygous) and lane 19: *S. pennellii* 1942 (resistant, heterozygous).

#### 4. Discussion

Molecular markers have several applications in plant breeding programs. The availability of molecular markers associated with genes which suggest desirable traits allows the shortening of the breeding programs. Many resistance genes discovered in different wild tomato species have been introgressed in the cultivated tomato. Some of them are mapped to chromosome 6, and are genetically very close. Identifying the loci of a marker linked specifically with one of these resistance genes can be complex. Some tomato genotypes integrating many genes from different wild species often share the same alleles for a marker. This can give false positive results (Slater *et al.*, 2013).

In the present study, one wild accession *S. corneliomulleri* 1274 was resistant to TYLCV which has not recorded any symptoms. Also, it was observed in this study that most the genotypes viz., *S. arcanum* 1346, *S. huaylasense* 1358, *S. peruvianum* 1333, *S. habrochaites* 1352 and 1739, *S. chilense* 56139, *S. corneliomulleri* 1283, *S. pimpinellifolium* 1332, and *S. pennellii* 2963 and 1942 were tolerant to the TYLCV infection. In contrast, eight tomato lines, including *S. hirsutum* 24036, *S. galapagense* 0317, *S. neoricki* 0247, *S. pennellii* 1733, *S. pimpinellifolium* 1342 and 1279, Super Marmande, and Strain B F1 were susceptible to TYLCV which showed the typical symptoms to TYLCV. These results were confirmed by amplification of 335 bp TYLCV DNA band in all of the studied tomato genotypes except *S. corneliomulleri* 1274. Similar studies were made by Chomdej *et al.*, (2007), Abdulbaset *et al.*, (2008) and Seo *et al.*, (2018) found that all genotypes of *S. lycopersicon* had shown various degrees of disease symptoms. Thus, six lines of *S. peruvianum* were resistant and remained symptomless.

In this study, five CAPS and three SCAR molecular markers tightly linked to *Ty-1*, *Ty-2*, *Ty-3* and *Mi-1.2* genes have been employed for nineteen tomato genotypes. Such data can assist plant breeders in fast screening against TYLCV resistance at the seedling stage and in the development of stable resistant lines by gene pyramiding through MAS. PCR amplification of DNA from nineteen

tomato lines and subsequent digestion by *TaqI* were performed using both JB-1 CAPS and TY-1CAPS-TG178 markers. For the JB-1CAPS marker, after restriction with *TaqI*, twelve tomato lines had a susceptible allele (*ty-1*) size of 450 bp such as *S. galapagense* 0317, *S. neoricki* 0247, *S. arcanum* 1346, *S. corneliomulleri* 1274, *S. huaylasense* 1358, *S. pimpinellifolium* 1342, 1279 and 1332, *S. habrochaites* 1739, and *S. pennellii* 1733, 2963 and 1942. Moreover, seven accessions exhibited heterozygous alleles (*Ty1/ty1*) of 450 and 500 bp including *S. hirsutum* 24036, *S. peruvianum* 1333, *S. habrochaites* 1352, *S. chilense* 56139, Super Marmande, Strain B F1 and *S. corneliomulleri* 1283. JB-1 CAPS have not discriminated between resistant and susceptible genotypes. These findings were in agreement with Prasanna *et al.*, (2015) who observed that the JB1 marker linked to TYLCV resistance *Ty-1* showed inconsistent amplification, and hence was not considered for further evaluation.

For the TY-1CAPS-TG178 marker, three genotypes showed two homozygous bands of 200 and band slightly larger than 200 bp thus conferring the presence of the dominant gene *Ty-1* such as *S. huaylasense* 1358, *S. peruvianum* 1333 and *S. corneliomulleri* 1283. These accessions appeared tolerant or resistant to TYLCV. Moreover, the other genotypes which showed three amplicons of 160, 200 and band slightly larger than 200 bp were heterozygous (*Ty1/ty1*) such as *S. arcanum* 1346, *S. corneliomulleri* 1274, and *S. pennellii* 1942. They displayed resistance or tolerance to the TYLCV infection. However, the remaining genotypes which had a recessive gene for *ty-1* showed two alleles with the molecular sizes of 200 and 160 bp. Ji *et al.*, (2007b) mentioned that *Ty-1*, which originated from *S. chilense* LA1969 accession and *Ty-1* is almost completely dominant to TYLCV. Milo, (2001) found out that resistance to TYLCV is controlled by *Ty-1* dominant gene, which has been mapped to chromosome 6.

For *Ty-2*, the two markers, TY-2CAPS-TG105A and Ty-2SCAR T0302 were used for the detection of homozygous *Ty-2/Ty-2* and *ty-2/ty-2* and heterozygous *Ty-2/ty-2* in nineteen tomato genotypes. In this study, Ty-2SCAR T0302 primer set separated the homozygous and heterozygous plants better than the TY-2CAPS-TG105 primer. Thus, the latter primer gave false positive results, when nineteen lines were evaluated. Also, this marker has not detected all the lines that have the *Ty-2* gene. In addition, TY-2CAPS-TG105 marker amplified PCR fragments from the recessive homozygous tomato such as Super Marmande, Strain B F1, *S. pimpinellifolium* 1279, 1332 and 1342, *S. peruvianum* 1333, *S. chilense* 56139, *S. galapagense* 0317, *S. neoricki* 0247 and *S. arcanum* 1346. So, the Ty-2SCAR T0302 primer has been a better marker than the TY-2CAPS-TG105 marker. These results concerning this marker are consistent with the results previously observed by Garcia *et al.*, (2007) who mentioned that the SCAR T0302 primer is a better marker than the TG105 CAPS marker, as the latter may also discover an introgression that might be linked with the *I2* gene, and this would give false positive results. Kalloo and Banerjee, (1990) found out that *Ty-2* originated from *S. habrochaites* in the resistant tomato line H24 and showed completely dominant TYLCV inheritance (Ji *et al.*,

2007b). *Ty-2* has been mapped to a 19-cM region on the long arm of chromosome 11 (Barbieri *et al.*, 2010).

In the current study, the two markers TY-3CAPS-FER-G8 and Ty3SCAR P6-25 have been used for the detection of the *Ty-3* gene. Only, co-dominant Ty3SCAR P6-25 marker distinguished between *Ty-3*, *Ty-3a*, *Ty-3b* and *ty-3* alleles. In contrast, TY-3CAPS-FER-G8 gave false positive results. Thus, all of the tested tomato lines recorded resistance to TYLCV except *S. neoricki* 0247, using TY-3CAPS-FER-G8. On the other hand, one locus of 450 bp (*Ty3/Ty3*) revealed using Ty3SCAR P6-25 primer in homozygous seven tomato accessions e.g., *S. hirsutum* 24036, *S. corneliomulleri* 1274, *S. habrochaites* 1352, *S. corneliomulleri* 1283 and *S. pennellii* 1733, 2963 and 1942. The expected 320 bp *ty3* fragment was recorded in the susceptible seven tomato genotypes such as *S. galapagense* 0317, *S. neoricki* 0247, *S. pimpinellifolium* 1342, 1279 and 1332, Super Marmande, and Strain B F1. Two alleles of 660 and 320 bp, were amplified from heterozygous lines (*Ty3b/ty3*) such as *S. arcanum* 1346 and *S. peruvianum* 1333. In addition, three heterozygous lines (*Ty3/ty3*), namely *S. huaylasense* 1358, *S. chilense* 56139, and *S. habrochaites* 1739 were easily detected by this primer which amplified two alleles of 320 and 450 bp. Moreover, there have not been any tomato lines which have the *Ty3a* gene. These results are in agreement with Neha *et al.*, (2016) and Ji *et al.*, (2007b) who used a co-dominant SCAR analysis to differentiate between the *S. lycopersicum* recessive allele *ty-3* and the *S. chilense* dominant allele *Ty-3*. Jensen Katie *et al.*, (2007) detected a new locus of introgression (*Ty-3b*) in the tomato. Mejia *et al.*, (2010) found out that *Ty-2* alone gave no resistance to TYLCV in the tomato, but pyramiding *Ty-2* and *Ty-3* together supplied a higher level of resistance better than *Ty-3* alone.

For the *Mi-1.2* locus, it was observed that MI-REXCAPS scored more accurate results than the *Mi-1.2SCARMi23* marker. Some accessions gave results with MI-REXCAPS and have not recorded any results with *Mi-1.2SCARMi23* such as *S. hirsutum* 24036, *S. neoricki* 0247, *S. corneliomulleri* 1274 and 1283, *S. huaylasense* 1358, *S. chilense* 56139, and *S. habrochaites* 1739. Furthermore, eleven heterozygous tomato lines (*Mi/mi*) displayed three alleles of 180, 570 and 750 bp, using MI-REXCAPS i.e., *S. hirsutum* 24036, *S. arcanum* 1346, *S. corneliomulleri* 1274 and 1283, *S. pennellii* 1733, *S. huaylasense* 1358, *peruvianum* 1333, *S. habrochaites* 1352 and 1739, *S. chilense* 56139, and Strain B F1. In contrast, the other eight genotypes were recessive homozygous have not digestion site by *TaqI* using the MI-REXCAPS marker. Veremis and Roberts, (2000) mentioned that resistance to whitefly or root-knot nematodes originates from wild tomatoes e.g., *S. peruvianum*, *S. arcanum*, *S. corneliomulleri* and *S. huaylasense*. The latter formerly belongs to *S. peruvianum* complex for tomato. Cortada *et al.*, (2010) reported that *S. huaylasense* accession LA1358 is a new source of whitefly or root-knot nematode resistance; this resistance can be attributed to the presence of *Mi*-genes. Firdaus *et al.*, (2012) discovered different levels of whitefly resistance in tomato wild relatives such as *S. chilense*, *S. pimpinellifolium*, *S. pennellii*, *S. habrochaites*, and *S. habrochaites* f. *glabratum*. In the current study, the MI-REXCAPS marker has been explored alternatively to the SCAR method because CAPS

detected new accessions carrying the *Mi-1.2* resistant gene to whitefly or root-knot nematode. These results were in agreement with Williamson *et al.*, (1994) who mentioned that The CAPS marker is widely applied to detect the *Mi-1.2* in the tomato, and has been reported relatively reliable. El-Mehrach *et al.*, (2005) found out that the REXCAPS marker could not be applied in tomato hybrid lines with introgressions of *S. chilense* and *S. habrochaites*.

## 5. Conclusion

In this study, CAPS and SCAR markers have been employed to detect resistance genes to TYLCV and whitefly in nineteen tomato accessions. The researchers have identified one line *S. corneliomulleri* 1274 carrying (*Ty-1*, *Ty-2*, *Ty-3*) and (*Mi-1.2*) and showing resistance to TYLCV and whitefly, respectively. In addition, ten genotypes were TYLCV tolerant carrying one or more TYLCV and whitefly resistant alleles. So, molecular markers can be applied in the breeding programs to expedite the procedures of pyramiding these resistance genes of several genotypes into a single line, hence improving the resistance to *begomoviruses*.

## References

- Abdulbaset A, Javad M and Masud B. 2008. Phenotypic and molecular screening of tomato germplasm for resistance *Tomato yellow leaf curl virus*. *Iran J Biotechnol.*, **6**:199-206.
- Allam EK, Abo El-Nasr MA, Othman BA and Thabeet SA. 1994. A new method for mechanical transmission of *Tomato Yellow Leaf Curl Virus*. *Egyptian Phytopathol. Soc.*, **7**: 91.
- Anbinder I, Reuveni M, Azari R, Paran I, Nahon S, Shlomo H, Chen L, Lapidot M and Levin I. 2009. Molecular dissection of *Tomato yellow leaf curl virus* (TYLCV) resistance in tomato line TY172 derived from *Solanum peruvianum*. *Theor Appl Genet.*, **119**(3):519-530.
- Barbieri M, Acciarri N, Sabatini E, Sardo L, Accotto GP and Pecchioni N. 2010. Introgression of resistance to two Mediterranean virus species causing *Tomato yellow leaf curl* into a valuable traditional tomato variety. *J Plant Pathol.*, **92** (2): 485-493.
- Belabess Z, Peterschmitt M, Granier M, Tahiri A, Blenzar A and Urbino C. 2016. The non-canonical *Tomato yellow leaf curl virus* recombinant that displaced its parental viruses in southern Morocco exhibits a high selective advantage in experimental conditions. *J Gen Virol.*, **97**: 3433-3445.
- Chen HM, Lin CY, Yoshida M, Hanson P and Schafleitner R. 2015. Multiplex PCR for detection of *Tomato yellow leaf curl disease* and root-knot nematode resistance genes in tomato (*Solanum lycopersicum* L.). *Inter J Plant Breeding and Genet.*, **9**(2): 44-56.
- Chomdej O, Chatchawankanpanich O, Kositratana W and Chunwongse J. 2007. Response of resistant breeding lines of tomato germplasm and their progenies with Seedathip3 to *Tomato yellow leaf curl virus*, Thailand isolate (TYLCTHV-[2]). *Songklanakarini J Sci Technol.*, **29**(6): 1469- 1477.
- Cortada L, Manzano P, Sorribas FJ, Ornat C and Verdejo-Lucas S. 2010. The resistance response of *Solanum huaylasense* spp. *Nematropica*, **40**:31-40.
- Czosnek H. (Ed.) 2007. *Tomato Yellow Leaf Curl Virus Disease: Management, Molecular Biology, Breeding for Resistance*. Springer, Berlin.

- El-Mehrach K, Chouchane SG, Mejía L, Williamson VM, Vidavski F, Hatimi A, Salus MS, Martin CT and Maxwell DP. 2005. PCR-based methods for tagging the *Mi-1* locus for resistance to root-knot nematode in begomovirus-resistant tomato germplasm. *Acta Hortic.*, **695**: 263-270.
- Feng Y, Wu Q, Wang S, Chang X, Xie W, Xu B and Zhang Y. 2010. Cross-resistance study and biochemical mechanisms of thiamethoxam resistance in B-biotype *Bemisia tabaci* (Hemiptera: Aleyrodidae). *Pest Manag Sci.*, **66**(3):313-318.
- Firdaus S, Van Heusden AW, Hidayati N, Supena EDJ., Visser RGF and Vosman B. 2012. Resistance to *Bemisia tabaci* in tomato wild relatives. *Euphytica*, **187**:31-45.
- García BE, Graham E, Jensen KS, Hanson P, Mejia L and Maxwell DP. (2007). Co-dominant SCAR marker for detection of the begomovirus-resistance *Ty2* locus derived from *Solanum habrochaites* in tomato germplasm. *Rep Tomato Genet Coop.*, **57**: 21-24.
- Geng L, Lx Q, Rx S, Yq L, Ss L and XW W. 2018. Transcriptome profiling of whitefly guts in response to *Tomato yellow leaf curl virus* infection. *Virus J.*, **15**(1):1-12.
- Hanson P, Green SK and Kuo G. 2006. *Ty2*, a gene in chromosome 11 conditioning geminivirus resistance in tomato. *Tomato Genet Coop Rep.*, **56**:17-18.
- Hanson PM, Bernacchi D, Green S, Tanksley SD, Muniyappa V, Padmaja AS, Chen H, Kuo G, Fang D and Chen J. 2000. Mapping a wild tomato introgression associated with *Tomato yellow leaf curl virus* resistance in a cultivated tomato line. *J Am Soc Hortic Sci.*, **15**:15-20.
- Jensen Katie S, Martin CT and Maxwell DP. 2007. A CAPS marker FER-G8 for detection of *Ty3* and *Ty3a* alleles associated with *S. chilense* introgression for begomovirus resistance in tomato breeding lines. University of Wisconsin, Madison. <http://www.plantpath.wisc.edu/GeminivirusResistantTomatoes/index.htm>.
- Ji Y, Schuster DJ and Scott JW. 2007a. *Ty-3*, a begomovirus resistance locus near the *Tomato yellow leaf curl virus* resistance locus *Ty-1* on chromosome 6 of tomato. *Mol Breed.*, **20**:271-284.
- Ji Y, Salus MS, Van Betteray B, Smeets J, Jensen KS, Martin CT, Mejia L, Scott JW, Havey MJ and Maxwell DP. 2007b. Co-dominant SCAR markers for detection of the *Ty-3* and *Ty-3a* loci from *Solanum chilense* at 25 cM of Chromosome 6 of tomato. *Tomato Genet Coop Rep.*, **57**:25-28.
- Ji Y, Betteray B, Smeets J, Jensen KS and Mejia L. 2008. Co-dominant SCAR marker, P6-25, for detection of *Ty-3*, *Ty-3a* and *Ty-3b* introgressions from three *Solanum chilense* accessions at 25 cM of chromosome 6 of Begomovirus-resistant tomatoes. <http://www.plantpath.wisc.edu/GeminivirusResistantTomatoes/Markers/MAS-Protocols/P6-25-locus.pdf>
- Ji Y, Scott JW and Schuster DJ. 2009. Molecular mapping of *Ty-4*, a new *Tomato yellow leaf curl virus* resistance locus on chromosome 3 of tomato. *J Am Soc Hortic Sci.*, **134**(2): 281-288.
- Kaloo G and Banerjee MK. 1990. Transfer of *Tomato leaf curl virus* resistance from *Lycopersicon hirsutum* f. *glabratum* to *L. esculentum*. *Plant Breed.*, **105**:156-159.
- Mahfouze SA, Mahfouze HA and Esmail RM. 2015. Detection of the *Mi-1.2* gene from tomato confers resistance against whitefly (*Bemisia tabaci*). *Wulfenia*, **22**(12): 136-146.
- Mahfouze SA, Saxena S, Mahfouze HA and Rajam MV. 2017. Characterization of *Mi<sub>1.2</sub>* whitefly (*Bemisia tabaci*) resistance gene. *Online J Biol Sci.*, **17**(4): 323-334.
- Maxwell DP, Martin C, Salus MS, Montes L and Mejía L. 2006. Breeding tomatoes for resistance to tomato-infecting begomoviruses. International Plant Virology Laboratory, University of Wisconsin, Madison.
- <http://www.plantpath.wisc.edu/GeminivirusResistantTomatoes/index.htm>.
- Mejía L, Teni RE, García BE, Fulladolsa AC, Méndez L, Melgar S and Maxwell DP. 2010. Preliminary observations on the effectiveness of five introgressions for resistance to begomoviruses in tomatoes. *Rept Tomato Genet Coop.*, **60**:41-53.
- Messeguer R, Ganai M, de Vicente MC, Young ND, Bolkan H and Tanksley SD, 1991. High resolution RFLP map around the root knot nematode resistance gene (*Mi*) in tomato. *Theor Applied Genet.*, **82**: 529-536.
- Michelson I, Zamir D and Czosnek H. 1994. Accumulation and translocation of *Tomato yellow leaf curl virus* (TYLCV) in a *Lycopersicon esculentum* breeding line containing the *L. chilense* TYLCV tolerance gene *Ty-1*. *Phytopathol.*, **84**: 928-933.
- Milligan SB, Bodeau J, Yaghoobi J, Kaloshian I, Zabel P and Williamson VM. 1998. The root knot nematode resistance gene *Mi* from tomato is a member of the leucine zipper, nucleotide binding, leucine-rich repeat family of plant genes. *Plant Cell*, **10**: 1307-1319.
- Milo J. 2001. The PCR-based marker REX-1, linked to the gene *Mi*, can be used as a marker to TYLCV tolerance. *Proceedings of Tomato Breeders Round Table*, Antigua.
- Neha P, Solankey SS, Vati L, and Chattopadhyay T. 2016. Molecular screening of tomato (*Solanum lycopersicum* L.) genotypes for resistance alleles against important biotic stresses. *J Appl Natural Sci.*, **8**(3): 1654 -1658.
- Nombela G, Williamson VM and Muniz M. 2003. The root-knot nematode resistance gene *Mi-1.2* of tomato is responsible for resistance against the whitefly *Bemisia tabaci*. *Mol Plant-Microbe Interact.*, **16**: 645-649.
- Peralta IE, Spooner DM and Knapp S. 2008. Taxonomy of wild tomatoes and their relatives (*Solanum* sections *Lycopersicoides*, *Juglandifolia*, *Lycopersicon*; *Solanaceae*). *Syst Bot Monogr.*, **84**:1-186.
- Pérez de Castro A, Blanca JM, Diez MJ and Nuez Viñals F. 2007. Identification of a CAPS marker tightly linked to the *Tomato yellow leaf curl disease* resistance gene *Ty-1* in tomato. *Eur J Plant Pathol.*, **117**:347-356.
- Prasanna HC, Sinha DP, Rai GK, Krishna R, Kashyap SP, Singh NK, Singh M and Malathi VG. 2015. Pyramiding *Ty-2* and *Ty-3* genes for resistance to monopartite and bipartite *Tomato leaf curl viruses* of India. *Plant Pathol.*, **64**:256-264.
- Rossi M, Goggin FL, Milligan SB, Kaloshian I, Ullman DE and Williamson VM, 1998. The nematode resistance gene *Mi* of tomato confers resistance against the potato aphid. *Proc Natl Acad Sci USA*, **95**: 9750-9754.
- Rozen S and Skaletsky H. 2000. Primer3 on the WWW for general users and for biologist programmers. *Methods Mol Biol.*, **132**: 365-386.
- Schuster DJ, Mann RS, Toapanta M, Cordero R, Thompson S, Cyman S, Shurtleff A and Morris RF. 2010. Monitoring neonicotinoid resistance in biotype B of *Bemisia tabaci* in Florida. *Pest Manag Sci.*, **66**(2):186-195.
- Scott JW. 2007. Breed for resistance to viral pathogens. In: Razdan MK, Mattoo AK (Eds.), **Genetic improvement of Solanaceous crops**. Science Publisher, Inc., Enfield, pp. 447-474.
- Seah S, Williamson VM, Garcia BE, Mejia L, Salus MS, Martin CT and Maxwell DP. 2007. Evaluation of a co-dominant SCAR marker for detection of the *Mi-1* locus for resistance to root-knot nematode in tomato germplasm. *Rep Tomato Genet Coop.*, **57**: 37-40.
- Seo JK, Kim MK, Kwak HR, Choi HS, Nam M, Choe JY, Choi B, Han SJ, Kang JH and Jung Ck. 2018. Molecular dissection of distinct symptoms induced by *Tomato chlorosis*



virus and Tomato yellow leaf curl virus based on comparative transcriptome analysis. *Virology*, 516: 1-20.

Slater AT, Cogan NO and Forster JW. 2013. Cost analysis of the application of marker-assisted selection in potato breeding. *Mol Breed.*, **32**: 299-310.

Veremis JC and Roberts PA. 2000. Diversity of heat-stable genotype specific resistance to *Meloidogyne* in Maranon races of *Lycopersicon peruvianum* complex. *Euphytica*, **111**: 9-16.

Vidavski F, Czosnek H, Gazit S, Levy D and Lapidot M. 2008. Pyramiding of genes conferring resistance to Tomato yellow leaf curl virus from different wild tomato species. *Plant Breed.*, **127**: 625-631.

Williamson VM, Ho JY, Wu FF, Miller N and Kaloshian I. 1994. A PCR-based marker tightly linked to the nematode resistance gene, *Mi*, in tomato. *Theor Appl Genet.*, **87**:757-763.

Yang X, Caro M, Hutton SF, Scott JW, Guo Y, Wang X, Rashid MH, Szinay D, de Jong H, Visser RG, Bai Y, Du Y. 2014. Fine mapping of the Tomato yellow leaf curl virus resistance gene *Ty-2* on chromosome 11 of tomato. *Mol Breed.*, **34**: 749-760.

Zamir D, Ekstein-Michelson I, Zakay Y, Navot N, Zeidan M, Sarfatti M, Eshed Y, Harel E, Pleban T, Vanoss H, Kedar N, Rabinowitch HD and Czosnek H. 1994. Mapping and introgression of a Tomato yellow leaf curl virus tolerance gene, *TY-1*. *Theor Appl Genet.*, **88**:141-146.



# Determination of the Immunogenic and Hematologic Effects of Titanium Nanoparticles Manufactured from *Aspergillus flavus* in Vivo

Mohammed N. Maaroo<sup>1,\*</sup> and Asmaa E. Mahmood<sup>2</sup>

<sup>1</sup>Department of Biology, College of Education for Pure Sciences, University of Tikrit;

<sup>2</sup>Department of Pathological Analyzes, College of Applied Sciences, Samarra University, Iraq

Received June 9, 2018; Revised July 14, 2018; Accepted August 15, 2018

## Abstract

The Titanium dioxide nanoparticles (TiO<sub>2</sub> NPs) have been synthesized via biological methods using *Aspergillus flavus*, and were subjected to numerous tests to confirm the formation of nanoparticles such as UV visible spectroscopy X-ray diffraction (XRD), Fourier transform infrared (FTIR), Atomic force microscope (AFM) and Scanning electron microscope (SEM) analysis. This study evaluates the immunogenic and hematologic effects of TiO<sub>2</sub> NPs *in vivo* in rabbit groups as treatment after infection by two pathogenic bacteria; *Escherichia coli* (G1) and *Staphylococcus aureus* (G2). A dosage of 20 mg/kg of TiO<sub>2</sub> NPs was administrated orally to the rabbit groups (G1, G2) and the results were compared with the control group (G3) which received the same dosage of TiO<sub>2</sub> NPs without any prior bacterial infection. The infected groups showed a significant reduction in the values of RBC, PCV, Hb compared with the control group (G3) and the groups (TG1, TG2, TG3) that were treated with TiO<sub>2</sub> NPs. Neutrophils percentages were higher than Lymphocytes in the infected groups compared with the control group before and after the treatment. The titers of IgG and IgM showed a significant increase in the infected animals compared with the control group and the group that was administrated TiO<sub>2</sub> NPs only. The levels of IL-10, IL-6, IFN- $\gamma$  and TNF- $\alpha$  showed a significant elevation ( $P < 0.05$ ) in the serum of infected groups (G1, G2) compared to those treated with TiO<sub>2</sub> NPs or that found in the control. The oral dosage of TiO<sub>2</sub> NPs showed no significant differences at ( $P > 0.05$ ) in group (TG3) compared with the control group (G3).

**Key words:** TiO<sub>2</sub> NPs, Hematological parameters, Immunoglobulin level, Cytokines

## 1. Introduction

According to recent studies, the effectiveness of nanoparticles has been evaluated in stimulating the immune system. Nanoparticles that target immune cells can manipulate or control the immunological diseases such as infectious diseases or tumor therapy. If the immune system cannot recognize any foreign substance as body-threatening, this substance is ignored or tolerated. Therefore, the immune response must be considered when it deals with nanoparticles within the body of the organism, (Moyano *et al.*, 2012). There are critical issues that should be highlighted in this regard; the most important of which is the immune system's rejection of nanoparticles, which the body identifies as foreign substances. The toxicity of nanoparticles should be assessed and considered, as they could introduce pathological changes to the immune system, and that would render the nanoparticles incompatible with the immune system (Boraschi *et al.*, 2012). Nanoparticles can be used as adjuvants (Li *et al.*, 2014), for example, the HIV-2 virus vaccine in mice consists of Polymethylmethacrylate (PMMA) nanoparticles which are

used as adjuvants that can enhance the response of the antibodies one hundred times higher than the conventional adjuvant aluminum hydroxide [Al(OH)<sub>3</sub>] (Stieneker *et al.*, 1991). The mechanism of nanoparticle usage as an adjuvant is not well understood, but nanoparticles are thought to improve the ingestion of antigen, or stimulate the action of antigen-presenting cells (APCs) (Dobrovolskaia and McNeil, 2007). A number of studies are carried out *in vitro* and *in vivo* focusing on the direct toxic effects, crystal phase composition, size, charge, the route of administration, and amount of dosage of TiO<sub>2</sub> NPs. These are important factors when considering TiO<sub>2</sub> NPs as a drug (Ivo Iavicoli *et al.*, 2012). The American Food and Drug Administration (FDA) has determined that TiO<sub>2</sub> NPs are non-toxic, and have been used in human food, medicine, food contact materials (Wist *et al.*, 2004). The continual resistance of microorganisms to conventional antibiotics stimulates scientific researchers to find out alternatives to them especially against the multidrug-resistant bacteria. The unique properties of TiO<sub>2</sub> NPs render them important in the pharmaceutical and medical industries (Gerhardt *et al.*, 2007). TiO<sub>2</sub> NPs have a broad spectrum of activity against microorganisms, including Gram-negative, Gram-positive and fungi as well

\* Corresponding author e-mail: : mohammednather78@yahoo.com.

(Josset *et al.*, 2008). The other prosperity is that when manipulating TiO<sub>2</sub> NPs biologically, no toxic substances will be produced. Consequently, TiO<sub>2</sub> NPs are environmental friendly (Llorens *et al.*, 2012).

## 2. Material and Methods

TiO<sub>2</sub> NPs have been synthesized from *Aspergillus flavus*. The biomass of the fungus was prepared by cultivation according to Baskar *et al.* (2013), and the synthesis of TiO<sub>2</sub> NPs was preformed according to Tarafdar *et al.* (2013). The manufactured nanoparticles were subjected to numerous tests to confirm the formation of nanoparticles such as UV visible spectroscopy ((UV-1800 series-Shimadzu/Japan), X-ray diffraction (XRD) (XRD-6000- Shimadzu/ Japan), Fourier transform infrared (FTIR) (Bruker/ Germany), atomic force microscope (AFM) (Phywe measure nano/ England), and scanning electron microscope (SEM) (Angstrom/ advanced/ USA) analysis.

### 2.1. Preparation of Bacterial Suspension

The bacterial suspension was prepared according to (Baron *et al.*, 1998), which used to induce experimental infection in rabbits.

### 2.2. Preparation of Laboratory Animals

Twelve males of local rabbits (*laguscaniculus orycto/* SDI/ Samarra) were used in this experiment. Their ages are 6 months, and their weights range from 700 to 950 g. To ensure their safety, they were examined by a specialist veterinarian, and were set under observation for seven days before the experiment, providing adequate ventilation and lighting conditions and a temperature between 23 and 25°C. The rabbits were fed the optimal formula according to (NAS-NRC, 2002). Food was provided, and the cleanliness of the cages has been observed, and sawdust was periodically changed throughout the experiment.

### 2.3. Distribution of Experimental Animals

As illustrated in Figure 1, three laboratory experiments were carried out as follows:

#### 1. First experiment: Incubation Period

In the first stage of the experiment, all the animals were incubated under the same conditions.

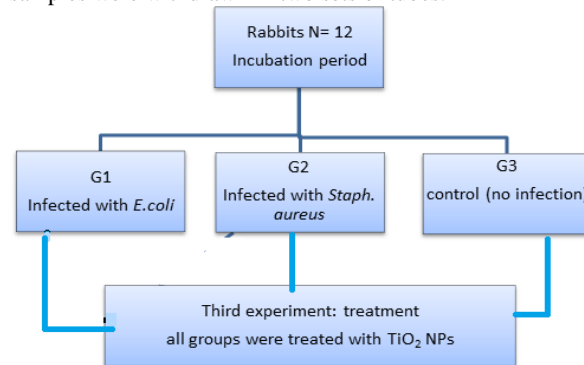
#### 2. Second experiment: Feeding

The animals were divided into three groups (each group has four animals): G1 was given the bacterial suspension of *Escherichia coli* (*E. coli*), and G2 was given a bacterial suspension of *Staphylococcus aureus* (*S. aureus*) with an amount of 1 mL per day ( $1 \times 10^8$  cell/ mL). G3 was left without being given any kind of dosage. The health status of the animals was monitored and the changes were recorded daily. Symptoms began to appear clearly on the fifth day, and were clearer on the seventh day; these include inactivity, solitude, lack of movement, lack of appetite, as well as diarrhea in the animals infected with *E. coli*, and conjunctivitis in the animals infected with *S. aureus*. All the animals have been examined by a specialist veterinarian to ascertain their infection. Blood samples were withdrawn from the animals, and these samples were dispensed in two tubes, one without EDTA for serological tests, and the

other with EDTA for hematological tests (Theml, *et al.*, 2004).

#### 3. Third Experiment: Treatment

The animals that were subjected to the infection (G1, G2) and the control group (G3) were administrated TiO<sub>2</sub> NPs with a concentration of 20 mg/ mL (Sankar *et al.*, 2013) via mouth. The health status of all animals was monitored, and the procedure continued until the complete disappearance of the disease symptoms. Again, their safety was checked by a specialist veterinarian. Then, the blood samples were withdrawn in two sets of tubes.



**Figure 1.** Illustrate the experiment design

G1: animals infected with *E. coli*; G2: animals infected with *S. aureus*; G3: control group; TG1: Infected G1 treated with TiO<sub>2</sub> NPs; TG2: Infected G2 treated with TiO<sub>2</sub> NPs; TG3: G3 treated with TiO<sub>2</sub> NPs.

### 2.4. Parameters Studies

#### 2.4.1. Hematological Parameters

Blood was withdrawn from all groups to perform the hematological tests. One mL of blood was withdrawn by cardiac puncturing using sterile medical syringes. Blood was collected in plastic tubes containing anticoagulant EDTA. The total number of white blood cells and the differential number of white blood cells (the lymphocyte and granulocyte), RBC, Hb, PCV and PLT were calculated using automation automatic analysis (Company/ Minaray BC-3000 plus/ Germany).

#### 2.4.2. Serological Parameters

Immunological tests were carried out on the serum of the rabbits to detect the presence of IL-6, IL-10, IFN- $\gamma$ , TNF- $\alpha$ , IgG and IgM in all groups. Blood was collected by cardiac puncture. 5 ml of blood was collected in plastic tubes free of anticoagulant to obtain the serum using centrifuge 3000 rpm for five minutes. The serum samples were kept at -20°C until the time of testing using (Elisa kit/ eBioscience and Abnova / UK).

## 3. Results and Discussion

### 3.1. Hematological Parameters

Only few studies have investigated the influence of TiO<sub>2</sub> NP exposure on the hematological parameters (Ivo Iavicoli *et al.*, 2012). Table 1 illustrates some of these parameters in the treated rabbit groups. The results revealed that there are many effects of *E. coli* and *S. aureus* infection in male rabbit's blood parameters. The hematological parameters in the infected groups (G1, G2)

which are administered 1 mL of *E. coli* and *S. aureus* suspension, showed significant changes ( $p < 0.05$ ) when compared with the normal control group (G3). The total white blood cells (WBC) count was found to be increased with the reduction in the total red blood cell (RBC) count, hemoglobin (Hb), PCV and PLT. The total white blood cells count in the group infected with *E. coli* and *S. aureus* reached 17.5, 16.1 ( $\times 10^3$  cell / mm<sup>3</sup>) respectively compared with 3.9 ( $\times 10^3$  cell / mm<sup>3</sup>) in the control group.

The increase in the number of white blood cells after being infected with bacteria is attributed to inflammation, which usually occurs after bacterial infections. The lipopolysaccharide (endotoxin) of gram negative and exotoxin of gram positive was found to be immunogenic and mitogenic for many immune cells such as B cells and T cells (Pulendran *et al.*, 2001; Su *et al.*, 2002). However, there were no significant changes of these parameters in the treated groups (G1 and G2) which received oral doses of 20 mg/mL of TiO<sub>2</sub> NPs compared with the control group. The results of this study agree with (Aysa, 2017).

Table 1 shows the significant reduction in the hemoglobin level ( $p < 0.05$ ) for the study groups compared with the control group; for the groups infected with *E. coli* and *S. aureus* it decreased to 9.1, 8.9 (dl/mL) respectively while for the control group it was 12.5 (dl/mL). The groups infected with *E. coli* and *S. aureus* showed a significant reduction in the percentage of PCV reaching 29.1%, 27 % respectively, compared to 41% for the control group. Also, there was a significant decrease in platelets count in the infected groups compared with the control group. This table shows that the treatment of the groups, (G1, G2), with TiO<sub>2</sub> NPs restored the number of white blood cells close to the control groups. This can be ascribed to the positive effects of these inorganic oxides in removing the harmful effects of bacteria and the recovery of the natural parameters' values. Accordingly, there was a significant decrease in the white blood cells numbers in the infected groups after being treated with TiO<sub>2</sub> NPs reaching 4.9, 4.6 ( $\times 10^3$  cell / mm<sup>3</sup>) respectively. The reason for this significant decrease in the level of Hb and PCV can be attributed to the ability of the pathogenic bacteria to produce hemolysin enzyme (Nester *et al.*, 2001). Since PCV is a measure of the volume of packed cells, the hemolysin in red blood cells leads to a decrease in their level. It can also be attributed to the bacterial infection impact on the animals' appetite and the lack of nutritional elements that are necessary for the formation of red blood cells such as minerals and vitamins. The results were consistent with those found in Al-Zamely and Shaymaa (2011) regarding the experimental infection in male rats with *E. coli* which resulted in a significant decrease in PCV and Hb compared to the control group. Also, the results showed that the treatment of the infected groups (G1 and G2) with TiO<sub>2</sub> NPs leads to a significant increase

in Hb and PCV levels. Table 1 indicates an improvement in the condition of animals and a recovery of red blood cells to their natural composition and formation of hemoglobin. This can be ascribed to the ability of TiO<sub>2</sub> NPs to control the infection in a short time, and the high oxidizing power of the free radicals that can directly destroy bacteria. TiO<sub>2</sub> NPs can inhibit the activity of ATPase which leads to the reduction of the essential ATP to sustain the bacterial cell life (Cui *et al.*, 2011).

Table 2 shows that the types of white blood cells (eosinophils, monocytes, and basophils) of G1 and G2 after infection have no significant changes in their levels when compared to the control group ( $P > 0.05$ ). The results showed that the percentages of neutrophils in the G1 and G2 were 19.0 %, 22.3 % respectively, while in the control group (G3) it was 53.3 % demonstrating a significant decrease. The Lymphocytes showed a significant increase in the percentages in G1 and G2 after infection reaching 47.6 %, 50.7 % respectively compared to the control group which reached to 22.6 %. The increased number of lymphocytes may be attributed to the infection by the two types of bacteria which stimulated the immune system to form defensive cells that caused an increase in the total number of white blood cells generally and lymphocytes particularly. These cells play an important role in immunity by secreting the chemical immunoglobulins consequently, controlling the pathogenic microorganisms (Stites, 1987). The reason behind the decrease of neutrophils is the production of leucocidin that destroys neutrophils through the lysis of the granule cytoplasm (Todar, 2004). When the bacterial infection is severe, these cells cannot resist the infection, and the body is forced to use lymphocytes as a second line of defense. After treatment with TiO<sub>2</sub> NPs, the results showed a significant increase in the neutrophils proportions at 43.0 % and 47.3% respectively compared to the proportion in the infected groups (G1 and G2) before treatment. The outcomes of the treatment resulted in the lymphocytes reduction reaching 30.3, 26.6 in G1 and G2, respectively.

The reason for the ability of the cells to recover their normal level is the action of nano-oxides in inhibiting pathogenic bacteria. The small size enables the nanoparticles to penetrate the cell membrane and to destruct it leading to loss of minerals, proteins, genetic material and finally to the cell death (Foster *et al.*, 2011). Adams *et al.*, (2006) noted that ZnO NPs can inhibit about 90 % of the Gram-positive bacteria and less than that in the case of Gram-negative bacteria. The mechanisms of cellular toxicity of nanoparticles, including ROS, increase the antioxidant system; consequently the cells enter oxidative stress that leads to the breakdown of cellular components such as lipids, proteins, and genetic material (Lovric *et al.*, 2005).

**Table 1.** Effect of TiO<sub>2</sub>NPs in some hematological parameters in infected animals.

Parameters Groups	WBC ( $\times 10^3$ cell / mm <sup>3</sup> )	PCV %	RBC ( $\times 10^3$ cell / mm <sup>3</sup> )	Hb (dl/ml)	PLT ( $\times 10^6$ cell / mm <sup>3</sup> )
infection stage					
G1	17.5 $\pm$ 1.17 a	29.1 $\pm$ 1.2 b	2.6 $\pm$ 0.35 b	9.1 $\pm$ 1.1 c	34.6 $\pm$ 14.1c
G2	16.1 $\pm$ 1.08 a	27.0 $\pm$ 2.7 b	2.5 $\pm$ 0.50 b	8.9 $\pm$ 0.4 c	28.0 $\pm$ 4.3 c
G3	3.9 $\pm$ 0.64 b	41.2 $\pm$ 4.1 a	4.8 $\pm$ 0.34 a	12.5 $\pm$ 0.8 a	253.6 $\pm$ 55.5a
treatment stage with TiO <sub>2</sub> NPs					
TG1	4.9 $\pm$ 0.50 b	37.4 $\pm$ 3.0 a	3.7 $\pm$ 0.20 a	11.7 $\pm$ 0.6ab	136.7 $\pm$ 41.6 b
TG2	4.6 $\pm$ 0.80 b	36.4 $\pm$ 1.2 a	3.4 $\pm$ 0.5 ab	10.5 $\pm$ 1. cb	123.3 $\pm$ 25.1 b
TG3	3.7 $\pm$ 1.00 b	39.1 $\pm$ 2.7 a	4.3 $\pm$ 0.9 a	11.6 $\pm$ 0.7ab	190 $\pm$ 45.8 ab

a, c: Values within columns followed by different letters differ significantly at ( $p < 0.05$ ).

**Table 2.** The effect of oral administration of TiO<sub>2</sub> NPs in the differential number of white blood cells in rabbits infected with bacteria.

Parameters Groups	Neutrophils %	Lymphocytes %	Monocytes %	Eosinophils %	Basophils %
infection stage					
G1	19.0 $\pm$ 3.6 c	47.6 $\pm$ 2.6 a	0.0 $\pm$ 0.0 a	0.0 $\pm$ 0.0 a	0.0 $\pm$ 0.0 a
G2	22.3 $\pm$ 3.0 c	50.7 $\pm$ 6 a	0.0 $\pm$ 0.0 a	0.0 $\pm$ 0.0 a	0.0 $\pm$ 0.0 a
G3	53.3 $\pm$ 4.7 a	22.6 $\pm$ 2.5 c	1.0 $\pm$ 0.0 a	0.0 $\pm$ 0.0 a	0.0 $\pm$ 0.0 a
treatment stage with TiO <sub>2</sub> NPs					
TG1	43.0 $\pm$ 3 b	30.3 $\pm$ 3.2 b	0.6 $\pm$ 0.5 a	0.0 $\pm$ 0.0 a	0.0 $\pm$ 0.0 a
TG2	47.3 $\pm$ 6.8 ab	26.6 $\pm$ 2.8 b	1.0 $\pm$ 1.0 a	0.0 $\pm$ 0.0 a	0.0 $\pm$ 0.0 a
TG3	50.6 $\pm$ 4 a b	23.6 $\pm$ 4 bc	1.0 $\pm$ 0.0 a	0.0 $\pm$ 0.0 a	0.0 $\pm$ 0.0 a

a, b: Values within columns followed by different letters differ significantly at ( $p < 0.05$ ).

### 3.2. Immunological Parameters

Table 3 demonstrates the levels of immunoglobulins; IgG, IgM that are produced as a result of the infection with pathogenic bacteria and treatment with TiO<sub>2</sub> NPs using Elisa kit. The effects of the pathogenic bacteria *E. coli* and *S. aureus* on the level of IgG and IgM are clear through the significant increase ( $P < 0.05$ ) in the titers values 10.3, 12.3 for IgG and 15.3, 13.3 for IgM in comparison to the results obtained from the samples before infection which were 6.7 and 10.3 respectively. It was found that the oral administration of TiO<sub>2</sub> NPs significantly increased the titer of IgM, and IgG in G1 and G2 respectively. Table 3 reveals that the value of IgG in G3 treated with TiO<sub>2</sub> NPs was higher than that in the control group, while IgM is the same in both groups. However, the statistical results show that there are no significant differences between G3 and TG3. The slight elevation can be attributed to different factors such as the genetic effects on the IgG levels including the immune state and environmental factors. The results concerning the elevation of the immunoglobulin might be interpreted as a beneficial host response for recovery from the injury.

**Table 3.** The effect of oral administration of TiO<sub>2</sub>NPs on immunoglobulin values in the infected animals.

Parameters Groups	IgG. mg/dl	IgM mg/dl
infection stage		
G1	10.3 $\pm$ 1.5 ab	15.3 $\pm$ 1.5 a
G2	12.3 $\pm$ 2.3 a	13.3 $\pm$ 1.4 ab
G3	6.7 $\pm$ 0.5 c	10.3 $\pm$ 1.5 c
treatment stage with TiO <sub>2</sub> NPs		
G1T	11.0 $\pm$ 1.0 ab	11.0 $\pm$ 1.0 bc
G2 T	10.6 $\pm$ 1.5 ab	10.0 $\pm$ 2.0 c
G3 T	9.0 $\pm$ 1.0 bc	10.0 $\pm$ 1.0 c

a, c: Values within columns followed by different letters differ significantly at ( $p < 0.05$ ).

The treatment of animals with TiO<sub>2</sub> NPs showed lower levels of TNF- $\alpha$  and IL-6 in the control group (G3) and in the pre samples that were collected before the beginning of the experiment compared with G1 and G2 before treatment with TiO<sub>2</sub> NPs (Table 4). For cytokines TNF- $\alpha$  and IL-6, high expression levels were observed in rabbits seven days following the bacterial infection. Thus seven days post-infection, the TNF- $\alpha$  was 11.0, 11.2 pg/mL in the infected groups (G1 and G2) respectively, while IL-6 level was 31.6, 27.6 pg/mL in the same groups. Under such conditions, feeding the infected animals with TiO<sub>2</sub> NPs can reduce the expression level of both cytokines (TNF- $\alpha$ , IL-6) significantly, and enhance the anti-inflammatory cytokines that could reduce the inflammatory response of animals (Chih-Yuan *et al.*, 2013). A recent study (Rossi *et al.*, 2010) demonstrated that, in ovalbumin-sensitized mice, silica, coated rutile TiO<sub>2</sub> NP inhalation decreased TNF- $\alpha$  and IL-13 expression in spleen cells. The results of the present study show a significant increase in the IL-10

concentration ( $P < 0.05$ ) 32.4, 31.1 pg/ mL for the G1 and G2 after infection compared with 18.3 pg/ mL values obtained from control group (G3) before infection. These results are similar to those obtained by Moore *et al.* (2002) and Yoshida *et al.* (2001) who indicated that the level of IL-10 increased in rats injected with *K. pnemaniae*. The IL-10 is characterized by an immunological regulation that includes positive and negative effects. As shown in Table 4, the level of IFN- $\gamma$  significantly increased in the infected groups (G1, G2) compared to the control group (G3). This finding agrees with the results of (AL-Refaei, 2016) who found that the concentration rate of the IFN- $\gamma$  in serum after the injection with (O), and (K) antigen of *K. pneumoniae* was elevated in the experimental animals. When all groups are treated with TiO<sub>2</sub> NP, the level of IFN- $\gamma$  significantly decreased to be closer to the value of the control group. IFN- $\gamma$  is an immune regulator of macrophages and T and B cells (Talaro, 2012).

**Table 4.** The effect of oral administration of TiO<sub>2</sub>NPs in some levels of cytokines in the infected animals.

Parameters	IL-6 pg/mL	IL-10 pg/mL	IFN- $\gamma$ pg/mL	TNF- $\alpha$ pg/mL
Groups				
Infection stage				
G1	31.6 $\pm$ 3.2a	32.4 $\pm$ 3a	53.0 $\pm$ 8.1a	11.0 $\pm$ 1.0 a
G2	27.6 $\pm$ 3.7a	31.1 $\pm$ 4.1a	46.3 $\pm$ 3.2 a	11.2 $\pm$ 0.6 a
G3	2.9 $\pm$ 0.6 b	18.3 $\pm$ 1.5c	28.3 $\pm$ 1.5c	1.26 $\pm$ 0.25d
treatment stage with TiO <sub>2</sub> NPs				
TG1	5.8 $\pm$ 1.5 b	27.6 $\pm$ 4.9 ab	37.0 $\pm$ 3b	6.4 $\pm$ 0.5b
TG2	4.8 $\pm$ 0.3 b	24.0 $\pm$ 4.5 bc	36.3 $\pm$ 2.8b	4.8 $\pm$ 0.3c
TG3	1.8 $\pm$ 0.3 b	22.3 $\pm$ 2.5 bc	32.0 $\pm$ 3.6bc	1.8 $\pm$ 0.3d

a,d: Values within columns followed by different letters differ significantly at ( $P < 0.05$ ).

#### 4. Conclusion

The laboratory animals that have been infected with pathogenic bacteria and treated with TiO<sub>2</sub> NPs showed improvement in the values of hematological and immunological parameters in addition to the significant restore of the rates of white blood cells, lymphocytes, and granules after treatment with TiO<sub>2</sub> NPs. Also, the results indicate stimulating the immune response of immunoglobulins by increasing the value of IgG and IgM in the rabbits treated with TiO<sub>2</sub> NPs. Cytokines showed different levels of cellular interleukins, IFN- $\gamma$  and TNF- $\alpha$ .

#### Acknowledgements

This work was supported by the Department of Pathological Analysis/ College of Applied Sciences/ University of Samarra.

#### References

Adams LK, Lyon DY and Alvarez PJJ. 2006. Comparative ecotoxicity of nanoscale TiO<sub>2</sub>, SiO<sub>2</sub>, and ZnO water suspensions. *Water Res.*, **40** (19): 3527–3532.

AL-Refaei, OMS. 2016. Effect some antigens of *Klebsiella pneumoniae* as a immune catalyzer for laboratory rabbits against infected by *Entamoeba histolytica*. Ph.D thesis. College of Education for pure Science. University of Tikrit.

Al-Zamely H. and Shaymaa Z. 2011. The effect of experimental *Escherichia coli* infection on some blood parameters and histological changes in male rats. *Iraqi J. Vet. Med.* **35** (2): 22 – 27.

Aysa AHA. 2017. Detection the Inhibition Activity of Some Oxides Nanoparticals and Fruits of Graviola *Annona muricata* Against Some Bacterial Species Isolated from Different Sources of Infections. PH.D thesis. College of Science. University of Tikrit.

Baron EJ, Peterson LR and Feingold SM. 1998. **Diagnostic Microbiology**. "15<sup>th</sup> ed". The C.V. Moisyby Co. Toronto. Canada.

Baskar G, Chandhuru J, Sheraz Fahad K and Praveen AS. 2013. Mycological synthesis, characterization and antifungal activity of zinc oxide nanoparticles, *Asian J Pharm Tech.*, **3** (4):142-146.

Boraschi D, Costantino L, and Italiani P. 2012. Interaction of nanoparticles with immunocompetent cells: nanosafety considerations, *Nanomedicine (London)*, **7**(1): 121–131.

Chih-Yuan Chen, Hau-Yang Tsen, Chun-Li Lin, Chien-Ku Lin, Li-Tsen Chuang, Chin-Shuh Chen and Yu-Cheng Chiang. 2013. Enhancement of the immune response against Salmonella infection of mice by heat-killed multispecies combinations of lactic acid bacteria. *J Med Microbiol.*, **62**: 1657–1664

Cui Y, Liu H, Zhou M, Duan Y, Li N, Gong X, Hu R, Hong M and Hong F. 2011. Signaling pathway of inflammatory responses in the mouse liver caused by TiO<sub>2</sub> nanoparticles. *J Biomed Mater Res A.*, **96**: 221-229.

Dobrovolskaia MA and McNeil SE .2007. Immunological properties of engineered nanomaterials. *Nat Nanotechnol.*, **2**: 469-78

Foster HA, Ditta IB, Varghese S and Steele A. 2011. Photocatalytic disinfection using titanium dioxide: spectrum and mechanism of antimicrobial activity. *Appl Microbiol Biotechnol.*, **90**: 1847–1868.

Gerhardt LC, Jell GMR and Boccaccini AR. 2007. Titanium dioxide (TiO<sub>2</sub>) nanoparticles filled poly (D,L lactic acid) (PDLLA) matrix composites for bone tissue engineering, *J Mater Sci: Mater Med.* **95**: 69–80.

Ivo Iavicoli I, Leso V and Bergamaschi A. 2012. Toxicological effects of titanium dioxide nanoparticles: A Review of *In Vivo* studies. *J Nanomaterials*, Article ID 964381, 36.

Josset S, Keller N, Lett MC, Ledoux MJ and Keller V. 2008. Numeration methods for targeting photoactive materials in the UV-A photocatalytic removal of microorganisms. *Chem Soc Rev.*, **37**:744–755.

Li X, Aldayel AM and Cui Z. 2014. Aluminum hydroxide nanoparticles show a stronger vaccine adjuvant activity than traditional aluminum hydroxide microparticles. *J Control Release*, **173**:148-157.

Llorens A, Lloret E, Picouet PA, Trbjevich R and Fernáandez A. 2012. Metallic-based micro and nanocomposites in food contact materials and active food packaging. *Trends Food Sci. Technol.*, **24**: 19–29.

Lovric J, Cho SJ, Winnik FM and Maysinger D. 2005. Unmodified cadmium telluride quantum dots induce reactive oxygen species formation leading to multiple organelle damage and cell death. *Chem Biol.*, **12**:1227-34.

- Moore TA, Perry ML, Getsoian AG, Newstead MW, Standiford TJ. 2002. Divergent role of gamma interferon in a murine model of pulmonary versus systemic *Klebsiella pneumoniae* infection. *Infect Immun.*, **70**: 116310-631.
- Moyano DF, Goldsmith M, Solfiell DJ, Landesman-Milo D, Miranda OR, Peer D and Rotello VM. 2012. Nanoparticle hydrophobicity dictates immune response. *JACS.*, **134** (9): 3965–3967.
- National Research Council Recommended (NAS-NRC). 2002. **Dietary Allowance**. 15<sup>th</sup> Ed Washington D.C.
- Nester EW, Anderson DG, Roberts CE, Pearsall NN and Nestor MT. 2001. **Microbiology a Human Perspective**, 3<sup>rd</sup> Ed. McGraw-Hill Higher Education., PP. 295-512, 691-712.
- Pulendran B, Kumar P, Cutler CW, Mohamadzahe M, VanDyke T and Banchereau J. 2001. Lipopolysaccharide from distinct pathogens induce different classes of immune response *in vivo*. *J Immunol.*, **167** (9): 5067-5076.
- Rossi, E., Pylkkanen, L., Koivisto, A., Nykasenoja, H., Wolff, H., Savolainen, K. and Alenius, H. 2010. Inhalation exposure to nanosized and fine TiO<sub>2</sub> particles inhibits features of allergic asthma in a murine model. *Particle and Fibre Toxicol.*, **7**: 35.
- Sankar R, Dhivya R, Ravikumar V. 2013. Wound healing activity of *Origanum vulgare* engineered titanium dioxide nanoparticles in Wistar Albino rats. *J Mater Sci: Mater Med*. DOI 10.1007/s10856-014-5193-5.
- Stieneker F, Kreuter J and Löwer J. 1991. High antibody titres in mice with polymethyl methacrylate nanoparticles as adjuvant for HIV vaccines. *AIDS*, **5**:431-5.
- Stites DP. 1987. **Basic and Clinical Immunology**. 6<sup>th</sup> Ed. Apleton and Lange, San Francisco.
- Su L, Goyert SM, Fan M, Aminlari A, Gong KQ, Klein RD, Myc A, Alarcon WH, Steintraesser L, Remick DG and Wang SC. 2002. Activation of human and mouse Kupffer cells by lipopolysaccharide is mediated by CD14. *Am J Physiol Gastrointest Liver physiol*, **283**(3): 640-645.
- Talaro, KP. 2012. **Foundation in Microbiology Basic Principles**. 8<sup>th</sup> Ed. McGraw Hill.
- Tarafdar A, Raliya R, Wei-Ning W, Biswas P and Tarafdar JC. 2013. Green synthesis of TiO nanoparticle using, *Aspergillus tubingensis*. *Adv Sci Eng Med.*, **5**: 1–7.
- Thieml H, Diem H and Haeflrich T 2004. **Color Atlas of Hematology, Practical Microscopic and Clinical Diagnosis**. 2nd revised Ed., Stuttgart. New York.
- Todar K. 2004. **Text book of Bacteriology** University of Wisconsin -Madison, Department of Bacteriology. U. S. A.
- Wist J, Sanabria J, Dierolf C, Torres W and Pulgarin . 2004. Evaluation of photocatalytic disinfection of crude water for drinking water production . *J Photochem. Photobiol A, Chem.*, **147**: 241-246.
- Yoshida K, Tetsuya M, Kazuhiro T, Kou U, Shiro T and Keizo Y. 2001. Induction of interleukin-10 and down regulation of cytokine production by *Klebsiella pneumoniae* capsule in mice with pulmonary infection. *J Med Microbiol.*, **50**:456-461.



# Isolation of Blood Group Non-specific Lectin from *Calotropis gigantea* Seeds

Vishwanath B. Chachadi\*

Department of Biochemistry, Karnatak University, Dharwad-580 003; India

Received July 18, 2018; Revised August 12, 2018; Accepted August 15, 2018

## Abstract

An altered expression of glycans on the cell surface can act as a marker of various diseases including cancer and AIDS. The identification of these altered glycans can be easily achieved by using glycan binding proteins, specifically antibodies and lectins. Identifying lectins, specific towards carbohydrates that are markers of various diseases will help towards an early diagnosis of diseases. The present study describes the isolation, carbohydrate specificity, and heat stability of lectin from the *Calotropis gigantea* seeds. *Calotropis gigantea* lectin (CGL), showed a blood group non-specificity strongly inhibited by glycans of mucin glycoprotein. The Ammonium sulphate precipitation of *Calotropis gigantea* crude extract results in the concentration of hemagglutination activity at 30-60 % saturation. Lectin retained its activity when exposed to as high as 50°C for one hour. Since *Calotropis gigantea* is commonly used as a medicinal plant, lectin from this plant may have haematological applications and can be used in the purification of glycoproteins.

**Keywords:** Lectins, Glycans, Hemagglutination, *Calotropis gigantea*, Hapten

## 1. Introduction

Various key biological processes including cell-cell interactions, cell migration, and induction of apoptosis, molecular trafficking, receptor activation, signal transduction and endocytosis are invariably mediated by carbohydrate ligands (Zeng *et al.*, 2012). Understanding the qualitative as well as quantitative expression of these glycans which tend to change at various conditions of cell, can provide useful information on whether the cell is normal or diseased along with their mechanisms. Among different molecules that recognize carbohydrates both in qualitative and quantitative manners are lectins (Sharon and Lis, 2004). Lectins are the carbohydrate binding proteins of a non-immune origin which recognize glycans that are specifically either expressed on cell surface or free in solutions. This glycan recognition property of lectins has been exploited in different fields of life sciences (Sharon and Lis, 2004). Some lectins bind specifically to tumor-associated carbohydrates, and therefore have the potential to serve as biomarkers to differentiate between normal and cancerous conditions of mammalian cells. Many of these specific glycans are considered as disease markers and are targets for diagnosis as well as for therapeutics (Brockhausen, 2006). Lectins from plant sources were the first proteins of this class to be studied, and to date most of the lectins studied so far are mainly from plant sources. Since the discovery of the first lectin from castor bean by Stillmark in 1888, many lectins from almost all parts of plants have been reported (Van Damme EJ, 2014). Although numerous plant lectins have been

studied for their great structural detail, the physiological role of these proteins is still poorly understood. Recently, there are many speculated roles for plant lectins 'as storage proteins', and 'as defense molecules', in symbiosis that have been assigned. A number of lectins have been isolated from storage tissues in plants (seeds or vegetative storage tissues) where they make for a very large proportion of the total protein content in the tissue (Van Damme *et al.*, 1995). Some plant lectins have been implicated in the defense mechanism of plants (Bellande *et al.*, 2017). In contrast, some plant lectins are involved in the cell wall extension and recognition (Ghequire *et al.*, 2012).

Considering the application of lectins in various fields such as immunology (Ashraf and Khan, 2003), cancer biology (Gastman *et al.*, 2004), microbiology (Oppenheimer *et al.*, 2008), insect biology (Fitches *et al.*, 2010), the current research is conducted to screen lectin activity in various plant sources. The study describes the, isolation and partial purification of lectin from *Calotropis gigantea* and its carbohydrate specificity.

## 2. Materials and Methods

*Calotropis gigantea* seeds were collected during March month from botanical garden, Karnatak University, Dharwad. Seeds were separated and used for lectin extraction, EDTA, Trypsin, Bovine serum albumin (BSA), Ammonium sulphate, Folin-Ciocalteu reagent, Sodium dodecyl sulfate, Acrylamide, N,N1-Methylene-bis-acrylamide, N,N,N1,N1-tetra methyl ethylene diamine (TEMED), and Commassie brilliant blue were from either

\* Corresponding author e-mail: vish2879@gmail.com.

Sisco Research Laboratory or from Himedia Laboratory, India. Sugars used for hapten inhibition studies were from Sigma Chemicals, USA. All other chemicals, plastic wares, glassware are of analytical grade unless they are specified with company names.

### 2.1. Extraction of Lectin from *Calotropis gigantea* Seeds

To extract lectin, *Calotropis gigantea* seeds were collected, washed with distilled water and dried. Next, the seeds were homogenized (5 gm in 25 mL) using mortar and pestle at room temperature with phosphate buffered saline (pH 7.2; 100 mM), containing 200 mM EDTA and 200 mM PMSF (Phenylmethylsulphonyl fluoride). The extraction procedure was carried out for overnight at 4°C. The extract was filtered through muslin cloth and was clarified by centrifugation at 8000 rpm for fifteen minutes at 4°C. The supernatant was stored at 4°C till further analysis. A similar procedure was also adopted for other plant seeds.

### 2.2. Preparation of Trypsinized Erythrocytes

Human blood of different blood groups (A, B and O) was collected in 1 mL of 4 % sodium citrate solution. The erythrocytes were separated by centrifugation at 1500 rpm for five minutes. Erythrocytes were washed three times with saline and finally in PBS, and were adjusted to an OD of 2.5 at 660 nm. The total volume was measured, and a final concentration of 0.025 % trypsin was added and incubated at 37 °C for one hour. The excess trypsin was removed by repeated washing in saline and was finally adjusted to OD 3.5 at 660 nm and used for hemagglutination assay and inhibition assays.

### 2.3. Hemagglutination Assay (HA)

To perform the hemagglutination assay, U-bottom 96-well micro titer plates were used. Initially, 50 µl of saline was added to all the wells of respective rows. Next, to the first well of each row, 50 µl of assay solution was added and 2-fold serial dilution was made up to the 11<sup>th</sup> well. From the 11<sup>th</sup> well, 50 µl was discarded. Trypsinized erythrocytes of each blood groups were added (50 µl per well) to each row in the plate. For each blood group and sample, the wells containing only saline and erythrocytes were included as negative controls. The plates were incubated at room temperature for one hour and visualized. The plates were photographed, and the geometric mean titers (GMTs) were calculated. The highest dilution of the extract causing visible agglutination was arbitrarily considered as the "titer", and the lowest concentration of the protein required for hemagglutination was considered as the "Minimum Concentration of Agglutinin" (MCA) which equals one unit of hemagglutinating activity (1 HAU). The specific activity of hemagglutination was expressed as activity in 1 mg of (unit mg<sup>-1</sup>) protein.

### 2.4. Hapten Inhibition Assay

Inhibition assays were carried out by incubating the lectin sample in serially diluted sugar/glycoproteins prior to the addition of erythrocytes in 25 µl of assay solution. The lowest concentration of the sugar/glycoprotein, which inhibited the agglutination, was taken as the inhibitory titre of the hapten. To the 10<sup>th</sup> well, saline is added instead of sugar/glycoproteins solutions, while in 11<sup>th</sup> well, saline is added instead of lectin. These wells served as both positive

and negative controls respectively for inhibition studies. The 12<sup>th</sup> well served as the regular control which had received only 50 µL of saline and erythrocyte suspension. The wells were mixed and incubated for one hour at room temperature, and then 50 µL of erythrocyte suspension was added and incubated further for one hour at room temperature. Finally, Inhibition of lectin activity was visualized and photographed as described earlier, and the minimum inhibitory concentration (MIC) which is defined as "the lowest concentration of the sugar/glycoprotein, which inhibited the agglutination" was determined for each sugars/glycoprotein.

### 2.5. Effect of pH

In order to know the optimum pH for lectin activity, lectin was extracted in different buffers with varied pH. For extraction, the same procedure was followed as described above containing appropriate protease inhibitors and sodium chloride. Various buffer systems used for obtaining the desired pH are sodium acetate (pH 4.0), phosphate buffer (pH 7.2), and carbonate buffer (pH 9.5). After extraction, the clear extract was used to determine the lectin activity using trypsinized erythrocytes.

### 2.6. Ammonium Sulphate Precipitation

The crude extract was subjected to 0-30, 30-60 and 60-90 % ammonium sulfate [(NH<sub>4</sub>)<sub>2</sub>SO<sub>4</sub>] precipitation. Ammonium sulfate was added at room temperature and the precipitated proteins were separated by centrifugation at 8000 rpm for thirty minutes. The supernatant was saved while the precipitate (residue) was re-dissolved in 2 mL of PBS. Both the precipitate and the supernatant were extensively dialyzed against PBS, and the hemagglutination activity was determined in all fractions.

### 2.7. SDS-PAGE

Protein samples from the crude extract, and ammonium sulfate precipitations were separated on 15 % acrylamide gel. The protein sample was treated with 6x SDS buffer and boiled for five minutes at 100°C. The cooled protein was loaded into the wells, and electrophoresed at 80 V for four hours. After completion of electrophoresis, the gels were stained with Coomassie brilliant blue R-250. A standard molecular weight protein ladder ranging from 14.3-97.4 kDa was also processed and electrophoresed under similar conditions.

### 2.8. Protein Estimation

The protein content in various steps including crude extracts was estimated according to the protocol described by Lowry et al., (Lowery *et al.*, 1951).

## 3. Results

Among different plant seeds, only seeds of *Calotropis gigantea* exhibited highest hemagglutination activity (Titre-16) as determined by serial two-fold dilution technique using rabbit erythrocytes (Table 1). Apart from *Calotropis gigantea*, seeds of *Lantana camara* has also exhibited hemagglutination activity but with lower titer (04). Since maximum hemagglutination activity was observed in *Calotropis gigantea* plant, further studies were carried out using this plant for lectin isolation, hapten inhibition assay etc.




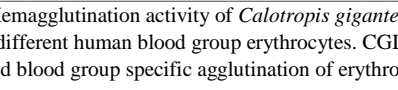
**Table 1.** Hemagglutination activity in different plant seeds

Sl No.	Plant name	Activity titer*	Protein conc. (mg/mL)	Specific activity
1	<i>Chenopodium album</i>	-	1.18	
2	<i>Lantana camara</i>	04	2.76	029
3	<i>Barnyard grass</i>	-	1.09	-
4	<i>Calotropis gigantea</i>	16	4.10	312
5	<i>Parthenium hysterophorus</i>	-	0.98	-
6	<i>Chromolaena odorata</i>	-	0.66	-

\*Hemagglutination activity was determined using rabbit erythrocytes

### 3.1. *Calotropis gigantea* lectin (CGL) did not discriminate human blood group erythrocytes.

Since lectin agglutinated rabbit erythrocytes, A, B, and O human blood group erythrocytes were used for the assay. It was found that CGL did not discriminate between A, B, and O blood group erythrocytes. However, lectin did bind with varied intensity, and recognized the "O" blood group erythrocytes with the maximum titer (64) and the "B" blood group erythrocytes with the least titer (08). These results are presented in Figure 1. For further studies, blood group O erythrocytes were used and maximum activity was obtained with these RBCs.

Blood group		Titre
Rabbit		16
A (+ve)		16
B (+ve)		08
O (+ve)		64

**Figure 1.** Hemagglutination activity of *Calotropis gigantea* lectin with different human blood group erythrocytes. CGL did not exhibit blood group specific agglutination of erythrocytes.

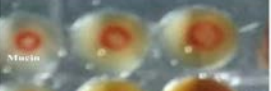



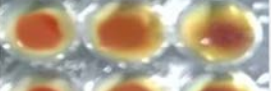

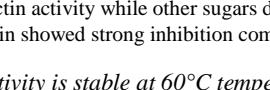
### 3.2. CGL lectin is strongly inhibited by glycans of mucin glycoproteins.

To determine the carbohydrate specificity of lectin, various monosaccharides, disaccharides and glycoproteins were used to perform hapten inhibition assay. The list of different sugars and glycoproteins used for this assay is given in table 2. As presented in Figure 2, hemagglutination activity of CGL lectin was strongly inhibited by mucin followed by fetuin. The lectin activity was not inhibited by any of the monosaccharides and disaccharides tested. These results indicate that lectin is not specific for simple sugars but recognizes complex sugars that are present in mucin or fetuin glycoproteins. This could be another reason why this lectin is blood group non-specific in nature.

**Table 2.** Sugars/glycoproteins used for hapten inhibition assay

Sl No.	Sugars/Glycoprotein	Inhibition	MIC*
1	Glucose (200 mM)	No	---
2	Galactose (200 mM)	No	---
3	Mannose (200 mM)	No	---
4	Xylose (200 mM)	No	---
5	Arabinose (200 mM)	No	---
6	D-Fucose (200 mM)	No	---
7	Lactose (200 mM)	No	---
8	Glucosamine (200 mM)	No	---
9	Mucin (1 mg/mL)	Yes	3.12 µg
10	Fetuin (1 mg/mL)	Yes	12.5 µg

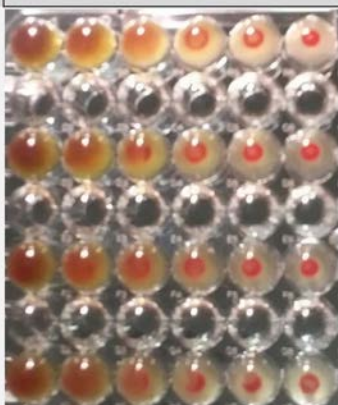


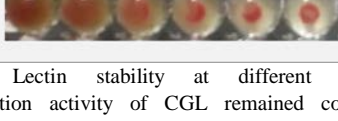
Minimum inhibitory concentration (MIC)

Sugars		MIC
Mucin		3.125 µg
Fetuin		12.50 µg
Lactose		
Maltose		
Glucose		
Galactose		
Arabinose		

**Figure 2.** Hapten inhibition assay of CGL. Mucin and fetuin inhibited the lectin activity while other sugars did not show any inhibition. Mucin showed strong inhibition compared to fetuin.

### 3.3. Lectin activity is stable at 60°C temperature.


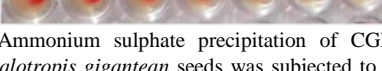
In order to determine the stability of lectin activity over different temperature, lectin was extracted and incubated at different temperature for one hour, and then, the hemagglutination activity was determined. As depicted in Figure. 3, lectin exhibited steady stability in its activity from 40°C-60°C. Although the titer decreased in 40°C-60°C treatments, but the same activity remained for several days. This may be attributed by the inactivation of proteases that are present in the extract. Furthermore, lectin activity was also stable for at least seven days, when it was kept at room temperature.

Treatment		Titre
RT		16
40°C		16
50°C		08
60°C		08

**Figure 3.** Lectin stability at different temperature. Hemagglutination activity of CGL remained constant after exposing lectin to different temperature for 1 h. Lectin also exhibited sustained stability at room temperature even after seven days.

### 3.4. Maximum hemagglutination activity of CGL was found in 30-60 % of ammonium sulphate saturation.

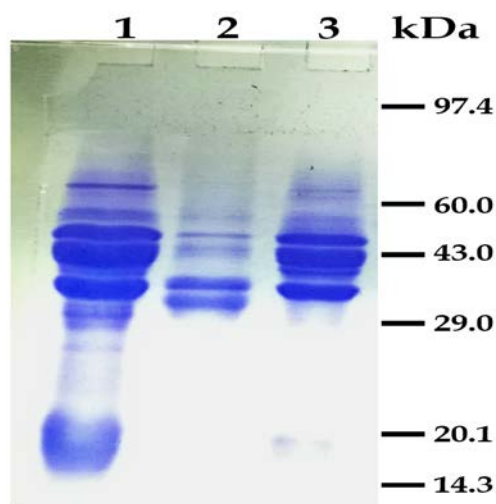
Next, ammonium sulphate precipitation of crude extract was performed to fractionate the proteins. The results of ammonium sulphate precipitation are presented in Figure 4. The results indicate that lectin concentration has increased in 30-60 % of ammonium sulphate precipitated fraction as evidenced by increased hemagglutination activity (titre-64). It is evident from Figure. 4 that some of the contaminated proteins can be removed by this step. Fraction 0-30 % showed some hemagglutination activity with titer 08. This may be attributed by the residual presence of lectin in this fraction. Although a good quantity of proteins was precipitated in 60-80 % fraction, but it did not show any hemagglutination activity.

Amm. Sul pptn		Titre
0-30 %		08
30-60 %		64
60-80 %		-

**Figure 4.** Ammonium sulphate precipitation of CGL. Crude extract of *Calotropis gigantean* seeds was subjected to 0-30, 30-60 and 60-80% saturation of ammonium sulphate. Lectin activity was mainly concentrated in 30-60% fraction.

### 3.5. SDS-PAGE analysis of partially purified lectin.

SDS-Polyacrylamide gel electrophoresis of crude and ammonium sulphate precipitated fractions was performed to analyze the number of proteins present in the samples. As shown in Figure 5, after 30-60 % of ammonium sulphate precipitation, the number of protein bands was reduced significantly (Lane-3) compared to the crude sample (Lane-1). The common protein bands that are present in all the fractions are near the molecular weight ranging from 40 to 50 kDa. These could be the protein bands which may be associated with lectin activity.



**Figure 5.** SDS-PAGE analysis of proteins precipitated from *Calotropis gigantean* crude extract. Common bands that are present in crude extract (lane-1), 0-30% (lane-2) and 30-60% (lane-3) ammonium sulphate precipitated proteins are closely associated with molecular weight from 40 to 50 kDa.

### 3.6. Fold purification of lectin.

Since lectin activity was increased in ammonium sulphate precipitated fraction, fold increase in purification of lectin was calculated based on a specific activity present in each step. Table 3 summarizes the fold purification of lectin in each step. In accordance with SDS-PAGE, it is clear from table 3 that there is a removal of some of the contaminated proteins in 30-60 % of ammonium sulphate fraction as evidenced by the increase in specific activity by 5.7-fold.

**Table 3.** Fold change in hemagglutination activity of CGL after ammonium sulphate fractionation.

Sl No.	Steps	Activity (titer)	Protein Conc. (mg/mL)	MCA (µg)	Specific Activity (HAU)	Fold change in activity
1	Crude	64	4.10	3.203	312	1.00
2	0-30%	08	1.07	6.687	149	0.47
3	30-60%	64	0.72	0.563	1776	5.70

## 4. Discussion

In the current study, the presence of lectin activity was screened in many plant sources. It was found that the seeds of *Calotropis gigantean* exhibited maximum lectin activity with all the human blood group erythrocytes. *Calotropis gigantean* plant is widely used as a medicinal plant (Kadiyala *et al.*, 2013), therefore, the researchers carried out a detailed study on the seeds of this plant to isolate and purify lectin.

Since the crude extract of *Calotropis gigantean* did not agglutinate any of the human blood group erythrocytes specifically, it was assumed that lectin probably recognizes complex sugars that are present on the cell surface of erythrocytes. This prediction was confirmed by hapten inhibition assay which revealed that lectin indeed exhibited specificity towards O-linked glycans of mucin and fetuin. These results are inconsistent with the blood group non-specificity of lectin.

In order to know the stability of lectin, the lectin extract was exposed to different temperatures and it was found that lectin is stable up to 60°C and when it was kept at room temperature for more than seven days. This result suggested that lectin is less prone to protease attack making it easy to operate during purification procedures. Many lectins are heat-labile (Devi *et al.*, 2011); however, CGL did not denature at high temperature. Ammonium sulphate fractionation not only increased the lectin concentration. In addition, it has also helped to remove most of the contaminated proteins that are present in the crude extract. The electrophoretic pattern of crude and ammonium sulphate precipitated proteins revealed that bands below 30 kDa are effectively removed during the ammonium sulphate precipitation step.

## 5. Conclusion

The current study describes the isolation and partial purification of lectin from *Calotropis gigantea* seeds and its carbohydrate specificity. Given the fact that *Calotropis gigantea* is regularly used as a medicinal plant, the presence of lectin activity may have implication in its medicinal properties. Furthermore, the results of the ammonium sulphate precipitation and SDS-PAGE steps provide important information that this lectin could be purified to homogeneity by employing these steps coupled with other chromatographic techniques.

## References

- Ashraf MT and Khan RH. 2003. Mitogenic lectins. *Med Sci Monit.* **9**(11): 265-269.
- Bellande K, Bono J-J, Savelli B, Jamet E and Canut H. 2017. Plant lectins and lectin receptor-like kinases: How do they sense the outside? *Inter J Mol Sci.* **18**(6):1164
- Brockhausen I. 2006. Mucin-type O-glycans in human colon and breast cancer: glycodynamics and functions. *EMBO Reports*, **7**(6): 599-604.
- Devi SK, Singh SS, Singh SJ, Rully H and Singh LR. 2011. Purification and characterization of a magnesium ion requiring N-acetyl-D-glucosamine specific lectin from seeds of *Quercus ilex* L. *Biosci, Biotechnol, Biochem.*, **75**(9): 1752-1757.
- Fitches EC, Bell HA, Powell ME, Back E, Sargiotti C, Weaver RJ and Gatehouse JA. 2010. Insecticidal activity of scorpion toxin (ButaIT) and snowdrop lectin (GNA) containing fusion proteins towards pest species of different orders. *Pest Management Sci.*, **66**(1): 74-83.
- Gastman B, Wang K, Han J, Zhu Z, Huang X, Wang G-Q, Rabinowich H and Gorelik E. 2004. A novel apoptotic pathway as defined by lectin cellular initiation. *Biochem Biophys Res Commun.*, **316**(1): 263-271.
- Ghequire MGK, Loris R and De Mot R. 2012. MMBL proteins: from lectin to bacteriocin. *Biochem Soc Trans.*, **40**(6): 1553-1559.
- Kadiyala M, Ponnusankar S and Elango K. 2013. *Calotropis gigantea* (L.) R. Br (Apocynaceae): a phytochemical and pharmacological review, *J Ethnopharmacol.* **150**(1): 32-50.
- Lowry OH, Rosebrough NJ, Farr AI and Randall RJ. 1951. Protein measurement with the Folin phenol reagent. *J Biol Chem.* **193**(1): 265-275.
- Oppenheimer SB, Alvarez M and Nnoli J. 2008. Carbohydrate-based experimental therapeutics for cancer, HIV/AIDS and other diseases. *Acta Histochemica*, **110**(1): 6-13.
- Sharon N and Lis H. 2004. History of lectins: from hemagglutinins to biological recognition molecules. *Glycobiol.* **14**(11): 53R-62R.
- Van Damme EJ, Goossens K, Smeets K, Van Leuven F, Verhaert P and Peumans WJ. 1995. The major tuber storage protein of araceae species is a lectin. Characterization and molecular cloning of the lectin from *Arum maculatum* L. *Plant Physiol.* **107**(4): 1147-1158.
- Van Damme EJ. 2014. History of plant lectin research. *Methods Mol Biol.* **1200**: 3-13.
- Zeng X, Andrade CAS, Oliveira MDL and Sun X-L. 2012. Carbohydrate-protein interactions and their biosensing applications. *Anal Bioanal Chem*, **402**(10): 3161-3176.



# A Morphological Study of the Pharmacological Effects of the *Nigella sativa* on the Reproductive System in Experimental Rats

Raith A. S. Al-Saffar<sup>\*</sup> and Mohammad K. M. Al-Wiswasy

Department of Basic Medical Sciences, Faculty of Medicine, The Hashemite University, Al-Zarka, Jordan.

Received July 2, 2018; Revised August 4, 2018; Accepted August 28, 2018

## Abstract

*Nigella sativa* (Black seed or Black cumin or Habbat Albaraka), which belongs to the Ranunculaceae family, is an annual herb used in food as a spice. In addition, *N. sativa* is an important medicinal herb used traditionally against a wide range of diseases. This herb has been well-studied for its pharmacological activities. However, there is limited information regarding its effects on the female reproductive system. This study describes the effects of the aqueous extract of the seeds of *N. sativa* on the endometrium in female rats. A single daily dose of 0.2g / 100g body weight (B\wt) of the crude aqueous extract of the seeds of *N. sativa* was administered orally to mature fertile female albino rats for ten days. The rats were subdivided into subgroups, according to the phase of the estrus cycle. The uterus of these animals were routinely processed for general histological studies, using carboy's fixed paraffin embedded sections. Compared with the control subgroups, the results showed an increase in the uterine wet weight of all the experimental subgroups, with a profound and persistent diffuse endometrial hypertrophy, and enhanced glandulogenesis. In conclusion, the crude aqueous extract of the seeds of *N. sativa* seemed to have achieved its effects via stimulating the endogenous release of estrogen and/or progesterone. However, direct estrogen and/or progesterone-like actions of the seeds could not be excluded.

**Keywords:** Black seeds (*Nigella sativa* L), Uterine wet weight, Glandulogenesis, Subnuclear Zone, Metrail gland, Diffuse Endometrial hypertrophy.

## 1. Introduction

The black seed *Nigella sativa* is an indigenous herbaceous plant, more commonly known as the fennel flower plant, which belongs to the buttercup or Ranunculaceae family. It is a native plant from the Mediterranean area, and found growing in some other regions in the world such as Saudi Arabia and North Africa. The herb is widely cultivated throughout South Europe, Asia, Turkey, Pakistan, and India. The plant is used especially in the Middle East and South Asia as a spice, condiment, carminative, and for aromatic and medical purposes. There are several names attributed to *N. sativa* in various countries around the world (Gilani *et al.*, 2004; El-Tahir *et al.*, 2006; Assi *et al.*, 2016; Randhawa and Alenazi, 2016). In Arab countries, the seeds are called 'Alhabba Alswda', 'Habbat Albaraka' or 'Alkamoun Alaswad'. In Urdu and Hindi, they are 'Kalonji', and in Sanskrit 'Krishnajirika'. Moreover, they are referred to as 'Kalajira' in Bangali, 'Shonaiz' or 'Siyah Daneh' in Persian, and 'cörek Out' in Turkish. In English, they are called Black cumin', 'Ajenue' in Europe, 'Schwarz' in Germany, and 'Black Caraway' in American English. The scientific name is a derivative of the Latin word 'niger' meaning 'black'.

The active constituents of the seeds include volatile oil. Pharmacologically active constituents of volatile oil are: thymoquinone, dithymoquinone, thyoquinone, and

thymol (Ghosheh *et al.*, 1999). Among these active components, thymoquinone (TQ) is the most abundant constituent (57-78 %) of the volatile oil of the *N. sativa* seeds (Gilani *et al.*, 2004), and is the constituent to which most properties of this herb are attributed (Tavakkoli *et al.*, 2018).

During the last two decades, literature has been replete with the subject of the pharmacological activities of *Nigella sativa* seeds. These studies revealed that *N. sativa* seeds, its oil, various extracts, and its active components have several therapeutic activities including: Bronchodilatory, anti-allergic (anti-histaminic), anti-inflammatory, analgesic, antipyretic, hypoglycemic, antibacterial, antifungal, anti-parasitic, antiviral, anti-cancer, antihypertensive, antioxidant, anticonvulsant, anti-parkinsonism, antidepressant, and anxiolytic effects. The seeds have also been reported to reduce the volume of gastric acid secretion and ulcer index, and modulate the lipid profile (Khan, 1999; Gelani *et al.*, 2004; Kanter *et al.*, 2005; El-Tahir and Bakeet, 2006; Ahmad *et al.*, 2013; Sandhu and Rana, 2013; Latiff *et al.*, 2014; Heshmati *et al.*, 2015; Randhawa and Alenazi, 2016; Zafar *et al.*, 2016; Daryabeygi-Khotbehsara *et al.*, 2017; Tavakkoli *et al.*, 2018). However very few studies have discussed the influence of the *N. sativa* seeds on the reproductive system, yet most of these limited studies have focused on the male reproductive system only (Agarwal *et al.*, 1990; Gilani *et al.*, 2004). Therefore, the effects of the seeds on

<sup>\*</sup> Corresponding author e-mail: Raith\_alsaffar@yahoo.com.

the female reproductive system have remained largely unknown (Kabir *et al.*, 2001; Yildiz and Balıkcı, 2016).

Moreover, the various preparations of *N. sativa* and its constituents have relaxant effects on various types of smooth muscles (Chakma *et al.*, 2001; Keyhanmanesh *et al.*, 2014). Aqel and Shaheen (1996) stated that the volatile oil of the black seeds of *N. sativa* prevents the spontaneous contraction of the uterine smooth muscle of rats and guinea pigs, and those induced by oxytocin.

Agarwal *et al.* (1990) stated that *N. sativa* ethanolic extract showed antifertility effects in male rats, probably due to its inherent estrogenic nature. In another study, (Kolahadooz *et al.*, 2014) stated that *N. sativa* could enhance sperm parameters, including sperm count, motility and morphology, semen volumes and pH. Other beneficial effects of the seeds on leydig cells and sexual hormones in infertile men have also been confirmed (Mahdavi *et al.*, 2015). In Unani medicine, *N. sativa* is recommended for use in the oligomenorrhoea therapy, infertility, and for inducing menstruation (Al-Jishi and Hozaifa, 2000). Parhizkar *et al.* (2016) stated that *N. sativa* plays a beneficial role in the treatment of postmenopausal symptoms, as its extracts displayed estrogenic activities. Other studies (Saha *et al.*, 1961; Agarwala *et al.*, 1971 and 1986, Al-Snafi *et al.*, 2014) showed that the seeds have beneficial effects on breast milk production in lactating women.

In 1995, a group of Indian workers (Keshri *et al.*) used the hexane extract of the seeds as a post-coital contraceptive in rats, when given at a single oral daily dose of 0.2g/100 g B.wt. on day 1-10 post-coitum. They reported a mild uterotrophic effect of such an extract, comparable almost to the ovulation dose of 17- $\alpha$ -estuarial, in the ovariectomized immature rat bioassay.

Accordingly, this study was conducted to investigate, for the first time, the effect of the crude aqueous extract of the seeds of *Nigella sativa* on the endometrium of mature rats during different physiological states. Comparative histological procedures at the level of light microscopy are attempted for this purpose.

## 2. Materials and Methods

### 2.1. Animals Used

Fifty fertile Norway albino female rats, aged 12-16 weeks, and weighting 194-199 g, were used in this study. Each animal was carefully selected to match the following criteria: (1) Being a mature female rat of a proven fertility that is decided by the history of previous deliveries. The last delivery should not be less than four weeks. (2) Had not been mixed with male partner(s) for the last two

weeks. (3) Having regular estrus cycles, as judged by their vaginal smears cytology, done on a regular daily basis.

The animals were grouped according to their physiological state and the substance they received (Table 1). All rats were kept in air-conditioned quarters ( $30 \pm 2^\circ\text{C}$ ), under standard husbandry conditions, with alternated 12h /12h dark/light cycle (Parhizkar *et al.*, 2016). Animals were fed with a protein-standard pellet diet.

### 2.2. Experimental Animals

Thirty animals were used in this experiment. They were divided into three subgroups: (1) Proestrus (P), (2) Estrus (E), and (3) Diestrus (D), as shown in Table 1. Each rat received the crude aqueous extract of the crushed *N. sativa* seeds at the dose of 0.2g/100g B. wt (Keshri *et al.*, 1995), starting at the P, E, and D phase, respectively (Table 1). The seeds' powder was mixed with 4 mL of distilled water (Al-Khateeb, 1996; Sakran, 1999), administered via an orogastric tube (5.5 X 0.13), and was given once a day for the duration of ten days (Keshri *et al.*, 1995).

### 2.3. Control Animals

Twenty animals were used as control animals. They were divided into two subgroups: (1) Non-treated controls ( $C_n$ ), which were used as standard reference models, and (2) A treated subgroup ( $C_R$ ) which received four mL of distilled water (D.W.) only, via the orogastric tube, once a day for the duration of ten days (Table 1).

### 2.4. Uterine Wet Weight Measurement and Tissue Processing

For each animal (experimental and control), the exposure of the peritoneal cavity, and the removal of the body of uterus were done under open ether anesthesia. The wet weight of each respected uterus was recorded. Immediately afterwards, the specimens were fixed for a period of two hours in Carnoy's fluid (6 volumes absolute ethanol: 3 volumes chloroform: 1 volume Glacial acetic acid). The fixed tissue-specimens were processed for routine paraffin wax-embedding. Serial sections, each of a 5 $\mu$  thickness were stained with the progressive Hematoxylin and Eosin stain.

### 2.5. Counts (Metrial Gland and Eosinophils Count)

The point-counting technique (Weibel and Gomez, 1962) with a Zeiss point-counting eyepiece graticule had been attempted in counting metrial gland sections per unit area at estrus. This was achieved by counting the number of metrial gland sections on each of a total of sixteen power fields (each of 0.37 mm diameter), in corresponding areas of adjacent sections.

**Table 1.** Animal groups and subgroups used in this study. All animals, were sacrificed after ten days.

Groups	Subgroups	No. of Animals	Substance received	Specific Phase of the cycle during which treatment commenced.	Dosage (g/100 g B.wt.)
Control	$C_n$	10	None	—	—
	$C_R$	10	D.W. only	Irrespective	—
Experimental	D	10	Crude aqueous extract of the <i>N. sativa</i> seeds	Diestrus	0.2
	P	10	Crude aqueous extract of the <i>N. sativa</i> seeds	Proestrus	0.2
	E	10	Crude aqueous extract of the <i>N. sativa</i> seeds.	Estrus	0.2



Counting the infiltrating eosinophils was achieved by virtue of the method described by Al-Hadithi, 1994: the mean count of five randomly selected high power fields; they were taken to represent the eosinophils count of an individual section. For individual animals, the mean of at least four serial sections was taken to represent its infiltrating eosinophils count.

### 2.6. Data Analysis

The statistically significant difference between two groups' mean values, with continuous variables was calculated, using the two-tailed student t-test, and  $P < 0.05$  was taken as significant. The Schiff's f-test was also used for multiple comparisons between pairs of means when appropriate (Daniel, 1983).

## 3. Results

Vaginal smears of rats treated with the crude aqueous extract of the seeds of *Nigella sativa* showed a shortening of the vaginal cycle with prolongation of both the estrus and the metestrus phases; the diestrus phase was undetectable.

The experimental rats treated with the aqueous extract of the *Nigella sativa* seeds showed a significant increase in their uterine weights (almost ten times elevation) compared to their control fellows ( $P < 0.05$ ). No significant differences among the individual experimental subgroups were found (Figure 1).

Control rats' uteri, under a low power objective (X 22), were seen as pear-shaped elongated, cylindrical organs.

The two uterine horns were diverging proximally; while their outlets, approaching each other at the cervix, and were directed distally.

The examination of sections of the control rats' uteri at the proestrus phase showed that the uterine lumen was seen as distended, and the luminal epithelium was low cuboidal (Figure 2 A, inset arrow). The endometrial surface was thrown into marked longitudinal folds, but with very narrow crypts (Figure 4 A). The endometrial stromal glands were relatively scarce (Figure 2 B head arrows), and are lined with a single layer of low cuboidal cells (Figure 2C, head arrow); the stromal cells were generally elongated or spindle in shape with darkly stained oval nuclei. Nucleoli were generally absent, and the chromatin granules were evenly distributed. (Figure 2 C, thin arrow). Eosinophilic granulocytes were seen moderately infiltrating the stroma (Figure 2C inset), and different types of blood vessels were seen throughout the stroma (Figure 2B small arrows).

Sections of the control rats' uteri at the estrus phase showed that the luminal epithelium was tall columnar in type with large vesicular nuclei occupying a parabasal position (Figure 3 A inset arrows). Luminal crypts were dilated, and its lumen was distended with fluid (Figure 3 A). At a low power, the endometrial stroma showed increased cellularity (Figure 3 B). The metrial glands were lined with darkly stained columnar cells (Figure 3C head arrow). Endometrial stroma was heavily infiltrated with eosinophil granulocyte (Figure 3 C double arrow), and

stromal cells were more or less spindle-shaped with darkly stained elongated nuclei. Mitosis was quite frequent amongst these cells (Figure 3 C, thin arrow).

The examination of sections of the control rats' uteri at the metestrus, showed that the endometrium was found shrunk, with a general distorted appearance. The functional layer of the endometrium (superficial layer) was disintegrated, and sheets of stromal elements, as well as surface epithelium were seen casted-off the endometrium (Figure 4 A, B, and C). However, the basalis layer of the endometrium (containing the deep part of the endometrial glands as well as its blood vessels) were relatively intact. Eosinophil granulocytes were remarkably absent amongst the stromal section (Figure 4 C).

The uterine sections of rats treated with *N. sativa* at the proestrus phase, showed profound endometrial hyperatrophy, with enhanced glandulogenesis (Figure 5 A and B). The luminal epithelium consists of tall columnar cells, with a characteristic subnuclear zone (Figure 5 C, white arrows), and subepithelial decidualization.

The uterine sections of the rats treated with *N. sativa*, at the estrus phase, showed diffuse endometrial hyperatrophy, with enhanced glandulogenesis (Figure 6A and B). Eosinophil granulocytes were absent (Figure 6 A). The surface epithelium was high columnar in shape, with well-developed subnuclear zones (Figure 6 C, thin arrows).

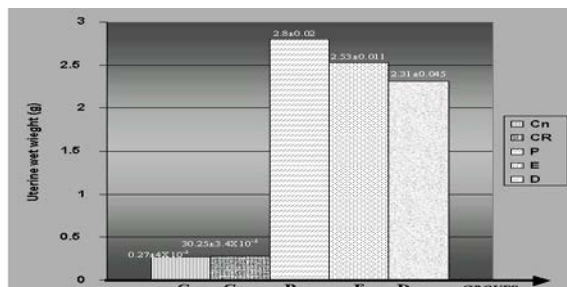
Stromal cells showed marked nuclear changes; being large and round or oval with coarsely granular and unevenly distributed chromatin materials, and eccentric nucleoli (Figure 6 C). Cells with reniform nuclei were also seen scattered throughout the stroma (Figure 6C, open arrow). Vascularity of the endometrium was well-established (Figure 6 C, open arrow). Mitosis of many stromal cells was frequent.

During the metestrus phase, the uterine sections of rats treated with *N. sativa* showed the persistence of metrial glands (Figure 7 A, arrows), as well as well-developed endometrial stroma and subepithelial decidualization reaction (Figure 7B, arrows), with a pseudostratification of nuclei (Figure 7B, head arrow). The luminal epithelium showed subnuclear vacular spaces (Figure 7 C, head arrow). The stromal cells nuclei showed vesicular patterns (Figure 7C, long arrow), and those of the reniform type (Figure 7 C, small head arrow).

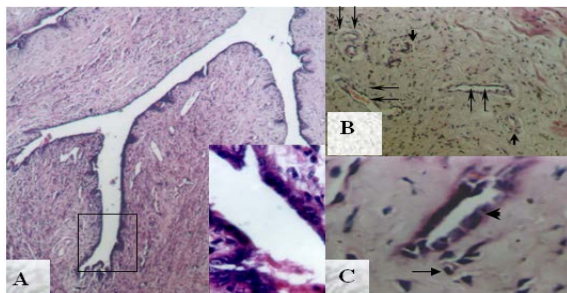
The statistical analysis of eosinophil count, as well as mean numbers of metrial gland sections, counted per unit area of the estrus specimens, for both the control and the experimental rats, are presented in Table 2, respectively. Statistically, these data showed: (1) A significant increase in the mean number of glandular sections per unit area amongst the estrus endometrial sections of experimental rats ( $P < 0.05$ ). However, no significant differences could be elicited amongst individual subgroups of the same group (Table 2); (2) A significant decline in the number of infiltrating eosinophils granulocytes endometrial sections ( $P < 0.005$ ) amongst all experimental rats, at the estrus (Table 2).

**Table 2.** Mean number of infiltrating eosinophils granulocytes per HPF, and that of metrial gland sections per unit area of estrus endometrial sections. Data expressed as means of at least forty sections (ten rats)  $\pm$  SD.

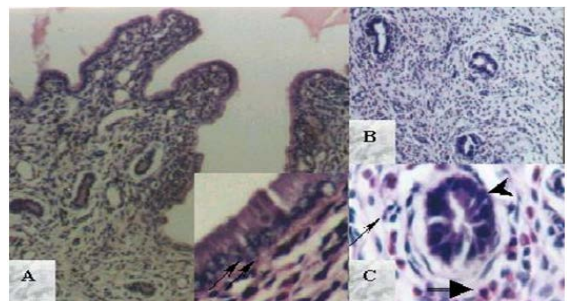
Group	Subgroups	Eosinophils per HPF $\pm$ SD	Metrial gland sections/unit area $\pm$ SD
Control	Treated	111 $\pm$ 4.5	1.3 $\pm$ 0.47
	Non-treated	113 $\pm$ 6.4	1.4 $\pm$ 0.35
Experimental	D	4.3 $\pm$ 3.8	5.2 $\pm$ 0.49
	P	5.3 $\pm$ 3.5	5.1 $\pm$ 1.1
	E	5.6 $\pm$ 3.5	4.7 $\pm$ 1.2



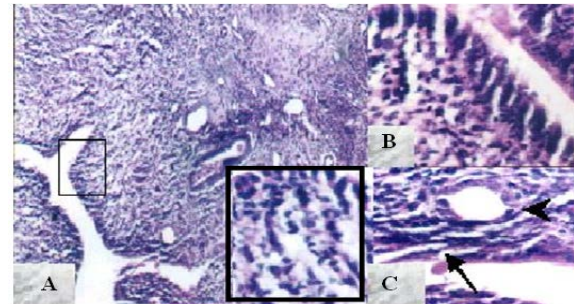
**Figure 1.** Frequency histogram showing values for uterine wet weight for the control and the experimental rats. Data expressed as mean  $\pm$  SD of readings obtained from ten rats at the end of experiment.



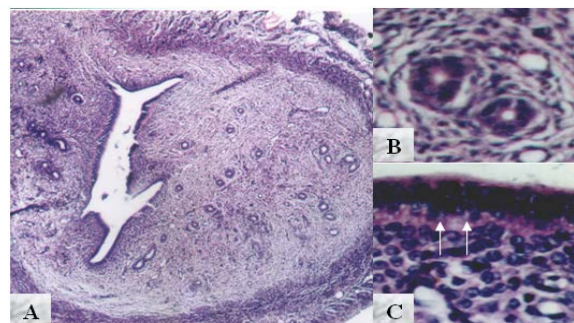
**Figure 2.** Proestrus section of control animals. A: Endometrial surface was thrown into marked longitudinal folds and narrow crypts (X 330); Note the low cuboidal lining of the crypts [inset arrow, (X 1320)]. B: General architecture of the endometrial stroma (X 330); Note the scarcity of the glands (head arrows), and relative abundance of the blood vessels (small arrows). C: Finer details of the stroma (X 1320), showing the low cuboidal lining of the glands (head arrow), the moderate eosinophils granulocytes infiltration [inset, (X 1320)], and the generally spindle shaped stromal cells with darkly stained oval nuclei (thin arrow).



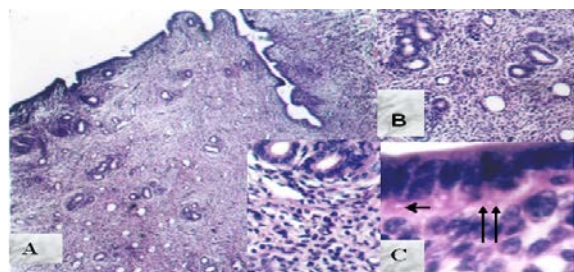
**Figure 3.** Estrus section of control animals. A: Dilatation and widening of the luminal crypts (X 330). Note the columnar type luminal epithelium, and the parabasal position of the nuclei [inset arrows (X 1320)]. B: Endometrial stroma, showing increased stromal cellularity (X 1320). C: Finer stromal details. Note the increased eosinophils granulocytes infiltration (double arrow), frequent mitotic figures (thin arrow) and the columnar lining of the glands (head arrow), cf., Fig. (4C). (X 1320).



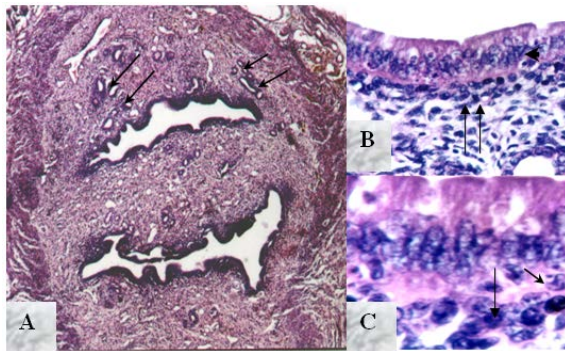
**Figure 4.** Metestrus section of control animals. A: General appearance of the sloughing endometrium (X 330). Note the absence of glands and loss of normal tissue architecture, of the superficial layers [inset, (X 1320)]. B: Degenerated luminal epithelium (X 1320). C: Loss of normal glands architecture (head arrow), and sheets of degenerated stromal elements (thin arrow). Note the absence of eosinophils granulocytes, cf., Fig. (5C) (X 1320).



**Figure 5.** Habbat-Baraka (*Nigella sativa* Linn. seeds) treated proestrus. A & B: Showing profound endometrial hypertrophy, with enhanced glandulogenesis, cf. Fig. (4A & B). [B (X 330)]. C: Luminal epithelium showing well-developed tall columnar cells, with characteristic subnuclear zones (white arrows), and subepithelial decidualization, cf. Fig. (4C). (X 1320).



**Figure 6.** Habbat-Baraka (*Nigella sativa* Linn. seeds) treated Estrus. A & B: showing diffuse endometrial hypertrophy, with enhanced glandulogenesis [B (X 330)]. Note the absence of eosinophils granulocytes infiltration of the stroma, cf. Fig. (5C). [A, inset (X 1320)]. C: luminal epithelium showing well-developed sub-nuclear zones (thin arrows). Note the vesicular pattern of stromal cells nuclei, and those of reniform type (open arrow). (X 1320).



**Figure 7.** Habbat-Baraka (*Nigella sativa* Linn. Seeds) treated metestrus. A: showing the persistence of metrial glands (arrows), and well-maintained endometrial stroma, cf. Fig.(6 A). (X 330). B: Subepithelial decidualization reaction (arrows). Note the pseudostratification of nuclei (head arrow). (X 1320). C: Luminal epithelium showing subnuclear vacuolar spaces (head arrow). Note the vesicular pattern of the stromal cells nuclei (long arrow), and those of the reniform type (small head arrow). (X 1320)

#### 4. Discussion

Vaginal smears of rats treated with the crude aqueous extract of *Nigella sativa* seeds showed a shortening of the vaginal cycles with the prolongation of both the estrus and the metestrus phases; the diestrus was undetectable.

The shortening of a five-day vaginal cycle reported earlier (Vander-Schoot and Uilenbroek, 1983), suggested mechanism of a prolonged exposure to progesterone after the metestrus, a consecutive effect to the inhibition of luteolysis. *Nigella sativa* was shown to prolong the life-span expectancy of the ovulatory corpus luteum, amongst locally bred hybrid albino female rats (Hassen, 2000). This provides supplementary evidence to the observed post-ovulatory, progesterone-like action of the administrated crude aqueous extract of the *N. sativa* seeds as shown from the vaginal smears of treated rats. Thus, this provides a clue that whole *N. sativa* might have achieved its effects by stimulating the endogenous release of estrogen and/or progesterone. However, direct estrogen and /or progesterone-like actions of the Black seeds, could not be excluded.

The results of this study showed that the crude aqueous extract of the *N. sativa* L. seeds at the dose of 0.2g/100g B. wt, leads to a significant increase ( $P < 0.05$ ) in the uterine weights of rats (almost ten times elevation) compared to their control fellows (Figure 1). Similar results were obtained by Parhizkar *et al.*, 2016. The number of the metrial glands was significantly elevated (Table 2), suggesting an increased rate of glandulogenesis. On the other hand, the vesicular pattern of the stromal cells nuclei, and the ostensibly increased nucleocytoplasmic ratio among such cells, can be a suggestive histological feature indicating an increase in the metabolic activities (Robertson, 1981; Junqueira and Carneiro, 2005). Berene and Levy, 1988; Ganong, 2010 stated that estrogen has a rapid effect on cell replication, but has a slower effect on cytoplasmic differentiation.

Mitosis was frequently seen amongst the stromal cells, and cells with indented, bilobed and/or reniform nuclei, were also produced and were predominantly seen at the immediate subepithelial zones. Such types of stromal cells had been reported (Robertson, 1981). These cells

were implicated in the process of decidualization of the rodent endometrial, and are shown to be responsible for the endometrial production of the polypeptide hormone Relaxin (Robertson, 1981). Relaxin has been found to stimulate the uterine edema via the activation of estrogen receptors (Pillai *et al.*, 1999). Such endometrial edematous changes might be responsible for some of the observed increment in the uterine wet weight values obtained in this study.

The luminal epithelial cells were persistently high columnar in type. Throughout the phases of the endometrial cycle, these cells developed the characteristic sub-nuclear vacuolar spaces. Since estrogen supports the growth of the luminal epithelial cells (Bere and Levy, 1988), the height of these cells was taken as a sensitive parameter in assessing the estrogen site of a given compound (Fuhrman *et al.*, 1998), and in accordance with the fact that the development of the sub-nuclear spaces amongst the luminal epithelium was shown to be functionally associated with ovulation (Lesson *et al.*, 1988), and is brought out by progesterone actions on the estrogen-primed luminal epithelium (Stenchever, 1987; Lesson *et al.*, 1988). The results obtained from this study indicate that the crude aqueous extract of the *Nigella sativa* seeds might possibly have an estrogen and/or progesterone-like action on mature rats' endometrium. Such indication is supported by other authors (Liu *et al.*, 2004; Parhizkar *et al.*, 2011, 2012, and 2016).

The failure to detect diestrus on the vaginal cytology (Hassen, 2000) of the experimental rats is supported by their endometrial histology: the absence of degenerative changes amongst metestrus endometrial sections was quite evident when compared with those of their controls (Figure 6) since the mechanisms of endometrial sloughing involved estrogen and/or progesterone withdrawal (Ganong, 2010) because blood estrogen concentrations should be above a critical level together with progesterone for both the maintenance and the proliferation of the secretory phase of the endometrium of the uterus (Laurence *et al.*, 1997). These findings provide further supporting evidence that the crude aqueous extract of the *N. sativa* seeds has an estrogen and/or progesterone-like action(s).

Stromal infiltration with eosinophils granulocytes is a unique feature of rodents' Estrus, which coincides with the periovulatory peak of estrogen (Hebel and Stromberg, 1986), and is considered as one of the histological parameters in assessing the uterotrophic effect of a given compound (Patriarca *et al.*, 1996). In this study, eosinophils granulocytes infiltration of the endometrial stroma, at Estrus, was significantly reduced after the administration of the aqueous extract of the *N. sativa* seeds. A low eosinophils count, at the Estrus of rats, had been reported earlier, and showed that anti-estrogens can induce it with intrinsic estrogen-agonist activity (Patriarca *et al.*, 1996).

However, inhibited eosinophils granulocytes infiltration of the decidualized endometrium is a well-known fact amongst rodents, and this suggests a possible role of these cells in the initiation of implantation (Hebel and Stromberg, 1986).

The current study reported that the inhibition of eosinophils granulocytes infiltration of the endometrial stroma at Estrus, suggests the presence of anti-estrogens



with intrinsic estrogen-agonist activity (Patriarca *et al.*, 1996); or this could be a consecutive effect of the observed utilization of the promoting effects of the herb on rats' ovaries (Hassen, 2000; Parhizkar *et al.*, 2011). However, direct decidualization promoting effect(s) of the crude aqueous extract of the seeds on the endometrial-stromal elements might not be ruled out by the present work.

## 5. Reference

- Agarwal C, Narula A, Vyas DK and Jacob D. 1990. Effect of seeds of "kalaunji" (*Nigella sativa*) on fertility and sialic acid content of the reproductive organs of the male rat. *Geobios.*, **17**: 269-272.
- Agrawala IP, Achar MVS, and Tamankar BP. 1971. Galactagogue action of *Nigella sativa*. *Indian J Med Sci.*, **25**(8): 535-537.
- Agrawala IP, Achar MVS, Boradker RV, and Roy N. 1986. Galactagogue action of *Cuminum cyminum* and *Nigella sativa*. *Indian J Med Res.*, **56** (6): 841-844.
- Ahmad A, Husain A, Mujeeb M, Khan SA, Najmi AK, Siddique NA, Damanhour ZA and Anwar F. 2013. A review on therapeutic of *Nigella sativa*: A miracle herb. *Asian Pacific J Tropic Biomed.*, **3** (5): 337-352.
- Al-Hadithi NK. 1994. **A study on Myogenesis with use of Organ Elements**. MSc Thesis, Baghdad University, Iraq.
- Al-Jishi SA and Abu-Hozaifa B. 2000. A study the effect of *Nigella sativa* on blood hemostatic functions in rats. *J Ethnopharmacol.*, **85**(1): 7-14.
- Al-Khateeb HM. 1996. **Some Morphological and Histochemical Studies on Rat's Mammary Gland**. PhD Thesis, University of Baghdad, Iraq.
- Al-Snafi AE, Majid WJ, and Talab TA. 2014. Galactagogue action of *Nigella sativa* seeds. *J Pharm*, **4**(6): 58-61.
- Aqel M and Shaheen R. 1996. Effects of the violet oil of *Nigella sativa* seeds on the uterine smooth muscle of rat and guinea pig. *J Ethnopharmacol.*, **52**(1): 23-26.
- Assi MA, Noor MHM, Bacheck NF, Ahmad H, Haron AW, Yussof MSM, and Rajion MA. 2016. The various effects of *Nigella sativa* on multiple body system in human and animals. *Pertanika J Schol Res Rev.*, **2**(3): 1-19.
- Berene RM and Levy RM. 1988. The reproductive glands. In: Berene RM and Levy RM (Eds.). **Physiology**. C. V. Mosby Company, St Louis-Washington DC-Toronto. pp: 983-1024.
- Chakma TK, Choudhuri MSK, Jabbar S, Khan MTH, Alamgir M, Gafur MA, Ahmed K and Roy BK. 2001. "Effect of some medicinal plants and plant parts used in ayurvedic system of medicine in isolated guinea pig ileum preparations". *Hamdard Medicus*, **44**(2): 70-73.
- Daniel WW. 1983. Hypothesis testing. In: **Biostatistics, A Foundation for Analysis in the Health Sciences**. Wiley J & Sons, London. pp: 161-205.
- Daryabeygi-Khotbehsara R, Golzarand M, and Djafarian K. 2017. *Nigella sativa* improves glucose homeostasis and serum lipids in type 2 diabetes: A systematic review and meta-analysis. *Complement Ther Med.*, **35**: 6-13.
- El-Tahir KEH and Bakeet DM. 2006. The black seed *Nigella sativa* Linnaeus – A mine for multi cures: a plea for urgent clinical evaluation of its volatile oil. *J Taibah Univ Med Sci.*, **1**(1): 1-19.
- Fuhrmann U, Fritzermeier KH, Stockemann K and Chwalisz K. 1998. Modulation of estrogen effects by progesterone antagonists in the rat uterus. *Hum Reprod.*, **4**: 570-583.
- Ganong FW. 2010. The female reproductive system; the Gonads: Development function of the reproductive system. In: Ganong F.W (Eds.) **Ganong, Review of Medical Physiology** 23<sup>rd</sup> ed. McGraw-Hill Companies (USA), PP: 391-428.
- Ghosheh, OA Houdi AA and Crooks PA. 1999. High performance liquid chromatography analysis of pharmacologically active quinines and related compounds in the oil of the black seed (*Nigella sativa*). *J Pharm Biomed Anal.*, **19**(5): 757-762.
- Gilani AH, Jabeen Q and Khan MA. 2004. A review of medicinal uses and pharmacological activities of *Nigella sativa*. *Pakistan J Biol Sci*, **7**(4): 441-451.
- Hassen AJ. 2000. **The Effect of the Black cumin Seeds *Nigella sativa* Linn. on Mature Rat Endometrium**. MSc Thesis, University of Baghdad, Iraq.
- Hebel R and Stromberg MW. 1986. Embryology. In: Hebel R. and Stromberg MW, **Anatomy and Embryology of the laboratory Rat**. Bio Med Verlage Wörthsee: 231-257; 771-783.
- Heshmati J, Namazi N, Memarzadeh MR, Taghizadeh M and Kolandooz F. 2015. *Nigella sativa* oil effects glucose metabolism and lipid concentrations in patients with type 2 diabetes: A randomized, double-blind, placebo-controlled trial. *Food Res Int.*, **70**: 87-93.
- Junqueira LC and Carneiro J. 2005. The Female Reproductive System.. In: Junqueira LC and Carneiro J (Eds.). **Basic Histology**, 11<sup>th</sup> ed. McGraw-Hill Companies, New York. PP: 435-455.
- Kabir KK, Varshney JP, Rawal CVS, Sirvastava RS and Ansari MR. 2001. Comparative efficacy of herbal preparations in the management of anoestrus in non descriptive rural buffaloes. *Indian J Anim Reprod*; **22**: 143-145.
- Kanter M, Demir H, Karakaya C and Ozbek H. 2005. Gastroprotective activity of *Nigella sativa* L oil and its constituent, thymoquinone against acute alcohol-induced gastric mucosal injury in rats. *World J Gastroenterol*, **11**(42): 6662-6666.
- Keshri G, Singh MM, Lakshmi V and Kamboj VP. 1995. Post-coital contraceptive efficacy of the seeds of *Nigella sativa* in rats. *Indian J Physiol Pharmacol.*, **39**(1): 59-62.
- Keyhanmanesh R, Gholamnezhad Z and Boskabady MH. 2014. The relaxant effect of *Nigella sativa* on smooth muscles, its possible mechanisms and clinical applications. *Iran J Basic Med Sci.*, **17** (12): 939-949.
- Khan MA. 1999. Chemical composition and medicinal properties of *Nigella sativa* Linn. *Inflammopharmacol.*, **7**(1): 15-35.
- Kolahdooz M, Nasri S, Modarres SZ, Kianbakht S and Huseini HF. 2014. Effects of *Nigella sativa* L. seed on abnormal semen quality in infertile men; a randomized, double-blind, placebo-controlled clinical trial. *Phytomedicine*, **21**(6): 901-905.
- Latiff LA, parhizkar S, Dollah MA and Tajuddin Syed Hassan S. 2014. Alternative supplement for enhancement of reproductive health and metabolic profile among perimenopausal women: a novel role of *Nigella sativa*. *Iran J Basic Med Sci.*, **17**(12): 980-985.
- Laurence DR, Bennett PN and Brown MJ. 1997. Oestrogens and Antioestrogens, In: Laurence DR, Bennett PN and Brown MJ (Eds.). **Clinical Pharmacology**, 8<sup>th</sup> ed. Churchill Livingstone N.Y. Edinburgh, London; pp: 649-652.
- Lesson TS, Lesson CR and Parao AA. 1988. The Female Reproductive system. In: Lesson TS, Lesson CR and Parao AA (Eds.). **Textbook of Histology** 5<sup>th</sup> ed. Lesson W.B.Saunders Company Pub. Philadelphia (USA); pp: 472-478.
- Liu M, Xu X, Rang W, Li Y and Song Y. 2004. Influence of ovariectomy and 17 $\beta$ -estradiol treatment on insulin sensitivity, lipid metabolism and post-ischemic cardiac function. *Int J Cardiol.*, **97**(3): 485-493.

- Mahdavi R, Heshmati J and Namazi N. 2015. Effects of black seeds (*Nigella sativa*) on male infertility: a systematic review. *J Her Med.*, **5**(3): 133-139.
- Parhizkar S, Abdul-Latiff L, Abdul-Rahman S, Dollah MA and Parichehr DH. 2011. Assessing estrogenic activity of *Nigella sativa* in ovariectomized rat, using vaginal cornification assay. *African J Pharm.*, **5**(2): 137-142.
- Parhizkar S, Abdu-Rahman S and Abdul-Latiff L. 2012. In vivo estrogenic activity of *Nigella sativa* different extracts using vaginal cornification assay. *J Medic Pl Res.*, **5**(32): 6939-6945.
- Parhizkar S, Abdul-Latiff L and Parsa A. 2016. Effect of *Nigella sativa* on reproductive system in experimental menopause rat model. *Avicenna J Phytomed.*, **6**(1): 95-103.
- Patriarca MT, Simaes MDJ, Smaniotto S, De-Teves DC, Simoes M-de-D, Evencio-Neto J, DeFreitas V and De-Lima GR. 1996. Morphological action of tamoxifen in the endometrium of persistent estrus rat. *Acta Obstet Gynecol Scand*, **75**(8): 707-710.
- Pillai SB, Rockwell C, Sherwood OD and Koss RD. 1999. Relaxin stimulate uterine edema via activation of estrogen receptors: Blockade of its effects using ICI 182, 789, a specific estrogen receptor antagonist. *Endocrinol*, **140**(5): 2426-2429.
- Randhawa MA and Alenazi SA. 2016. Neuropsychiatric effects of *Nigella sativa* (black seed) A review. *Altern Integr Med.*, **5**(1):209-216.
- Robertson WB. 1981. Normal Endometrium. In: Robertson WB (Eds). **The Endometrium**. Butter Worths & Co. Pub. pp: 7-44.
- Saha JC, Savini EC, and Kasinathan, S. 1961. Ecobolic properties of Indian medicinal plants. Part 1 *Indian J. Med Res.*, **49**: 130-151.
- Sakran A M. 1999. **The Effect of Fenugreek Seeds on Rat's Ovary: Histological and Histochemical Studies**. MSc Thesis, University of Baghdad, Iraq.
- Sandhu KS and Rana AC. 2013. A review of plant *Nigella sativa*: A brief consideration of its pharmacognostic character, chemical constituents and therapeutic benefits. *Inter J Pharmacut Sci.*, **4**(4): 323-343.
- Stenchever MA. 1987. Endometrial histology. In: Stenchever MA, Mishell DR, Herbst AL and Drogemuller W. (Eds). **Comprehensive Gynecology**. The C.V. Mosby Company, West line Industrial Drive, St. Louis, Missouri (USA) PP: 112-116.
- Tavakkoli A, Mahdian V, Razavi BM and Hosseinzadeh H. 2018. Review on clinical trials of black seed (*Nigella sativa*) and its active constituent, thymoquinone. *J Pharmacopuncture*, **20**(3): 179-193.
- Van-der-Schoot P and Uilenbroek JT. 1983. Reduction 5-days cycle length of female rats by treatment with bromocriptine. *J Endocrinol*, **97**(1): 83-89.
- Weibel ER and Gomez DM. 1962. A principle for counting tissue structures on random sections. *J Appl Physio.*, **17**: 343-348.
- Yildiz A and Balikci E. 2016. Antimicrobial, anti-inflammatory and antioxidant activity of *Nigella sativa* in clinically endometritic cows. *J Appl Anim Res.*, **44**(1): 431-435.
- Zafar K, Noorul H, Nesar A, Vatikas S, Khalid M, Prashant S, Zeeshan A and Zohrameena S. 2016. Pharmacological activity of *Nigella sativa*. A review. *World J Pharm Sci.*, **4**(5): 234-241.



# First Record of the Cochineal Scale Insect, *Dactylopius opuntiae* (Cockerell) (Hemiptera: Dactylopiidae), in Jordan

Ahmad M. Katbeh Bader<sup>1\*</sup> and Asem H. Abu-Alloush<sup>2</sup>

<sup>1</sup>Department of Plant Protection, School of Agriculture, The University of Jordan, Amman; <sup>2</sup>National Center for Agricultural Research and Extension, Plant Protection Department, Al Baqa'a, Jordan.

Received September 3, 2018; Revised September 14, 2018; Accepted September 18, 2018

## Abstract

The cochineal scale, *Dactylopius opuntiae* (Cockerell, 1896) (Hemiptera: Dactylopiidae), is reported from Jordan for the first time from several localities in the north of the country. This scale insect attacks the Indian-fig prickly pear, *Opuntia ficus-indica* (L.) Miller (Cactaceae), and plants are killed by heavy infestations. The distribution and the relative degree of infestations in Jordan are shown in a map. Voucher specimens of the collected samples were preserved in the University of Jordan Insect Museum. Slides of adult females were prepared, and digital images were taken to illustrate important diagnostic characters. World distribution, morphology, control methods, natural enemies and the probable means of the introduction of this serious pest are discussed.

**Keywords:** Cochineal scale insect, Prickly-pear cactus.

## 1. Introduction

The cochineal insects are sources of red dye. They are potential agents for the control of certain pest species of *Opuntia* or prickly pears (De Lotto, 1974). They have been used for commercial purposes since the 16<sup>th</sup> century in Central and South America, in Mexico and Spain (De Lotto 1974 and Chávez-Moreno *et al.*, 2009). *D. opuntiae*, was described by Cockerell in 1896 from Mexico (De Lotto, 1974). It was introduced into Australia, India, South Africa, and Saudi Arabia to control the prickly pear cacti which were considered noxious weeds (Hosking *et al.*, 1994; Foxcroft and Hoffmann 2000; Aldawood and Tuwariqi, 2014). The current distribution of this insect includes twenty countries: Australia (New South Wales), Brazil Cape Verde, France, Hawaii, India, Jamaica, Kenya, Lebanon, Madagascar, Mauritius, Mexico, Morocco, Pakistan, Palestine, Reunion, South Africa, Sri Lanka, United States (Arizona California Texas ), and Zimbabwe (García *et al.*, 2016). Additionally, it is found in Lebanon (Moussa *et al.*, 2017), Saudi Arabia (Aldawood and Tuwariqi, 2014), Morocco (Bouharroud *et al.*, 2016) and Cyprus (EPPO Reporting Service, 2017).

*D. opuntiae* females have three developmental stages – egg, nymph (two instars) and adult- whereas males have egg, nymph, pre-pupa, pupa and adult stages (De Lotto, 1974). This cochineal scale produces carminic acid to protect itself from predators (Eisner *et al.*, 1994). The longevity of the female is 38.4 days, while male longevity is only 4.2 days. The complete biological cycle is 77 and 43 days for the female and male insects respectively. Sexual reproduction is most common, but parthenogenetic females were found (Flores-Hernandez *et al.*, 2006).

Cactus was introduced into Palestine centuries (400 years) ago from Central America (Protasov *et al.*, 2017). In Jordan, *Opuntia ficus-indica* is planted at the edges of farms and gardens as a fence, and also for its fruits, which have a good market value. It can also be used as animal feed. The cultivated area of this plant in Jordan is estimated at 3000,000 m<sup>2</sup> mainly in the Jordan Valley and Madaba area. Recently, farmers from the northern parts of Jordan complained from the scale insect that attacked cactus severely. The objective of the current work is to document the first record of *D. opuntiae* (Cockerell) in Jordan, its recent distribution in the country, and to propose effective control pest methods.

## 2. Materials and Methods

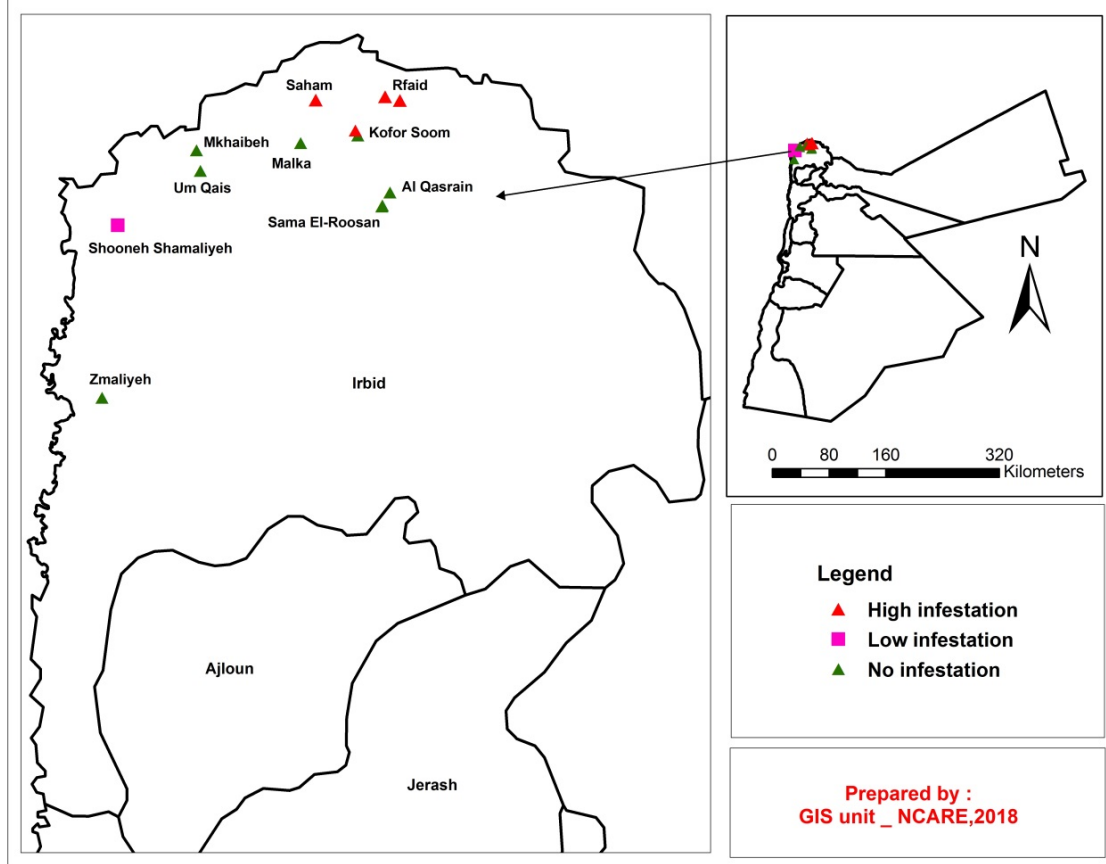
Six field trips were conducted on the 9<sup>th</sup>, 14<sup>th</sup>, 17<sup>th</sup>, 24<sup>th</sup> of February and the 3<sup>rd</sup> of March in 2018 to several localities in northern Jordan (Map 1). The elevations of sites were recorded by GPS. All cactus plants were observed, and examined for the presence of the Cochineal scale insect in all of the visited sites. The severity of infestation was estimated as follows: 0, no infestation; 1, low infestation if less than 25 % of the pad surface was infested; 2, medium infestation if 25-50 % of the pad surface was infested; 3, high infestation if more than 50 % of the pad surface was infested (Moussa *et al.*, 2017).

The heavily infested cladodes of cactus were collected from several sites in the northern parts of Jordan. The specimens were removed from the cladodes with a fine brush, and were boiled gently in 75 % alcohol for few minutes. They were then washed with distilled water, and placed in 10 % KOH for 24 hours until the specimens became translucent. Afterwards, all body contents were

\* Corresponding author e-mail: Ahmadk@ju.edu.jo.

removed by pressing the insect with a small spatula. The specimens were then rinsed in distilled water for about ten minutes placed in few drops of glacial acetic acid and acid fuchsin, and were then washed in absolute alcohol. Slide mounts were prepared in clove oil. Voucher specimens of the collected samples and the prepared slides were

preserved at the University of Jordan Insect Museum. The adult female was photographed using a dissecting microscope (Leica M165 C) provided with a dome illumination unit. Enlargements were carried out under light microscope by a digital camera (CMEX 5.0 M pixel digital USB2 camera Euromex) attached to the eye tube.



Map 1. Current distribution of *Dactylopius opuntiae* in Jordan.

### 3. Results

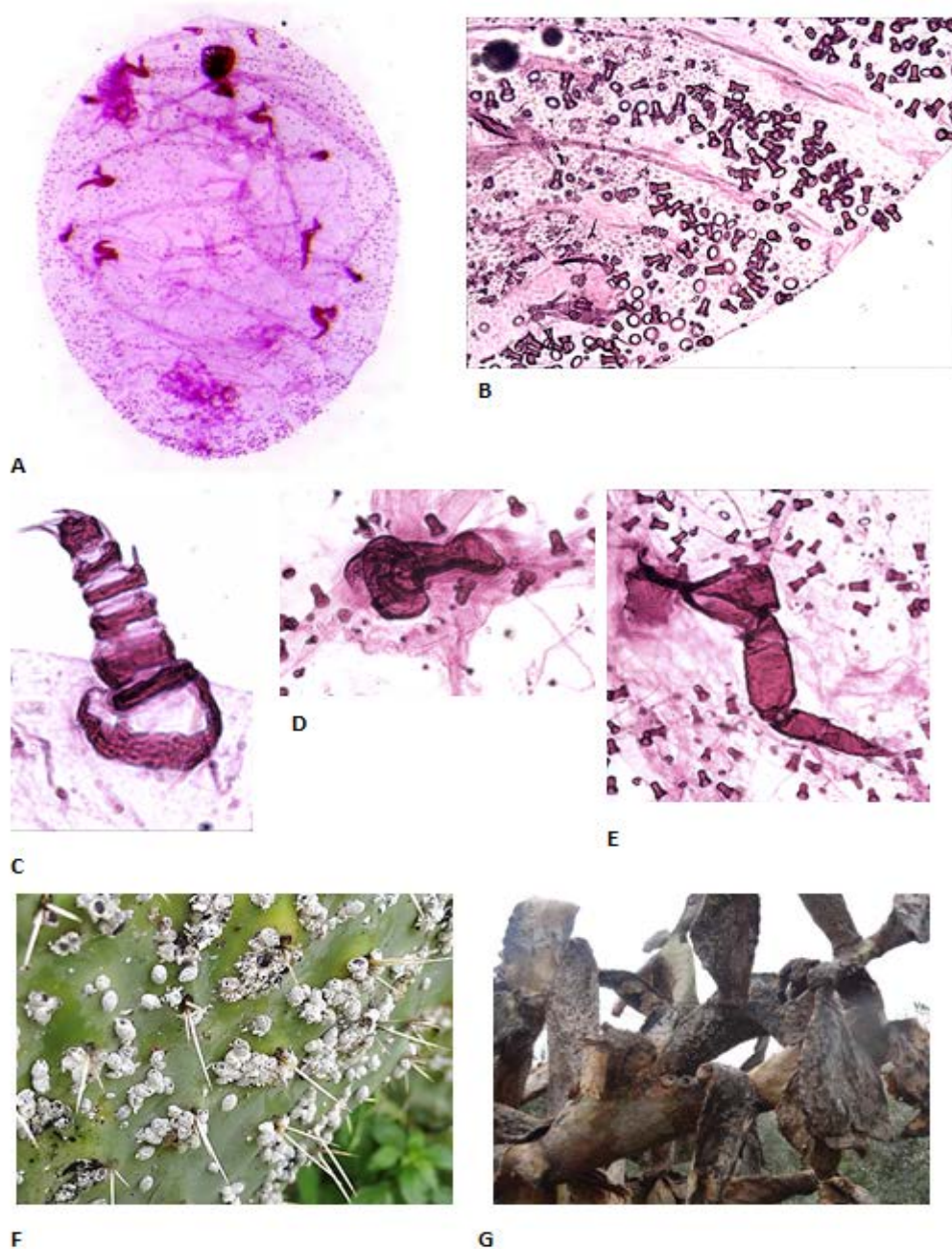
The mounted specimens of the examined scale insect were found by the first author to belong to *D. opuntiae* (Cockerell) according to the key of (De Lotto, 1974). Mounted adult female is elongate oval (Plate 1, A), dorsal and ventral lateral modified body setae short, cylindrical, moderately to strongly stout; rather numerous (Plate 1, B). Antennae with seven segments (Plate 1, C). Anterior and posterior spiracles large with the sclerotized operculum well developed and having the lateral edges rough or provided with a few minute indentations (Plate 1, D). Legs short and stout (Plate 1, E). *D. opuntiae* was recorded from few sites in the north of the country (Map 1). The infestation was high (cladodes totally covered with the scale) in Saham and Rfaid where *D. opuntiae* was first observed (Plate 1, F) and low (few colonies on the cladode) in Alshouna Shamaliyah (Table 1). Heavy infestation led to the death of cactus plants (Plate 1, G).

**Table 1.** Cactus localities sampled, their elevations and the severity of *Dactylopius opuntiae* in Jordan.

Location	Sampling date	Elevation (m)	Severity*
Saham	14.2.18	330	3
Kufr Soom	14.2.18	380	3
Rafaïd	9.2.18	440	3
Rafaïd	9.2.18	380	3
Sama Rousan	14.2.18	470	0
Al-Qasrin	14.2.18	470	0
Malka	17.2.18	390	0
Um-Qias	17.2.18	310	0
Alshouna Shamaliyah	24.2.18	-210 (below sea level)	1
Zmalyeh	3.3.18	-190 (below sea level)	0
Mukhaibah	3.3.18	20	0

\* Severity scale: 0 (no infestation); 1 (low infestation, less than 25 % of the pad surface was infested); 2 (medium infestation, 25-50 % of the pad surface was infested); 3 (high infestation, more than 50 % of the pad surface was infested).





**Plate 1.** *D. opuntiae*: A. Adult female (3 mm length); B. Dorsal cylindrical setae (40x); C. Antenna (40x); D. Spiracle (40x); E. leg (40x); F. Cochineal scale infested cladode; G. Dead cactus due to heavy infestation.

#### 4. Discussion

This is the first record of *D. opuntiae* from Jordan. Subsequent observations on cactus plants in areas southwards from the sites of initial records during March and April of 2018 in Amman area, Madaba, Wadi Al Walah and Wadi al Hidan, Dayr Alla, Wadi Al Huwarat, Abu Az Zeeghan, Sawalhah showed that cactus plants were uninfested which may suggest that the introduction of this insect into Jordan is recent. It may have been introduced naturally by wind, livestock, or birds coming from Palestine and/or Lebanon. It is highly expected that it has been recently introduced into Syria because most of the study records were from areas close to the Syrian border. It is probable that this invasive insect will spread

southwards in Jordan, and may infest most cactus plantations in the country unless an effective control program is implemented.

Moussa *et al.*, (2017) stated that the risk of the spread of this pest to new areas in Lebanon is very high and urgent eradication programs must be implemented. The predator *Cryptolaemus montrouzieri* Mulsant (Coleoptera: Coccinellidae) was found in association with the colonies of *D. opuntiae*, but its densities were too low to regulate the population of this new invasive pest.

After the first detection of *D. opuntiae* in Palestine in 2013 (Spodek *et al.*, 2014), its management with inundated releases of 100,000 adult predatory beetles of *C. montrouzieri* was apparently unsuccessful. Accordingly, two natural enemies were introduced from Mexico into Palestine; a predatory beetle, *Hyperaspis trifurcata*

(Coleoptera: Coccinellidae) and a predatory fly, *Leucopis bellula* (Diptera: Chamaemyiidae). Recently, individuals of *H. trifurcata* were released in the cochineal infested sites in the Galilee (Protasov *et al.*, 2017). The efficiency of these bioagents is not reported so far.

*D. opuntiae* is not attacked by parasitoids due to the presence of the carminic acid. Its predators in Mexico were studied by Vanegas-Rico *et al.* (2010). The most common species were *Leucopis bellula* (Diptera: Chamaemyiidae), *Symphorobius barberi* (Neuroptera: Hemerobiidae), and *Laetilia coccidivora* (Lepidoptera: Pyralidae). García *et al.*, (2016) listed the natural enemies of this pest which included the predatory fly larvae of Chamaemyiidae (*Leucopis bellula*), beetles of Coccinellidae (*Chilocorus cacti*, *Cryptolaemus montrouzieri*, *Exochomus* sp. *Hyperaspis trifurcata* and *Tenuisvalvae notata*), the brown lacewings of Hemerobiidae (*Symphorobius angustus* and *Symphorobius barberi*), the moth larvae of Pyralidae (*Laetilia coccidivora*), and larvae of the syrphid flies of Syrphidae (*Eosalingogaster cochenillivora* and *Salpingogaster* sp.).

Resistant cactus cultivars may be used to control *D. opuntiae* (Borges *et al.*, 2013). One biotype of *D. opuntiae*, the 'stricta' biotype, only survives on low-growing species such as *O. stricta*, while the other, the 'ticus' biotype, is associated with tree-like cacti, including *O. ficus-indica*. The 'stricta' biotype was used, with considerable success, for the biological control of *O. stricta* in Australia for over sixty years (Githure *et al.*, 1999).

The application of pyrethroid and organophosphate insecticides, mineral oils and neem oils were used in Mexico (Vannegas-Rico *et al.*, 2010) giving partial control. Heavy rain was reported to reduce the development of cochineal insects by dropping crawlers from the cladodes (Moran *et al.*, 1987).

An urgent action plan for controlling *D. opuntiae* in Jordan is needed. First of all, the current distribution of this pest should be determined by surveying all cactus plantations in Jordan. Heavily infested plantations should be eradicated which may include the destruction of the first clusters of infested plants, collecting fallen cladodes and burning abandoned cultivations. The transport of cactus plants or fruits from infested areas to pest-free areas must be prevented through internal quarantine regulations. The search for local natural enemies (predators) is important, and the release of introduced bioagents may be implemented if native populations were found insufficient or ineffective. The use of entomopathogenes such as *Fusarium incarnatum-equiseti* in combination with plant extracts may be a good option (Santos *et al.*, 2016; Carneiro-Leao *et al.*, 2017). Insecticidal sprays including powdered soap or liquid detergents in urgent situations could be used. In addition, Jordanian farmers should be encouraged to plant the resistant variety, *Nopalea cochenillifera* after conducting the necessary assessments regarding the suitability of this variety to Jordanian soils and climate.

## 5. Conclusions

The cochineal scale insect, *D. opuntiae* (Cockerell), was recorded from Jordan for the first time in several localities in the northern parts of the country. This invasive

insect species was most probably introduced from nearby countries only recently. Controlling procedures must be implemented urgently.

## Acknowledgment

The researchers extend their thanks to the workers at the GIS Unit in NCARE for drawing the distribution map for this research.

## References

- Aldawood AS, Al-Tuwariqi HA and Zimmermann HG. 2014. The biological control of *Opuntia stricta* var. *dillenii* (balas) in the Jizan Emirate of Saudi Arabia. Entomological Society of America. 62th Annual meeting "Grand Challenges Beyond Our Horizons". Portland, Oregon, USA.
- Borges LR, Santos DC, Cavalcanti VALB, Gomes EWF, Falcao HM and Da Silva DMP. 2013. Selection of cactus pear clones regarding resistance to carmine cochineal *Dactylopius opuntiae* (Dactylopiidae). *Acta Hort.*, **995**: 359–365.
- Bouharrou R, Amarraque A, Qessaoui R. 2016. First report of the *Opuntia* cochineal scale *Dactylopius opuntiae* (Hemiptera: Dactylopiidae) in Morocco. *Bulletin OEPP/EPPO Bulletin*, **46**(2):308-310.
- Carneiro-Leao MP, Tiago, PV, Medeiros, LV, Costa, AF and Oliveira, N. 2017. *Dactylopius opuntiae*: control by the *Fusarium incarnatum-equiseti* species complex and confirmation of mortality by DNA fingerprinting. *J Pest Sci.*, **90**: 925–933.
- Chávez-Moreno CK, Tecante A, and Casas A. 2009. The *Opuntia* (Cactaceae) and *Dactylopius* (Hemiptera: Dactylopiidae) in Mexico: a historical perspective of use, interaction and distribution. *Biodivers Conserv.*, **18**: 3337–3355.
- De Lotto G. 1974. On the status and identity of the cochineal insects (Homoptera: Coccoidea: Dactylopiidae). *J Entomol Soc Southern Afr.*, **37**: 167–193.
- Eisner T, Ziegler R, McCormick JL, Eisner M, Hoebeke ER and Meinwald J. 1994. Defensive use of an acquired substance (carminic acid) by predaceous insect larvae. *Experientia*, **50**: 610–615.
- EPPO Reporting Service no. 04 .2017. First report of *Dactylopius opuntiae* in Cyprus. Num. article: 2017/082.
- Flores-Hernandez A, Murillo-Amador B, Rueda-Puente EO, Salazar- Torres JC, Garcia-Hernandez JL and Troyo-Dieguez E. 2006. Reproduccion de cochinilla silvestre *Dactylopius opuntiae* (Homoptera: Dactylopiidae). *Revista Mexicana de Biodivers.*, **77**: 97–102.
- Foxcroft LC, and Hoffmann, JH. 2000. Dispersal of *Dactylopius opuntiae* (Cockerell) (Hemiptera: Dactylopiidae), a biological control agent of *Opuntia stricta* (Haw.) Haw (Cactaceae), in the Kruger National Park, South Africa. *Koedoe*, **43**: 1–5.
- García Morales M, Denno BD, Miller DR, Miller GL, Ben-Dov Y, Hardy NB. 2016. ScaleNet: A literature-based model of scale insect biology and systematics. Database. doi: 10.1093/database/bav118. <http://scalenet.info> Accessed August 2018.
- Githure CW, Zimmermann HG, Hoffmann JH. 1999. Host specificity of biotypes of *Dactylopius opuntiae* (Cockerell) (Hemiptera: Dactylopiidae): prospects for biological control of *Opuntia stricta* (Haworth) Haworth (Cactaceae) in Africa. *Afr. Entomol.*, **7**: 43–48.
- Hosking JR, Sullivan, PR, and Welsby, SM. 1994. Biological control of *Opuntia stricta* (Haw.) Haw. var. *stricta* using *Dactylopius opuntiae* (Cockerell) in an area of New South Wales,

Australia, where *Cactoblastis cactorum* (Berg) is not a successful biological control agent. *Agri Ecosys Environ.*, **48**: 241–255.

Moran VC, Hoffmann JH and Basson NCJ. 1987. The effects of simulated rainfall on cochineal insects (Homoptera: Dactylopiidae): colony composition and survival on cactus cladodes. *Ecol Entomol.* **12**: 51–60.

Moussa Z, Yammouni, D and Azar, D. 2017. *Dactylopius opuntiae* (Cockerell, 1896), a new invasive pest of the cactus plants *Opuntia ficus-indica* in the South of Lebanon (Hemiptera, Coccoidea, Dactylopiidae). *Bull Soc Entomol France*, **122** (2): 2017: 173-178.

Protasov A, Mendel Z, Spodek M and Carvalho CJ. 2017. Management of the Opuntia cochineal scale insect, *Dactylopius opuntiae* (Cockerell) in Israel. 'Alon Hanotea', **71**: 48-51.

Santos A, Oliveira R, Costa A, Tiago P and Oliveira N. 2016. Controlling *Dactylopius opuntiae* with *Fusarium incarnatum-mequiseti* species complex and extracts of *Ricinus communis* and *Poincianella pyramidalis*. *J Pest Sci.*, **89**: 539–547.

Spodek M, Ben-Dov Y, Protasov A, Carvalho CJ and Mendel Z. 2014: First record of *Dactylopius opuntiae* (Cockerell) (Hemiptera: Coccoidea: Dactylopiidae) from Israel. *Phytoparasitica*, **42**: 377-379.

Vanegas-Rico JM, JR Lomeli-Flores E. Rodríguez-Leyva, G Mora-Aguilera and JM Valdez. 2010. Natural enemies of *Dactylopius opuntiae* (Cockerell) on *Opuntia ficus-indica* (L.) Miller in Central Mexico. *Acta Zool. Mex. (n.s.)*, **26**(2): 415-433.



# The Genotoxic Potential of Alugbati Leaf Extracts on MCF-7 Cells

Darcy L. Garza<sup>1,\*</sup>, Rechel G. Arcilla<sup>3</sup>, Ma. Luisa D. Enriquez<sup>2,4</sup>, Maria Carmen S. Tan<sup>1</sup> and Marissa G. Noel<sup>1</sup>

<sup>1</sup>Chemistry Department; <sup>2</sup>Biology Department; <sup>3</sup>Mathematics Department; De La Salle University, 2401 Taft Avenue, Manila 1004, <sup>4</sup>Research and Biotechnology Division, St. Luke's Medical Center, 279 E. Rodriguez Sr. Avenue, Quezon City, Metro Manila, Philippines.

Received June 20, 2018; Revised August 24, 2018; Accepted August 28, 2018

## Abstract

To determine the genotoxicity of alugbati (*Basella alba* Linn. var. *rubra*) leaf extracts on breast adenocarcinoma, the Comet assay was employed on MCF-7 cells incubated with the following: lyophilized alugbati juice extracts reconstituted with 2 % DMSO (AJ) and in aqueous media (AJ2), and lyophilized alugbati hydrolysate (exogenous myrosinase (E.C. 3.2.3.1) assisted) re-dissolved with 2 % DMSO in culture media (AH). Untreated MCF-7 cells in 2 % DMSO served as the negative control. MANOVA and Post hoc Tukey's HSD were employed to determine statistically significant differences among the samples. First, mutant cells in AJ and AH formed pronounced comet tails indicating that DNA damage had occurred significantly compared to that of the control. Post hoc comparisons between AJ and AH indicated that both samples exhibited comparable effects to MCF-7 cells. Due to the similarity of AJ to AH, it was presumed that hydrolysis occurred during the mechanical process of juice extraction. Second, AJ2 exhibited analogous results with the control; whereas, AJ was found to be statistically different. Aberrant cells incubated with the control and AJ2 trials exhibited relatively minimal genotoxicity as evidenced by intact nuclei. Overall, multiple comparisons illustrated that the most prominent DNA damage was observed by extracts AJ and AH in all parameters. The results of this study suggested that alugbati leaves subjected to enzyme-assisted hydrolysis or juice extractions prepared in DMSO caused considerable DNA damage in MCF-7 cells.

**Keywords:** Alugbati, Glucosinolates, Myrosinase, Genotoxicity, Comet Assay, MCF-7, *Basella alba* Linn. var. *rubra*

## 1. Introduction

As of 2014, statistics showed that Asia accounts for approximately 50 % of the global incidence of cancer, and is projected to increase from 6.1 million in 2008 to 10.6 million cases in 2030 (Sankaranarayanan *et al.*, 2014). Among the fifteen Asian countries assessed by the Pfizer Medical Division, the Philippines was found to be ranked third with the highest cancer prevalence (McDonald *et al.*, 2008). In fact, the occurrence of malignant neoplasm continued to increase in the ten leading causes of mortality in the Philippines from 9<sup>th</sup> to 3<sup>rd</sup> in occurrence in only a span of two decades in the Philippines (Tayag *et al.*, 2011). In this regard, different dietary practices and nutrition have become a focus of several researches which are associated with the prevention of noncommunicable diseases such as cancer (Vainio and Weiderpass, 2006); (Key, 2011). Several epidemiological studies show that the consumption of fruits and vegetables was strongly linked to risk reduction of prevailing forms of cancer and that a diet rich in this food was suggested as a primary preventive factor (Tayag *et al.*, 2011; Rick *et al.*, 2013). Riboli and Norat (2003) proposed an intake of approximately of 350 grams of fruits and vegetables per day as proportional to the preventable level of cancer types

such as colorectal, esophageal and gastric. The high intake of fruits and vegetables were also correlated to the risk reduction of breast cancer by the hormone steroid receptor status (Emaus *et al.*, 2015). In addition, a large cohort of case studies recommended that the intake of cruciferous vegetables, such as broccoli, reduces the risk of stomach, colon and lung cancer. In general, dietary components such as flavonoids, phenolic compounds, and glucosinolates are the potential factors contributing to such health benefits (Johnson, 2002).



**Figure 1.** *Basella alba* Linn. var. *rubra* (alugbati).

*B. alba*, a relatively understudied but widely consumed vegetable grown in Asia is believed to exhibit a wide range of biological functions. This plant is very popular in the

\* Corresponding author e-mail: darcy.garza@dlsu.edu.ph.

central and southern Philippines, and is often a popular component of a concoction vegetable dish called “laswa” with its characteristic jelly-like consistency (Figure 1). Alugbati is recognized as a medicinal plant known for its antioxidant, antibacterial and anticancer potentials (Sushila *et al.*, 2010). The leaves and stem of alugbati have been used in Indian Ayurvedic treatments for curing diseases such as melanoma, leukemia and oral cancer. The traditional use of alugbati has been attributed and correlated to the presence of bioactive phenolics and flavonoids in the plant (Adhikari *et al.*, 2012). Moreover, preliminary screening in the laboratory showed that the extracts of alugbati species contain significant levels of glucosinolates (GSLs) (Malabed and Sandoval, De La Salle University – Manila, unpublished data). GSLs are phytochemicals and secondary metabolites known for the anticancer properties of their hydrolysis products. They are present along with myrosinase which is responsible for their enzymatic breakdown into various hydrolytic products such as isothiocyanates (ITCs) which are known to possess a number of marked biological activities (Calmes *et al.*, 2015). For instance, isothiocyanates were established to block metabolic activation and enhance the detoxification of chemically-induced carcinogens. Other breakdown products such as allyl-ITCs and benzyl-ITCs exhibited high bioavailability of up to 90 % in orally administered trials in bladder cancer cells, and decreased the growth of pancreatic tumor cells (Zhang, 2010; Boreddy *et al.*, 2011). Several studies have led to the proposal of some mechanisms and actions of GSL hydrolysis products on cancer. The induction of Phase II enzymes such as glucuronosyl transferase (GT) and glutathione S-transferase (GST), modification of steroid hormone metabolism, and protection against oxidative damages are the general ways by which these compounds exhibit their anticancer properties (Das *et al.*, 2000).

This research is aimed at determining the genotoxic capabilities of the juice and semi-purified enzymatically-hydrolyzed preparations of *B. alba* on breast adenocarcinoma immortalized cell line. To the best of the researchers' knowledge, this is the first reported study using this methodology of genotoxicity analyses on the extracts of *B. alba* against the aforementioned MCF-7 cells.

## 2. Materials and Methods

### 2.1. Preparation of Alugbati Juice Samples

Fresh alugbati leaves were chopped and blended with a small amount of water. The mixture was filtered to separate the juice from the pulp. The alugbati juice was frozen and lyophilized using a Labconco Freeze Dry System/Frozone®. Prior to the assay, 0.034 g lyophilized alugbati juice was reconstituted in 10 mL DMSO (AJ), and 0.095 g of the powdered sample was reconstituted in 10 mL distilled water (AJ2).

### 2.2. Preparation of Alugbati Hydrolysate

Fresh alugbati leaves were cut into small pieces, and were frozen and lyophilized. About 2.0 g of ground freeze-dried samples were mixed with 30.0 mL distilled water, and 100.0 µL myrosinase (E.C. 3.2.3.1) (3 units/mL). The hydrolysis mixture was homogenized and incubated for one hour at room temperature. 30.0 mL of the solvent

DCM was added to the hydrolysate. The mixture was centrifuged for three minutes at 4000 rpm, and the organic layer was separated from the aqueous layer. The organic layer was dried over anhydrous Na<sub>2</sub>SO<sub>4</sub> and was subsequently concentrated in a rotary evaporator (Malabed and Noel, 2012). The extract weighing 0.017g was dissolved in 10 mL DMSO (AH).

### 2.3. Comet Assay (Single cell gel electrophoresis)

Human breast adenocarcinoma cell line (MCF-7) was treated with extracts AJ, AJ2 and AH. Untreated MCF-7 cells in DMSO served as the negative control. MCF-7 cells, in complete growth medium, composed of Dulbecco's Modified Eagle Medium (DMEM, ThermoFisher Scientific Gibco®, USA) containing 10 % fetal bovine serum (FBS, Thermo Fisher Scientific, Gibco®, USA), and 1x antibiotic- antimycotic (Thermo Fisher Scientific, Gibco®, USA), and kept at 37°C with 5 % CO<sub>2</sub> in a 98 % humidified incubator, were placed in separate flat-sided culture test tubes and were incubated with 15 µL extract AJ, 10 µL of extract AJ2 and 25 µL of hydrolysate AH resulting in 0.75 % (v/v) DMSO, 0.53 % (v/v) water and 1.25 % (v/v) DMSO in solution, respectively. After twenty-four hours, the cells were harvested and incubated with 2 mL trypsin-EDTA and 5 % CO<sub>2</sub> at 37°C for five minutes. Subsequently, 4 mL 1 x PBS was added, and the mixture was centrifuged for ten minutes at 22°C and 1,200 rpm. The pellet was re-dissolved in PBS, transferred to an Eppendorf tube, and subjected to comet assay.

The bioassay was performed using Trevigen's reagent kit for Comet Assay® and the assay protocol specified by Trevigen Inc. (Gaithersburg, USA) was followed. About 50 µL of the cell culture mixture (250 µL low melting agarose and 25 µL of the MCF-7 cells) was layered onto the wells of the Comet slide and placed in the dark at 4°C until the mixture solidified. After that, the slides were immersed in a pre-chilled lysis solution for one hour at 4°C. Consequently, the slides were incubated in the dark with 50 mL alkaline unwinding solution (pH>13 (200 mM NaOH, 1 mM EDTA)) for twenty minutes at room temperature. Electrophoresis was performed as described in the Trevigen's Alkaline Comet Assay protocol. Following electrophoresis, the air-dried slides were stained with 50 µL of SYBR Green, and after subsequent drying, the images were captured using fluorescence microscopy.

Statistical evaluations of the different preparations of *B. alba* leaves (AJ, AJ2, and AH) were done on all the accumulated data gathered from the Comet assay. DNA damage was evaluated by measuring three parameters: tail length (TL) of the resulting fragmented DNA, the percentage of DNA in tail (%DNA), and the tail moment (TM). Cells with extensive DNA single and double stranded fragmentations were characterized according to the degree of nucleic dispersion and migration visualized as pronounced tails. The resulting images of cells or comets were scrutinized using OpenComet and ImageJ software.

### 2.4. Statistical Analyses

Multivariate analysis of variance (MANOVA) test was performed using SAS 9.3 Software and graphical representations were plotted using GraphPad Prism 7.04. Pillai's Trace was used with statistical significance level



(a) of  $p \leq 0.05$ . Post-hoc Tukey's honest significant difference (Tukey's HSD) was performed in the three dependent variables, and values of the least square means were also compared. Treatments having the same letter were considered not significantly different at 95 % confidence level.

### 3. Results

#### 3.1. Comparison of the Alugbati Juice Extract and Hydrolysates in DMSO

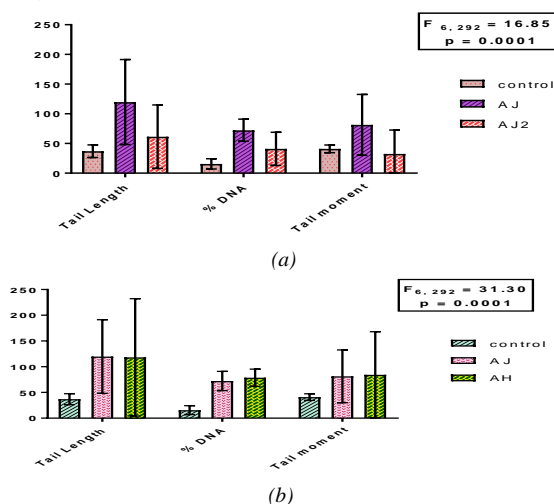
Lyophilized alugbati juice (AJ) and alugbati hydrolysate (AH), both in DMSO, were assessed for possible genotoxic effects on MCF-7 cell lines. The mean scores and corresponding standard deviations (SD) in the three parameters (TL, %DNA, and TM) for the control, AJ and AH were presented in Table 1 and Figure 2. The control exhibited minimal DNA damage for TL ( $36.98 \pm 10.56$ ), %DNA ( $15.55 \pm 8.66$ ) and TM ( $40.95 \pm 6.37$ ).

**Table 1.** Post hoc comparison: Tukey's HSD on *B. alba* trials.

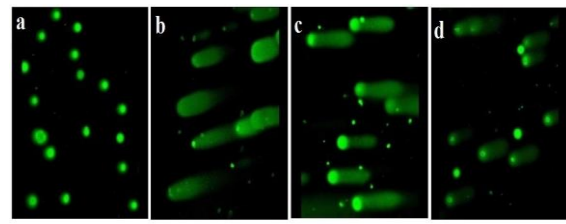
Extract	Parameter		
	TL	%DNA	TM
control	$36.99 \pm 10.56^b$	$40.95 \pm 8.66^b$	$15.55 \pm 6.37^b$
AJ	$119.74 \pm 71.61^a$	$72.27 \pm 18.65^a$	$81.40 \pm 51.30^a$
AH	$118.18 \pm 114.11^a$	$78.64 \pm 16.69^a$	$84.22 \pm 83.75^a$
AJ2	$61.40 \pm 53.47^b$	$40.96 \pm 27.89^b$	$32.44 \pm 40.12^b$

\* Means with the same letter are not significantly different.

MCF-7 cells incubated with AJ and AH extracts showed loss of DNA integrity and substantial migration represented in numerous comets with extensive tails compared to the control with intact nuclei (Figure 3). Moreover, comets parameters of AJ (TL =  $119.74 \pm 71.61$ ; % DNA =  $72.27 \pm 18.65$ ; TM =  $81.40 \pm 51.30$ ) and AH (TL =  $118.18 \pm 114.11$ ; % DNA =  $78.64 \pm 16.69$ ; TM =  $84.22 \pm 83.75$ ) (Table 1 and Figure 2). Multivariate testing indicated that there was a statistically significant difference between the parameters of the control with both AJ and AH ( $F(6, 292) = 31.30$ ,  $p = 0.0001$ ; Pillai's trace = 0.78).



**Figure 2.** Comparison of the comet assay parameters incubated with the (a) AJ and AH and with (b) AJ and AJ2.



**Figure 3.** Images of MCF-7 cells subjected to Comet assay: (a) control (b) AJ (c) AH (d) AJ2.

#### 3.2. Comparison of Alugbati Juice Extracts in Water and DMSO

The effect of changes in the matrix (lyophilized alugbati juice in DMSO (AJ) and in water (AJ2)) was observed to verify if the solubility of the constituents played a role in the genotoxicity of *B. alba* extracts. In addition, untreated MCF-7 cells in 2 % DMSO served as the negative control, and the results of the assay divulged that the solvent did not exhibit significant genotoxicity to the untreated cells. As seen in Table 1, data gathered for AJ were considerably different compared to the control (TL =  $36.98 \pm 10.56$ ; %DNA =  $40.95 \pm 8.66$ ; TM =  $15.55 \pm 6.37$ ) and AJ2 (TL =  $61.40 \pm 53.47$ ; %DNA =  $40.96 \pm 27.89$ ; TM =  $32.44 \pm 40.12$ ) in all the generated data. AJ (TL =  $119.74 \pm 71.61$ , %DNA =  $72.27 \pm 18.65$  and TM =  $81.40 \pm 51.30$ ) showed the most substantial DNA damage. However, the resulting images for AJ2 (Figure 3) exhibited fewer moderate to extensive diffused nuclei. In comparison with AJ, comets from AJ2 exhibited relatively shorter comet tails and the fluorescence of the comets were faint and less prominent. The findings dictate that greater DNA damage occurred in MCF-7 incubated with AJ compared to AJ2.

The outcome of the Pillai's trace statistics,  $F(6, 292) = 16.85$ ,  $p = 0.0001$ ; Pillai's trace = 0.51, signified that there were statistical differences between the control, AJ, and AJ2. Post hoc analyses showed that AJ was significantly different from the control and AJ2. This implied that the alugbati juice in DMSO exhibited significant DNA damage and genotoxicity to MCF-7 cell lines. On the other hand, the control and AJ2 were statistically equivalent indicating that the two exhibited the same effect.

### 4. Discussion

The Comet assay is one of the most sensitive techniques that can observe genotoxic effects in cancer cells (Florent *et al.*, 1999). Several factors could initiate DNA damage such as ionizing radicals, topoisomerases inhibitors, alkylating agents, sulfonates, *etc.* (Cann and Hicks, 2007). Bioactive constituents have been found to initiate DNA double strand breaks through the alkylation of DNA bases; consequently, DNA helices are disrupted and DNA breaks are induced. Elevation of reactive oxygen species levels trigger oxidative stress which also leads to unstable genomic processes of cells and double strand breaks (George and Rupasinghe, 2017). The appearance and formation of comets with pronounced tails in the assay were indicative of DNA strand breaks caused by pretreatments of the cells. The present investigation was performed to determine whether the extracts from *B. alba*

leaves could cause substantial DNA damage on MCF-7 cells and possess chemopreventive properties.

Alugbati juice's pharmacognosy has been reported to be linked to constituents such as flavonoids, phenolics and intact GSLs (Tongco *et al.*, 2015); Myrosinase assisted hydrolysis of GSLs primarily produce degradation products specifically ITCs (Angelino *et al.*, 2015). The evaluation of the collected images of comets from **AJ** and **AH** trials suggested that the presence of bioactive compounds in the juice extract which could consist of hydrolysis products can cause genotoxicity against breast adenocarcinoma. During the preparation of extracts **AJ** and **AJ2**, it was observed that powdered alugbati juice was soluble in DMSO, but partially dissolved in water. The results of the Comet assay exhibited that the extracts reconstituted with DMSO had greater efficacy due to the polar-aprotic solvent which had the capability to dissolve both polar and small nonpolar compounds (Capriotti and Capriotti, 2012). Even though the results of the water extract did cause minimal nucleic fragmentation, the bioactive constituents may not have been completely soluble, and therefore did not contribute to substantial genotoxicity on the MCF-7 cell line. Since the two extracts, **AJ** and **AJ2**, were prepared using the same freeze-dried alugbati juice, it may be inferred that the difference in their genotoxicity could be attributed to the solvent used.

Herbal extracts of *B. alba* were shown to exhibit immense anti-inflammatory, antioxidant, antibacterial, antifungal, and anti-ulcer activities (Sushila *et al.*, 2010). Such observations were correlated to the considerable concentrations of flavonoids, phenolics and betalains present in the plant (Kumar *et al.*, 2015). Cytotoxicity studies proposed that alugbati extracts exhibit chemotherapeutic actions through the following: modification of the permeability of mutagens through membranes, and prevention of mutagen transfer into cytosols by binding or inserting phenolics into the transporters of the outer cell membrane (Adhikari *et al.*, 2012). In another research, MTT assay showed that the red-stem variety of alugbati showed strong cytotoxicity against cervical carcinoma cells after a twenty-four-hour treatment with 50 mg/mL *B. alba* extract. Morphological changes, such as shrinkage and blebbing of the cancer cells, and the significant decrease of the live cancer cell count were indicative of the genotoxic activity of the alugbati extract (Kumar *et al.*, 2015).

It was found from preliminary studies in the laboratory that alugbati contained significant levels of GSLs which could be a possible cause of its genotoxic activities against MCF-7 cells. Fifteen local vegetables were analyzed for their total GSL content, and it was found that alugbati contains the highest levels of GSLs (85.30  $\mu\text{mol/g}$ ) (Malabed and Sandoval, De La Salle University – Manila, unpublished data). Moreover, initial identification of GSLs in *B. alba* indicated that extracts could also contain breakdown products such as isothiocyanates. Tan, *et al.* (2017) proposed pathways by which ITCs which could direct cell death. Inhibition of Phase I enzyme generates electrophiles, and introduces polar groups to xenobiotics. Consequently, activation of Phase II enzymes via antioxidant response factors (ARE) detoxifies and aids in the excretion of these carcinogens. It was observed that ITCs participate in mercapturic acid pathway in certain

cancer cells. In this pathway, depletion of GSH level result in the activation of caspase dependent pathways, and the increase of S-thiocarbamoyl derivatives activates the expression of tumor suppressor genes (p53, Ink 4A, BRCA 1 & 2, ATF 2) both of which leads to cell death. Cell toxicity of hydrolysis products such as ITCs and indole-3-carbinol had been primarily studied on human lung, breast and prostate cancer cell lines in order to determine their anti-tumor activities. ITCs are known to cause pathogen and fungal death through the induction of cellular oxidative stress and redox homeostasis which causes glutathione depletion. It was found that such mechanisms were similar to its cellular targets in the said mammalian cancer cells. This observation corroborates the effects of ITCs in human lung, breast and prostate cancer cell lines (Calmes *et al.*, 2015).

## 5. Conclusion

The analyses of the Comet assay on MCF-7 cells exhibited that lyophilized alugbati juice (**AJ**) and hydrolysate (**AH**) trials, both in 2 % DMSO, displayed notable DNA damage to the mutant cells observed by the appearance of pronounced tails. No significant differences were found between the genotoxic effects of the **AJ** and **AH** extracts which were attributed to the possibility of hydrolysis also taking place during the juice extraction. Moreover, determining the effects of change in the matrix revealed that alugbati juice in 2 % DMSO (**AJ**) exhibited greater DNA damage compared to the alugbati juice extract reconstituted in water (**AJ2**). Evidence was found to indicate that the bioactive constituents which possibly induced nucleic fragmentation were more soluble in DMSO than in water. Generally, extracts **AJ** ( $TL = 119.74 \pm 71.61$ ;  $PD = 72.27 \pm 18.65$ ;  $TM = 81.40 \pm 51.30$ ) and **AH** ( $TL = 118.18 \pm 114.11$ ;  $PD = 78.64 \pm 16.69$ ;  $TM = 84.22 \pm 83.75$ ) resulted in the most significant damage to MCF-7 cells. Overall, the current research shows that the extracts from *B. alba* caused significant DNA damage to MCF-7 cells. It supports preliminary studies on the biochemical constituents of alugbati as well as possible GSLs affirming significant chemotherapeutic properties of the plant extracts. To the researchers' knowledge, this is the first research that reports the genotoxic activity of alugbati extracts against breast cancer cells. A thorough and extensive investigation is recommended to further characterize the bioactive compounds and glucosinolates present in alugbati, and it will now be of interest to establish specific mechanisms by which alugbati constituents trigger cell cycle arrest on MCF-7 cells.

## Acknowledgement

The authors would like to thank the Research and Biotechnology Division of St. Luke's Medical Center.

**Financial support and sponsorship:** Metro Manila Health Research and Development Consortium, Philippine Council for Health Research and Development – Department of Science and Technology, De La Salle University Challenge Grant and St. Luke's Medical Center are gratefully acknowledged.



## References

- Adhikari R, HN Kumar N and SD S. 2012. A review on Medicinal Importance of *Basella alba* L. *Int J Pharm Sci Drug Res.*, **4(2)**: 110-114.
- Angelino D, Dosz EB, Sun J, Hoefflinger JL, Van Tassell M, Chen P, Harnly JM, Miller MJ and Jeffrey EH. 2015. Myrosinase-dependent and -independent formation and control of isothiocyanate products of glucosinolate hydrolysis. *Front Plant Sci.*, **6(831)**: 1-6.
- Boreddy SR, Sahu RP and Srivastava SK. 2011. Benzyl Isothiocyanate Suppresses Pancreatic Tumor Angiogenesis and Invasion by Inhibiting HIF- $\alpha$ /VEGF/Rho-GTPases: Pivotal Role of STAT-3. *PLoS ONE*, **6(10)**: 1-12.
- Calmes B, N'Guyen G, Dumur J, Brisach CA, Campion C, Iacomini B, Pigne S, Dias E, Marcheret D, Guillemette T and Simoneau P. 2015. Glucosinolate-derived isothiocyanate impact mitochondrial function in fungal cells and elicit and oxidative stress response necessary for growth recovery. *Front Plant Sci.*, **6(414)**: 1-14.
- Cann, KL and Hicks GG. 2007. Regulation of the cellular DNA Double Strand Break Response. *Cell Biol.*, **85**: 663-674.
- Capriotti K and Capriotti JA. 2012. Dimethyl Sulfoxide: History, Chemistry and Clinical Utility in Dermatology. *J Clin Aesthet Dermatol.*, **5(9)**: 24-26.
- Das S, Tyagi AK and Kaur H. 2000. Cancer modulation by glucosinolates: a review. *Dairy Cattle Nutrition Division*, **79(12)**: 1665-1671.
- Florent M, Godard T, Ballet JJ, Gauduchon P and Sola B. 1999. Detection by the comet assay of apoptosis induced in lymphoid cell lines after growth factor deprivation. *Cell Biol Toxicol.*, **15**: 185-192.
- George VC and Rupasinghe HPV. 2017. Apple Flavonoids Suppress Carcinogen-Induced DNA Damage in Normal Human Bronchial Epithelial Cells. *Oxid Med Cell Longev*, **2017**.
- Emaus MJ, Peeters PH, Bakker MF, Overvad K, Tjønneland A, Olsen A, ... van Gils CH. 2015. Vegetable and fruit consumption and the risk of hormone receptor-defined breast cancer in the EPIC cohort. *Am J Clin Nutr.*, **103(1)**: 168-177.
- Key TJ. 2011. Fruits and vegetables and cancer risk. *British Journal of Cancer*, **104(1)**: 6-11.
- Kumar SS, Manoj P, Giridhar P, Shrivastava R and Bharadwaj M. 2015. Fruit Extracts of *Basella rubra* that are rich in bioactives and betalains exhibit antioxidant and cytotoxicity against human cervical carcinoma cells. *J. Funct. Foods*, **15**:509-515.
- Johnson IT. 2002. Glucosinolates in the human diet. Bioavailability and implications for health. *Phytochem Reviews*, **1**: 183-188.
- Malabed RS and Noel MG. 2012. Characterization of the glucosinolates and Isothiocyanates in
- Malunggay (*Moringa oleifera* L.) Extracts and Determination of their Myrosinase Activity and Anticancer Properties. De La Salle University – Manila, Philippines.
- McDonald M, Hertz R and Lowenthal P. 2008. **Pfizer Facts: The Burden of Cancer in Asia**. Pfizer Medical Division, USA.
- Riboli E and Norat T. 2003. Epidemiologic evidence of the protective effect of fruit and vegetables on cancer risk. *Am J Clin Nutr.*, **78(3)**: 559-569.
- Rick A, Barnes C, Burke A, Gansler T, Gapstur S, Gaudet M, Kramer J, Newman LA, Niemeyer D, Richards C, Runowicz C, Saslow D, Simpson S, Smith R, Runowicz C, Saslow D, Simpson S and Sullivan K. 2013. **Breast Cancer Facts and Figures 2013-2014**. American Cancer Society, Inc. Atlanta, USA.
- Tan MCS, Enriquez MLD, Arcilla RG and Noel MG. 2017. Determining the Apoptotic-Inducing Property of Isothiocyanates Extracted from Three Cultivars of *Raphanus sativus* Linn. Using the Comet Assay. *J App Pharm Sci.*, **7(9)**: 044-051.
- Sankaranarayanan R, Ramadas K and Qiao Y. 2014. Managing the changing burden of cancer in Asia. *BMC Med.*, **12(3)**: 1-17.
- Sushila R, Deepti A, Permender R, Madhavi T and Dharmender R. 2010. Cytotoxic and antibacterial activity of *Basella Alba* whole plant: A Relatively unexplored plant. *Pharmacol online*, **3**:651-658.
- Tayag EA, Benegas-Segarra A, Sinson FA, Rebanal LMR and Timbang T. 2011. **The 2011 Philippine Health Statistics, Department of Health, National Epidemiology Center**. Statistics and Publication Section, Philippines.
- Tongco JVV, Anis AD and Tamayo JP. 2015. Nutritional analysis, phytochemical screening, and total phenolic content of *Basella alba* leaves from the Philippines. *Int. J. Pharmacognosy Phytochem. Res*, **7(5)**: 1031-1033.
- Vainio H and Weiderpass E. 2006. Fruit and vegetables in cancer prevention. *Nutr Cancer*, **54(1)**: 111-142.
- Zhang Y. 2010. Allyl isothiocyanate as a cancer chemopreventive phytochemical. *Mol. Nutr. Food Res*, **54(1)**: 1-16.



# The Importance of Zinc-Mobilizing Rhizosphere Bacteria to the Enhancement of Physiology and Growth Parameters for Paddy under Salt-Stress Conditions

Yachana Jha\*

N. V. Patel College of Pure and Applied Sciences, S. P. University, V. V. Nagar, Anand (Gujarat), India.

Received July 15, 2018; Revised August 15, 2018; Accepted August 30, 2018

## Abstract

Rhizosphere bacteria are a group of metal-mobilizing and plant growth-promoting bacteria having the ability to solubilize minerals such as zinc. This plant growth-promoting bacterium, which lives symbiotically in/on the root surface, helps directly or indirectly in promoting plant growth. Zinc is one of the essential micronutrients required for optimum plant growth, and plays a vital role in metabolism. It is necessary in low concentrations, and is critically required for the functioning of several plant physiological processes. Zinc deficiency is the most widespread micronutrient disorder in rice (*Oryza sativa*). Out of the twenty-five isolates used in this study, two selected ones, namely, *Bacillus pumilus* and *Pseudomonas pseudoalcaligenes*, were evaluated for the ability to solubilize zinc and for their growth-promotion efficiency on rice in the greenhouse. Zinc-mobilizing bacteria protect plants from salinity injuries by enhancing their growth-related physiology, such as chlorophyll, carotenoid, and antioxidant enzymes catalase (CAT), peroxidase (PO). Plants inoculated with Zn-mobilizing bacteria (ZMB) also accumulate soluble carbohydrates in leaves under salinity, which helps plants overcome osmotic stress.

**KeyWords-** Zinc mobilizing bacteria, Paddy, Salinity, Chlorophyll, Carotenoid, Catalase (CAT), Peroxidase (PO).

## 1. Introduction

Salt stress is an increasingly global problem which affects major parts of the global agricultural lands. Some states of India, such as the Gujarat state, have a total coastal length of about 1600 Km, as many districts of the Gujarat state including Valsad, Navsari, Surat and Bharuch have their western boundaries on the Arabian Sea (Garg and Patel, 2007). A high amount of salinity may affect the plant in several ways such as water stress, reduction and expansion of cell division, oxidative stress, and nutritional disorders (Zhu, 2007). The long-term exposure of plants to salinity makes plants experience ionic stress, which may lead to a premature deterioration of adult leaves, affecting the photosynthetic area available to support the continued growth. In fact, excess sodium and more importantly chloride have the potential to affect plant enzymes and cause cell swelling, resulting in reduced energy production and other physiological changes (Larcher, 1980). Hence, arid and semiarid areas of Indian agro ecosystems are often deficient in important minerals including phosphorus, potassium, and zinc. For a proper growth and development, plants need several macro- and micronutrients. The macronutrients including nitrogen (N), phosphorus (P), potassium (K), calcium (Ca), and the micronutrients including iron (Fe), boron (B), chlorine (Cl), manganese (Mn), zinc (Zn), and copper (Cu) are

supplemented through inorganic or organic forms when taken up by the plant roots along with water.

Zinc (Zn) is one of the eight essential micronutrients required for the healthy growth and reproduction of crop plants. For an optimum plant growth, Zinc is required relatively in small concentrations ( $5\text{--}100\text{mg kg}^{-1}$ ), and plays an important role in metabolism. Similar to nitrogen, phosphorus and potassium, zinc deficiency has been found widespread and responsible for yield reduction in rice (Fageria *et al.* 2002). In plants, zinc also acts as a regulator being a constituent of more than sixty-five different enzyme systems of drought tolerance and water-use efficiency (Assunção *et al.* 2010). Cereal species greatly differ in their zinc efficiency which is defined as the ability of a plant to grow and yield well under Zn deficiency. All crops require Zn, especially high carbohydrate plants such as rice, potatoes, etc. Although Zn is not an essential component of cell structure, it regulates many biochemical processes essential for growth, development and seed production. Zn solubility is highly dependent upon soil pH and moisture. Bacteria play an important role in mobilizing nutrients' requisites by the plants to some extent. Microbes are a potential alternate which can provide plant zinc requirements by solubilizing the complex zinc in the soil. Microbes solubilize the metal forms by protons, chelated ligands, and oxido-reductive systems that are present on the cell surface and membranes (Hughes and Poole, 1991). Rhizobacteria genera belonging to *Pseudomonas* spp. and *Bacillus* spp. are reported to

\* Corresponding author e-mail: yachanajha@gmail.com.

solubilize zinc. Thus, the identification of efficient microbial strains capable of solubilizing minerals rapidly can conserve the existing resources, and avoid environmental pollution hazards caused by the excessive usage of chemical fertilizers.

Salt stress adversely affects plant nutrient acquisition, especially in the root, resulting in a significant decrease in shoots dry biomass (Jha and Subramanian, 2016). The collaboration of plant growth-promoting bacteria, especially Zn-mobilizing bacteria (ZMB), and their effect on the biological growth response of plants under soil salinity are complex. The effect of the inoculation of ZMB in plants, alone or in groups in conferring tolerance to plants against adverse environmental conditions has been analysed. Its effect in improving other nutrient availability to help the plant overcome osmotic stress by the accumulation of soluble sugar has also been analysed. Such change has been correlated with variation in the antioxidant enzymes such as catalase and peroxidase activity, photosynthesis rate, leaf greenness, and other growth-promotion parameters including plant height, dry weight, etc.

## 2. Materials and Methods

### 2.1. Isolation, Identification and Zinc Solubilization Assay

Rhizobacteria were isolated and identified by 16S rDNA analysis from the rice field as per the researchers' published method (Jha, 2017). The growth-promotion efficiency of the isolates was analyzed in terms of their ability to solubilize zinc by inoculating it on to the modified Pikovskaya medium (Pikovskaya, 1948), containing 1 % insoluble zinc compounds (a) ZnO, (b) ZnCO<sub>3</sub>, and (c) Zn (PO<sub>3</sub>)<sub>4</sub>. A loopful of a forty-eight-hour bacterial culture was inoculated on the prepared plates. All the plates were incubated for forty-eight hours at 28°C for five days. The halo zone around the colony and the colony growth were measured, and the Zn solubilization efficiency was tested (Gontia-Mishra *et al.*, 2017).

Solubilization efficiency = Solubilization diameter/ Diameter of colony growth X 100.

They were subjected to further experimental studies such as quantitative estimation (broth assay), the influence of the isolates on the pH of the medium, and the production of gluconic acid and auxin.

### 2.2. Quantitative Estimation of Zinc Mobilization

A loopful of a forty-eight- hour bacterial culture was inoculated into 25 mL modified Pikovskaya broth in a 50 mL capacity flask and was incubated at 28±2°C for ten days. The growth suspension was centrifuged at 7,000 g for ten minutes to separate the supernatant from the cell growth and the insoluble Zn. One mL of the supernatant was taken in a 50 mL volumetric flask, and the volume was made to 50 mL with distilled water and was mixed thoroughly. The solution was fed to an atomic absorption spectrometer to determine the Zn content. A standard curve was prepared using various concentrations of a 10 ppm ZnCl solution. The amount of zinc solubilized by the bacterial isolates was calculated from the standard curve.

### 2.3. Influence of Zinc Solubilizing Organisms on pH of the Growth Medium

The selected strains were inoculated in the flasks containing 50 mL of sterilized modified Pikovskaya medium containing 0.1% of ZnO, ZnCO<sub>3</sub> and Zn(PO<sub>3</sub>)<sub>4</sub> as insoluble sources. An un-inoculated sample was also maintained. The samples were analyzed on the sixth, eighth, and tenth day after incubation. The bacterial cultures were centrifuged at 15,000 rpm for ten minutes and were filtered using Whatman No. 42 filter paper. The pH of the ZMB culture filtrates was measured using a pH meter (Elico).

### 2.4. Quantitative Estimation of IAA by Zinc Solubilization

The selected bacterial isolates were tested for their ability to produce IAA by inoculation in the flasks containing 50 mL of sterilized modified Pikovskaya medium supplemented with 0.1 % ZnO. Another set devoid of Zn material was also inoculated. All the treatments were amended with 0.1 % tryptophan and were incubated for seven days. The quantity of IAA produced by the organisms was estimated by the method of Brick *et al.* (1991).

### 2.5. Rice Cultivation and Inoculation

Seeds of rice, variety GJ17, were germinated, and the seedling was inoculated with isolates as per the published method of the researchers (Jha and Subramanian, 2014a). Seven-day-old ZMB inoculated rice plants were carefully removed from different test tubes inoculated with the strain of bacterium, and were planted in a pot. Similarly, the control plants (un-inoculated) were also transferred to a fresh pot. Soil samples were collected from wet rice fields possessing the following physio-chemical properties, pH: 7.79, electrical conductivity 1063 µS/cm, CEC:3 cmol, organic carbon: 5500 mg per kg, available nitrogen 200 mg per square decimeter, available Ca: 12.1cmol, available P 205 : 9.5 mg per square decimeter, available K 20 : 265 mg per kg, Fe: 3.1 mg per kg, Zn: 285 mg per kg, Mn: 3.7 mg per kg, and Cu : 2.2 mg per kg. All the seedlings were grown for four weeks without any fertilizer treatment. The experiment was conducted in a greenhouse at 20 to 25 °C with a relative humidity of 70 to 80 % according to the published method of (Jha and Subramanian, 2014b).

### 2.6. Effect of Isolates on Chlorophyll and Carotenoid Content under Salinity

Pigments were extracted from the leaves of the seedlings treated with 13.0 dS m<sup>-1</sup> salt for fourteen days. The extraction of the leaf pigments was performed with 80 % acetone, and the absorbance at 663 and 645 nm was measured with a Hitachi U-2000 dual length spectrophotometer. The chlorophyll a, chlorophyll b, and total chlorophyll quantities were calculated according to the method of Arnon (1949). The total carotenoid content was measured at 470 nm. The pigment concentrations were expressed as µg g<sup>-1</sup> fresh weight (FW).

### 2.7. Enzyme Extraction and Enzyme Assay

Leaves (2 g) were homogenized with a mortar and pestle in 4 ml of ice-cold 50 mM Tris-acetate buffer pH 6.0, containing 0.1mM of ethylene diamine tetra-acetic acid (EDTA), 5 mM of cysteine, 2 % (w/v)

polyvinylpyrrolidone (PVP), 0.1mM of phenyl methyl sulphonyl fluoride (PMSF) and 0.2 % (v/v) Triton X 100. The homogenate was centrifuged at 12,000 g for twenty minutes, and the supernatant was filtered through Sephadex G-25 column equilibrated with the same buffer used for homogenization. The column elution was used as the enzyme source for the determination of enzyme activity. All operations were performed at 4°C. Protein concentration was determined by taking OD at 595 nm according to Bradford, (1976) using bovine serum albumin as a standard.

### 2.8. Measurement of Soluble Sugar Contents

Soluble sugars were determined based on the method of phenolsulfuric acid (Dubois *et al.* 1956). A half gram (0.5g) fresh weight of the roots and shoots was homogenized with deionized water. The extract was filtered and treated with 5 % phenol and 98 % sulfuric acid. The mixture remained for one hour, and the absorbance was determined at 485 nm by a spectrophotometer (Biochrom S 2100). Contents of soluble sugar were expressed as mg g<sup>-1</sup> FW.

### 2.9. Estimation of Catalase (CAT) Activity

CAT activity was assayed by measuring the initial rate of disappearance of H<sub>2</sub>O<sub>2</sub> (Bergmeyer, 1970). The reaction mixture consisted of 3 % H<sub>2</sub>O<sub>2</sub> and 0.1 m mol L<sup>-1</sup> EDTA in a 0.05 mol L<sup>-1</sup> Na-phosphate buffer (pH 7) and 0.1mL enzyme from the plant source. The decrease in H<sub>2</sub>O<sub>2</sub> is followed as the decline in optical density at 240 nm, and the activity is calculated as mmol H<sub>2</sub>O<sub>2</sub> consumed per minute. All tests were carried out in triplicate.

### 2.10. Estimation of Peroxidase (PO)

A leaf sample (1g) was homogenized in 1 mL of 0.1 M phosphate buffer, pH 7.0 at 4 °C. The homogenate was centrifuged at 12000 g at 4 °C for fifteen minutes, and the supernatant was used as the enzyme source. The reaction mixture consisted of 1.5 mL of 0.05 M pyrogallol, 0.5 mL of the enzyme extract and 0.5 ml of 1 % H<sub>2</sub>O<sub>2</sub>. The reaction mixture was incubated at room temperature. The change in O.D was recorded at 420 nm at thirty-second intervals for three minutes. The enzyme activity was expressed as changes in the absorbance min<sup>-1</sup>g<sup>-1</sup>protein (Hammerschmidt *et al.*; 1982). All tests were carried out in triplicate.

### 2.11. Statistical Analysis

Each pot was considered as replicate, and all of the treatments were repeated three times. A two-way analysis of variance (ANOVA) was performed using STATISTICA program. The means and the calculated standard errors are reported. Significance was tested at a 5 % level.

## 3. Results

Out of twenty-five isolates, the *P. pseudoalcaligenes* and *B. pumilus* strong Zn solubilizers were identified and inoculated in the modified Pikovskaya medium containing different insoluble sources (ZnO, ZnCO<sub>3</sub> and Zn(PO<sub>3</sub>)<sub>4</sub>) of Zn at 0.1 % and area of zone of inhibition was maximum 23.6 mm<sup>2</sup> by *P. pseudoalcaligenes*. The solubilization efficiency of the isolates was calculated by measuring the diameter of the colony growth and the solubilization zone.

The zinc- solubilizing potential varied from one isolate to another, and the solubilization efficiency ranged between 312 % and 341% in ZnO, indicating its dependence on the zinc sources used (Table 1).

In the quantitative assay, the bacterial isolates were tested after being grown in a modified Pikovskaya liquid medium supplemented with 0.1 % of ZnO, ZnCO<sub>3</sub> and Zn (PO<sub>3</sub>)<sub>4</sub>. The bacterial cultures were withdrawn after the sixth, eighth, and tenth day of incubation at 30°C for the estimation of the soluble Zn in the broth using atomic absorption spectrophotometric. The amount of Zn solubilized by both isolates varied, and *P. pseudoalcaligenes* recorded maximum solubilization of Zn in all of the three insoluble sources. The maximum solubilization of Zn was in Zn(PO<sub>3</sub>)<sub>4</sub> (33.26 mgL<sup>-1</sup>) at the tenth day of incubation (Table1).

Zinc forms an important metalloprotein which is responsible for the synthesis of tryptophan, which in turn acts as a precursor for the production of IAA. The results show that both isolates produce IAA in the medium supplemented with tryptophan, and that there is further enhancement in the IAA production by the isolates due to the addition of Zn sources. This may be attributed to the induction of high Zn solubilizing efficiency of the isolates, which results in the stimulation of IAA synthesis. Moreover, *P. pseudoalcaligenes* was found to produce more IAA (33.20 mgL<sup>-1</sup>) in the presence of ZnO (Table 2). Both bacteria were able to solubilize zinc with the production of organic acid resulting in a change in the pH of the medium; with time it became more acidic by both isolates and in all of the three insoluble sources (Table 2).

The plants inoculated with ZMB reduced the effect of salinity, on growth suppression of paddy under salinity. The plant inoculated with ZMB showed a 52 % greater plant height under normal conditions, and 32 % higher under salinity conditions. Similarly, the dry weight increased by 26 % under normal conditions, and by 30 % under salinity (Table 3). Plants inoculated with *P. pseudoalcaligenes* and *B. pumilus* also showed higher chlorophyll a, chlorophyll b, total chlorophyll, and carotenoid content at normal conditions as well as under salinity (Table 3).

It has been shown that soluble sugars increase under osmotic stress for osmotic adjustment in paddy under salinity. So the accumulation of soluble sugars significantly increased in the ZMB inoculated plant at normal conditions, but there was no significant change observed in the *P. pseudoalcaligenes* and *B. pumilus* inoculated paddy under salinity as shown in Figure 1.

CAT scavenges H<sub>2</sub>O<sub>2</sub> by breaking it down directly to form water and oxygen, and an increase in its activity is related to the increase in stress tolerance. In paddy plants grown in soils devoid of NaCl, catalase activity increased with the inoculation of ZMB. The CAT in non-stressed control plants varied from 40 (plant non treated) to 62 (Plants treated with ZMB) mmol min<sup>-1</sup>g<sup>-1</sup>FW, while under salinity stress, it ranged between 63 and 69 mmol min<sup>-1</sup>g<sup>-1</sup>FW as shown in Figure 2.

The peroxidase (PO) activity was significantly high in the control paddy plant due to salinity. There is no significant change in the PO activity with the inoculation of ZMB, but the saline stress increased the PO activity in the control plants and plants treated with *P. pseudoalcaligenes* as shown in Figure 3.

**Table 1.** *In vitro* zinc-solubilizing potential of the bacterial isolates.

Zinc-mobilizing bacteria	Zinc source	Area of halo zone (mm <sup>2</sup> )	Solubilization efficiency	Zn Solubilization on Day 6	Zn Solubilization on Day 8	Zn Solubilization on Day 10
<i>P. pseudoalcaligenes</i>	ZnO	23.6	341%	17.02 ± 0.12	13.09±0.16	11.22±0.24
	ZnCO <sub>3</sub>	19.7	276%	11.29 ± 0.14	10.01±0.11	8.62 ±0.12
	Zn(PO <sub>3</sub> ) <sub>4</sub>	18.2	121%	23.02 ±1.13	27.23±2.01	33.26±0.28
<i>B. pumilus</i>	ZnO	19.5	312%	19.42 ± 0.23	15.06±0.11	10.34±0.41
	ZnCO <sub>3</sub>	19.1	266%	12.36 ±0.28	11.02±0.34	8.35 ±0.47
	Zn(PO <sub>3</sub> ) <sub>4</sub>	17.2	147%	11.02 ±0.11	09.25±1.06	7.22±0.21

Values are mean ± SD of three samples in each group, and are significantly different at  $P < 0.05$

**Table 2.** Influence of zinc-solubilizing organisms on the pH of the growth medium and the IAA production.

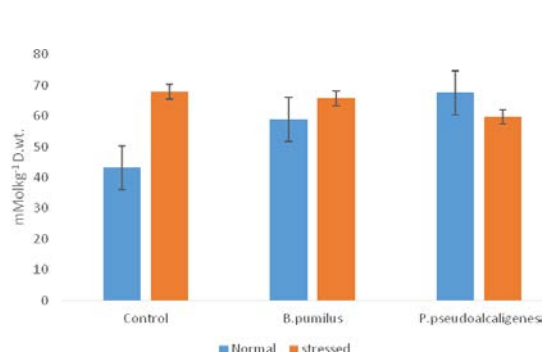
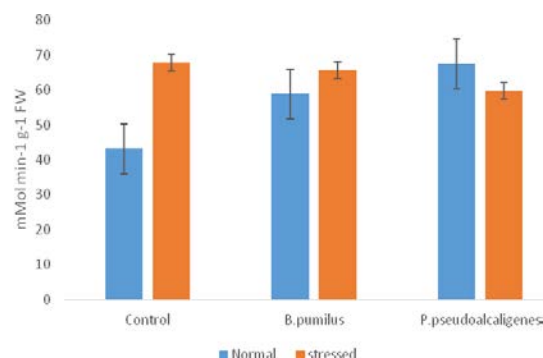
Zinc-mobilizing bacteria	Zinc source	pH of medium on Day 6	pH of medium on Day 8	pH of medium on Day 10	IAA production (mg l <sup>-1</sup> )
Control	Nil				12.11± 0.51
<i>P. pseudoalcaligenes</i>	ZnO	5.13 ± 0.21	4.34 ± 0.24	3.23 ± 0.31	33.20 ± 1.58
	ZnCO <sub>3</sub>	4.45 ± 0.17	4.01 ± 0.21	3.11 ± 0.25	25.15 ± 1.72
	Zn(PO <sub>3</sub> ) <sub>4</sub>	3.24 ± 0.41	3.01 ± 0.31	2.77 ± 0.26	19.87 ± 0.51
<i>B. pumilus</i>	ZnO	5.71 ± 0.20	4.55 ± 0.10	3.33 ± 0.50	28.74 ± 2.41
	ZnCO <sub>3</sub>	4.61± 0.52	6.24± 0.25	4.21± 0.23	22.62 ± 5.57
	Zn(PO <sub>3</sub> ) <sub>4</sub>	4.10 ± 0.30	3.93 ± 0.31	3.37 ± 0.32	15.80 ± 0.40

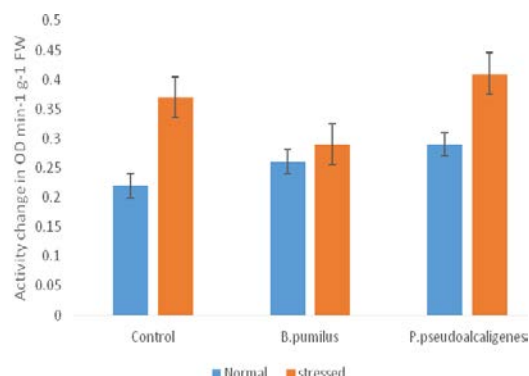
Values are mean ± SD of three samples in each group, and are significantly different at  $P < 0.05$

**Table 3.** Effect of ZMB on chlorophyll content and other growth parameters.

Zinc-mobilizing bacteria	Plant Height (m)	Dry weight (kg)	chlorophyll a, (mg g <sup>-1</sup> FW)	chlorophyll b, (mg g <sup>-1</sup> FW)	total chlorophyll (mg g <sup>-1</sup> FW)	Total carotenoid (mg g <sup>-1</sup> FW)
Control						
Non-inoculated Control	0.167 <sup>c</sup>	0.39 <sup>bc</sup>	1.271 <sup>c</sup>	0.542 <sup>c</sup>	0.386 <sup>c</sup>	0.418 <sup>bc</sup>
<i>P. pseudoalcaligenes</i>	0.192 <sup>b</sup>	0.46 <sup>ab</sup>	1.321 <sup>a</sup>	0.633 <sup>a</sup>	0.452 <sup>a</sup>	0.535 <sup>a</sup>
<i>B. pumilus</i>	0.254 <sup>a</sup>	0.49 <sup>a</sup>	1.082 <sup>b</sup>	0.612 <sup>ab</sup>	0.412 <sup>b</sup>	0.517 <sup>ab</sup>
Stressed						
Non-inoculated Control	0.141 <sup>c</sup>	0.34 <sup>bc</sup>	0.561 <sup>c</sup>	0.348 <sup>bc</sup>	0.296 <sup>c</sup>	0.272 <sup>abc</sup>
<i>P. pseudoalcaligenes</i>	0.161 <sup>b</sup>	0.42 <sup>ab</sup>	0.691 <sup>a</sup>	0.411 <sup>a</sup>	0.382 <sup>a</sup>	0.354 <sup>a</sup>
<i>B. pumilus</i>	0.187 <sup>a</sup>	0.43 <sup>a</sup>	0.678 <sup>b</sup>	0.376 <sup>b</sup>	0.341 <sup>ab</sup>	0.316 <sup>ab</sup>

Values are the means of replicates. Values with different letters are significantly different at  $P < 0.05$  (Duncan's Test).

**Figure 1.** Effect of *B.pumilus* and *P. pseudoalcaligenes* on the accumulation of soluble sugars in paddy under salinity stress. Values are means from five replications. Vertical bars indicate ±S.D.**Figure 2.** Effect of *B.pumilus* and *P. pseudoalcaligenes* on catalase activity in paddy under salinity stress. Values are means from five replications. Vertical bars indicate ±S.D.



**Figure 3.** Effect of *B. pumilus* and *P. pseudoalcaligenes* on peroxidase activity in paddy under salinity stress. Values are means from five replications. Vertical bars indicate  $\pm$ S.D.

#### 4. Discussion

India is considered as one of the main regions for rice cultivation, covering forty-four million hectares of land. In India, rice accounts for 40 % of the nation's food production, and is a staple food for around 65 % of the total population. Crop production in the arid and semi-arid environments is highly unstable and unsustainable due to uncongenial climates (Sharma *et al.* 2011). Low soil fertility is one of the most important factors which not only seriously affect the rice production, but also reduce the quality of the rice. Chaudhary *et al.* (2007) reported Zn deficiency as a key factor in determining the rice production in several parts of India. Zinc plays an important role in maintaining the structure and function of a large number of macromolecules, and is also found responsible for controlling over 300 enzymatic reactions (Tapiero and Tew, 2003). Graham (2008) stated that zinc deficiency is the highest priority among micronutrients for agriculture experts to address. The use of chemical fertilizers to enhance soil fertility and crop productivity is an option, but the continuous application of chemical fertilizers as well as their low use efficiency cause leaching and runoff of nutrients, leading to environmental degradation (Gyaneshwar *et al.* 2002). One of the possible methods to increase crop productivity and food quality without creating environmental hazards is the use of zinc-mobilizing bacteria (ZMB). Several efforts have been made to identify the zinc solubilizers with their varying abilities. Bacterial genera such as *Azotobacter*, *Bacillus*, *Beijerinckia*, *Burkholderia*, *Enterobacter*, *Erwinia*, *Flavobacterium*, *Microbacterium*, *Pseudomonas*, *Rhizobium* and *Serratia* are reported to be the most significant mineral solubilizing bacteria (Bhattacharyya and Jha, 2012).

In the present study, two bacterial isolates, *P. pseudoalcaligenes* and *B. pumilus* were found to be efficient with reference to their zinc mineralization capability. Zaidi *et al.* (2009) reported that the mineral solubilization by the bacteria may be attributed to the secretion of organic acids. So in the present study, change in the pH of the medium has been studied, and the results showed that the medium had become acidic with time. The production of organic acids for the solubilization of minerals, such as zinc, and potassium, is a well-known

mechanism. In the present study, the reason for the reduction in pH may also be attributed to the production of organic acids by the isolates. Auxin may function as an important signal molecule in the regulation of plants' development. This hormone influences many cellular functions, the orientation of root and shoot growth in response to light and gravity, the differentiation of vascular tissue, apical dominance, the initiation of lateral and adventitious roots, and the stimulation of cell division and elongation of stems and roots. In this study, both of the bacterial isolates were positive for auxin production, and *P. pseudoalcaligenes* was found to be better than *B. pumilus* in presence of Zn in the medium compared to the control. Patten and Glick, (2002) also reported that auxin producing *P. putida* increased the length of canola seedling roots.

Salinity affects the crop productivity and yield as salt stress affects plant growth negatively (Parida and Das, 2005). In the present study, the physiological and biochemical changes in a paddy cultivar were studied in the presence of ZMB. However, when the plants were inoculated with ZMB, the extent of growth suppression was ameliorated and the treated plants showed growth in terms of dry weight compared to non-inoculated control plants as also was reported by Vaid *et al.* (2014) and Jha and Subramanian, (2018a). The zinc application increased the plant height significantly. This may be attributed to the adequate supply of zinc which contributes to acceleration of the enzymatic activity and auxin metabolism in plants. These results are also in agreement with the findings of Khan *et al.* (2009).

Different stress situations directly result in the accumulation of ROS and are associated with soluble sugar accumulation, which has generally been considered to be an adaptive response to the stress condition. Carbohydrates such as soluble sugars (glucose, fructose, sucrose, fructans) accumulate under salt stress to accommodate the ionic balance in the plant (Ivan Couee *et al.* 2006). Their major functions include osmoprotection, osmotic adjustment, carbon storage, radical scavenging and the stabilization of the structure of proteins (Jha and Subramanian, 2018b). In the present study, the contribution of total accumulation of soluble sugars to osmotic adjustment was significant, since the total soluble sugars content increased with the increase of salinity in both the ZMB inoculated and non-inoculated plants. Similar results were obtained by Rejsiková *et al.* (2007), who reported that the concentrations of sugars change in response to salt stress in plants. Soluble sugars accumulation may be attributed to the further transformation of starch to sugars, or to the less consumption of carbohydrates by the tissues under saline conditions.

In order to allow the adjustment of the cellular redox state and to reduce the toxic effects of salinity, plant antioxidant system, peroxidase (POX), and catalase (CAT), are common and important indices for evaluating the redox status of plants. Increasing salinity stress affects the CAT and POX activity in the ZMB inoculated and non-inoculated plants. Hafeez *et al.* (2013) reported that under salinity non-inoculated plants had an increased antioxidant activity compared to the ZMB inoculated plants. These antioxidant enzymes are involved in eliminating  $H_2O_2$  from salt-stressed plants. In the present

study, CAT and POX activities were higher in the plants inoculated with the isolates under normal conditions, but under salinity, CAT activity decreased in the plants inoculated with *P. pseudoalcaligenes*. The POX activity decreased in the plants inoculated with *B. pumilus*. This may be attributed to the free radical scavenging activities of these isolates, due to the decreased  $H_2O_2$  levels (Jha and Subramanian, 2015). The salt stress results in the induction of CAT and POX activities in the plants, but the activities of these enzymes were significantly higher in the presence of ZMB under normal conditions. The further induction of CAT and POX activities are attributed to the ZMB inoculation, pointing to its signaling role in the generation of  $H_2O_2$  and the detoxifying activity of enzymes in rice leaves, similar to other abiotic stresses as reported by Sairam *et al.* (2005). The present study shows that *P. pseudoalcaligenes* and *B. pumilus* have zinc solubilizing abilities, and are able to induce stress-related proteins and enzymes and protect the paddy plant under salinity. The results suggested that the inoculation of salt-stressed plants with ZMB strains reduced the negative effects of salinity stress, improved tolerance, and enhanced plant growth.

## 5. Conclusions

Crop productivity is decreasing due to climatic changes. Moreover, human populations are increasing daily, which results in starvation problems in the developing countries. Nowadays, research is more focused on enhancing crop yields in spite of various unfavorable environmental conditions. Plants inoculated with ZMB have an enhanced growth and acquired a better capacity for salt tolerance, correlated with the regulation of ion concentrations. To grow food for all, the use of such biofertilizers, especially ZMB, may be a beneficial means for the enhancement of plant growth and yield for the growing populations.

## Reference

- Arnon DI. 1949. Copper enzymes in isolated chloroplasts, polyphenoxidase in beta vulgaris. *Plant Physiol.*, **24**: 1-15.
- Assunção AG, Schat H and Aarts MG. 2010. Regulation of the adaptation to zinc deficiency in plants. *Plant Signal Behav.*, **5**:1553-1555.
- Bergmeyer N. 1970 **Methoden der Enzymatischen Analyse**, vol. I. Akademie Verlag, Berlin, 636-647.
- Bhattacharyya PN and Jha D. 2012. Plant growth-promoting rhizobacteria (PGPR): emergence in agriculture. *World J Microbiol Biotechnol.*, **28**: 1327-1350.
- Bradford MM. 1976. Rapid and sensitive method for the quantization of microgram quantities of protein utilizing the principle of protein-dye binding. *Anal Biochem.*, **72**: 248-254.
- Brick JM, Bostock RM and Silverstone SE. 1991. Rapid in situ assay for indole acetic acid production by bacteria immobilized on nitrocellulose membrane. *Appl Environ Microbiol.*, **57**: 535-538
- Chaudhary SK, Thakur SK and Pandey AK. 2007. Response of wetland rice to nitrogen and Zinc. *Oryza*. **44**: 44-47.
- Dubois M, Gilles KA, Hamilton JK, Rebers PA and Smith F. 1956. Colorimetric method for determination of sugars and related substances. *Anal Chem.*, **38**: 350-356.
- Fageria NK, Baligar VC and Clark RB. 2002. Micronutrients in crop production. *Adv Agron.*, **77**: 185-268.
- Garg JK and Patel JG. 2007. National Wetland Inventory and Assessment, Technical Guidelines and Procedure Manual, Technical Report, SAC/EOAM/AFEG/NWIA/TR/01/2007, June 2007, Space Applications Centre, Ahmedabad,
- Graham RD. 2008. Micronutrient deficiencies in crops and their global significance. In: Alloway B J (Ed). **Micronutrient Deficiencies in Global Crop Production**. Springer, New York, 41-61.
- Gyaneshwar P, Kumar GN, Parekh LJ and Poole PS. 2002. Role of soil microorganisms in improving P nutrition of plants. *Plant Soil*, **245**: 83-93.
- Gontia-Mishra I, Sapre S and Tiwari S. 2017. Zinc solubilizing bacteria from the rhizosphere of rice as prospective modulator of zinc biofortification in rice. *Rhizosphere*, **3**: 185-190.
- 32.Hafeez B, Khanif YM and Saleem M. 2013. Role of zinc in plant nutrition – A review. *Am J Exp Agricul.*, **3**(2): 374-391,
- Hammerschmidt R and Kuc J. 1982. Lignification as a mechanism for induced systemic resistance in cucumber. *Physiol Plant Pathol.*, **20**: 61-71.
- Hughes MN and Poole RK. 1991. Metal speciation and microbial growth—the hard (and soft) facts. *J Gen Microbiol.*, **137**:725-734.
- Ivan Coue'e, Ce'cile Sulmon, Gwenola G and Abdelhak ELA. 2006. Involvement of soluble sugars in reactive oxygen species balance and responses to oxidative stress in plants. *J Exp Bot.*, **57**: 449-459.
- Jha Y and Subramanian RB. 2014a. Under saline stress plant growth- promoting bacteria affect growth, photosynthesis and antioxidant activities in paddy. *IJAEB*. **7**: 205-212.
- Jha Y and Subramanian RB. 2014b. Characterization of root associated bacteria from paddy and its growth promotion efficacy. *Biotech*. **4**: 325-330.
- Jha Y and Subramanian RB. 2015. Reduced cell death and improved cell membrane integrity in rice under salinity by root associated bacteria. *Theor Exp Plant Physiol.*, **27**: 227-235.
- Jha Y and Subramanian RB. 2016. Rhizobacteria enhance oil content and physiological status of *Hyptis suaveolens* under salinity stress. *Rhizosphere*, **1**:33-35.
- Jha Y. 2017. Potassium mobilizing bacteria: enhance potassium intake in paddy to regulate membrane permeability and accumulate carbohydrates under salinity stress. *Braz J Biol Sci.*, **4**: 333-344.
- Jha Y and Subramanian RB. 2018a. From interaction to gene induction: An eco-friendly mechanism of PGPR-mediated stress management in the plant. *Plant Microbiome: Stress Response*, 217-232.
- Jha Y and Subramanian RB. 2018b. Effect of root-associated bacteria on soluble sugar metabolism in plant under environmental stress. In: Ahmad P, Ahanger M A, Singh V P, Tripathi D K, Alam P and Alyemeni MN (Eds). **Plant Metabolites and Regulation under Environmental Stress**, Elsevier Inc., UK, pp 231-239.
- Khan MS, Zaidi A, Wani PA and Oves M. 2009. Role of plant growth-promoting rhizobacteria in the remediation of metal contaminated soils. *Environ Chem Lett.*, **7**: 1-19.
- Larcher W. 1980. **Physiological plant Ecology**. In 2nd totally rev. edition ed. (303). Berlin and New York: Springer-Verlag.
- Parida AK and Das AB. 2005. Salt tolerance and salinity effects on plants: a review. *Ecotoxicol Environ Saf.*, **60**: 324-349.



- Pikovskaya RI. 1948. Mobilization of phosphorus in soil connection with the vital activity of some microbial species. *Microbiologiya* **17** : 362–370.
- Patten CL and Glick BR. 2002. Bacterial biosynthesis of indole-3-acetic acid. *Can J Microbiol.*, **42**: 207-220.
- Rejsiková A, Patková L, Eva Stodulková E and Lipavská H. 2007. The effect of abiotic stresses on carbohydrate status of olive shoots (*Olea europaea* L.) under *in vitro* conditions. *J Plant Physiol.*, **164**: 74–184.
- Sairam RK, Srivastava GC, Agarwal S and Meena RC. 2005. Differences in antioxidant activity in response to salinity stress in tolerant and susceptible wheat genotypes. *Biol Plantarum*. **49**: 85-91.
- Sharma SK, Johri BN, Ramesh A, Joshi OP and Prasad SVS. 2011. Selection of plant growth-promoting *Pseudomonas* spp. that enhanced productivity of soybean-wheat cropping system in central India. *J Microbiol Biotechnol.*, **21**: 1127-1142.
- Tapiero H and Tew KD. 2003. Trace elements in human physiology and pathology: zinc and metallothioneins. *Biomed. Pharmacother.*, **57**: 399-411.
- Vaid SK, Kumar B, Sharma A, Shukla AK and Srivastava PC. 2014. Effect of zinc solubilizing bacteria on growth promotion and zinc nutrition of rice. *J Soil Sci Plant Nutr.*, **14**: 889-910.
- Zaidi A, Khan MS, Ahemad M and Oves M. 2009. Plant growth promotion by potassium solubilizing bacteria. *Acta Microbiol Immunol Hung.*, **56**: 263-284.
- Zhu JK. 2007. Plant Salt Stress: John Wiley & Sons, Ltd. A. K. Parida, A. B. Das, 2005 Salt tolerance and salinity effects on plants: A review. *Ecotoxicol Environ Saf.*, **60**:324-49.



# Life-History Traits of the Climbing perch *Anabas testudineus* (Bloch, 1792) in a Wetland Ecosystem

Dalia Khatun<sup>1</sup>, Md. Yeamin Hossain<sup>1,\*</sup>, Md. Aatur Rahman<sup>1</sup>, Md. Akhtarul Islam<sup>1</sup>, Obaidur Rahman<sup>1</sup>, Md. Abul Kalam Azad<sup>1</sup>, Most. Shakila Sarmin<sup>1</sup>, Most. Farida Parvin<sup>1</sup>, Ahnaf Tausif Ul Haque<sup>2</sup>, Zannatul Mawa<sup>1</sup> and Md. Akhtar Hossain<sup>1</sup>

<sup>1</sup>Department of Fisheries, Faculty of Agriculture, University of Rajshahi, Rajshahi 6205,

<sup>2</sup>Department of Environmental Science and Management, North South University, Dhaka 1229, Bangladesh

Received June 2, 2018; Revised July 25, 2018; Accepted August 19, 2018

## Abstract

The freshwater climbing perch, *Anabas testudineus* (Bloch, 1792), is an economically important, and nutritionally valuable food fish in south Asia. The present study provides the first complete description of life-history traits, i.e., length-frequency distributions (LFDs), length-weight relationships (LWRs), length-length relationship (LLR), condition factors (allometric,  $K_A$ ; Fulton's,  $K_F$ ; relative,  $K_R$ ; relative weight,  $W_R$ ), form factor ( $a_{3.0}$ ), size at sexual maturity ( $L_m$ ), and natural mortality ( $M_w$ ) of *A. testudineus* in a wetland known as Gajner Beel, Pabna, in northwestern Bangladesh. Sampling was done using different traditional fishing gears during July to December, 2017. Total length (TL) and whole body weight (BW) were measured by the digital slide calipers and an electronic balance with 0.01cm and 0.01 g accuracy, respectively. A total of 239 specimens were measured ranging from 7.40-14.50 cm TL and 7.89- 63.78 g BW during this study. The estimated  $b$  values indicated an isometric growth pattern ( $b=3.00$ ) in *A. testudineus*. The LWRs were highly significant ( $p<0.001$ ) with  $r^2$  values  $>0.956$ .  $K_F$  best indicated the well-being of *A. testudineus* among the four types of condition factors in the Gajner Beel. A Wilcoxon sign-ranked test for  $W_R$  showed no significant dissimilarity from 100, signifying the balanced habitat for *A. testudineus*. The estimated  $a_{3.0}$  was 0.021, and  $L_m$  was calculated as 8.41 (~8.40) cm TL in the Gajner Beel. The  $M_w$  of *A. testudineus* was 1.05 year<sup>-1</sup>. The results should benefit the sustainable management of *A. testudineus* species in Bangladesh and its neighboring countries.

**Keywords:** *Anabas testudineus*, Growth pattern, Conditions, Size at sexual maturity, Natural mortality

## 1. Introduction

Perciformes is the largest and most diverse order of teleosts in the world, containing about 41 % of all bony fish comprising more than 10,000 species and about 160 families (Nelson, 2006). Anabantidae is a Perciformes family with thirty-four species in it. The climbing perch, *A. testudineus* (Bloch, 1792) is a member of this family, being abundant in different parts of Asia: Bangladesh, China, India, Malaysia, Myanmar, Pakistan, Philippines, Sri Lanka, and Thailand (Talwar and Jhingran, 1991; Rahman, 2005). It is a fresh- and brackish water potamodromous species that mostly dwells in canals, lakes, ponds, swamps, and estuaries (Menon, 1999; Vidhayanon, 2002), even though adults usually inhabit rivers, flooded fields, and stagnant water bodies (slow moving canals) (Pethiyagoda, 1991). This species is known as Koi in Bangladesh, Kawai in India, Kabai in Nepal, and Kavaia in Sri Lanka (Froese and Pauly, 2018). It is a hardy fish that can endure extremely unfavorable water conditions including low oxygen, polluted water, etc. (Pethiyagoda, 1991) through an accessory air-

breathing organ called the labyrinth organ (Rahman, 1989). This species is considered commercially important, as it has a high market value for being a delicious food fish in Southeast Asia (Herre, 1935; Vidhayanon, 2002). Furthermore, it is an indigenous commercial target fish and a vital source of subsistence for small- and large-scale fishers, who employ a variety of traditional fishing gears (Craig *et al.*, 2004; Hossain, 2010a; Hossain *et al.*, 2016a). Although this species is facing some potential threats such as habitat destruction and dry-out, it is a very hardy, habitat-generalist fish that is categorized as 'least concern' in Bangladesh (IUCN Bangladesh, 2015).

Knowledge of the life-history traits of fish species is very important for the implementation of proper management strategies for conserving the commercially important fish such as *A. testudineus* (Hossain *et al.*, 2013a). Studies of length-frequency distributions (LFDs) usually express the life-history traits and ecology of fishes (Ranjan *et al.*, 2005). Length-weight relationships (LWRs) are considered a useful tool in fisheries studies for the estimation of weight, biomass, and condition indices (Anderson and Gutreuter, 1983; Froese, 2006; Froese *et al.*, 2011). Moreover, condition factors help evaluate the

\* Corresponding author e-mail: hossainyeamin@gmail.com.

status of fish from which the present and future population success can be predetermined (Richter, 2007; Rypel and Richter, 2008). Additionally, relative weight ( $W_R$ ) is one of the most accepted indices for fish condition in the USA for the last two decades (Rypel and Richter, 2008), and now it is being used in Bangladesh for assessing freshwater fishes (Rahman *et al.*, 2012; Hossain *et al.*, 2012a, 2015a, 2016b).

Although, several authors have reported on LWRs and the condition factors (Kumar *et al.*, 2013; Hossain *et al.*, 2015b; Kumary and Raj, 2016), morphometric and meristic variations (Hossen *et al.*, 2017), morphometric and gonadal studies (Ziauddin *et al.*, 2016), captive breeding (Sarkar *et al.*, 2005), reproduction and spawning behavior (Zworykin, 2012; Uddin *et al.*, 2017), fecundity (Marimuthu *et al.*, 2009), induced breeding (Mandal *et al.*, 2016), and growth performance of *A. testudineus* (Alam *et al.*, 2007; Bhaskar *et al.*, 2015), this economically important species has not been studied for life-history traits from Bangladesh or elsewhere. Therefore, the current study provides a complete and informative depiction of the life-history traits of *A. testudineus* - including LFDs, LWRs, LLR, condition factors (allometric,  $K_A$ ; Fulton's,  $K_F$ ; relative,  $K_R$ ), relative weight ( $W_R$ ), form factor ( $a_{3.0}$ ), size at first sexual maturity ( $L_m$ ), and natural mortality ( $M_w$ ) from the Gajner Beel wetland, Pabna in northwestern Bangladesh using many specimens of small to large sizes over a study period of six months.

## 2. Material and Methods

### 2.1. Study area and Sampling

The present study was carried out in the Gajner Beel (Lat. 23°55' N; Long. 89° 33' E), NW Bangladesh. It is one of the largest wetlands (floodplain) in the area, which is considered an important breeding and feeding ground for many freshwater fishes (Hossain *et al.*, 2017a) and is located in Sujanagar Upazilla, Pabna, Bangladesh. A total of 239 individuals of *A. testudineus* were collected monthly from that region over the period from July to December, 2017, using different types of fishing gears; gill net (mesh size: 1.5–2.5 cm), cast net (mesh size: 1.0–2.0 cm), and square lift net (mesh size ~1.0 cm). Samples were rapidly chilled in ice on site and preserved with 10% buffered formalin back in the laboratory. For each individual, lengths (total length, TL and standard length, SL) were measured by digital slide calipers, and the whole body weight (BW) was measured using an electronic balance, to the nearest 0.01cm and 0.01 g precision, respectively.

### 2.2. Length-frequency Distributions (LFDs)

LFDs for *A. testudineus* was constructed using 1.0 cm intervals of TL. The normal-frequency distribution was fitted to the TL frequency distribution of *A. testudineus* using a computer program Microsoft Excel-add-in-solver, based on Hasselblad's maximum-likelihood method (Hasselblad, 1966).

### 2.3. Length-weight Relationships and Length-length Relationship (LWRs and LLR)

The growth pattern was estimated through LWRs with the equation:  $W = a \cdot L^b$ , where  $W$  is the total body weight

(g), and  $L$  is the total length (cm). The parameters  $a$  and  $b$  were estimated by linear regression analyses based on natural logarithms:  $\ln(W) = \ln(a) + b \ln(L)$ . Extremes outliers were removed from the regression analyses according to Froese (2006). A t-test was used to verify whether  $b$  values acquired in the linear regressions were significantly different from the isometric value ( $b = 3$ ), according to the equation of Sokal and Rohlf (1987) as:  $t_s = (b-3) / s_b$ , where  $t_s$  is the t-test value,  $b$  is the slope, and  $s_b$  is the standard error of the slope ( $b$ ). Additionally, on the basis of the  $b$  values of LWRs (TL vs. BW and SL vs. BW), the growth pattern of *A. testudineus* was determined. In addition, the LLR for TL vs. SL was estimated by linear regression analysis (Hossain *et al.*, 2006). Additionally linear regression analysis was conducted using untransformed TL-SL data to recognize the growth type for LLR. Significant divergence of the  $b$  value from the theoretical isometric value ( $b = 1$ ) specifies the growth type as either positively ( $b > 1$ ) or negatively ( $b < 1$ ) allometric for LLR (Hartnoll, 1982), which was confirmed with Student's t-tests according to the equation of Sokal and Rohlf (1987) as  $t_s = (b-1) / s_b$ .

### 2.4. Condition Factors

The allometric condition factor ( $K_A$ ) was estimated by the equation of Tesch (1968):  $W/L^b$ , where  $W$  is the body weight (g),  $L$  is the TL (cm), and  $b$  is the LWR parameter. Fulton's condition factor ( $K_F$ ) was calculated using the equation of Fulton (1904):  $K_F = 100 \times (W/L^3)$ , where  $W$  is the body weight (g), and  $L$  is the TL in cm. The scaling factor of 100 was used to bring the  $K_F$  close to unit (Froese, 2006). Furthermore, the relative condition factor ( $K_R$ ) was analyzed following the equation of Le Cren (1951):  $K_R = W/(a \times L^b)$ , where  $W$  is the body weight (g),  $L$  is the total length (cm), and  $a$  and  $b$  are LWR parameters. For estimating the relative weight ( $W_R$ ), the equation of Froese (2006) was used:  $W_R = (W / W_s) \times 100$ , where  $W$  is the weight of a particular individual and  $W_s$  is the predicted standard weight as calculated by  $W_s = a \times L^b$ , where the  $a$  and  $b$  values are obtained from the relationships between TL vs. BW.

### 2.5. Form Factor ( $a_{3.0}$ )

The  $a_{3.0}$  of *A. testudineus* was estimated using the equation of Froese (2006) as:  $a_{3.0} = 10^{\log a - s(b-3)}$ , where  $a$  and  $b$  are the regression parameters of LWR, and  $s$  is the regression slope of  $\ln a$  vs.  $b$ . The researchers used a mean slope  $S = -1.358$  for calculating the form factor because there was no available information on LWR for this species to estimate the regression ( $S$ ) of  $\ln a$  vs.  $b$ .

### 2.6. Size at First Sexual Maturity ( $L_m$ )

Size at first sexual maturity ( $L_m$ ) for *A. testudineus* was estimated by the empirical equation,  $\log(L_m) = -0.1189 + 0.9157 * \log(L_{max})$ , where  $L_{max}$  is the maximum TL (Binohlan and Froese, 2009). Moreover, the maximum length of *A. testudineus* obtained from available literature in the FishBase was used to estimate  $L_m$  for water bodies throughout the world.

### 2.7. Natural Mortality ( $M_W$ )

$M_W$  of *A. testudineus* was estimated using the model,  $M_W = 1.92 \text{ year}^{-1} * (W)^{-0.25}$  (Peterson and Wroblewski, 1984), where,  $M_W$  = natural mortality at mass  $W$ ; and  $W = a * L^b$ , where  $a$  and  $b$  are the regression parameters of LWR.

### 2.8. Statistical Analysis

For statistical analysis, Microsoft® Excel-add-in DDXL and GraphPad Prism 6.5 software were used. The Spearman rank-correlation test was applied to analyze the relationship of condition factors with TL and BW. Wilcoxon sign-ranked test was used in this study to compare the mean relative weight ( $W_R$ ) with 100 (Anderson and Neumann, 1996). All statistical analyses were considered significant at 5 % ( $p < 0.05$ ).

## 3. Results

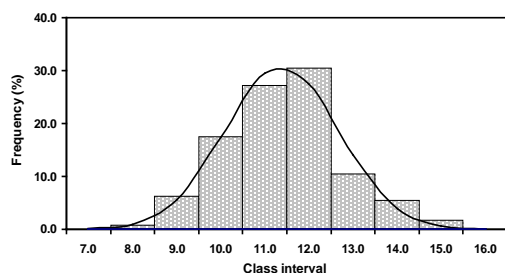
### 3.1. Length-frequency Distributions (LFDs)

A total of 239 *A. testudineus* were collected from fishermen throughout the Gajner Beel, Pabna, Bangladesh during the study period (July to December 2017). Table 1 shows the descriptive statistics of maximum and minimum length and weight measurement, and 95% confidence limits (CLs) of *A. testudineus*. LFDs showed that the range of TLs was 7.40 to 14.50 cm (Figure 1), and that body weight ranged from 7.89 to 63.78 g there. The 10.00-10.99 and 11.00-11.99 cm TL size groups were numerically dominant and constituted together 57.70 % of the total population (Figure 1).

**Table 1.** Length (cm) and weight (g) measurements with 95% confidence limit of combined sexes of *Anabas testudineus* (Bloch, 1792) in a wetland (Gajner Beel, Pabna, Bangladesh) ecosystem.

Measurement	<i>n</i>	Min	Max	Mean±SD	95% CL
Total length(TL)		7.40	14.50	10.85 ± 1.33	10.68 – 11.02
Standard length(cm)	239	6.10	11.70	8.64 ± 1.07	8.50 – 8.77
Body weight(BW)		7.89	63.78	26.46 ± 10.24	25.15 – 27.76

*n*, sample size; Min, minimum; Max, maximum; SD, standard deviation; CL, confidence limit for mean values



**Figure 1.** Total length frequency distribution of *Anabas testudineus* (Bloch, 1792) in a wetland (Gajner Beel, Pabna, Bangladesh) ecosystem.

### 3.2. Length-weight Relationships (LWRs)

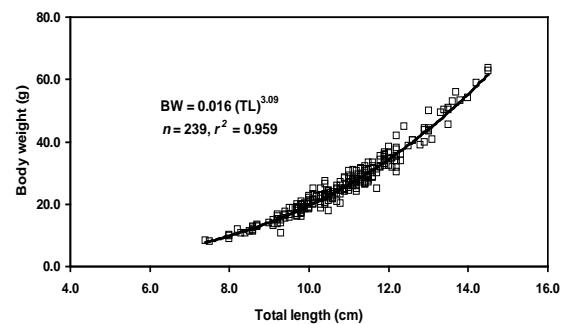
The sample size (*n*), regression parameter, 95% confidence interval of *a* and *b*, coefficient determination ( $r^2$ ), and growth type (GT), of *A. testudineus* are shown in Table 2. In this study, the calculated allometric coefficient

(*b*) of TL vs. BW indicates an isometric growth pattern (Figure 2), as did the SL-BW relationship (Table 2 and Figure 3) in the Gajner Beel. The LWRs were highly significant ( $p < 0.001$ ) with  $r^2$  values  $> 0.956$ .

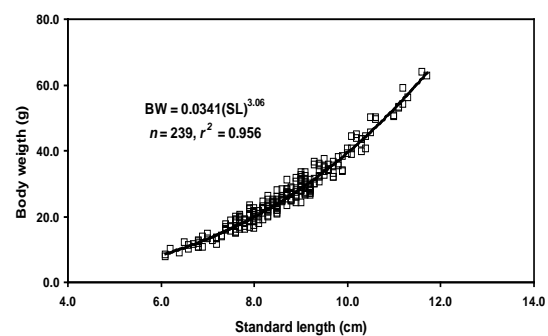
**Table 2.** Descriptive statistics and estimated parameters of the length-weight and length-length relationships of *Anabas testudineus* (Bloch, 1792) (*n* = 239) in a wetland (Gajner Beel, Pabna, Bangladesh) ecosystem.

Equation	Regression parameter		95% CL of <i>a</i>	95% CL of <i>b</i>	$r^2$	$t_s$	GT
	<i>a</i>	<i>b</i>					
$BW = a * TL^b$	0.0160	3.09	0.0132 – 0.0194	3.01 – 3.17	0.959	1.11	I <sup>ns</sup>
$BW = a * SL^b$	0.0341	3.06	0.0285 – 0.0409	2.98 – 3.15	0.956	0.77	I <sup>ns</sup>
$TL = a + b * SL$	0.3048	1.22	0.0615 – 0.5481	1.19 – 1.25	0.969	0.94	I <sup>ns</sup>

*a*, intercept; *b*, slope; CL, confidence limit for mean values;  $r^2$ , coefficient of determination; GT, growth type; I, isometric; *ns*, not significant



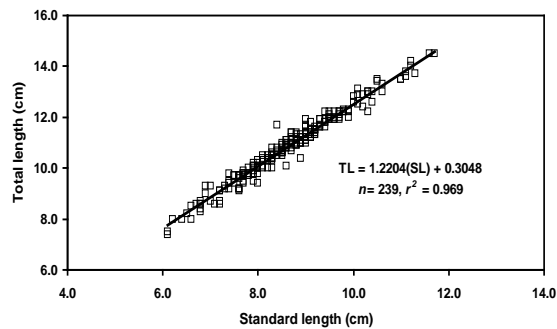
**Figure 2.** Total length-body weight relationship of *Anabas testudineus* (Bloch, 1792) in a wetland (Gajner Beel, Pabna, Bangladesh) ecosystem.



**Figure 3.** Standard length-body weight relationship of *Anabas testudineus* (Bloch, 1792) in a wetland (Gajner Beel, Pabna, Bangladesh) ecosystem.

### 3.3. Length-length Relationship (LLR)

The relationship between TL and SL of *A. testudineus* along with the estimated parameters of the LLR and the coefficient of determination ( $r^2$ ), are shown in Table 2 and Figure 4. During this study, the calculated *b* value of the LLR indicates an isometric growth pattern. The LLR was highly significant ( $p < 0.001$ ) with a coefficient of determination values of 0.969.



**Figure 4.** Total length-standard length relationship of *Anabas testudineus* (Bloch, 1792) in a wetland (Gajner Beel, Pabna, Bangladesh) ecosystem.

### 3.4. Condition Factors

#### 3.4.1. Allometric Condition Factor ( $K_A$ )

The estimated  $K_A$  of *A. testudineus* ranged from 0.0109-0.0198 (Mean  $\pm$ SD, 0.0161 $\pm$ 0.0012) (Table 3). According to Spearman rank-correlation tests, there was a significant relationship between BW vs.  $K_A$  ( $r_s = 0.1780$ ,  $p = 0.0058$ ), but not between TL vs.  $K_A$  ( $r_s = -0.0194$ ,  $p = 0.7660$ ) (Table 4).

**Table 3.** Condition factors of *Anabas testudineus* (Bloch, 1792) ( $n = 239$ ) in a wetland (Gajner Beel, Pabna, Bangladesh) ecosystem.

Condition factors	Min	Max	Mean $\pm$ SD	95% CL
Allometric condition factor ( $K_A$ )	0.0109	0.0198	0.0161 $\pm$ 0.0012	0.0159 – 0.0162
Fulton's condition factor ( $K_F$ )	1.33	2.43	1.98 $\pm$ 0.15	1.96 – 1.20
Relative condition factor ( $K_R$ )	0.68	1.24	1.00 $\pm$ 0.08	0.99 – 1.01
Relative weight ( $W_R$ )	68.35	123.82	100.44 $\pm$ 7.76	99.46 – 101.43

Min, minimum; Max, maximum; SD, standard deviation; CL, confidence limit for mean values

**Table 4.** Relationships of condition factor with total length (TL) and body weight (BW) of *Anabas testudineus* (Bloch, 1792) ( $n = 239$ ) in a wetland (Gajner Beel, Pabna, Bangladesh) ecosystem.

Relationship	$r_s$ value	95% CL of $r_s$	$p$ values	Significance
TL vs. $K_A$	-0.019	-0.150 to 0.112	0.766	Ns
TL vs. $K_F$	0.345	0.485 to 0.188	< 0.001	***
TL vs. $K_R$	-0.031	-0.161 to 0.100	0.634	Ns
TL vs. $W_R$	-0.031	-0.161 to 0.099	0.632	Ns
BW vs. $K_A$	0.178	0.048 to 0.302	0.006	**
BW vs. $K_F$	0.310	0.187 to 0.424	< 0.001	***
BW vs. $K_R$	0.171	0.041 to 0.295	0.008	**
BW vs. $W_R$	0.171	0.041 to 0.295	0.008	**

TL, total length; BW, body weight;  $K_A$ , allometric condition factor;  $K_F$ , Fulton's condition factor;  $K_R$ , relative condition factor;  $W_R$ , relative weight;  $r_s$ , Spearman rank-correlation values; CL, confidence limit;  $p$ , shows the level of significance; Ns, not significant; \* significant; \*\* highly significant; \*\*\*very highly significant.

#### 3.4.2. Fulton's Condition Factor ( $K_F$ )

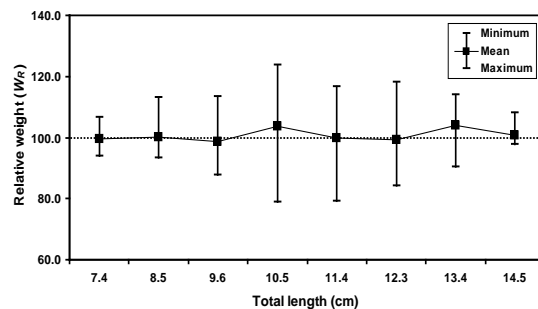
The calculated  $K_F$  ranged from 1.33-2.43 (Mean  $\pm$  SD, 1.98 $\pm$ 0.15) (Table 3). Spearman rank-correlation tests showed that  $K_F$  had highly significant relationships with both TL ( $r_s = 0.345$ ,  $p < 0.001$ ) and BW ( $r_s = 0.310$ ,  $p < 0.001$ ) (Table 4).

#### 3.4.3. Relative Condition Factor ( $K_R$ )

The  $K_R$  of *A. testudineus* ranged from 0.68-1.24 (Mean  $\pm$  SD, 1.00 $\pm$ 0.08) during this study (Table 3). From Spearman rank-correlation tests,  $K_R$  showed a significant relationship with BW ( $r_s = 0.171$ ,  $p = 0.008$ ), but not with TL ( $r_s = -0.031$ ,  $p = 0.634$ ) (Table 4).

#### 3.4.4. Relative Weight ( $W_R$ )

$W_R$  of *A. testudineus* ranged from 68.35-123.82 (Mean  $\pm$  SD, 100.44 $\pm$ 7.76) during this study (Table 3). According to Spearman rank-correlation tests, there was a significant relationship between BW vs.  $W_R$  ( $r_s = 0.171$ ,  $p = 0.008$ ), but not between TL vs.  $W_R$  ( $r_s = -0.031$ ,  $p = 0.632$ ) (Table 4). According to a Wilcoxon sign-ranked test,  $W_R$  showed no significant variation from 100 for *A. testudineus* ( $p = 0.452$ ). The relationship between TL vs.  $W_R$  is shown in Figure 5.



**Figure 5.** The relationship between total length and relative weight of *Anabas testudineus* (Bloch, 1792) in a wetland (Gajner Beel, Pabna, Bangladesh) ecosystem.

### 3.5. Form Factor ( $a_{3.0}$ )

The  $a_{3.0}$  was calculated as 0.021 for combined sex of *A. testudineus* in the Gajner Beel, Pabna, Bangladesh, and this value indicates that this fish is short and deep in body shape. The researchers also calculated the  $a_{3.0}$  of *A. testudineus* from various water bodies worldwide using available data to compare the findings with the current study's (Table 5).

### 3.6. Size at First Sexual Maturity ( $L_m$ )

$L_m$  for *A. testudineus* was estimated as 8.41 (~ 8.4) (95% CL= 6.08-11.62) cm TL in the Gajner Beel (Figure 6). Moreover, the researchers calculated the  $L_m$  of *A. testudineus* from different water bodies worldwide using the available literature (Table 5).

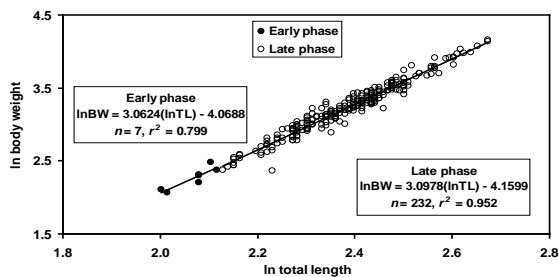
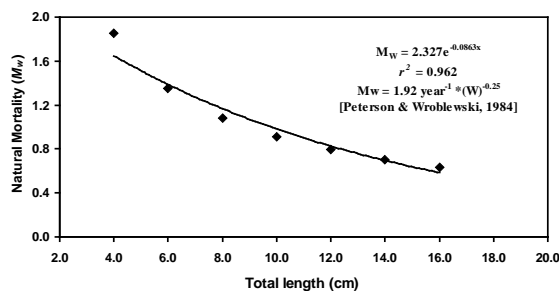
### 3.7. Natural Mortality ( $M_w$ )

$M_w$  for the population of *A. testudineus* in the current study was estimated as 1.05 year<sup>-1</sup> in the Gajner Beel (Figure 7). In addition,  $M_w$  of *A. testudineus* acquired from various water bodies worldwide were calculated using the available data (Table 5).

**Table 5.** The calculated form factor ( $a_{3.0}$ ), size at first sexual maturity ( $L_m$ ) and natural mortality ( $M_w$ ) of *Anabas testudineus* in different waterbodies worldwide.

Water body	Sex	Regression parameter		$L_{max}$ (cm)	$a_{3.0}$	$L_m$ (cm)	95% CL of $L_m$	$M_w$	Reference
		$a$	$b$						
Chi River, Thailand	Unsexed	0.078	2.51	16.5	0.0167	9.47	6.81–13.18	0.82	Satrawaha and Pilasamorn (2009)
Dacca city, ponds, Bangladesh	Male	0.047	2.73	-	0.0200	-	-	-	Shafi and Mustafa (1976)
	Female	0.034	2.80	-	0.0184	-	-	-	
Pampanga River, Philippines	Unsexed	0.056	2.84	11.7 (SL)	0.0340	6.90	5.05–9.43	1.14	Garcia (2010)
Agushan Marsh, Philippines	Mixed	0.086	2.86	17.0	0.0555	9.74	6.99 – 13.57	0.57	Jumawan and Seronay (2017)
	Unsexed	0.086	2.86	17.0	0.0555	9.74	6.99 – 13.57	0.57	
Tetulia River, Bangladesh	Unsexed	0.022	2.90	16.1	0.0161	9.26	6.67 – 12.87	0.89	Hossain <i>et al.</i> (2015b)
Kuttanad, Kerala	Unsexed	0.011	2.84	18.4	0.0070	10.48	7.49 – 14.65	0.96	Kumary and Raj (2016)
Kausalyaganga, India	Unsexed	0.275	2.62	17.5	0.0859	10.00	7.17 – 13.96	0.91	Kumar <i>et al.</i> (2013)
	Unsexed	0.217	2.76	17.5	0.1053	10.00	7.17 – 13.96	0.87	
	Unsexed	0.011	2.77	17.5	0.0056	10.00	7.17 – 13.96	1.07	
West Bengal, India	Mixed	0.119	2.13	17.0	0.0077	9.74	6.99 – 13.57	0.81	Ziauddin <i>et al.</i> (2016)
<b>Gajner Beel, Bangladesh</b>	<b>Unsexed</b>	<b>0.016</b>	<b>3.09</b>	<b>14.5</b>	<b>0.021</b>	<b>8.41</b>	<b>(6.08 – 11.62)</b>	<b>1.05</b>	<b>Present study</b>

$a$  and  $b$  are regression parameters of length-weight relationships;  $L_{max}$ , Maximum length;  $a_{3.0}$ , form factor;  $L_m$ , Size at first sexual maturity;  $M_w$ , Natural mortality.

**Figure 6.** Size at first sexual maturity of *Anabas testudineus* (Bloch, 1792) in a wetland (Gajner Beel, Pabna, Bangladesh) ecosystem.**Figure 7.** Natural mortality of *Anabas testudineus* (Bloch, 1792) in a wetland (Gajner Beel, Pabna, Bangladesh) ecosystem.

#### 4. Discussion

The information on the life history of *A. testudineus* is scant in literature from Bangladesh and elsewhere. Therefore, this study focuses on the complete depiction on life-history traits - including LFDs, LWRs, LLR, condition factors ( $K_A$ ,  $K_F$ ,  $K_R$ ),  $W_R$ ,  $a_{3.0}$ ,  $L_m$  and  $M_w$  - using a number of specimen of various body sizes from the Gajner Beel, NW Bangladesh.

The researchers could not sample individuals of *A. testudineus* below 7.40 cm TL, for one or more of the following reasons: the biased selection of fishing gear, or because fishermen did not go where the smaller fish were (Hossain *et al.*, 2012b; 2016b, c; Azad *et al.*, 2018, Khatun *et al.*, 2018), or perhaps because of the small fish's absence on the fishing grounds (Hossain, 2010a, b; Hossain *et al.*, 2012b, c, d, 2013a, b; 2017b, c), and/or because fishermen discarded smaller fish (Rahman *et al.*, 2018). The maximum length of *A. testudineus* within the Gajner Beel was 14.50 cm TL which is lower than the maximum recorded value of 25.0 cm TL (Froese and Pauly, 2018). Moreover, Satrawaha and Pilasamorn (2009) reported the maximum length of *A. testudineus* as 16.50 cm TL from the Chi River in northeastern Thailand, Hossain *et al.* (2015b) reported a value of 16.10 cm TL in the Tetulia River in Bangladesh, and Jumawan and Seronay (2017) reported the maximum TL in Agushan Marsh of the Philippines as 17.0 cm TL, all of which being higher than those in the current study. Maximum length is considered as a functional tool for fisheries resource planning and management, and is crucial for the

determination of asymptotic length and growth coefficient of fishes (Ahmed *et al.*, 2012; Hossain *et al.*, 2016c, 2017b, c; Nawer *et al.*, 2017; Hossen *et al.*, 2016, 2018).

In the current study of *A. testudineus*, the estimated *b* values ranged from 3.00 to 3.17 for LWRs from the Gajner *Beel* which were within the usual range (2.50 to 3.50) of *b* values for fishes (Carlander, 1969; Froese, 2006). Whereas the *b* values being close to 3 signify that fish grow isometrically, and values >3 indicate positive allometry, and <3 indicate negative allometry (Tesch, 1971). In this study, *b* values of the LWRs were ~3 indicating isometric growth for *A. testudineus* in the Gajner *Beel*. However, other Asian studies have found negative allometric growth for this species: Jumawan and Seronay (2017) reported *b*=2.86 in Agushan Marsh, Philippines; Hossain *et al.* (2015b) observed *b*=2.91 from the Tetulia River in Bangladesh; and Kumar *et al.* (2013) found *b*=2.77 from ponds in Kausalyaganga, India. Such differences may arise due to variation in observed length class, preservation technique, stock health, stomach fullness, gonadal maturity, gender, season, or geographic location (Hossain *et al.*, 2017b, Khatun *et al.*, 2019), which were not considered for this study. However, LLR in this study was highly significant (*p*<0.001), and the calculated *b* value suggests isometric growth, similar to the LWRs (see above). Other LLR data for *A. testudineus* are unavailable for comparison.

In the present study, four condition factors (*K<sub>A</sub>*; *K<sub>F</sub>*; *K<sub>R</sub>* and *W<sub>R</sub>*) were estimated to evaluate the health and habitat status of *A. testudineus*, though most studies deal with a single condition factor. Spearman rank-correlation test indicated that, among these condition factors, Fulton's *K<sub>F</sub>* was significantly correlated with TL and BW (Table 4), so *K<sub>F</sub>* is the best condition index for assessing the well-being of *A. testudineus* in the Gajner *Beel* and nearby ecosystems. It is the first study on condition factor for *A. testudineus*, so future comparisons with other findings are needed.

According to Rypel and Richter (2008), *W<sub>R</sub>* helps judge the overall health and fitness, as well as ecosystem disturbances at the population-level. In this study, the Wilcoxon sign-ranked test indicates that *W<sub>R</sub>* had no remarkable distinction from 100, for combined sex *A. testudineus* in the Gajner *Beel*. This suggests that the population was of balanced condition, with few predators relative to food availability. However, the lack of available literature regarding *W<sub>R</sub>* of *A. testudineus* prevents comparison with other studies.

According to Froese (2006), form factor (*a<sub>3.0</sub>*) can help determine whether the body profile of individuals in a particular population or species differs from others. The *a<sub>3.0</sub>* for *A. testudineus* was 0.021, indicating that this fish is short and deep-bodied in the Gajner *Beel*. There are no references dealing with *a<sub>3.0</sub>* for this species to make comparisons across water bodies.

The size at first maturity can be used to set minimum-permissible capture size and for stock assessment (Lucifora *et al.*, 1999). Size at first sexual maturity (*L<sub>m</sub>*) was estimated as 8.41 cm for *A. testudineus* in the Gajner *Beel*. This is the first attempt to estimate *L<sub>m</sub>* for *A. testudineus* worldwide, so it constitutes a baseline for future studies of environmental factors affecting *L<sub>m</sub>* and spawning season. The natural mortality (*M<sub>w</sub>*) of *A.*

*testudineus* was calculated as 1.05 year<sup>-1</sup> in the Gajner *Beel*, also the first worldwide assessment.

## 5. Conclusion

The present results provide the first inclusive information on the life history traits of *A. testudineus* in the Gajner *Beel* wetland including length-frequency distribution, length-weight and length-length relationships, condition factors (allometric, Fulton's, relative, and relative weight), form factor, first sexual maturity, and natural mortality. The findings from this study can be used as an important tool for fishery biologists, conservationists, and managers to initiate management and fishery regulations for the sustainable conservation of the remaining stocks of this species. Additionally, information on the life history of *A. testudineus* is clearly lacking in the literature and databases, including FishBase. Therefore, the results of the current study provide fundamental information for the online FishBase database, and offer an important baseline as well for future studies within South Asian wetland ecosystems.

## Acknowledgments

The authors extend their sincere appreciation to the PIU-BARC, NATP-2, Sub-Project ID: 484 for funding the project (Management of indigenous fishes in the wetland (Gajner *Beel*, Pabna) ecosystem) and it is a partial work of this CRG (Competitive Research Grants) Project.

## Conflicts of Interest

The authors declare that there is no conflict of interest regarding the publication of this paper.

## References

- Ahmed ZF, Hossain MY and Ohtomi J. 2012. Modeling the growth of silver hatchet chela *Chela cachius* (Cyprinidae) from the Old Brahmaputra River in Bangladesh using multiple functions. *Zool Stud*, **51**: 336-344.
- Alam MA, Noor AM, Khan MMR and Rahman L. 2007. Growth performance and morphological variations of local and Thai climbing perch (*Anabas testudineus*, Bloch). *Fish Res*, **11**: 163-171.
- Anderson RO and Gutreuter SJ. 1983. Length, weight, and associated structural indices. In: Nielsen L and Johnson D (Eds), **Fisheries Techniques**, Bethesda: American Fisheries Society. pp 284-300.
- Anderson RO and Neumann RM. 1996. Length, weight and associated structure indices. In: Murphy B.R. and Willis, W.D (Eds) **Fisheries Techniques**, 2<sup>nd</sup> Ed. American Fisheries Society Bethesda, Maryland, pp 447-482.
- Azad MAK, Hossain MY, Khatun D, Parvin MF, Nawer F, Rahman O and Hossen MA. 2018. Morphometric relationships of the tank goby *Glossogobius giuris* (Hamilton, 1822) in the Gorai River using multi-linear dimensions. *Jordan J Biol Sci*, **11**: 81-85.
- Bhaskar P, Pyne SK and Ray AK. 2015. Growth performance study of koi fish, *Anabas testudineus* (Bloch) by utilization of poultry viscera, as a potential fish feed ingredient, replacing fishmeal. *Int J Recycl Org Waste Agricult*, **4**: 31-37.



- Binohlan C and Froese R. 2009. Empirical equations for estimating maximum length from length at first maturity. *J Appl Ichthyol*, **25**: 611-613.
- Carlander KD. 1969. **Handbook of Freshwater Fishery Biology**. vol.1. The Iowa State University Press. Ames, IA, 752 p.
- Craig JF, Halls AS, Barr JJF and Bean CW. 2004. **The Bangladesh Floodplain Fisheries**. *Fish Res*, **66**: 271-286.
- Froese R and Pauly D. (Eds.) 2018. **Fish Base 2018**, World Wide Web electronic publication. Available at: <http://www.fishbase.org> (Accessed on 22 February 2018).
- Froese R, Tsikliras AC and Stergiou KI. 2011. Editorial note on weight-length relations of fishes. *Acta Ichthyol Pisc*, **41**: 261-263.
- Froese R. 2006. Cube law, condition factor and weight-length relationships: History, meta-analysis and recommendations. *J Appl Ichthyol*, **22**: 241-253.
- Fulton TW. 1904. **The Rate of Growth of Fishes**. *Twenty-second Annual Reports*, Part III. Fisheries Board of Scotland, Edinburgh, 141-241 pp.
- Garcia LMB. 2010. Species composition and length-weight relationship of fishes in the Candaba wetland on Luzon Island, Philippines. *J Appl Ichthyol*, **26**: 946-948.
- Hasselblad V. 1966. Estimation of parameters for a mixture of normal distributions. *Technometrics*, **8**: 431-444.
- Herre AWCT. 1935. **Philippine Fish Tales**. D.P. Perez Company, Manila, Philippines, 302 p.
- Hossain MY. 2010a. Morphometric relationships of length-weight and length-length of four cyprinid small indigenous fish species from the Padma River (NW Bangladesh). *Turk J Fish Aquat Sci*, **10**: 213-216.
- Hossain MY. 2010b. Length-weight, length-length relationships and condition factor of three schibid catfishes from the Padma River, northwestern Bangladesh. *Asian Fish Sci*, **23**: 329-339.
- Hossain MY, Ahmed ZF, Leunda PM, Islam AKMR, Jasmine S, Scoz J, Miranda R and Ohtomi J. 2006. Length-weight and length-length relationships of some small indigenous fish species from the Mathabhangra River, southwestern Bangladesh. *J Appl Ichthyol*, **22**: 301-303.
- Hossain MY, Jewel MAS, Nahar L, Rahman MM, Naif A and Ohtomi J. 2012a. Gonadosomatic index-based size at first sexual maturity of the catfish *Eutropiichthys vacha* (Hamilton, 1822) in the Ganges River (NW Bangladesh). *J Appl Ichthyol*, **28**: 601-605.
- Hossain MY, Rahman MM and Abdallah EM. 2012b. Relationships between body size, weight, condition and fecundity of the threatened fish *Puntius ticto* (Hamilton, 1822) in the Ganges River, northwestern Bangladesh. *Sains Malays*, **41**: 803-814.
- Hossain MY, Rahman MM, Miranda R, Leunda PM, Oscoz J, Jewel MAS, Naif A and Ohtomi J. 2012c. Size at first sexual maturity, fecundity, length-weight and length-length relationships of *Puntius sophore* (Cyprinidae) in Bangladeshi waters. *J Appl Ichthyol*, **28**: 818-822.
- Hossain MY, Rahman MM, Fulanda B, Jewel MAS, Ahamed F and Ohtomi J. 2012d. Length-weight and length-length relationships of five threatened fish species from the Jamuna (Brahmaputra River tributary) River, northern Bangladesh. *J Appl Ichthyol*, **28**: 275-277.
- Hossain MY, Rahman MM, Jewel MAS, Hossain MA, Ahamed F, Tumpa AS, Abdallah EM and Ohtomi J. 2013a. Life-history traits of the critically endangered catfish *Eutropiichthys vacha* (Hamilton, 1822) in the Jamuna (Brahmaputra River distributary) River, northern Bangladesh. *Sains Malays*, **42**: 265-277.
- Hossain MY, Khatun MM, Jasmine S, Rahman MM, Jewel MAS and Ohtomi J. 2013b. Life history traits of the threatened freshwater fish *Cirrhinus reba* (Hamilton 1822) (Cypriniformes: Cyprinidae) in the Ganges River, northwestern Bangladesh. *Sains Malays*, **42**: 1219-1229.
- Hossain MY, Jahan S, Jewel MAS, Rahman MM, Khatun MM and Jasmine S. 2015a. Biological aspects of the critically endangered fish, *Labeo boga* in the Ganges River, Northwestern Bangladesh. *Sains Malays*, **44**: 31-40.
- Hossain MY, Sayed SRM, Rahman MM, Ali MM, Hossen MA, Elgorban AM, Ahmed ZF and Ohtomi J. 2015b. Length-weight relationships of nine fish species from the Tetulia River, southern Bangladesh. *J Appl Ichthyol*, **31**: 967-969.
- Hossain MY, Hossen MA, Pramanik MNU, Yahya K, Bahkali AH, Elgorban AM. 2016a. Length-weight relationships of *Dermogenys pusilla* Kuhl and van Hasselt, 1823 (Zenarchopteridae) and *Labeo bata* (Hamilton, 1822) (Cyprinidae) from the Ganges River (NW Bangladesh). *J Appl Ichthyol*, **32**: 744-746.
- Hossain MY, Naser SMA, Bahkali AH, Yahya K, Hossen MA, Elgorban AM., Islam MM and Rahman MM. 2016b. Life history traits of the flying barb *Esomus danricus* (Cyprinidae) in the Ganges River, northwestern Bangladesh. *Pakistan J Zool*, **48**: 399-408.
- Hossain MY, Rahman MM, Bahkali AH, Yahya K, Arefin MS and Hossain MI. 2016c. Temporal variations of sex ratio, length-weight relationships and condition factor of *Cabdio morar* (Cyprinidae) in the Jamuna (Brahmaputra River distributary) River, northern Bangladesh. *Pakistan J Zool*, **48**: 1099-1107.
- Hossain MY, Hossen MA, Ahmed ZF, Hossain MA, Pramanik MNU, Nawer F, Paul AK, Khatun D, Haque, N and Islam MA. 2017a. Length-weight relationships of 12 indigenous fish species in the Gajner *Beel* floodplain (NW Bangladesh). *J Appl Ichthyol*, **33**: 842-845.
- Hossain MY, Hossen MA, Khatun D, Nawer F, Parvin MF, Rahman O and Hossain MA. 2017b. Growth, condition, maturity and mortality of the Gangetic leaffish *Nandus nandus* (Hamilton, 1822) in the Ganges River (northwestern Bangladesh). *Jordan J Biol Sci*, **10**: 57-62.
- Hossain MY, Hossen MA, Ali MM, Pramanik MNU, Nawer F, Rahman MM, Sharmin S, Khatun D, Bahkali AH, Elgorban AM and Yahya K. 2017c. Life-history traits of the endangered carp *Botia dario* (Cyprinidae) from the Ganges River in northwestern Bangladesh. *Pakistan J Zool*, **49**: 801-809.
- Hossen MA, Hossain MY, Pramanik MNU, Nawer F, Khatun D, Parvin MF and Rahman MM. 2016. Morphological characters of *Botia lohachata*. *J Coast Life Med*, **4**: 689-692.
- Hossen MA, Hossain MY, Pramanik MNU, Khatun D, Nawer F, Parvin MF, Arabi A and Bashir MA. 2018. Population Parameters of the Minor carp *Labeo bata* (Hamilton, 1822) in the Ganges River of northwestern Bangladesh. *Jordan J Biol Sci*, **11**: 179-186.
- Hossen MB, Sharker MR, Rahman MA and Hoque MS. 2017. Morphometric and meristic variation of indigenous and Thai koi, *Anabas testudineus* available in coastal region of Bangladesh. *Int J Innov Res*, **2**: 01-08.
- IUCN Bangladesh. 2015. **Red List of Bangladesh Volume 5: Freshwater Fishes**. IUCN, International Union for Conservation of Nature, Bangladesh Country Office, Dhaka, Bangladesh, xvi+360 p.
- Jumawan JC and Seronay RA. 2017. Length-weight relationships of fishes in eight floodplain lakes of Agusan Marsh, Philippines. *Phil J Sci*, **146**: 95-99.

- Khatun D, Hossain MY, Parvin MF and Ohtomi J. 2018. Temporal variation of sex ratio, growth pattern and physiological status of *Eutropiichthys vacha* (Schilbeidae) in the Ganges River, NW Bangladesh. *Zool Ecol.*, **28**: 343-354.
- Khatun D, Hossain MY, Nawer F, Mostafa AA and Al-Askar AA. 2019. Reproduction of *Eutropiichthys vacha* (Schilbeidae) in the Ganges River (NW Bangladesh) with special reference to potential influence of climate variability. *Environ Sci Pollut Res.*, **26**:10800-10815.
- Kumar K, Lalrinsanga PL, Sahoo M, Mohanty UL, Kumar R and Sahu AK. 2013. Length-weight relationship and condition factor of *Anabas testudineus* and *Channa* species under different culture systems. *World J Fish Mar Sci.*, **5**: 74-78.
- Kumary KSA and Raj S. 2016. Length-weight relationship and condition of climbing perch *Anabas testudineus* Bloch population in Kuttanad, Kerala. *Int J Adv Res Biol Sci.*, **3**: 21-26.
- Le Cren, ED. 1951. The length-weight relationships and seasonal cycle in gonad weight and condition in the perch (*Perca fluviatilis*). *JAnim Ecol.*, **20**: 201-219.
- Lucifora LO, Valero JL and Garcia VB. 1999. Length at maturity of the green-eye spurdog shark, *Squalus mitsukuii* (Elasmobranchii: Squalidae) from the SW Atlantic, with comparisons with other regions. *Mar Freshwater Res.*, **50**: 629-632.
- Mandal B, Kumar R and Jayasankar P. 2016. Efficacy of exogenous hormone (GnRH $\alpha$ ) for induced breeding of climbing perch *Anabas testudineus* (Bloch, 1792) and influence of operational sex ratio on spawning success. *Ani Repr Sci.*, **171**: 114-120.
- Marimuthu K, Arumugam J, Sandragasan D and Jegathambigai R. 2009. Studies on the fecundity of native fish climbing perch (*Anabas testudineus*, Bloch) in Malaysia. *Am.-Eurasian J Sustain Agric.*, **3**: 266-274.
- Menon AGK. 1999. **Check list - Freshwater Fishes of India.** *Rec Zool Surv India, Misc Publ, Occas. Pap. No. 175*, 366 p.
- Nawer F, Hossain MY, Hossen MA, Khatun D, Parvin MF, Ohtomi J and Islam MA. 2017. Morphometric relationships of the endangered ticto barb *Pethia ticto* (Hamilton, 1822) in the Ganges River (NW Bangladesh) through multi-linear dimensions. *Jordan J Biol Sci*, **10**: 199-203.
- Nelson JS. 2006. **Fishes of the World** (4th ed.). Hoboken, NJ: John Wiley & Sons. ISBN 978-0-471-25031-9. sk JS.
- Peterson I and Wroblewski JS. 1984. Mortality rates of fishes in the pelagic ecosystem. *Can J Fish Aquat Sci*, **41**: 1117-1120.
- Pethiyagoda R. 1991. **Freshwater Fishes of Sri Lanka.** The Wildlife Heritage Trust of Sri Lanka, Colombo. 362 p.
- Rahman AKA. 1989. **Freshwater Fishes of Bangladesh.** Zoological Society of Bangladesh. Department of Zoology, University of Dhaka. 364 p.
- Rahman AKA. 2005. **Freshwater Fishes of Bangladesh (2nd edition).** Zoological Society of Bangladesh, Department of Zoology, University of Dhaka, Dhaka. 394 p.
- Rahman MM, Hossain MY, Jewel MAS, Billah MM and Ohtomi J. 2018. Population biology of the pool barb *Puntius sophore* (Hamilton 1822) (Cyprinidae) in the Padma River, Bangladesh. *Zool Ecol*, **28**: 100-108.
- Rahman MM, Hossain MY, Jewel MAS, Rahman MM, Jasmine S, Abdallah EM and Ohtomi J. 2012a. Population structure, length-weight and length-length relationships, and condition- and form-factors of the Pool barb *Puntius sophore* (Hamilton, 1822) (Cyprinidae) from the Chalan bel, north-central Bangladesh. *Sains Malays*, **41**: 795-802.
- Ranjan JB, Herwig W, Subodh S and Michael S. 2005. Study of the length frequency distribution of sucker head, *Garragotyla gotyla* (Gray, 1830) in different rivers and seasons in Nepal and its applications. *Kathmandu Univ J Sci Eng Technol*, **1**: 1-14.
- Richter TJ. 2007. Development and evaluation of standard weight equations for bridgelip suckers and largescale suckers. *N Am J Fish Manag.*, **27**: 936-939.
- Rypel AL and Richter TJ. 2008. Empirical percentile standard weight equation for the blacktail redhorse. *N Am J Fish Manag.*, **28**: 1843-1846.
- Sarkar UK, Deepak PK, Kapoor D, Negi RS, Paul SK and Singh S. 2005. Captive breeding of climbing perch *Anabas testudineus* (Bloch, 1792) with Wova-FH for conservation and aquaculture. *Aquacult Res*, **36**: 941-945.
- Satrawaha R and Pilasamorn C. 2009. Length-weight and length-length relationships of fish species from the Chi River, northeastern Thailand. *J Appl Ichthyol*, **25**: 787-788.
- Shafi M and Mustafa G. 1976. Observations on some aspects of the biology of the climbing perch, *Anabas testudineus* (Bloch) (Anabantidae: Perciformes). *Bangladesh J Zool*, **4**: 21-28.
- Sokal RR and Rohlf FJ. 1987. **Introduction to Biostatistics**, 2nd edn. Freeman Publication, New York, 225-227 pp.
- Talwar PK and Jhingran AG. 1991. *Inland Fishes of India and Adjacent Countries*. Vol. 2. Rotterdam: A. A. Balkema.
- Tesch FW. 1968. Age and growth. In: Ricker, W.E (Eds), **Methods for Assessment of Fish Production in Freshwaters**, Oxford: Blackwell Scientific Publications.
- Tesch FW. 1971. Age and Growth. In: Ricker WE (Eds), **Methods for Assessment of Fish Production in Fresh Waters.**, Oxford: Blackwell Scientific Publications, 98-130 pp.
- Uddin S, Hasan MH, Iqbal MM and Hossain MA. 2017. Study on the reproductive biology of Vietnamese climbing perch (*Anabas testudineus*, Bloch). *Punjab Univ J Zool*, **32**: 1-7.
- Vidthayanon C. 2002. Peat swamp fishes of Thailand. Office of Environmental Policy and Planning, Bangkok, Thailand, 136 p.
- Ziauddin G, Behera S, Sanjeev K, Rinku G, Jomang O and Baksi S. 2016. Morphometrical and gonadal studies of a threatened fish, *Anabas testudineus* with respect to seasonal cycle. *Int J Fish Aquacult Sci*, **6**: 7-14.
- Zworykin DD. 2012. Reproduction and spawning behavior of the climbing perch *Anabas testudineus* (Perciformes, Anabantidae) in an aquarium. *J Ichthyol*, **52**: 379-388.

# Virtual Screening for Inhibitors Targeting the Rod Shape-Determining Protein in *Escherichia coli*

Mohammed Z. Al-Khayyat<sup>1\*</sup>, Ammar Gh. Ameen<sup>2</sup> and Yousra A. Abdulla<sup>1</sup>

<sup>1</sup>Biology Department, College of Education for Pure Sciences, <sup>2</sup> Biology Department, College of Science, University of Mosul, Mosul city, Iraq

Received June 20, 2018; Revised August 26, 2018; Accepted August 28, 2018

## Abstract

The rod shape-determining protein, MreB, is a bacterial actin analog and is involved in determining the shape of non-spherical bacteria. A tertiary structure of MreB from *Escherichia coli* was constructed by an online server, RaptorX, and its accuracy was assessed by four validation tools. The docking software, AutoDock Vina was used to dock a total of one-hundred natural occurring compounds obtained from ZINC and PubChem databases. The pharmacokinetics and toxicity profiles of the compounds were predicted by Swiss ADME tool. The results indicate that amentoflavone, rutin, and chlorogenic acid had binding affinities of -10.9, -10.1 and -9.3 Kcal/mol respectively which were higher than the control, ATP, -9.2 Kcal/mol. In the pharmacokinetic profiling, these three compounds were not inhibitors of cytochromes, but had a low gastrointestinal absorption. MreB may serve as an alternative molecular target for new antibiotics against rod-shape resistant microbes, since the disruption of its function may lead to bacterial cell lysis.

**Keywords:** Amentoflavone, AutoDock Vina, Docking, Homology modeling, MreB.

## 1. Introduction

The rod shape-determining protein, MreB, is a component of bacterial cytoskeleton, and is an analog of the eukaryotic actin. MreB is a product of *mre* operon (murein gene cluster e) (Doi *et al.*, 1988). Unlike actin, MreB uses ATP to polymerize into helical filaments encircling the whole cell just under the cytoplasmic membrane (Jones *et al.*, 2001). This activity is essential for maintaining the rod shape of *Escherichia coli*, *Caulobacter crescentus*, and *Thermotoga maritima* (Salje *et al.*, 2011). Several proteins act for this purpose in non-spherical bacteria including two membrane proteins encoded by *mreC* and *mreD*. The cell wall biosynthetic component, Penicillin-binding protein 2 (PBP2), via interaction with MreC also participates in the process (Wachi *et al.*, 1989; Slovak *et al.*, 2006; van den Ent *et al.*, 2010). Another cell protein, RodZ, interacts with of MreB in the process of cell wall synthesis by affecting its biophysics. The expression of these two proteins varies in response to cell width and growth rate variations (Colavin *et al.*, 2018). Mutagenesis of *mreB* results in the loss of the normal rod-shape of *E. coli* and the formation of spherical cells. These slowly growing irregular cells are hypersensitive to antibiotics targeting cell wall synthesis such as mecillinam, and tend to lyse under normal growth conditions (Wachi *et al.*, 1987; Bendežú and de Boer, 2008).

The failure of the currently-used antimicrobials to combat infections caused by resistant microbes encouraged researchers to search for new molecular targets upon

which newer agents may work either to kill pathogenic microbes or eliminate their pathogenicity. A suggested approach is to screen libraries of natural or synthetic compounds capable of binding a selected molecular targets inside the bacterial cell. A selected compound should be able to abolish the function of this selected target. Docking experiments may be used to compute *in silico* the binding affinity of ligands with the molecular targets, and present the results in a scoring system (Allsop and Illingworth, 2002; Huang and Zou, 2010).

Due to difficulties in the purification of this protein, most structural studies of MreB were conducted on *T. maritima* because there is no experimental structure that has been determined for *E. coli* (Salje *et al.*, 2011). The only study of the MreB inhibition, is that of Iwai *et al.* (2002) in which the compound S-(3,4-dichlorobenzyl) isothioureia, affected MreB of *C. crescentus*, and resulted in converting the rod-shape cells into spherical ones (Iwai *et al.*, 2002). This study is aimed at building a model of *E. coli* MreB, and carrying out docking experiments in order to find possible inhibitors.

## 2. Materials and Methods

### 2.1. Homology Modeling

The amino-acid sequence of MreB (Doi *et al.*, 1988) was obtained from Uniprot database which can be accessed at <http://www.uniprot.org/>. The MreB accession number was (P0A9X4). The protein tertiary structure was built by an online server, RaptorX (Källberg *et al.*, 2012), at (<http://raptorx.uchicago.edu/>) which also predicts the

\* Corresponding author e-mail: mzsaeed19@hotmail.com.

binding site. The sequence was visualized by BioEdit 3.3.19.0 (Hall, 1999). The three-dimensional structure was visualized by ArgusLab 4.0.1 (Thompson, 2004) and for the protein-ligand interactions, LigPlot<sup>+</sup> was used (Wallace *et al.*, 1996).

## 2.2. Quality Assessment of the Model

The accuracy of the model was assessed by four online tools; (a) ERRAT (Colovos and Yeates, 1993) at (<http://services.mbi.ucla.edu/ERRAT/>), (b) PROSA (Sippl, 1993; Wiederstein and Sippl, 2007), accessed at (<https://prosa.services.came.sbg.ac.at/prosa.php>), (c) Qualitative Model Energy Analysis tool, QMEAN6 (Benkert *et al.*, 2009) at: (<https://swissmodel.expasy.org/>); (d) Ramachandran plot analysis by RAMPAGE (Lovell *et al.*, 2002), at (<http://mordred.bioc.cam.ac.uk/~rapper/rampage.php>). The model was submitted into the protein model database (PMDb) (Castrignano *et al.*, 2006) which can be accessed at <http://bioinformatics.cineca.it/PMDB>.

## 2.3. Molecular Docking

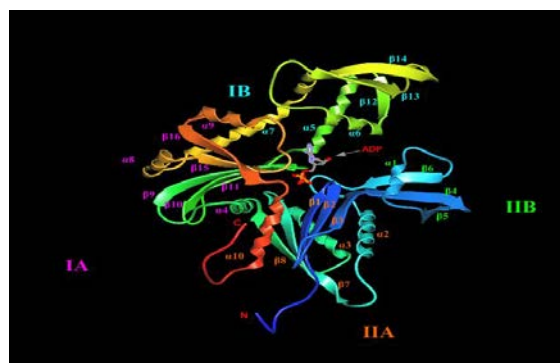
A total of one-hundred natural compounds were obtained from ZINC database (Irwin *et al.*, 2012) available at (<http://zinc.docking.org/>) and PubChem database (Kim *et al.*, 2016) available at (<http://pubchem.ncbi.nlm.nih.gov>). These two databases also provide the molecular properties: mass, H-bond donors, H-bond acceptors, and polar surface area. Molecular docking was performed using AutoDock Vina (Trott and Olson, 2010). The Autogrid tool was employed to pre-calculate a grid. This grid has a size of 60×60×60 and a box center of 1.615,-1.708 and 22.49 for x, y, and z respectively.

## 2.4. Pharmacologic Properties of the Compounds

The pharmacokinetics of the compounds were predicted by Swiss ADME (Daina *et al.*, 2017) at <http://www.swissadme.ch/>. The computed parameters were: (1) Gastro-intestinal absorption (GI absorption), (2) blood-brain barrier (BBB) penetration, (4) plasma glycoprotein (P-gp) substrate and (5) Cytochromes (CYP P<sub>450</sub>), inhibition.

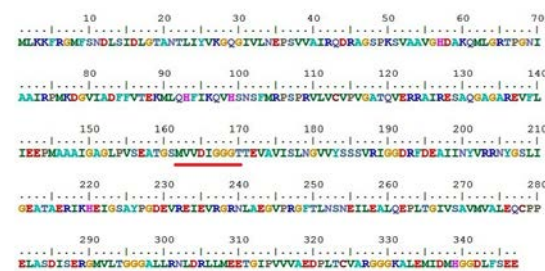
## 3. Results

The constructed model (Figure 1) appears to be composed of 40 %  $\alpha$ -helices, 25 %  $\beta$ -strands and 36 % as coils. Since there is no experimental structure of MreB for *E. coli*, the selected template was 2 Å X-ray crystal structure of rod shape-determining protein of *C. crescentus* (Löwe and van den Ent, 2014). This template has a PDB ID of 4cze.1A with a sequence identity of 63.75 % and 95 % coverage of the predicted model. The predicted model was submitted onto protein model database with PMDB ID: PM0080558. The constructed model of MreB has the following topology:  $\beta$ 1 D<sup>12</sup>→G<sup>18</sup>,  $\beta$ 2 A<sup>20</sup>→V<sup>26</sup>,  $\beta$ 3 G<sup>30</sup>→D<sup>36</sup>,  $\beta$ 4 V<sup>38</sup>→R<sup>45</sup>,  $\beta$ 5 S<sup>48</sup>→G<sup>56</sup>,  $\alpha$ 1 H<sup>57</sup>→Q<sup>61</sup>,  $\beta$ 6 N<sup>69</sup>→K<sup>77</sup>,  $\alpha$ 2 F<sup>84</sup>→V<sup>98</sup>,  $\beta$ 7 R<sup>109</sup>→V<sup>114</sup>,  $\alpha$ 3 Q<sup>120</sup>→A<sup>133</sup>,  $\beta$ 8 E<sup>137</sup>→I<sup>141</sup>,  $\alpha$ 4 P<sup>144</sup>→I<sup>149</sup>,  $\beta$ 9 S<sup>161</sup>→G<sup>167</sup>,  $\beta$ 10 T<sup>170</sup>→S<sup>177</sup>,  $\beta$ 11 G<sup>180</sup>→V<sup>187</sup>,  $\alpha$ 5 G<sup>191</sup>→Y<sup>206</sup>,  $\beta$ 12 G<sup>207</sup>→I<sup>209</sup>,  $\alpha$ 6 E<sup>212</sup>→I<sup>222</sup>,  $\beta$ 13 R<sup>232</sup>→L<sup>241</sup>,  $\beta$ 14 V<sup>245</sup>→S<sup>253</sup>,  $\alpha$ 7 N<sup>254</sup>→A<sup>276</sup>,  $\alpha$ 8 P<sup>280</sup>→R<sup>289</sup>,  $\beta$ 15 M<sup>291</sup>→T<sup>294</sup>,  $\alpha$ 9 L<sup>303</sup>→T<sup>311</sup>,  $\beta$ 16 I<sup>314</sup>→A<sup>318</sup> and  $\alpha$ 10 P<sup>321</sup>→L<sup>333</sup>.



**Figure 1.** The MreB model as predicted by RaptorX. Numbering starts from N-terminal towards (N) to C-terminal (C). MreB monomer consists of two domains I and II. Subdomain IA and IIA have the topology of five  $\beta$ -sheets surrounded by three  $\alpha$ -helices, while the smaller subdomains are variable. Subdomain IA comprises  $\alpha$ 4,  $\alpha$ 8,  $\beta$ 9,  $\beta$ 10,  $\beta$ 11,  $\beta$ 15,  $\beta$ 16 and  $\alpha$ 9 while subdomain IIA comprises  $\alpha$ 2,  $\alpha$ 3,  $\beta$ 1,  $\beta$ 2,  $\beta$ 3,  $\beta$ 7,  $\beta$ 8 and  $\alpha$ 10. The variable smaller subdomain IB comprises  $\alpha$ 5,  $\alpha$ 6,  $\beta$ 12,  $\beta$ 13,  $\beta$ 14 and  $\alpha$ 7 and while subdomain IIB comprises  $\alpha$ 1,  $\beta$ 4,  $\beta$ 5 and  $\beta$ 6. ADP occupies a cleft between domains I and II where its phosphate groups interact. These two sub-domains are connected via a helix,  $\alpha$ 4.

RaptorX predicted two binding sites of the model. The largest pocket is for ADP molecule and consists of following residues: G<sup>18</sup>, T<sup>19</sup>, A<sup>20</sup>, N<sup>21</sup>, G<sup>167</sup>, G<sup>168</sup>, G<sup>169</sup>, G<sup>191</sup>, E<sup>216</sup>, K<sup>219</sup>, H<sup>220</sup>, G<sup>295</sup>, G<sup>296</sup>, G<sup>297</sup>, L<sup>299</sup>, L<sup>300</sup> and L<sup>322</sup>. A second smaller pocket was predicted for binding Mg<sup>+2</sup> ion, which is composed of E<sup>143</sup> and D<sup>165</sup> (Figure 2).



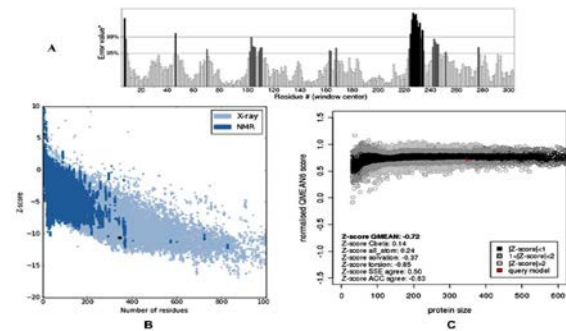
**Figure 2.** Amino acid sequence of MreB (Doi *et al.*, 1988). ATP binding motifs are marked with a red underline.

Four evaluation tools were used to measure the accuracy of the model. ERRAT overall quality of the model is 88.855 % (Figure 3 A). PROSA Z-score is -10.66 (Figure 3 B). The raw score of QMEAN6 is 0.713 which is in the normal range of 0-1. A comparison of Z-scores with experimentally determined structures is shown in (Figure 3 C). In the Ramachandran plot analysis, the constructed MreB model has 338(98.0 %) of the residues being in the favored region (Figure 4), and three residues (0.9 %) in the allowed region. These residues are S<sup>102</sup>, V<sup>231</sup> and M<sup>335</sup>. Four residues (1.2 %) were in the disallowed (outlier) region. These residues are R<sup>45</sup>, N<sup>101</sup>, F<sup>103</sup> and D<sup>229</sup>.

A total of one-hundred natural compounds were docked against the predicted model; the highest ten are shown in Table 1. Figure 5 shows ATP at its binding site in MreB and the interaction with the MreB amino acid residues. The results of AutoDock Vina show that there are three compounds, namely amentoflavone, rutin, and chlorogenic acid which had higher binding affinities than ATP. Figures 6-8 show the docking of the three ligands against MreB



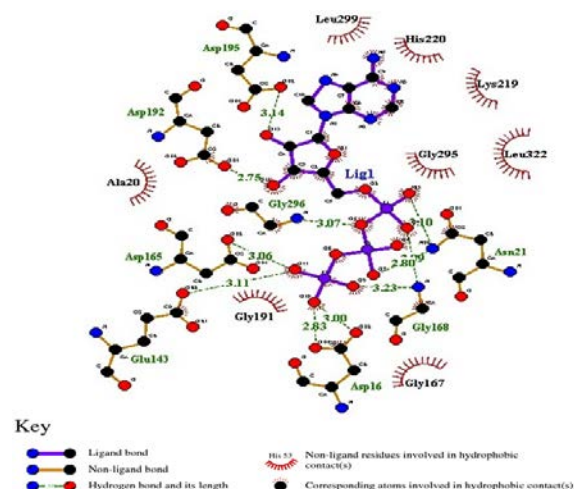
and the amino-acid residues involved. Figure 9 shows the chemical structure of these three compounds.



**Figure 3.** (A) ERRAT result of the generated model. Black bars represent misfolded regions. On the error axis two lines are drawn to indicate the confidence in which it is possible to reject regions (B) Z-score of MreB (black dot) computed by PROSA web tool compared with Z-scores of the experimentally determined proteins by NMR spectroscopy and X-ray crystallography (C) QMEAN6 plot of MreB model showing a comparison with non-redundant set of known experimental PDB structures in Z-scores.

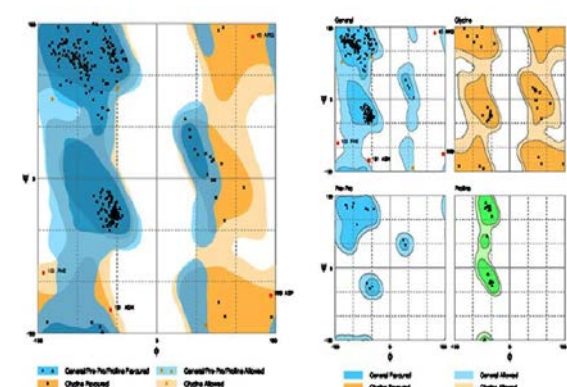
**Table 1.** Results of docking *E. coli* MreB

Compound	Database ID	Binding affinity (Kcal/mol)	Residues forming hydrogen bonds	Residues forming hydrophobic interactions
ATP	ZINC18456332	-9.2	D <sup>16</sup> , N <sup>21</sup> , E <sup>143</sup> , D <sup>165</sup> , G <sup>168</sup> , G <sup>192</sup> , G <sup>195</sup>	A <sup>20</sup> , G <sup>167</sup> , G <sup>191</sup> , K <sup>219</sup> , H <sup>220</sup> , G <sup>295</sup> , L <sup>299</sup> , L <sup>322</sup>
Amentoflavone	ZINC03984030	-10.9	D <sup>16</sup> , N <sup>21</sup> , E <sup>143</sup> , G <sup>168</sup>	G <sup>18</sup> , T <sup>19</sup> , A <sup>20</sup> , G <sup>167</sup> , F <sup>194</sup> , K <sup>219</sup> , H <sup>220</sup> , G <sup>295</sup> , G <sup>296</sup> , L <sup>299</sup> , L <sup>300</sup> , L <sup>322</sup> , V <sup>325</sup>
Rutin	ZINC59764511	-10.1	D <sup>16</sup> , R <sup>74</sup> , D <sup>165</sup> , G <sup>168</sup> , G <sup>296</sup> , G <sup>297</sup> , L <sup>322</sup>	G <sup>18</sup> , A <sup>20</sup> , N <sup>21</sup> , N <sup>34</sup> , E <sup>35</sup> , P <sup>36</sup> , K <sup>60</sup> , E <sup>143</sup> , G <sup>167</sup> , G <sup>191</sup> , D <sup>195</sup> , E <sup>216</sup> , K <sup>219</sup> , H <sup>220</sup> , G <sup>295</sup> , V <sup>325</sup>
Chlorogenic acid	ZINC02138728	-9.3	D <sup>16</sup> , T <sup>19</sup> , N <sup>21</sup> , E <sup>143</sup> , G <sup>169</sup> , T <sup>170</sup>	G <sup>18</sup> , A <sup>20</sup> , G <sup>79</sup> , D <sup>165</sup> , G <sup>167</sup> , G <sup>168</sup> , G <sup>191</sup> , G <sup>295</sup> , V <sup>325</sup>
Scutellarin	ZINC21902916	-9.2	D <sup>16</sup> , T <sup>19</sup> , G <sup>168</sup> , G <sup>296</sup> , L <sup>322</sup>	G <sup>18</sup> , A <sup>20</sup> , P <sup>36</sup> , N <sup>21</sup> , G <sup>167</sup> , G <sup>191</sup> , K <sup>219</sup> , G <sup>296</sup>
Takakin	ZINC14813980	-8.6	D <sup>16</sup> , T <sup>19</sup> , E <sup>143</sup> , G <sup>168</sup>	G <sup>18</sup> , A <sup>20</sup> , N <sup>21</sup> , G <sup>167</sup> , D <sup>195</sup> , K <sup>219</sup> , G <sup>295</sup> , G <sup>296</sup> , L <sup>322</sup> , V <sup>325</sup>
Coumestrol	ZINC00001219	-8.3	-	A <sup>20</sup> , G <sup>168</sup> , G <sup>191</sup> , K <sup>219</sup> , H <sup>220</sup> , G <sup>296</sup> , G <sup>297</sup> , L <sup>299</sup> , L <sup>300</sup>
Hinokinin	ZINC01872258	-8.3	-	D <sup>16</sup> , A <sup>20</sup> , N <sup>21</sup> , K <sup>60</sup> , E <sup>143</sup> , I <sup>166</sup> , G <sup>167</sup> , G <sup>168</sup> , G <sup>191</sup> , D <sup>195</sup> , E <sup>216</sup> , E <sup>216</sup> , K <sup>219</sup> , H <sup>220</sup> , G <sup>296</sup> , G <sup>297</sup> , L <sup>322</sup>
Bucegin	ZINC14757469	-8.3	G <sup>191</sup>	A <sup>20</sup> , N <sup>21</sup> , G <sup>167</sup> , G <sup>168</sup> , K <sup>219</sup> , H <sup>220</sup> , G <sup>223</sup> , G <sup>296</sup> , G <sup>297</sup> , L <sup>299</sup> , L <sup>300</sup> , R <sup>301</sup> , L <sup>322</sup>
Isoquercitrin	ZINC04096845	-8.2	I <sup>166</sup> , D <sup>195</sup> , K <sup>219</sup>	A <sup>20</sup> , N <sup>21</sup> , N <sup>34</sup> , E <sup>35</sup> , P <sup>36</sup> , K <sup>60</sup> , G <sup>167</sup> , G <sup>168</sup> , G <sup>191</sup> , E <sup>216</sup> , H <sup>220</sup> , G <sup>296</sup> , G <sup>297</sup> , L <sup>322</sup>
Vitexin	ZINC04339745	-8.1	D <sup>192</sup>	A <sup>20</sup> , N <sup>21</sup> , G <sup>168</sup> , G <sup>191</sup> , F <sup>194</sup> , D <sup>195</sup> , E <sup>216</sup> , K <sup>219</sup> , H <sup>220</sup> , G <sup>296</sup> , G <sup>297</sup> , L <sup>299</sup> , L <sup>300</sup> , L <sup>322</sup>

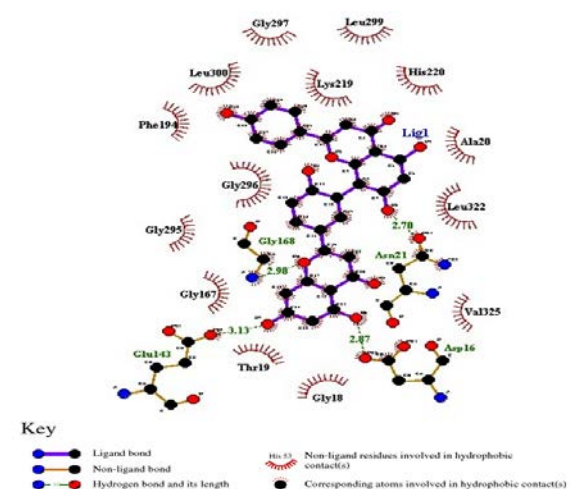


**Figure 5.** ATP interaction with MreB. ATP forms H-bonds with the amino-acid residues D<sup>16</sup> (2.83, 3.00 Å), N<sup>21</sup> (3.10, 2.09 Å), E<sup>143</sup> (3.11 Å), D<sup>165</sup> (3.06 Å), G<sup>168</sup> (2.80, 3.23 Å), G<sup>192</sup> (2.75 Å) and G<sup>195</sup> (3.14 Å). ATP also has hydrophobic interactions with A<sup>20</sup>, G<sup>167</sup>, G<sup>191</sup>, K<sup>219</sup>, H<sup>220</sup>, G<sup>295</sup>, L<sup>299</sup> and L<sup>322</sup>.

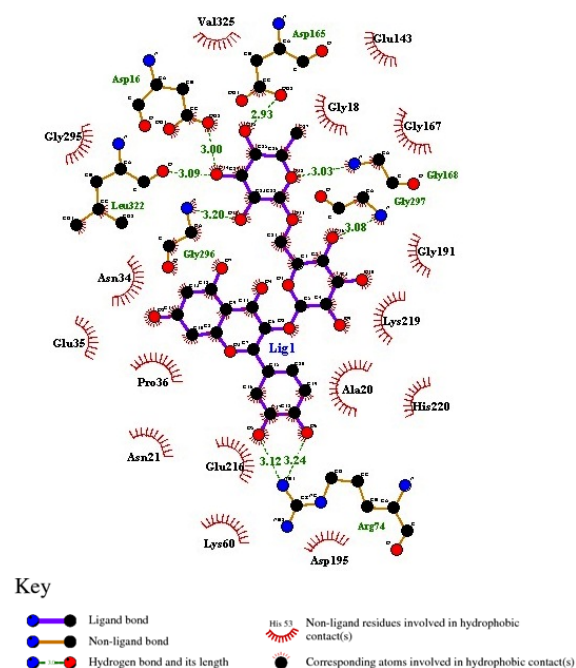
**Figure 4.** Ramachandran plot of the predicted model using RAMPAGE. Residues in the disallowed regions are red-colored



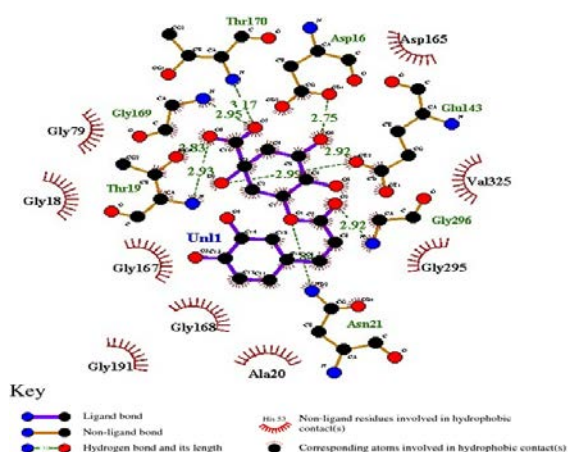
squares, while residues in the allowed region are brown-colored squares.



**Figure 6.** Amentoflavone interaction with MreB. Amentoflavone forms H-bonds with the amino-acid residues D<sup>16</sup> (2.87 Å), N<sup>21</sup> (2.70 Å), E<sup>143</sup> (3.13 Å) and G<sup>168</sup> (2.98 Å). It also has hydrophobic interactions with G<sup>18</sup>, T<sup>19</sup>, A<sup>20</sup>, G<sup>167</sup>, F<sup>194</sup>, K<sup>219</sup>, H<sup>220</sup>, G<sup>295</sup>, G<sup>296</sup>, L<sup>299</sup>, L<sup>300</sup>, L<sup>322</sup>, and V<sup>325</sup>.



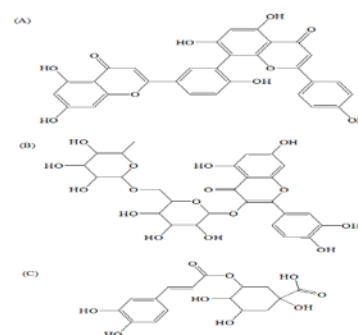
**Figure 7.** Rutin interaction with MreB. Rutin forms H-bonds with the amino-acid residues D<sup>16</sup> (3.00 Å), R<sup>74</sup> (3.12, 3.24 Å), D<sup>165</sup> (2.93 Å), G<sup>168</sup> (3.03 Å), G<sup>296</sup> (3.20 Å), G<sup>297</sup> (3.08 Å) and L<sup>322</sup> (3.09 Å). It also has hydrophobic interactions with G<sup>18</sup>, A<sup>20</sup>, N<sup>21</sup>, N<sup>34</sup>, E<sup>35</sup>, P<sup>36</sup>, K<sup>60</sup>, E<sup>143</sup>, G<sup>167</sup>, G<sup>191</sup>, D<sup>195</sup>, E<sup>216</sup>, K<sup>219</sup>, H<sup>220</sup>, G<sup>295</sup>, and V<sup>325</sup>.



**Figure 8.** Chlorogenic-acid interaction with MreB. Chlorogenic acid forms H-bonds with the amino-acid residues D<sup>16</sup> (2.75 Å), T<sup>19</sup> (2.83, 2.93 Å), N<sup>21</sup> (2.84 Å), E<sup>143</sup> (2.99, 2.92 Å) and G<sup>169</sup> (2.95 Å), T<sup>170</sup> (3.17 Å) and G<sup>296</sup> (2.92 Å). It also has hydrophobic interactions with G<sup>18</sup>, A<sup>20</sup>, G<sup>79</sup>, D<sup>165</sup>, G<sup>167</sup>, G<sup>168</sup>, G<sup>191</sup>, G<sup>295</sup> and V<sup>325</sup>.

**Table 3.** Swiss ADME predicted pharmacokinetics of the ligands.

Compound	GI absorption	BBB permeant	P-gp substrate	CYP 450 Inhibition				
				CYP1A2	CYP2C19	CYP 2C9	CYP2D6	CYP 3A4
Amentoflavone	Low	No	No	No	No	No	No	No
Rutin	Low	No	Yes	No	No	No	No	No
Chlorogenic acid	Low	No	No	No	No	No	No	No
Scutellarin	Low	No	Yes	No	No	No	No	No
Takakin	High	No	No	Yes	No	Yes	Yes	Yes
Coumestrol	High	No	No	Yes	No	No	Yes	No
Hinokinin	High	Yes	No	Yes	Yes	Yes	Yes	Yes
Bucegin	High	No	No	Yes	No	Yes	Yes	Yes
Isoquercitrin	Low	No	No	No	No	No	No	No
Vitexin	Low	No	No	No	No	No	No	No



**Figure 9.** The chemical structure of (A) amentoflavone (B) rutin (C) chlorogenic acid.

Table 2 shows the chemical properties of the ligands. The predicted ADME profiles, namely absorption, distribution, metabolism, elimination were computed by Swiss ADME, and are presented in Table 3. Swiss ADME shows that the three compounds cannot cross the blood-brain barrier, and have low absorption via the human gastrointestinal tract. Only Rutin is a substrate for P-glycoprotein. None of the compounds is inhibitory of the cytochromes. Amentoflavone and rutin show violation of the Lipinski's rule, since their molecular weights are more than 500, the logP of amentoflavone is greater than five, and rutin has its hydrogen bond acceptors being more than 10. In respect to this rule, chlorogenic acid appears to be better than the other two natural products.

**Table 2.** Molecular descriptors of the compounds.

Compound	Mass (g/mol)	xlogP	H-bond donors	H-bond acceptors	Polar surface area (Å <sup>2</sup> )
Amentoflavone	538.464	5.61	6	10	182
Rutin	610.521	-1.06	10	16	269
Chlorogenic acid	353.303	-0.45	5	9	168
Scutellarin	461.355	0.07	6	12	210
Takakin	300.266	2.74	3	6	100
Coumestrol	268.224	2.54	2	5	84
Hinokinin	354.358	3.02	0	6	63
Bucegin	314.293	3.02	2	6	89
Isoquercitrin	464.379	-0.36	8	12	211
Vitexin	432.381	0.52	7	10	181

#### 4. Discussion

The actin-like protein MreB regulates the synthesis of the cell wall. The length and number of polymer and its curvature are correlated to the cell width and cylindrical uniformity of the cell (Bratton *et al.*, 2018). The anionic phospholipids, phosphatidylglycerol and cardiolipin are essential to MreB activity since they would be deposited at the cell poles and an irregular shape is developed due to lack of these phospholipids (Kawazura *et al.*, 2017). Van den Ent *et al.*, (2001) suggested that MreB of *T. maritima* possesses a similar topology to actin. The tertiary structure appears to be composed of two domains (I and II) where a nucleotide-binding site is formed by the cleft between the two domains. Each domain is subdivided into two sub-domains A and B.

Walker *et al.* (1982) suggested that an ATP-binding motif, also called Walker A, having the sequence of GX<sub>4</sub>GK[S/T], is found in the nucleotide recognition sequences of many proteins (Walker *et al.*, 1982). Several Walker-A sequence variants have been identified; for example, the serine/threonine residue may be replaced by aspartic acid or glycine in some kinases. Several proteins that bind ATP may also have G-rich loops, GXGXXG, which bind the  $\alpha$  and  $\beta$  phosphates of ATP (Bossemeyer, 1994; Leipe *et al.*, 2003). A second sequence, the Walker-B motif, contains a conserved aspartic or glutamic-acid residue which is preceded by four hydrophobic residues. This second motif forms coordinate bonds with the Mg<sup>2+</sup> ion which is necessary for the catalysis of the ATPase reaction (Walker *et al.*, 1982). However, Bork *et al.*, (1992) suggested that MreB and its related division protein, FtsA, contain two ATP binding motifs one for phosphate: V<sup>163</sup>, V<sup>164</sup>, D<sup>165</sup>, I<sup>166</sup>, G<sup>167</sup>, G<sup>168</sup>, G<sup>169</sup> and T<sup>170</sup>, and a second for adenosine: V<sup>292</sup>, L<sup>293</sup>, T<sup>294</sup>, G<sup>295</sup> and G<sup>296</sup>.

Although many online automated servers have been developed for homology modeling, reliability and accuracy of these models for docking experiments should be explored and assessed. ERRAT is a statistical potential to detect regions of errors the basis of heavy atomic-pair distributions (CC, CN, CO, NN, NO and OO) of the amino-acid residues that are compared with a set of 96 experimental structures. A high-resolution experimental structure usually produces quality factors of 95 % or higher, but those had a lower resolution showing an average of 91 % as a quality factor (Colovos and Yeates, 1993). PROSA is another statistical potential method to measure the energy difference in terms of standard deviation between a native fold of protein and an ensemble of alternative folds to predict error in the constructed model. The energy of the model is shown against the known X-ray and the NMR solved structures of proteins deposited in the Protein Data Bank (Zhang and Skolnick, 1992; Wiederstein and Sippl, 2007).

QMEAN6 estimates the quality of the models by six indices. These are (a) the solvation potential, (b) the torsion angle potential, (c) two distance-dependent potentials: one based on  $\beta$ -atoms, and the second is based on all-atom, and (d) two terms: one compares the predicted secondary structure with a computed (SSE agree.), and the second is for the solvent accessibility (ACC agree.) (Benkert *et al.*, 2009, 2011). In the Ramachandran plot analysis, normally 98.0 % of the residues are expected to

be in the favored region, and 2 % are in the allowed region for accurate models (Lovell *et al.*, 2002).

Amentoflavone is a bioflavonoid extracted from *Selaginella tamariscina*. It has an antibacterial action and possesses a synergistic effect with antibiotics (ampicillin, cefotaxime and chloramphenicol) when tested on *Staphylococcus aureus*, *Enterococcus faecium*, *E. coli* and *Pseudomonas aeruginosa* (Hwang *et al.*, 2013). Moreover, Kaikabo *et al.* (2009) had isolated amentoflavone from *Garcinia livingstonei*, and suggested that it has an antibacterial activity against *S. aureus*, *E. faecalis*, *E. coli*, and *P. aeruginosa*.

Rutin is 3, 4, 4', 5, 7-pentahydroxyflavone-3-rhamnoglucoside, a flavonoid present in tea, apples and onions with many medicinal activities such as antifungal, antibacterial and anti-cancer potentials (Sharma *et al.*, 2013; Janbaz, 2002).

Chlorogenic acid is a polyphenolic compound found in apricots where its methanolic extract, containing 968.125  $\mu\text{g/ml}$  of the compound, inhibited *E. coli*, *Salmonella enteritidis* and *Helicobacter pylori* (Mujtaba *et al.*, 2017). Lou *et al.* (2011) suggested that chlorogenic acid has antimicrobial activities against bacteria at minimum inhibitory concentrations ranging between 20-80  $\mu\text{g/ml}$ . A possible mechanism of its action is the disruption of the plasma membrane which becomes permeable to cytoplasmic components including nucleotides.

Lipinski *et al.*, (2001) suggested a rule of five to predict the solubility and permeability of a candidate drug. In this rule, poor permeability probably occurs when there are more than five hydrogen bond donors, ten hydrogen bond acceptors, and when the molecular weight is greater than five-hundred, and the calculated Log P (logarithm of octanol-water partition coefficient) is greater than five. The polar surface area also estimates a drug's permeability. Compounds with a polar surface area being greater than 140  $\text{\AA}^2$  may have poor permeability across cell membranes, and for crossing the blood-brain barrier, compounds need to have a polar surface area less than 90  $\text{\AA}^2$  (Pajouhesh and Lenz, 2005). Lipinski *et al.* (2001) stated that in spite of the fact that a huge amount of compounds were used to predict this rule, several classes of drugs such as antifungal and antibacterial drugs are exceptions. Drugs that are subjected to transporters inside the human body are excluded from the rule as well.

Many factors affect the gastrointestinal tract absorption. Some of these factors are physicochemical such as the solubility and lipophilicity, while others are physiological such as active transport and efflux. The prediction of drug permeability across the blood-brain barrier is necessary when a drug is required to exert a therapeutic effect on the central nervous system, or when adverse effects of a drug in the brain are being questioned (de la Nuez and Rodríguez, 2008).

P-glycoproteins are members of the ATP-binding cassette transporter family and are responsible for multiple-drug resistance. By their efflux, P-glycoproteins decrease the bioavailability of a drug by reducing its levels inside human cells (Lin, 2003; van de Waterbreemd and Gifford, 2003). P-glycoproteins are found on the surface of biliary canalicular hepatocytes, the luminal surface of epithelial cells of the gastrointestinal tract, the proximal convoluted tubular cells of the kidney, and the capillary endothelial cells of the blood-brain barrier (Thiebut *et al.*,

1987). The human CYP isoforms CYP3A4, CYP2C9, CYP2C19 and CYP2D6 account for about 80 % of the oxidative metabolism of drugs, the first stage of elimination (Williams *et al.*, 2004).

In the pharmaceutical industry, the chemical and physical modifications of the parent compounds are implemented to enhance their properties including solubility and absorption, e.g. nanosuspension, solid dispersions, use of carriers and surfactants, and the reduction of particle size (Chaudry and Patel, 2013). Upretti *et al.* (2011) suggested adding a terpene glycoside and cyclodextrin to increase the solubility of drugs.

## 5. Conclusion

The bioinformatics' tools, including homology modeling and docking, may be implemented in the preliminary screening of drugs. The three compounds identified above may be capable of binding the active site of MreB, and may interfere with its ATPase activity. Amentoflavone, rutin, and chlorogenic acid can be useful as lead compounds to target MreB in *E. coli* and other bacilli affecting humans; however, in vitro and animal studies should be carried out to elucidate their effects. Pharmacokinetics and pharmacodynamics are essential in the drug discovery process. The pharmacological properties could be improved by the chemical and physical modifications of the drugs.

## References

- Allsop A and Illingworth R. 2002. The impact of genomics and related technologies on the search for new antibiotics. *J Appl Microbiol.*, **92**:7-11.
- Bendezú FO and de Boer PA. 2008. Conditional lethality, division defects, membrane involution, and endocytosis in *mre* and *mrh* shape mutants of *Escherichia coli*. *J Bacteriol.*, **190**: 1792-1811.
- Benkert P, Biasini M and Schwede T. 2011. Toward the estimation of the absolute quality of individual protein structure models. *Bioinformatics*, **27**(3): 343-350.
- Benkert P, Kunzli M and Schwede T. 2009. QMEAN server for protein model quality estimation. *Nucleic Acids Res.*, **37**: W510-W514.
- Bork P, Sander C and Valencia A. 1992. An ATPase domain common to prokaryotic cell cycle proteins, sugar kinases, actin and hsp70 heat shock proteins. *Proc Natl Acad Sci USA*, **89**:7290-7294.
- Bossemeyer D. 1994. The glycine-rich sequence of protein kinases: A multifunctional element. *Trends Biochem Sci.*, **19**:201-205.
- Bratton BP, Shaevitz JW, Gitai Z and Morgenstein RM. 2018. MreB polymers and curvature localization are enhanced by RodZ and predict *E. coli*'s cylindrical uniformity. *Nat Commun.* **9**(1):2797.
- Castrignano T, De Meo PD, Cozzetto D, Talamo IG and Tramontano A. 2006. The PMDB protein model database. *Nucleic Acids Res.*, **34**(1): D306-309.
- Chaudry VB and Patel JK. 2013. Cyclodextrin inclusion complex to enhance solubility of poorly water soluble drugs: A review. *Inter J Pharma Sci Res.* **4**(1):68-76.
- Colavin A, Shi H and Huang KC. 2018. RodZ modulates geometric localization of the bacterial actin MreB to regulate cell shape. *Nat Commun.* **9**(1):1280.
- Colovos C and Yeates TO. 1993. Verification of protein structures: Patterns of non-bonded atomic interactions. *Protein Sci.*, **2**:1511-1519.
- Daina A, Michielin O and Zoete V. 2017. SwissADME: A free web tool to evaluate pharmacokinetics, drug-likeness and medicinal chemistry friendliness of small molecules. *Sci Rep.*, **7**:42717.
- de la Nuez A and Rodríguez R. 2008. Current methodology for the assessment of ADME-Tox properties on drug candidate molecules. *Biotec Aplic.*, **25**(2): 97-110.
- Doi M, Wachi M, Ishino F, Tomioka S, Ito M, Sakagami Y, Suzuki A and Matsushashi M. 1988. Determinations of the DNA sequence of the *mreB* gene and of the gene products of the *mre* region that function in formation of the rod shape of *Escherichia coli* cells. *J Bacteriol.*, **170**:4619-4624.
- Hall TA. 1999. BioEdit: A user-friendly biological sequence alignment editor and analysis program for Windows 95/98/NT. *Nucl Acids Symp Ser.*, **41**:95-98.
- Huang S-Y and Zou X. 2010. Advances and challenges in protein-ligand docking. *Inter J Mol Sci.*, **11**:3016-3034.
- Hwang JH, Choi H, Woo E-R and Lee DG. 2013. Antibacterial effect of amentoflavone and its synergistic effect with antibiotics. *J Microbiol Biotechnol.*, **23**(7):953-958.
- Kaikabo AA, Samuel BB, Eloff JN. 2009. Isolation and activity of two antibacterial biflavonoids from leaf extracts of *Garcinia livingstonei* (Clusiaceae). *Nat Prod Commun.* **4**(10):1363-1366.
- Kawazura T, Matsumoto K, Kojiima K, Kato F, Kanai T, Niki H and Shiomi D. 2017. Exclusion of assembled MreB by anionic phospholipids at cell poles confers cell polarity for bidirectional growth. *Mol Microbiol.* **104**(3):472-486.
- Irwin JJ, Sterling T, Michael MM, Bolstad ES and Coleman RG. 2012. ZINC: A free tool to discover chemistry for biology. *J Chem Inf Model.*, **52**:1757-1768.
- Iwai N, Nagai K and Wachi M. 2002. Novel S-bezylisothiourea compound that induces spherical cells in *Escherichia coli* probably by acting on a rod-shaped-determining protein(s) other than penicillin-binding protein 2. *Biosci Biotechnol Biochem.*, **66**:2658-2662.
- Janbaz KH, Saeed SA and Gilani AH. 2002. Protective effect of rutin on paracetamol- and CCl4-induced hepatotoxicity in rodents. *Fitoterapia.*, **37**:557-563.
- Jones LJF, Carballido-Lopez R and Errington J. 2001. Control of cell shape in bacteria: helical, actin-like filaments in *Bacillus subtilis*. *Cell*, **104**:913-922.
- Källberg M, Wang H, Wang S, Peng J, Wang Z, Lu H and Xu J. 2012. Template-based protein structure modeling using the RaptorX web server. *Nat Protocols*, **7**:1511-1522.
- Kim S, Thiessen PA, Bolton EE, Chen J, Fu G, Gindulyte A, Han L, He J, He S, Shoemaker BA, Wang J, Yu B, Zhang J and Bryant SH. 2016. PubChem substance and compound databases. *Nucleic Acid Res.*, **44**: D1212-1213.
- Leipe DD, Koonin EV and Aravind L. 2003. Evolution and classification of P-loop kinases and related proteins. *J Mol Biol.*, **333**:781-815.
- Lin JH. 2003. Drug-drug interaction mediated by inhibition and induction of P-glycoprotein. *Adv Drug Deliv Rev.*, **55**: 53-81.
- Lipinski CA, Lombardo F, Dominy BW and Feeney PJ. 2001. Experimental and computational approaches to estimate solubility and permeability in drug discovery and development settings. *Adv Drug Delivery Rev.*, **46**:3-26.
- Lou Z, Wang H, Zhu S, Ma C and Wang Z. 2011. Antibacterial activity and mechanism of action of chlorogenic acid. *J Food Sci.*, **76**: M398-403.



- Lovell SC, Davis IW, Arendall 3rd WB, de Bakker PI, Word JM, Prisant MG, Richardson JS and Richardson DC. 2003. Structure validation by Ca geometry: Phi, psi and C $\beta$  deviation. *Proteins: Struct Funct Genet.*, **50**(3):437-450.
- Lowe J and van den Ent F. 2014. Bacterial actin MreB forms antiparallel double filaments. *Elife*, **3**:2634.
- Mujtaba A, Masud T, Ahmed A, Ahmed W, Jabbar S and Levin RE. 2017. Antibacterial activity by chlorogenic acid isolated through resin from apricot (*Prunus Armeniaca* L.). *Pakistan J Agric Res.*, **30**(2):144-148.s
- Pajouhesh H and Lenz GR. 2005. Medicinal chemical properties of successful central nervous system drugs. *Neuro Rx*, **2**(4):541-553.
- Salje J, van den Ent F, de Boer P and Löwe J. 2011. Direct membrane binding by bacterial actin MreB. *Mol Cell*, **43**:478-487.
- Sharma S, Ali A, Ali J, Sahni JK and Baboota S. 2013. Rutin: Therapeutic potential and recent advances in drug delivery. *Expert Opin Investig Drugs*, **22**:1063-1079.
- Sippl MJ. 1993. Recognition of errors in three-dimensional structures of proteins. *Proteins*, **17**:355-362.
- Slovak PM, Porter SL and Armitage JP. 2006. Differential localization of Mre proteins with PBP2 in *Rhodobacter sphaeroides*. *J Bacteriol.*, **188**:1691-1700.
- Thiebut F, Tsuruo T, Hamada H, Gottesman MM and Pastan I. 1987. Cellular localization of the multidrug resistance gene product P-glycoprotein in normal human tissues. *Proc Natl Acad Sci USA*, **84**:7735-7738.
- Thompson M. 2004. ArgusLab 4.0.1. Planaria Software LLC. Available at (<http://www.arguslab.com>). Seattle, Washington, USA.
- Trott O and Olson AJ. 2010. AutoDock Vina: Improving the speed and accuracy of docking with a new scoring function, efficient optimization and multithreading. *J Comput Chem.*, **31**(2):455-461.
- Upreti M, Prakash I and Chen YL. 2011. Solubility enhanced terpene glycosides(s). PCT/US2011/02436.
- van de Waterbeemd H and Gifford E. 2003. ADMET *in silico* modeling: Towards prediction paradise? *Nature*, **2**:192-204.
- van den Ent F, Johnson CM, Persons L, de Boer P and Löwe J. 2010. Bacterial actin MreB assembles in complex with cell shape protein RodZ. *EMBO J.*, **29**: 1081-1090.
- van den Ent V, Amos LA and Löwe J. 2001. Prokaryotic origin of the actin cytoskeleton. *Nature*, **413**(6):39-44.
- Wachi M, Doi M, Okada Y and Matsushashi M. 1989. New *mre* genes *mreC* and *mreD*, responsible for formation of the rod shape of *Escherichia coli* cells. *J Bacteriol.*, **171**:6511-6516
- Wachi M, Doi M, Tamaki S, Park W, Nakajima-Iijima S and Matsushashi M. 1987. Mutant isolation and molecular cloning of *mre* genes, which determine cell shape, sensitivity to mecillinam, and amount of penicillin-binding proteins in *Escherichia coli*. *J Bacteriol.*, **169**:4935-4940.
- Walker JE, Saraste M, Runswick M and Gay NJ. 1982. Distantly related sequences in the alpha- and beta-subunits of ATP synthase, myosin, kinases and other ATP-requiring enzymes and a common nucleotide binding fold. *EMBO J.*, **1**:945-951.
- Wallace AC, Laskowski RA and Thornton JM. 1996. LIGPLOT: A program to generate schematic diagrams of protein-ligand interactions. *Protein Eng.* **8**:127-134.
- Wiederstein M and Sippl MJ. 2007. ProSA-web: Interactive web service for the recognition of errors in three-dimensional structures of proteins. *Nucleic Acids Res.*, **35**:W407-410.
- Williams JA, Hyland R, Jones BC, Smith DA, Hurst S, Goosen TC, Peterkin V, Koup JR and Ball SE. 2004. Drug-drug interactions for UDP-glucuronosyltransferase substrates: A pharmacokinetic explanation for typically observed low exposure (AUC<sub>i</sub>/AUC) ratios. *Drug Metab. Dispos.*, **32**:1201-1208.
- Zhang L and Skolnick J. 1992. What should the Z-score of native structure be? *Protein Sci.*, **7**:1201-1207.



# Antibiotic Resistance and Type III Exotoxin Encoding Genes of *Pseudomonas aeruginosa* Isolates from Environmental and Clinical Sources in Northern West Bank in Palestine

Ghaleb M. Adwan<sup>\*</sup>, Awni A. Abu-Hijleh and Ne'ma M. Bsharat

Department of Biology and Biotechnology, An-Najah National University, P.O.Box 7, Nablus, Palestine

Received August 8, 2018; Revised August 25, 2018; Accepted August 28, 2018

## Abstract

A total of fifty-seven *Pseudomonas aeruginosa* isolates were collected from different sources of clinical (n=47) and environmental samples (n=10) during 2018, in Northern West Bank, Palestine. Molecular techniques were used to detect type III secretion exotoxin-encoding genes (T3SEEG), and clone identity. The antimicrobial susceptibility was carried out by the disk diffusion method. This study is aimed at comparing the distribution of the T3SEEG and antibiotic resistance between *P. aeruginosa* isolated from both sources. The correlation between T3SEEG and antibiotic resistance in both clinical and environmental isolates collected from a limited geographical area, in parallel, over a short period of time was also determined. In addition, clone identity between the clinical and environmental strains was determined. The results showed that all clinical and environmental *P. aeruginosa* isolates carried T3SEEG. *ExoT* was detected in all of the clinical and environmental isolates. The occurrence rates of *exoY* and *exoS* in *P. aeruginosa* isolates were 80.7 % and 36.8 %, respectively. More than one exotoxin gene was observed in 87 % of the clinical isolates and 70 % of the environmental isolates. The most common combination was *exoT* and *exoY*, with prevalence rates of 47 % and 50 % for the clinical and environmental isolates, respectively. *ExoU* was not detected in any isolate. There was no statistically significant difference between the distribution of T3SEEG according to the isolates' source. There were no significant associations between the carriage of T3SEEG and resistance to some antimicrobials such as ciprofloxacin, norfloxacin, levofloxacin, aztreonam, tetracycline, and kanamycin. The profile of RAPD-PCR typing of 44 *p. aeruginosa* isolates (nine environmental isolates recovered from hospital sinks and thirty-five clinical isolates recovered from different hospitals) was clustered into three groups at a 96 % similarity level. There was no significant difference between the strains isolated from both of the environmental and clinical sources according to antibiotic resistance and the prevalence of T3SEEG. In conclusion, there was high similarity between *P. aeruginosa* strains isolated from both environmental and clinical sources. In addition, no significant differences in antibiotic resistance and the distribution of T3SEEG were observed among the isolates from both sources.

**Keywords:** *Pseudomonas aeruginosa*, Type III secretion system, Environmental isolates, Clinical isolates, *ExoS*, *ExoT*, *ExoY*, *ExoU*.

## 1. Introduction

*Pseudomonas aeruginosa* is a major opportunistic human pathogen. It is an important cause of infections, particularly in immunodeficient patients, burn patients, patients using mechanical ventilation, and patients with cancer or cystic fibrosis (Elsen *et al.*, 2014; Azimi *et al.*, 2016). *P. aeruginosa* can also cause infections in healthy persons (McCallum *et al.*, 2002; Kang *et al.*, 2005). In addition, *P. aeruginosa* can cause community-acquired infections as well as hospital-acquired infections (Barbier *et al.*, 2013).

*P. aeruginosa* genomes isolated from environmental and clinical sources are highly conserved. All *P. aeruginosa* isolates are able to produce virulence factors, and are thus considered potential pathogens (Alonso *et al.*, 1999; Pirnay *et al.*, 2002; Pirnay *et al.*, 2009; Grosso-

Becerra *et al.*, 2014). The intrinsic and acquired resistance of *P. aeruginosa* to many types of antibiotics are attributed to several mechanisms, including reduced cell wall permeability, active efflux systems, expression of various enzymes, plasmid acquisition, and biofilm formation (Allydice-Francis and Brown, 2012).

Secreted exotoxins are either passively or actively secreted from the cell by type I secretion system (T1SS), type II secretion system (T2SS), or type III secretion system (T3SS) (Bradbury *et al.*, 2010). The T3SS of *P. aeruginosa* has four known secretion effector toxins; these are ADP-ribosylating enzymes exoenzyme (ExoS), exoenzyme T (ExoT), adenylate cyclase exoenzyme Y (ExoY), and acute cytolytic factor (a phospholipase) exoenzyme U (ExoU). Although the *P. aeruginosa* T3SS is not required for infection, it enhanced disease severity in several animal models (Hauser, 2009).

<sup>\*</sup> Corresponding author e-mail: adwang@najah.edu.

The prevalence of *exoS*, *exoT*, *exoU* and *exoY* in clinical and environmental *P. aeruginosa* isolates has been previously reported. All tested clinical and environmental *P. aeruginosa* isolates had *exoT* gene sequences (Feltman *et al.*, 2001; Strateva *et al.*, 2010; Gawish *et al.*, 2013; Adwan, 2017). The prevalence of *exoT* gene sequences in *P. aeruginosa* isolates recovered from both environmental and clinical sources ranged from 5 % to 92 % (Lomholt *et al.*, 2001; El-Solh *et al.*, 2012; Azimi *et al.*, 2016). The prevalence of *exoY* gene sequences among *P. aeruginosa* isolates ranged from 55 % to 97 % (Dacheux *et al.*, 2000; Azimi *et al.*, 2016; Adwan, 2017). The prevalence of *exoS* gene sequences among *P. aeruginosa* isolates ranged from 0 % to 96 % (Rumbaugh *et al.*, 1999; Azimi *et al.*, 2016; Adwan, 2017). Finally, the prevalence of *exoU* gene sequences among *P. aeruginosa* isolates ranged from 0 % to 80 % (Fleiszig *et al.*, 1997; Azimi *et al.*, 2016; Adwan, 2017). According to one report, *exoY* and *exoT* gene sequences were detected in all *P. aeruginosa* isolates recovered from hospital environments, and only 80 % and 25.7 % of the isolates carried *exoS* and *exoU* gene sequences, respectively (Bradbury *et al.*, 2010). In another study, *P. aeruginosa* isolates recovered from environmental sources were significantly more likely to have *exoU* gene sequences more than other isolates (Bradbury *et al.*, 2010). In contrast, in another study, there were no significant differences in the prevalence of type III secretion exotoxin-encoding genes (T3SEEG) between both nosocomial and environmental *P. aeruginosa* isolates, or between isolates recovered from different clinical infection sites (Gawish *et al.*, 2013).

**Table 1.** A sample source of 57 of *P. aeruginosa* isolates collected from different hospitals.

Hospital	Sample source (n)												Total
	wound	Urine	tissue	Blood	Bed sore	nasal	Fluid	skin	sputum	swabs	umbilicus	Environment (sink of hospital)	
N	5	4	1	3	1	0	0	0	0	0	0	0	14
W	0	0	0	0	1	0	0	0	0	0	0	0	1
T	1	1	0	0	0	3	0	0	0	0	0	3	8
J	1	7	0	1	0	0	1	2	4	3	0	7	26
TH	2	1	0	0	0	0	0	0	1	3	1	0	8
Total	9	13	1	4	2	3	1	2	5	6	1	10	57

N: An-Najah National University Hospital; W: Alwatany Hospital; T: Tubas Turk Hospital; J: Jenin Hospital; TH: Thabet Hospital.

## 2.2. Antibacterial Susceptibility Test

Antimicrobial sensitivity testing was performed according to Clinical and Laboratory Standard Institute (CLSI) guidelines using the disk diffusion method (CLSI, 2016). All *P. aeruginosa* isolates were examined using antimicrobial disks (Oxoid) to determine resistance against, ciprofloxacin (5 µg), kanamycin (30 µg), tetracycline (30 µg), norfloxacin (10 µg), aztreonam (30 µg), and levofloxacin (5 µg). Mueller Hinton agar (MHA) plates were seeded with a 6-8 h old culture of the isolates, followed by placement of the antimicrobial disks. The plates were incubated at 37°C for twenty-four hours. The inhibition zones (if any) were measured, and the isolates were classified as resistant, intermediate, or susceptible, according to CLSI guidelines (CLSI, 2016). The reference strain of *P. aeruginosa* ATCC 27853 was used as a quality control in all of the experiments of antimicrobial susceptibility testing.

The association between antimicrobial resistance, especially to fluoroquinolones, and the clinical isolates of T3SS<sup>+</sup> *P. aeruginosa* has been reported in different clinical studies (Wong-Beringer *et al.*, 2008; Mitov *et al.*, 2010; Agnello and Wong-Beringer, 2012; Cho *et al.*, 2014).

The present study is aimed at comparing the distribution of the T3SEEG and antibiotic resistance between *P. aeruginosa* strains that were isolated from clinical and environmental sources, and to investigate the presence of an association between them in both clinical and environmental isolates collected from a limited geographical area, in parallel, over a short period of time. In addition, clone identity among the clinical and environmental strains was determined and compared using molecular techniques.

## 2. Materials and Methods

### 2.1. Bacterial Isolates' Collection and Identification

A total of fifty-seven isolates of *P. aeruginosa* were collected from different clinical (n=47) and environmental samples (n=10) during 2018 (Table 1). Both clinical and environmental samples were collected from different hospitals in Northern West Bank, Palestine. All clinical isolates were identified using the API 20E system at the respective hospital laboratories, and were then confirmed using conventional methods at a microbiology research laboratory. The environmental isolates were identified using conventional methods at the microbiology research laboratory of An-Najah National University.

### 2.3. DNA Extraction and PCR Amplification

#### 2.3.1. DNA Extraction

The genome of *P. aeruginosa* was prepared for PCR according to the method described previously (Adwan *et al.*, 2013). Briefly, the cells were scraped off an overnight MHA plate, washed with 800 µL of 1X Tris-EDTA buffer (10 mM Tris-HCl, 1 mM EDTA [pH 8]), centrifuged, and the pellet was resuspended in 400 µL of sterile double distilled H<sub>2</sub>O, and boiled for 10-15 minutes. The cells were incubated on ice for ten minutes. The debris were pelleted by centrifugation at 11,500 X g for five minutes. The concentration of DNA was determined using a nanodrop spectrophotometer (Genova Nano, Jenway). The DNA samples were stored at -20°C.

#### 2.3.2. PCR Amplification of Type III Secretion Exotoxin-Encoding Genes

The detection of gene sequences encoding T3SEEG (*exoS*, *exoT*, *exoU* and *exoY* genes) was performed using multiplex PCR using specific oligonucleotide primer sets

as described previously (Ajayi *et al.*, 2003). Primer sequences and the size of amplicons are listed in Table 2. Each PCR mix (25 µL) consisted of 10 mM PCR buffer pH 8.3; 2.3 mM MgCl<sub>2</sub>; 0.3 mM of each dNTP; 0.3 µM of each primer; 1.25U of Taq DNA polymerase, and 3 µL (100-200 ng) of DNA template. A negative control without template DNA and a positive control strain (department collection) possessing a T3SEEG (*exoS*, *exoT*, *exoU* and *exoY* genes) were used during PCR. The cycling conditions were: initial denaturation at 94°C for three minutes; followed by thirty-six cycles of denaturation at 94°C for forty seconds, annealing at 56°C for forty seconds, and extension at 72°C for one minute; followed by a single final extension step at 72°C for five minutes. The PCR products were detected by electrophoresis on 1.5 % agarose gels to determine the size of amplified fragment after staining with a final concentration 0.5 µg/mL ethidium bromide.

**Table 2.** Target genes for PCR amplification, amplicon sizes, and primer sequences used.

Target gene	Primer sequence (5'→3')	Amplicon size (bp)
<i>exoS</i>	Exo S F: GCG AGG TCA GCA GAG TAT CG	118
	Exo S R: TTC GGC GTC ACT GTG GAT GC	
<i>exoT</i>	Exo T F: AAT CGC CGT CCA ACT GCA TGC G	152
	Exo T R: TGT TCG CCG AGG TAC TGC TC	
<i>exoU</i>	Exo U F: CCG TTG TGG TGC CGT TGA AG	134
	Exo U R: CCA GAT GTT CAC CGA CTC GC	
<i>exoY</i>	Exo Y F: CGG ATT CTA TGG CAG GGA GG	289
	Exo Y R: GCC CTT GAT GCA CTC GAC CA	

### 2.3.3. Random Amplified Polymorphic DNA (RAPD) PCR

Random amplified polymorphic DNA PCR products were generated from forty-four bacterial genomes. The RAPD-PCR was performed using Primer RAPD 208: 5'-

**Table 3.** Antimicrobial susceptibility profile of study isolates.

Antibiotic	Antimicrobial susceptibility result n (%)								
	Clinical source n=47			Environmental source n=10			Total n=57		
	S	I	R	S	I	R	S	I	R
Ciprofloxacin	27 (57.4 %)	3 (6.3 %)	17 (36.3 %)	3 (30 %)	2 (20 %)	5 (50 %)	30 (52.6 %)	5 (8.7 %)	22 (38.7 %)
Norfloxacin	27 (56 %)	6 (12 %)	14 (32 %)	6 (60 %)	2 (20 %)	2 (20 %)	33 (57 %)	8 (14 %)	16 (29 %)
Levofloxacin	27 (57 %)	1 (2 %)	19 (41 %)	6 (60 %)	1 (10 %)	3 (30 %)	33 (58 %)	2 (3.5 %)	22 (38.5 %)
Aztreonam	25 (53.1 %)	14 (29.7 %)	8 (17.2 %)	3 (30 %)	2 (20 %)	5 (50 %)	28 (49.1 %)	16 (28 %)	13 (22.9 %)
Tetracycline	9 (19.1 %)	6 (12.7 %)	32 (68.2 %)	2 (20 %)	2 (20 %)	6 (60 %)	11 (19.2 %)	8 (14 %)	38 (66.8 %)
Kanamycin	7 (14 %)	12 (24 %)	28 (62 %)	1 (10 %)	1 (10 %)	8 (80 %)	8 (14.1 %)	13 (22.8 %)	36 (63.1 %)

n: isolates' count; S: susceptible; I: intermediate; R: resistant

### 3.2. Detection of Type III Secretion Toxins-Encoding Genes

According to the PCR results, all the isolates carried T3SEEG. *ExoT* was detected among all clinical and

ACG GCC GAC C-3' as described earlier (Mahenthalingam *et al.*, 1996). Each PCR mix (25 µL) consisted of 10 mM PCR buffer pH 8.3; 3 mM MgCl<sub>2</sub>; 0.4 mM of each dNTP; 0.8 µM primer; 1.5 U of Taq DNA polymerase, and 3 µL (100-200 ng) of DNA template. The DNA amplification was carried out using the thermal cycler (Mastercycler personal, Eppendorf, Germany) according to the following protocol: initial denaturation for three minutes at 94°C; followed by thirty-five cycles of denaturation at 94°C for fifty seconds, annealing at 45°C for one minute, and extension at 72°C for one minute, followed by a final extension step at 72°C for five minutes. The PCR products were analyzed by electrophoresis on a 1.7 % agarose gel. The gel image was scored using a binary scoring system that recorded the absence and presence of bands as 0 and 1, respectively. A binary matrix was analyzed by the unweighted pair group method for arithmetic averages (UPGMA), using SPSS statistical software version 20 (IBM).

### 2.4. Statistical Analysis

The results were evaluated by the Fisher exact test using SPSS version 20. A *P* value less than 0.05 was considered significant.

## 3. Results

### 3.1. Antimicrobial Susceptibility

A total of fifty-seven isolates (forty-seven clinical isolates and ten environmental isolates) of *P. aeruginosa* were subjected for antimicrobial susceptibility testing. All isolates showed high resistance to tetracycline and kanamycin. The clinical isolates showed low resistance rates against aztreonam, while the environmental isolates showed low resistance rates against norfloxacin. There were no significant differences in the resistance profile between strains isolated from environmental and clinical sources (Fisher exact test; *p* 0.084-1). The antimicrobial susceptibility profile of the isolates is presented in Table 3.

environmental isolates. The prevalence of *exoY* and *exoS* in isolates from both sources was 80.7 % and 36.8 %, respectively. Two or more genes were observed among 87 % and 70 % of the clinical and environmental isolates, respectively. The most common combination was *exoT*



All the isolates recovered from both environmental and clinical sources were *exoT*<sup>+</sup>. These results were consistent with previous reports from USA (Feltman *et al.*, 2001), Bulgaria (Strateva *et al.*, 2010), Egypt (Gawish *et al.*, 2013), and Palestine (Adwan, 2017). The prevalence rate of *exoT* was inconsistent with the results of other studies, which showed the prevalence of the gene among environmental and clinical *P. aeruginosa* isolates at a range of 5 % to 92 % (Lomholt *et al.*, 2001; El-Solh *et al.*, 2012; Azimi *et al.*, 2016). In the present study, the prevalence rate of *exoY* among *P. aeruginosa* isolates recovered from clinical and environmental sources was 80.7 %. This is comparable to previously published results from Palestine (Adwan, 2017), which showed that 72.5 % of *P. aeruginosa* recovered from clinical isolates were *exoY*<sup>+</sup>. This result is also in agreement with other studies published elsewhere (Strateva *et al.*, 2010; Gawish *et al.*, 2013), which reported rates ranging from 83.5 % to 85.8 %. The prevalence rate of 80.7 % for *exoY* among the *P. aeruginosa* isolates was lower than that in other studies; 97 % (Dacheux *et al.*, 2000) and 89 % (Finck-Barbancon *et al.*, 1997), and even higher prevalence rates than these rates by other reports such as by Azimi *et al.*, 2016, at 55 %. The prevalence rate of *exoS* among the isolates from both sources was 36.8 %. This is in contrast to a previous report from Palestine (Adwan, 2017), which did not recover the gene among clinical isolates of *P. aeruginosa*. The prevalence rate for this gene among the *P. aeruginosa* isolates by other reports ranged from 0 % to 96 % (Rumbaugh *et al.*, 1999; Azimi *et al.*, 2016; Adwan, 2017). The product of the *exoS* gene is considered a main cytotoxin involved in the colonization, invasion, and spreading of the infection (Lee *et al.*, 2005). Increasing the gene expression results in increased pulmonary damage in cystic fibrosis patients and in animal models, and leads to *in vitro* cytotoxicity, and induction of apoptotic-like cell death (Lee *et al.*, 2005; Engel, 2003). In the current study, all the isolates recovered from clinical and environmental sources were *exoU*<sup>+</sup>. This result is consistent with a previous report from Palestine (Adwan, 2017), which showed that all the clinical *P. aeruginosa* isolates were *exoU*<sup>+</sup>. The prevalence rate of *exoU* gene sequences among *P. aeruginosa* isolates ranged from 0 % to 80 % according to reports published elsewhere (Fleiszig *et al.*, 1997; Azimi *et al.*, 2016; Adwan, 2017). The product of *exoU* demonstrates specificity to human neutrophils, and is associated with a severe *P. aeruginosa* infection in humans (Finck-Barbancon *et al.*, 1997). Strains of *P. aeruginosa* with deleted or mutated *exoU* gene had a lower toxicity during lung infection (Engel, 2003). In addition, an association had been proposed between the product of *exoU* and the invasive *P. aeruginosa* leading to bloodstream infections (Wareham and Curtis, 2007).

In the present study, no association was found between the resistance profile and the *P. aeruginosa* isolates recovered from both clinical and environmental sources that carried T3SEEG. A statistically significant association ( $p = 0.047$ ) was demonstrated between the absence of the *exoS* gene and resistance to norfloxacin. In a recent study from Palestine (Adwan, 2017), no associations were observed between ciprofloxacin, norfloxacin, meropenem, and imipenem resistance, and the carriage of T3SEEG among clinical *P. aeruginosa* isolates. A significant association between clinical *P. aeruginosa* isolates having

the *exoU* gene sequences and fluoroquinolone resistance has been proposed (Wong-Beringer *et al.*, 2008; Cho *et al.*, 2014). In another report (Bradbury *et al.*, 2010), no significant association was demonstrated between ciprofloxacin resistance and *P. aeruginosa* isolates carrying the *exoU* gene.

RAPD-PCR typing of *P. aeruginosa* genomes of both environmental and clinical isolates showed that the genome is highly conserved (96 % similarity), and that all *P. aeruginosa* isolates, whether from clinical or environmental sources, were able to produce virulence factors, and are thus potential pathogens. Cluster 1 and 2 had identical isolates recovered from both environmental and clinical sources. This indicates that the strains of environmental origin may cause human infections. These results are in accordance with the results published formerly (Hardalo and Edberg, 1997; Pirnay *et al.*, 2009). Moreover, others have proposed the absence of significant differences between the environmental and clinical isolates regarding the virulence aspects (Morgan *et al.*, 1999; Alonso *et al.*, 1999; Pirnay *et al.*, 2002). Finally, identical clones have been recovered from different hospitals. This may be attributed to medical referrals and the transportation of patients among different hospitals (Adwan, 2017).

## 5. Conclusion

According to RAPD-PCR typing, the results of this study revealed a high similarity between the *P. aeruginosa* strains isolated from environmental and clinical sources. In addition, strains from both sources had no significant differences in antimicrobials' resistance profiles and the presence of T3SEEG. These results indicate that the isolates from both sources have the ability to cause clinical infections.

## Conflict of Interest

No conflicts of interest have been declared by the authors

## References

- Adwan G, Shtayah A, Adwan K, Al-Sheboul S and Othman S. 2016a. Prevalence and molecular characterization of *P. aeruginosa* Isolates in the West Bank-Palestine for ESBLs, MBLs and Integrons. *J Appl Life Sci Int.*, **8**(2): 1-11.
- Adwan G, Abu Hasan N, Sabra I, Sabra D, Al-butmah S, Odeh S, Abd Albake Z and Badran H. 2016b. Detection of bacterial pathogens in surgical site infections and their antibiotic sensitivity profile. *Int J Med Res Health Sci.*, **5**(5): 75-82.
- Adwan G, Adwan K, Jarrar N and Salameh Y. 2013. Prevalence of *seg*, *seh* and *sei* genes among clinical and nasal swab of *Staphylococcus aureus* isolates. *Br Microbiol Res J.*, **3**(2):139-149.
- Adwan G. 2017. Detection of Type III Secretion Toxins encoding-genes of *Pseudomonas aeruginosa* isolates in the West Bank-Palestine. *J Adv Biol Biotechnol.*, **11**(3): 1-10.
- Agnello M and Wong-Beringer A. 2012. Differentiation in quinolone resistance by virulence genotype in *Pseudomonas aeruginosa*. *PLoS One.*, **7**(8): 1-8.
- Ajayi T, Allmond LR, Sawa T and Wiener-Kronish JP. 2003. Single-nucleotide-polymorphism mapping of the *Pseudomonas aeruginosa* type III secretion toxins for development of a diagnostic multiplex PCR system. *J Clin Microbiol.*, **41**(8): 3526-3531.



- Allydice-Francis K and Brown PD. 2012. Diversity of antimicrobial resistance and virulence determinants in *Pseudomonas aeruginosa* Associated with fresh vegetables. *Int J Microbiol.*, **2012**: 1-7.
- Alonso A, Rojo F and Martínez JL. 1999. Environmental and clinical isolates of *Pseudomonas aeruginosa* show pathogenic and biodegradative properties irrespective of their origin. *Environ Microbiol.*, **1**(5): 421-430.
- Azimi S, Kafil HS, Baghi HB, Shokrian S, Najaf K, Asgharzadeh M, Yousefi M, Shahrivar F and Aghazadeh M. 2016. Presence of *exoY*, *exoS*, *exoU* and *exoT* genes, antibiotic resistance and biofilm production among *Pseudomonas aeruginosa* isolates in Northwest Iran. *GMS Hyg Infect Control.*, **11**: 1-6.
- Barbier F, Andremont A, Wolff M and Bouadma L. 2013. Hospital-acquired pneumonia and ventilator-associated pneumonia: recent advances in epidemiology and management. *Curr Opin Pulm Med.*, **19**: 216-228.
- Bradbury RS, Roddam LF, Merritt A, Reid DW and Champion AC. 2010. Virulence gene distribution in clinical, nosocomial and environmental isolates of *Pseudomonas aeruginosa*. *J Med Microbiol.*, **59**(Pt 8):881-890.
- Cho HH, Kwon KC, Kim S and Koo SH. 2014. Correlation between virulence genotype and fluoroquinolone resistance in carbapenem-resistant *Pseudomonas aeruginosa*. *Ann Lab Med.*, **34**(4):286-292.
- Clinical and Laboratory Standards Institute (CLSI). 2016. Performance standards for antimicrobial susceptibility testing. 26<sup>th</sup> ed. CLSI supplement. M100S. Wayne, PA, USA.
- Dacheux D, Toussaint B, Richard M, Brochier G, Croize J and Attree I. 2000. *Pseudomonas aeruginosa* cystic fibrosis isolates induce rapid, type III secretion-dependent, but Exo-U independent, oncosis of macrophages and polymorphonuclear neutrophils. *Infect Immun.*, **68**: 2916-2924.
- Elsen S, Huber P, Bouillot S, Couté Y, Fournier P, Dubois Y, Timsit JF, Maurin M and Attrée I. 2014. A type III secretion negative clinical strain of *Pseudomonas aeruginosa* employs a two-partner secreted exolysin to induce hemorrhagic pneumonia. *Cell Host Microbe.*, **15**(2): 164-176.
- El-Solh AA, Hattemer A, Hauser AR, Alhajhusain A and Vora H. 2012. Clinical outcomes of type III *Pseudomonas aeruginosa* bacteremia. *Crit Care Med.*, **40**(4): 1157-1163.
- Engel JN. 2003. Molecular pathogenesis of acute *Pseudomonas aeruginosa* infections. In: Hauser AR and Dordrecht RJ (Eds.), **Severe Infections caused by *Pseudomonas aeruginosa***. Kluwer Academic Publishers, pp. 201-229.
- Feltman H, Schulert G, Khan S, Jain M, Peterson L and Hauser AR. 2001. Prevalence of type III secretion genes in clinical and environmental isolates of *Pseudomonas aeruginosa*. *Microbiol.*, **147**: 2659-2669.
- Finck-Barbancon V, Goranson J, Zhu L, Sawa T, Wiener-Kronish JP, Fleiszig SMJ, Wu C, Mende-Mueller L and Frank DW. 1997. *ExoU* expression by *Pseudomonas aeruginosa* correlates with acute cytotoxicity and epithelial injury. *Mol Microbiol.*, **25**:547-557.
- Fleiszig S M J, Wiener-Kronish JP, Miyazaki H, Vallas V, Mostov KE, Kanada D, Sawa T, Yen TSB and Frank DW. 1997. *Pseudomonas aeruginosa*-mediated cytotoxicity and invasion correlate with distinct genotypes at the loci encoding exoenzyme S. *Infect Immun.*, **65**: 579-586.
- Gawish AA, Mohammed NA, El-Shennawy GA and Mohammed HA. 2013. An investigation of type 3 secretion toxins encoding-genes of *Pseudomonas aeruginosa* isolates in a University Hospital in Egypt. *J Microbiol Infect Dis.*, **3**(3): 116-122.
- Grosso-Becerra MV, Santos-Medellín C, González-Valdez A, Méndez JL, Delgado G, Morales-Espinosa R, Servín-González L, Alcaraz LD and Soberón-Chávez G. 2014. *Pseudomonas aeruginosa* clinical and environmental isolates constitute a single population with high phenotypic diversity. *BMC Genomics.*, **15**: 318.
- Hardalo HC and Edberg SC. 1997. *Pseudomonas aeruginosa*: Assessment of risk from drinking water. *Crit Rev Microbiol.*, **23**: 47-75.
- Hauser AR. 2009. The type III secretion system of *Pseudomonas aeruginosa*: infection by injection. *Nat Rev Microbiol.*, **7**(9): 654-665.
- Kang CI, Kim SH, Park WB, Lee KD, Kim HB, Kim EC, Oh MD and Choe KW. 2005. Clinical features and outcome of patients with community-acquired *Pseudomonas aeruginosa* bacteraemia. *Clin Microbiol Infect.*, **11**(5): 415-418.
- Lee VT, Smith RS, Tümmler B and Lory S. 2005. Activities of *Pseudomonas aeruginosa* effectors secreted by the type III secretion system in vitro and during infection. *Infect Immun.*, **73**: 1695-1705.
- Lomholt JA, Poulson K and Kilian M. 2001. Epidemic population structure of *Pseudomonas aeruginosa*: evidence for a clone that is pathogenic to the eye and that has a distinct combination of virulence factors. *Infect Immun.*, **69**: 6284-6295.
- Mahenthiralingam E, Campbell ME, Foster J, Lam JS and Speert DP. 1996. Random amplified polymorphic DNA typing of *Pseudomonas aeruginosa* isolates recovered from patients with cystic fibrosis. *J Clin Microbiol.*, **34**: 1129-1135.
- McCallum SJ, Gallagher MJ, Corkill JE, Hart CA, Ledson MJ and Walshaw MJ. 2002. Spread of an epidemic *Pseudomonas aeruginosa* strain from a patient with cystic fibrosis (CF) to non-CF relatives. *Thorax.*, **57**(6): 559-560.
- Mitov I, Strateva T and Markova B. 2010. Prevalence of virulence genes among Bulgarian nosocomial and cystic fibrosis isolates of *Pseudomonas aeruginosa*. *Brazilian J Microbiol.*, **41**: 588-595.
- Morgan JA, Bellingham NF, Winstanley C, Ousley MA, Hart CA and Saunders JR. 1999. Comparison of flagellin genes from clinical and environmental *Pseudomonas aeruginosa* isolates. *Appl Environ Microbiol.*, **65**(3): 1175-1179.
- Pirnay JP, Bilocq F, Pot B, Cornelis P, Zizi M, Van Eldere J, Deschaght P, Vaneechoutte M, Jennes S, Pitt T and De Vos D. 2009. *Pseudomonas aeruginosa* population structure revisited. *PLoS One.*, **4**: 1-20.
- Pirnay JP, De Vos D, Mossialos D, Vanderkelen A, Cornelis P and Zizi M. 2002. Analysis of the *Pseudomonas aeruginosa oprD* gene from clinical and environmental isolates. *Environ Microbiol.*, **4**(12): 872-882.
- Rumbaugh KP, Hamood AN and Griswold JA. 1999. Analysis of *Pseudomonas aeruginosa* clinical isolates for possible variations within the virulence genes exotoxin A and exoenzyme S. *J Surg Res.*, **82**: 95-105.
- Strateva T, Markova B, Ivanova D and Mitov I. 2010. Distribution of the type III effector proteins-encoding genes among nosocomial *Pseudomonas aeruginosa* isolates from Bulgaria. *Ann Microbiol.*, **60**: 503-509.
- Wareham DW and Curtis MA. 2007. A genotypic and phenotypic comparison of type III secretion profiles of *Pseudomonas aeruginosa* cystic fibrosis and bacteraemia isolates. *Int J Med Microbiol.*, **297**: 227-234.
- Wong-Beringer R, Wiener-Kronish J, Lynch S and Flanagan J. 2008. Comparison of type III secretion system virulence among fluoroquinolon-susceptible and -resistant clinical isolates of *Pseudomonas aeruginosa*. *Clin Microbiol Infect.*, **14**: 330-336.



## Estimation of Biometric Indices for Snakehead *Channa punctata* (Bloch, 1793) through Multi-model Inferences

Md. Alomgir Hossen<sup>1</sup>, Alok Kumar Paul<sup>1</sup>, Md. Yeamin Hossain<sup>1,\*</sup>, Jun Ohtomi<sup>2</sup>, Wasim Sabbir<sup>1,3</sup>, Obaidur Rahman<sup>1</sup>, Julia Jasmin<sup>1</sup>, Md. Nuruzzaman Khan<sup>3</sup>, Md. Akhtarul Islam<sup>1</sup>, Md. Ataur Rahman<sup>1</sup>, Dalia Khatun<sup>1</sup> and Sk. Kamruzzaman<sup>1</sup>

<sup>1</sup>Department of Fisheries, Faculty of Agriculture, University of Rajshahi, Rajshahi 6205, Bangladesh; <sup>2</sup>Faculty of Fisheries, Kagoshima University, 4-50-20 Shimoarata, Kagoshima 890-0056, Japan; <sup>3</sup>Fisheries and Marine Resource Technology Discipline, Khulna University, Khulna 9208, Bangladesh

Received July 19, 2018; Revised September 4, 2018; Accepted September 14, 2018

### Abstract

The present study describes the biometric indices of *Channa punctata* including- length frequency distributions (LFDs), length-weight relationships (LWRs), length-length relationships (LLRs), condition factors (allometric,  $K_A$ , Fulton's,  $K_F$ , relative,  $K_R$  and relative weight,  $W_R$ ), form factor ( $a_{3.0}$ ), and natural mortality ( $M_W$ ) using multi-model indices from the Rupsha River in southern Bangladesh. For each individual, the total length (TL) and body weight (BW) were measured by digital slide calipers and an electric balance, respectively. The LFDs showed that the 13.0-14.0 cm TL size group was numerically dominant. The  $b$  values of LWRs (TL vs. BW) indicates positive allometric growth, ( $b = 3.10$ ) and  $K_F$  is the best for assessing the well-being of this species in the Rupsha River. The  $W_R$  indicates that the habitat was imbalanced with higher predators. The  $a_{3.0}$  and  $M_W$  were 0.0116 and 1.00 year<sup>-1</sup> for *C. punctata* in the Rupsha River, respectively. In addition, the present study calculates the  $a_{3.0}$  and  $M_W$  from world-wide different water bodies using the available literature. These results would be effective for further stock assessment and for the management of *C. punctata* in the Rupsha River and the surrounding ecosystems.

**Keywords:** *Channa punctata*, Conditions, Form factor, Natural mortality, Rupsha River.

### 1. Introduction

The spotted snakehead, *Channa punctata* (Bloch, 1793), is a freshwater fish belonging to the family Channidae. Locally it is known as taki in Bangladesh, mural, lata in India, and spotted snakehead in Sri-Lanka. This freshwater fish is distributed throughout the South Asian countries of Bangladesh, China, India, Myanmar, Nepal, Pakistan, and Sri-Lanka (Froese and Pauly, 2016). It is found in ponds, swamps, brackish water (Pethiyagoda, 1991), ditches, and *beels* (Rahman, 1989). The snakehead fish is used as food and is important for wound healing and for reducing post-operative pain (Gam *et al.*, 2006). This fish has an accessory respiratory organ to sustain itself in miserable conditions, but unfortunately it is declining due to habitat changes and indiscriminate fishing (Hossain *et al.*, 2015a, b, c; Hossen *et al.*, 2015). Globally, it is categorized as least concern (IUCN, 2017).

The length-weight relationship (LWR) is very essential for fisheries management and conservation. It is also important for comparing the life histories of fishes among different geographic locations (Le Cren, 1951; Hossain *et al.*, 2009, 2012a, 2013; Azad *et al.*, 2018; Nawer *et al.*,

2017). Condition factors are functional parameters that can be used for determining the possible differences among different stocks of the same species (King, 2007). Moreover, relative weight ( $W_R$ ) is one of the most popular indices to detect the condition of fishes in different water bodies (Rypel and Richter, 2008; Hossain *et al.*, 2012b; Hossen *et al.*, 2018). In addition, the form factor ( $a_{3.0}$ ) can be used to determine whether the body shape of a given population or species is significantly different from others (Froese, 2006). On the other hand, the natural mortality ( $M_W$ ) can be used to know fisheries stock' status and management strategies (Brodziak *et al.*, 2011).

To the best of the researchers' knowledge, to date, there have been no studies on biometric indices using multi-model inferences for *C. punctata*. Therefore, this study is aimed at focusing on the length-frequency distributions (LFDs), length-weight (LWRs), length-length relationships (LLRs), condition factors (allometric,  $K_A$ ; Fulton's,  $K_F$ ; relative,  $K_R$ ; relative weight,  $W_R$ ), form factor ( $a_{3.0}$ ), and natural mortality ( $M_W$ ) of *C. punctata* using a number of specimens with various body sizes from the Rupsha River in southern Bangladesh through multiple model inferences.

\* Corresponding author e-mail: hossainyamin@gmail.com; yeamin.fish@ru.ac.bd.

## 2. Materials and Methods

This study was conducted in the Rupsha River (Lat. 22°46' N; Long. 89°34' E), southern Bangladesh. A total of 132 individuals of *C. punctata* were occasionally sampled using cast net (the mesh size ranges from 1.5 to 2.0 cm) and gill net (mesh size ~ 2.5 cm) from September 2014 to August, 2015. The fresh samples were immediately preserved in ice on site and were fixed with 10 % buffered formalin upon arrival in the laboratory.

Individual lengths including- total length (TL), standard length (SL) and total body weight (BW) were measured to 0.1 cm and 0.1 g accuracy using digital slide calipers and an electronic balance, respectively.

The LFDs for *C. punctata* were constructed using 1 cm intervals of TL. The LWRs were calculated using the equation:  $W = a \cdot L^b$ , where  $W$  is the body weight (BW, g), and  $L$  is the length (TL, SL cm). The parameters  $a$  and  $b$  were estimated by linear regression analysis based on natural logarithms:  $\ln(W) = \ln(a) + b \ln(L)$ . A t-test was used to confirm whether the  $b$  values obtained in the linear regression were significantly different from the isometric value ( $b = 3$ ) (Sokal and Rohlf, 1987). Furthermore, LLR including TL vs. SL was estimated by linear regression analysis (Hossain *et al.*, 2006a).

The allometric condition factor ( $K_A$ ) was calculated using the equation of Tesch (1968):  $K_A = W/L^b$ , where  $W$  is the BW in g,  $L$  is the TL in cm, and  $b$  is the LWRs parameter. Fulton's condition factor ( $K_F$ ) was calculated using the equation:  $K_F = 100 \times (W/L^3)$ , where  $W$  is the BW in g, and  $L$  is the TL in cm. The scaling factor 100 was used to bring the  $K_F$  close to unit and the relative condition factor ( $K_R$ ) for each individual was calculated via the equation of Le Cren (1951):  $K_R = W/(a \cdot L^b)$  where  $W$  is the BW in g,  $L$  is the TL in cm,  $a$  and  $b$  are LWRs parameters. The relative weight ( $W_R$ ) was calculated by the equation of Froese (2006), as:  $W_R = (W/W_S) \times 100$ , where  $W$  is the weight of a particular individual, and  $W_S$  is the predicted standard weight for the same individual as calculated by  $W_S = a \cdot L^b$ , (where the  $a$  and  $b$  values were obtained from the relationships between TL vs. BW).

The form factor ( $a_{3.0}$ ) of *C. punctata* was calculated using the equation of Froese (2006), as:  $a_{3.0} = 10^{\log a - s(b-3)}$ , where  $a$  and  $b$  are regression parameters of LWR, and  $s$  is the regression slope of  $\ln a$  vs.  $b$ . In this study, a mean slope  $S = -1.358$ , was used for estimating the  $a_{3.0}$  because information on LWR is not available concerning this species for the estimation of the regression ( $S$ ) of  $\ln a$  vs.  $b$ . The natural mortality ( $M_W$ ) was calculated using the model of Peterson and Wroblewski (1984) as  $M_W = 1.92 \text{ year}^{-1} \cdot (W)^{-0.25}$ , where,  $M_W$  = Natural mortality at mass  $W$ , and  $W = a \cdot L^b$ , and  $a$  and  $b$  are regression parameters of LWR.

Statistical analyses were performed using GraphPad Prism 6.5 software. The one sample t-test was used to compare the mean relative weight ( $W_R$ ) with 100 (Anderson and Neumann, 1996). In addition, the Spearman rank test was used to correlate body measurements (e.g., TL, SL, and BW) with condition factors ( $K_A$ ,  $K_F$ ,  $K_R$ , and  $W_R$ ). Furthermore, the LWRs between waters were compared by the analysis of covariance (ANCOVA). All statistical analyses were considered significant at 5 % ( $P < 0.05$ ).

## 3. Results

Descriptive statistics on the length (cm) and weight (g) measurements with 95% confidence limit (CL) are presented in Table 1. The LFDs of *C. punctata* showed that the smallest and largest individuals were 4.6 cm and 22.7 cm TL, respectively; whereas the BW ranged from 1.6 g to 76.8 g. The maximum population stands on 13.0-14.0 cm TL size group in the Rupsha River (Figure 1).

The sample size ( $n$ ), regression parameters ( $a$  and  $b$ ) and 95% CL of  $a$  and  $b$  of the LWRs, co-efficient of determination ( $r^2$ ) and growth type of *C. punctata* are presented in Table 2 and Figure 2. The calculated  $b$  values (3.07) indicate a positive allometric growth in case of TL vs. BW, and a negative allometric growth for SL vs. BW relationships (Table 2) in the Rupsha River. All LWRs were highly significant ( $P < 0.001$ ), with all  $r^2$  values being greater than 0.971. The ANCOVA revealed significant differences in the LWRs of *C. punctata* between Bangladesh and Indian waters ( $df = 390$ ,  $F = 337.71$ ,  $P < 0.001$ ) (Figure 2). The LLR (TL vs. SL) of *C. punctata* are presented in Table 3. The LLR was highly significant ( $P < 0.001$ ) with  $r^2$  values being  $\geq 0.984$ .

The  $K_A$  varied from 0.005 to 0.018 (mean  $\pm$  SD =  $0.009 \pm 0.001$ ) (Table 4). According to Spearman rank correlation test, there was a significant relationship among the TL vs.  $K_A$  ( $r_s = 0.275$ ,  $P = 0.001$ ) and BW vs.  $K_A$  ( $r_s = 0.401$ ,  $P < 0.001$ ) (Table 5). The  $K_F$  values varied from 0.630 to 1.990 (mean  $\pm$  SD =  $1.120 \pm 0.170$ ) (Table 4), and the Spearman rank correlation test revealed that there was a strong correlation among TL vs.  $K_F$  ( $r_s = 0.353$ ,  $P < 0.001$ ), and BW vs.  $K_F$  ( $r_s = 0.474$ ,  $P < 0.001$ ) (Table 5). Also the  $K_R$  ranged from 0.590 to 2.000 (mean  $\pm$  SD =  $1.050 \pm 0.160$ ) (Table 4). The Spearman rank correlation test indicates that there was a significant relationship among TL vs.  $K_R$  ( $r_s = 0.272$ ,  $P = 0.001$ ) and BW vs.  $K_R$  ( $r_s = 0.398$ ,  $P < 0.0001$ ) (Table 5). In addition, the calculated minimum and maximum  $W_R$  were 59.020 and 200.240, with a mean value of  $105.020 \pm 15.980$  (Table 4). The Spearman rank correlation test shows that there was a significant relationship between TL vs.  $W_R$  ( $r_s = 0.271$ ,  $P = 0.001$ ) and BW vs.  $W_R$  ( $r_s = 0.396$ ,  $P < 0.001$ ) for *C. punctata* in the Rupsha River. The relationship between TL vs.  $W_R$  was also shown in Figure 3. The calculated  $a_{3.0}$  and  $M_W$  for *C. punctata* in the Rupsha River, and different water bodies world-wide are shown in Table 6.

**Table 1.** Descriptive statistics on the length (cm) and weight (g) measurements of the *Channa punctata* captured from the Rupsha River, southern Bangladesh

Measurements	Min	Max	Mean $\pm$ SD	Mode	95% CL
TL	4.6	22.7	13.59 $\pm$ 3.25	13.70	13.03-14.15
SL	3.7	19.9	11.47 $\pm$ 2.89	11.50	10.98-11.97
BW	1.6	76.8	32.63 $\pm$ 18.81	24.70	29.39-35.87

TL, total length; SL, standard length; BW, body weight; Min, minimum; Max, maximum; SD, standard deviation; CL, confidence limit for mean values

**Table 2.** Descriptive statistics and estimated parameters of the length-weight relationships ( $BW = a \times L^b$ ) of *Channa punctata* captured from the Rupsha River, southern Bangladesh

Equation	<i>a</i>	<i>b</i>	95% CL of <i>a</i>	95% CL of <i>b</i>	<i>r</i> <sup>2</sup>	GT
$BW = a \times TL^b$	0.0093	3.067	0.0073-0.0118	2.974-3.159	0.971	+A
$BW = a \times SL^b$	0.0224	2.923	0.0180-0.0278	2.834-3.012	0.984	-A

*a* and *b* are regression parameters of LWRs; CL, confidence limit for mean values; *r*<sup>2</sup>, co-efficient of determination; GT, growth type; +A, positive allometric, -A, negative allometric

**Table 3.** The estimated parameters on the length-length relationships ( $y = a + b \cdot x$ ) of *Channa punctata* captured from the Rupsha River, southern Bangladesh

Equation	<i>n</i>	Regression parameters		95% CL of <i>a</i>	95% CL of <i>b</i>	<i>r</i> <sup>2</sup>
		<i>a</i>	<i>b</i>			
TL = <i>a</i> + <i>b</i> × SL	132	0.7724	1.117	0.481-1.064	0.092-1.141	0.984

*n*, sample size; TL, total length; SL, standard length; *a*, intercept; *b*, slope; CL, confidence limit for mean values; *r*<sup>2</sup>, coefficient of determination

**Table 4.** Condition factors of the *Channa punctata* captured from the Rupsha River, southern Bangladesh

Condition factor	<i>n</i>	Min	Max	Mean $\pm$ SD	95% CL
<i>K<sub>A</sub></i>		0.005	0.018	0.009 $\pm$ 0.001	0.009-0.010
<i>K<sub>F</sub></i>	132	0.630	1.990	1.120 $\pm$ 0.170	1.090-1.150
<i>K<sub>R</sub></i>		0.590	2.000	1.050 $\pm$ 0.160	1.020-1.080
<i>W<sub>R</sub></i>		59.020	200.240	105.020 $\pm$ 15.980	102.27-107.77

*n*, sample size; Min, minimum; Max, maximum; SD, standard deviation; CL, confidence limit for mean values; *K<sub>A</sub>*, allometric condition factor; *K<sub>F</sub>*, Fulton's condition factor; *K<sub>R</sub>*, relative condition factor; *W<sub>R</sub>*, relative weight.

**Table 5.** Relationships of condition factor with total length (TL) and body weight (BW) of *Channa punctata* captured from the Rupsha River, southern Bangladesh

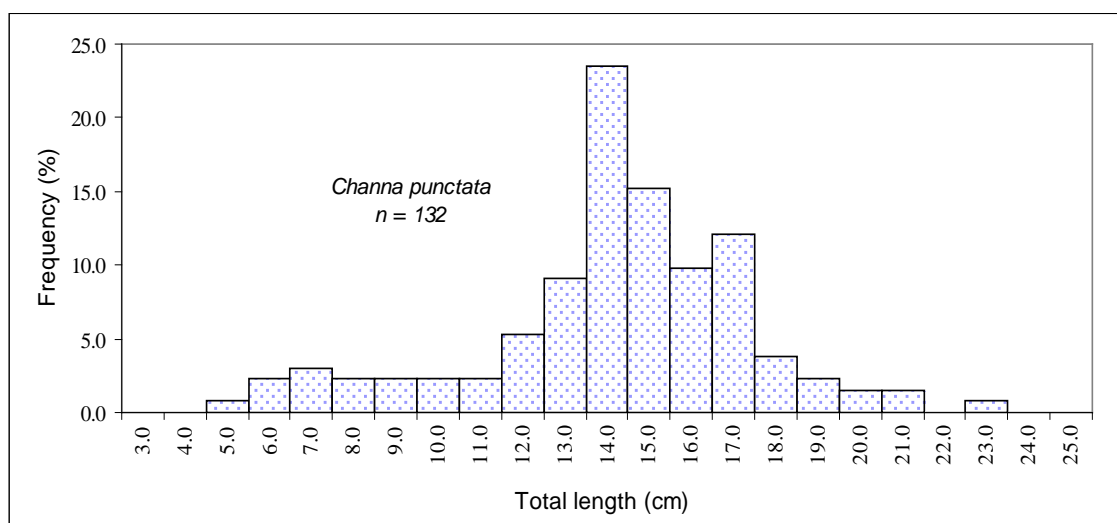
Condition factor	<i>r<sub>s</sub></i> value	95% CL of <i>r<sub>s</sub></i>	<i>P</i> value	Degree of significance
TL vs. <i>K<sub>A</sub></i>	0.275	0.104-0.430	<i>P</i> = 0.001	*
BW vs. <i>K<sub>A</sub></i>	0.401	0.242-0.538	<i>P</i> < 0.001	***
TL vs. <i>K<sub>F</sub></i>	0.353	0.188-0.498	<i>P</i> < 0.001	***
BW vs. <i>K<sub>F</sub></i>	0.474	0.325-0.599	<i>P</i> < 0.001	***
TL vs. <i>K<sub>R</sub></i>	0.273	0.102-0.428	<i>P</i> = 0.001	*
BW vs. <i>K<sub>R</sub></i>	0.399	0.240-0.537	<i>P</i> < 0.001	***
TL vs. <i>W<sub>R</sub></i>	0.271	0.099-0.426	<i>P</i> = 0.001	*
BW vs. <i>W<sub>R</sub></i>	0.397	0.238-0.535	<i>P</i> < 0.001	***

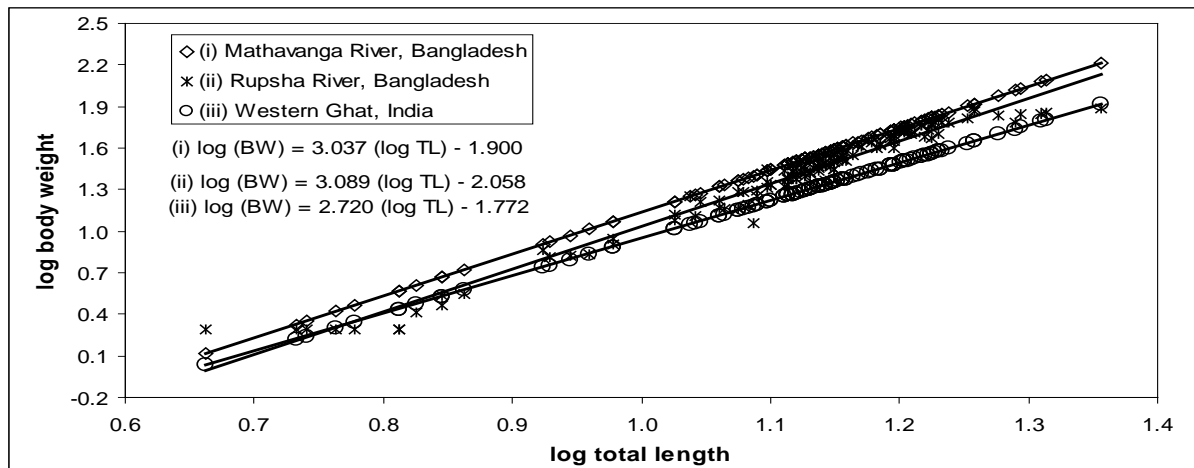
TL, total length; BW, body weight; *K<sub>A</sub>*, allometric condition factor; *K<sub>F</sub>*, Fulton's condition factor; *K<sub>R</sub>*, relative condition factor; *W<sub>R</sub>*, relative weight; *r<sub>s</sub>*, spearman rank correlation values; CL, confidence limit; *P*, shows the level of significance; \*significant; \*\*\* very significant.

**Table 6.** The calculated form factor (*a<sub>3.0</sub>*) and natural mortality (*M<sub>w</sub>*) of *Channa punctata* in different water bodies world-wide.

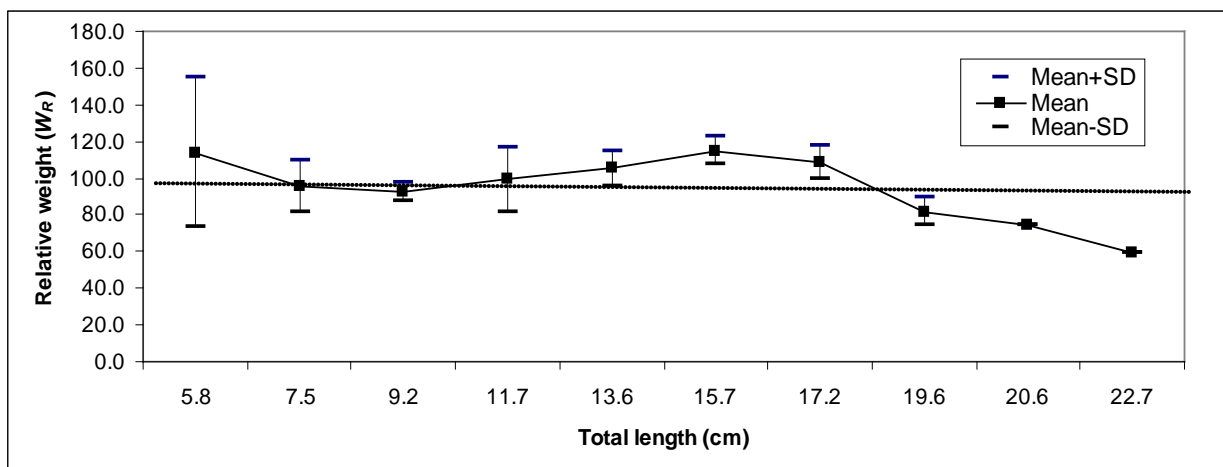
Water-bodies	<i>a</i>	<i>b</i>	Maximum TL(cm)	Reference	<i>a<sub>3.0</sub></i>	<i>M<sub>w</sub></i> year <sup>-1</sup>
Siruvani River, India	0.0169	2.72	24.4	Haniffa et al. (2006)	0.0070	0.7
Vellar River, India	0.0282	2.77	24.5	Haniffa et al. (2006)	0.0137	0.7
Tamirabrani River, Tamil Nadu, India	0.0105	2.99	26.8	Haniffa et al. (2006)	0.0102	0.6
Mathabhanga River, Bangladesh	0.0126	3.04	18.9	Hossain et al. (2006)	0.0141	0.6
Rupsha River, Bangladesh	0.0093	3.07	22.7	Present study	0.0116	1.0

*a* and *b* are regression parameters of length-weight relationships; TL, total length; *a<sub>3.0</sub>*, form factor; *M<sub>w</sub>*, natural mortality

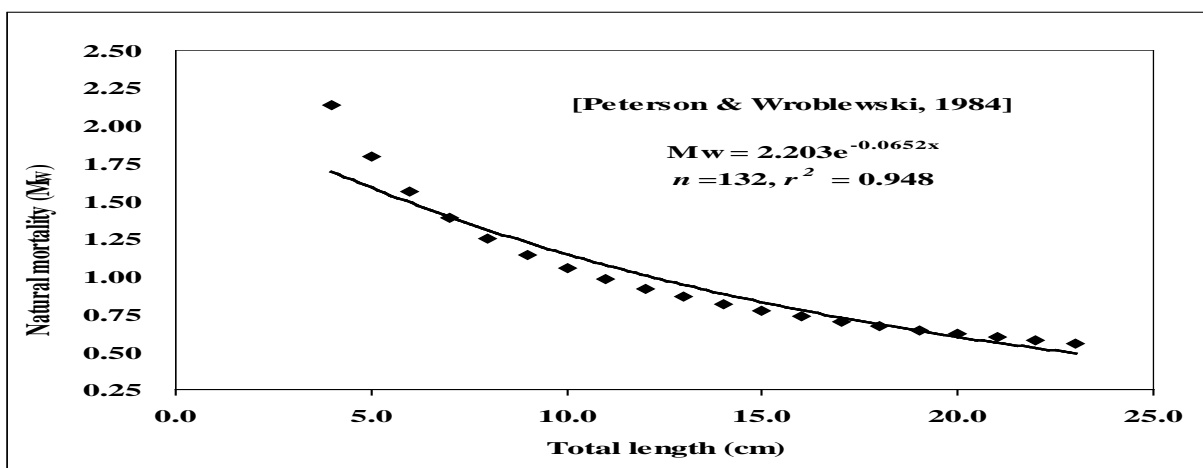
**Figure 1.** The length-frequency distribution of *Channa punctata* in the Rupsha River, southern Bangladesh.



**Figure 2.** Total length and body weight relationships ( $\log W = \log a + b \log L$ ) of *Channa punctata* in the (i) Mathabanga River, Bangladesh (ii) Rupsha River, Bangladesh (present study) and (iii) Western Ghat, India.



**Figure 3.** The relationships between total length and relative weight of *Channa punctata* in the Rupsha River, southern Bangladesh.



**Figure 4.** The relationships between natural mortality and total length of *Channa punctata* in the Rupsha River, southern Bangladesh.

#### 4. Discussion

Only few studies on LWRs and LLRs have been conducted on *C. punctata* in the Indian sub-continent (Haniffa *et al.*, 2006; Hossain *et al.*, 2006b). However, this study highlighted the biometric indices of *C. punctata* including LFDs, LWRs, LLRs, condition factors ( $K_A$ ,  $K_F$ ,

$K_R$  and  $W_R$ ),  $a_{3.0}$  and  $M_W$  from the Rupsha River in SW Bangladesh.

During the study, a total of 132 individuals of *C. punctata* with various body sizes were sampled. The LFDs stated that here it was not possible to sample *C. punctata* smaller than 4.6 cm in TL which may be ascribed to gear selectivity or because the fishermen did not go where smaller sizes exist (Hossain *et al.*, 2012c, 2015d, 2016a; Rahman *et al.*, 2012). The maximum length of *C.*

*punctata* was found 22.7 cm TL in the present study which is lower than the maximum recorded value of 31.0 cm TL (Talwar and Jhingran, 1991). Information on maximum length is necessary to estimate the asymptotic length and growth co-efficient of fishes, which is vital for fisheries resource-planning and management (Ahmed *et al.*, 2012, Hossen *et al.*, 2016; Khatun *et al.*, 2018).

Generally, the *b* values in LWRs should remain within the range of 2.5–3.5 (Froese, 2006); in this study all the *b* values fell within this expected range. This study reported positive allometric growth for *C. punctata* (*b* = 3.07) agrees with the findings of Hossain *et al.* (2006b) (*b* = 3.04), but is inconsistent with Haniffa *et al.* (2006) (*b* = 2.83), who estimated negative allometric growth sampled from the Western Ghat, India. However, this difference can be attributed to a number of factors including season, habitat, gonadal maturity, diet, health, and preservation techniques of the captured specimens (Tesch, 1968; Hossain *et al.*, 2016b, c; Khatun *et al.*, 2019), which were unaccounted for in the present study. The LLR was highly correlated, but it was not possible to make any comparisons due to the lack of available study.

Although most of the studies deal with a single condition factor, however the current study has worked with four condition factors ( $K_A$ ;  $K_F$ ;  $K_R$  and  $W_R$ ) to assess the health and habitat condition of *C. punctata* in the Rupsha River. This study postulates that the  $K_F$  is the best biometric index for assessing the well-being of this species in the study area. Additionally, the  $W_R$  was significantly different from 100 ( $P < 0.05$ ) indicating an imbalanced habitat with food availability relative to the presence of predators for *C. punctata* in the Rupsha River.

The calculated  $a_{3.0}$  value was 0.0116 for *C. punctata* in the Rupsha River. The  $a_{3.0}$  can be used to verify whether the body shape of individuals in a given population or species is significantly different from others (Froese, 2006). In addition, the calculated  $M_W$  was 1.00 year<sup>-1</sup>. The  $M_W$  was higher for smaller fish species (Figure 4). There is no reference regarding the condition factor, form factor, and natural mortality of this species, which restrains comparisons with the findings of this study.

## 5. Conclusion

The present study describes the biometric indices of *C. punctata* including LFDs, LWRs, LLRs, condition factors ( $K_A$ ,  $K_F$ ,  $K_R$  and  $W_R$ ),  $a_{3.0}$  and  $M_W$  from the Rupsha River in southern Bangladesh. The results of this study can be an effective tool for fishery managers, and for fish biologists and conservationists to initiate early management strategies and regulations for a more sustainable conservation of the remaining stocks of this species in the Rupsha River and the surrounding ecosystem.

## Acknowledgements

The authors would like to extend their sincere appreciation to the (i) Ministry of Education of Bangladesh for funding (No. 37.200000.004.003.005.2014-1309/1 (42); Date: 10-08-2014) and (ii) PIU-BARC, NATP-2, CRG, Sub-Project: 484 for technical supports.

## References

- Ahmed ZF, Hossain MY, and Ohtomi J. 2012. Modeling the growth of silver hatchet chela *Chela cachius* (Cyprinidae) from the old Brahmaputra River in Bangladesh using multiple functions. *Zoological Study* 51: 336-344.
- Anderson RO and Neumann RM. 1996. Length, weight and associated structure indices. In: Murphy, BR. and Willis, WD (Eds), **Fisheries Techniques** 2nd ed. American Fisheries Society, Bethesda, MD, 447-482 pp.
- Azad MAK, Hossain MY, Khatun D, Parvin MF, Nawar F, Rahman O and Hossen MA. 2018. Morphometric relationships of the Tank goby *Glossogobius giuris* (Hamilton, 1822) in the Gorai River using multi-linear dimensions. *Jordan J Biol Sci*, **11**: 81 -85.
- Brodziak J, Ianelli J, Lorenzen K and Methot Jr. RD.(eds). 2011. Estimating natural mortality in stock assessment applications. U.S. Dep. Commer., NOAA Tech. Memo. NMFS-F/SPO-119, 38 pp.
- Froese R. 2006. Cube law, condition factor and weight length relationship: history meta-analysis and recommendations. *J Appl Ichthyol.*, **22**: 241-253.
- Froese R and Pauly D. (Eds). 2016. Fish base 2016. World Wide Web electronic publication. Available at: <http://www.fishbase.org> (accessed on 21 September 2016).
- Gam LH, Leow CY and Baie S. 2006. Proteomic analysis of snakehead fish (*Channa striata*) muscle tissue. *Malaysian J Biochem Mol Biol.*, **14**: 25–32.
- Haniffa MA, Nagarajan M. and Gopalakrishnan A. 2006. Length-weight relationships of *Channa punctata* (Bloch, 1793) from Western Ghats Rivers of Tamil Nadu. *J Appl Ichthyol.*, **22**: 308-309.
- Hossain MY, Ahmed ZF, Leunda PM, Jasmine S, Oscoz J, Miranda R. and Ohtomi J. 2006a. Condition, length-weight and length-length relationships of the Asian striped catfish *Mystus vittatus* (Bloch, 1794) (Siluriformes: Bagridae) in the Mathabhangha River, southwestern Bangladesh. *J Appl Ichthyol.*, **22**: 304-307.
- Hossain MY, Ahmed Z F, Leunda PM, Islam AKMR, Jasmine S, Oscoz J, Miranda R and Ohtomi J. 2006b. Length-weight and length-length relationships of some small indigenous fish species from the Mathabhangha River, southwestern Bangladesh. *J Appl Ichthyol.*, **22**: 301-303.
- Hossain MY, Jasmine S, Ibrahim AHM., Ahmed ZF, Rahman MM and Ohtomi J. 2009. Length-weight and length-length relationships of 10 small fish species from the Ganges, Bangladesh. *J Appl Ichthyol.*, **25**: 117–119.
- Hossain MY, Rahman MM, Fulanda B, Jewel MAS, Ahamed F and Ohtomi J. 2012a. Length-weight and length-length relationships of five threatened fish species from the Jamuna (Brahmaputra river tributary) River, northern Bangladesh. *J Appl Ichthyol.*, **28**: 275-277.
- Hossain MY, Rahman MM, Jewel MAS, Ahmed ZF, Ahamed F, Fulanda B, Abdallah EM and Ohtomi J. 2012b. Condition-and form-factor of the five threatened fishes from the Jamuna (Brahmaputra River distributary) River, northern Bangladesh. *Sains Malaysiana* **41**: 671–678.
- Hossain MY, Rahman MM, Miranda R, Leunda PM, Oscoz J, Jewel MAS, Naif A and Ohtomi J. 2012c. Size at first sexual maturity, fecundity, length-weight and length-length relationships of *Puntius sophore* (Cyprinidae) in Bangladeshi waters. *J Appl Ichthyol.*, **28**: 818-822.
- Hossain MY, Rahman MM, Abdallah EM and Ohtomi J. 2013. Biometric relationships of the Pool Barb *Puntius sophore* (Hamilton 1822) (Cyprinidae) from three major Rivers of Bangladesh. *Sains Malays.*, **42**: 1571–1580.

- Hossain MY, Hossen MA, Pramanik MNU, Ahmed ZF, Yahya K, Rahman MM and Ohtomi J. 2015a. Threatened fishes of the world: *Anabas testudineus* (Bloch, 1792) (Perciformes: Anabantidae). *Croatian J Fisher.*, **73**: 128-131.
- Hossain MY, Hossen MA, Pramanik MNU, Nawer F, Ahmed ZF, Yahya K, Rahman MM and Ohtomi J. 2015b. Threatened fishes of the world: *Labeo calbasu* (Hamilton, 1822) (Cypriniformes: Cyprinidae). *Croatian J Fisher.*, **73**: 134-136.
- Hossain MY, Hossen MA, Yahya K, Islam MM, Islam MA, Ahmed KNU and Begum M. 2015c. Threatened Fishes of the World: *Ompok pabda* (Hamilton, 1822) (Siluriformes: Siluridae). *Croatian J Fisher.*, **73**: 183-185.
- Hossain MY, Sayed SRM, Rahman MM, Ali MM, Hossen MA, Elgorban AM, Ahmed ZF and Ohtomi J. 2015d. Length-weight relationships of nine fish species from the Tetulia River, southern Bangladesh. *J Appl Ichthyol.*, **31**: 967-969.
- Hossain MY, Hossen MA, Pramanik MNU, Yahya K, Bahkali AH and Elgorban AM. 2016a. Length-weight relationships of *Dermogenys pusilla* Kuhl & van Hasselt, 1823 (Zenarchopteridae) and *Labeo bata* (Hamilton, 1822) (Cyprinidae) from the Ganges River (NW Bangladesh). *J Appl Ichthyol.*, **32**: 744-746.
- Hossain M.Y, Naser SMA, Bahkali AH, Yahya K, Hossen MA, Elgorban AM, Islam MM and Rahman MM. 2016b. Life history traits of the Flying Barb *Esomus danricus* (Cyprinidae) in the Ganges River, northwestern Bangladesh. *Pakistan J Zool.*, **48**: 399-408.
- Hossain MY, Hossen MA, Pramanik MNU, Ahmed ZF, Hossain MA and Islam MM. 2016c. Length-weight and length-length relationships of three Ambassid fishes from the Ganges River (NW Bangladesh). *J Appl Ichthyol.*, **32**: 1279-1281.
- Hossen MA, Hossain MY, Pramanik MNU, Nawer F, Khatun D, Parvin MF and Rahman MM. 2016. Morphological characters of *Botia lohachata*. *J Coast Life Med*, **4**: 689-692.
- Hossen MA, Hossain MY, Pramanik MNU, Khatun D, Nawer F, Parvin MF, Arabi A and Bashir MA. 2018. Population Parameters of the Minor carp *Labeo bata* (Hamilton, 1822) in the Ganges River of Northwestern Bangladesh. *Jordan J Biol Sci*, **11**: 179-186.
- Hossen MA, Hossain MY, Yahya K and Pramanik MNU. 2015. Threatened Fishes of the World: *Labeo bata* (Hamilton, 1822) (Cypriniformes: Cyprinidae). *Croatian J Fisher.*, **73**: 89-91.
- IUCN. 2017. IUCN Red List of Threatened Species. Version 2017-1, Downloaded on 3 September 2018).
- Khatun D, Hossain MY, Parvin MF and Ohtomi J. 2018. Temporal variation of sex ratio, growth pattern and physiological status of *Eutropiichthys vacha* (Schilbeidae) in the Ganges River, NW Bangladesh. *Zool Ecol.*, **28**: 343-354.
- Khatun D, Hossain MY, Nawer F, Mostafa AA and Al-Askar AA. 2019. Reproduction of *Eutropiichthys vacha* (Schilbeidae) in the Ganges River (NW Bangladesh) with special reference to potential influence of climate variability. *Environ Sci Pollut Res.*, **26**: 10800-10815.
- King, M. 2007. Population Dynamics. In: **Fisheries Biology, Assessment and Management**, 2<sup>nd</sup> edition. Fishing News Books, Oxford, 79-197 pp.
- Le Cren ED. 1951. The length-weight relationship and seasonal cycle in gonad weight and condition in the perch (*Perca fluviatilis*). *J Animal Ecol.*, **20**: 201-219.
- Nawer F, Hossain MY, Hossen MA, Khatun D, Parvin MF, Ohtomi J and Islam MA. 2017. Morphometric relationships of the endangered Ticto barb *Pethia ticto* (Hamilton, 1822) in the Ganges River (NW Bangladesh) through multi-linear dimensions. *Jordan J Biol Sci*, **10**: 199-203.
- Peterson I and Wroblewski JS. 1984. Mortality rates of Fishes in the pelagic ecosystem. *Canadian J Fisher Aquatic Sci.*, **41**: 1117-1120.
- Pethiyagoda R. 1991. **Freshwater Fishes of Sri Lanka**. The Wildlife Heritage Trust of Sri-Lanka. 362pp.
- Rahman AKA. 1989. Freshwater fishes of Bangladesh. Zoological Society of Bangladesh. *Department of Zoology, University of Dhaka*. 364 pp.
- Rahman MM, Hossain MY, Jewel MAS, Rahman MM, Jasmine S, Abdallah EM and Ohtomi J. 2012. Population structure, length-weight and length-length relationships, and condition-and form-factors of the Pool barb *Puntius sophore* (Hamilton, 1822) (Cyprinidae) from the Chalan Beel, North-central Bangladesh. *Sains Malays.*, **41**: 795-802.
- Rypel AL and Richter TJ. 2008. Empirical percentile standard weight equation for the black tail red horse. *North Am J Fisher Manag.*, **28**: 1843-1846.
- Sokal R.R. and Rohlf FJ. 1987. **Introduction to Biostatistics**. 2<sup>nd</sup> ed. New York: Freeman Publication.
- Talwar, P. K. and Jhingran A. G. 1991. **Inland Fishes of India and Adjacent Countries**. vol 1. A.A. Balkema, Rotterdam, 541p.
- Tesch FW. 1968. Age and Growth. In: Ricker, W. E (Ed), **Methods for Assessment of Fish Production in Fresh Waters**, Oxford: Blackwell Scientific Publications.



# Differential Expression for Genes in Response to Drought and Salinity in *Ruta graveolens* Plantlets

Sabah M. Hadi<sup>1\*</sup>, Kadhim M. Ibrahim<sup>2</sup> and Shatha I. Yousif<sup>3</sup>

<sup>1</sup> Department of Biology, College of Sciences, Baghdad University, <sup>2</sup> Department of Plant Biotechnology, College of Biotechnology, Al-Nahrain University, <sup>3</sup> Agricultural Research Directors, Ministry of Science and Technology, Baghdad, Iraq

Received July 26, 2018; Revised September 4, 2018; Accepted September 14, 2018

## Abstract

Abiotic stress-induced genes may lead to understand the response of plants and adaptability to salinity and drought stresses. Differential display reverse transcriptase – polymerase chain reaction (DDRT-PCR) was used to investigate the differences in gene expression between drought- and salinity-stressed plantlets of *Ruta graveolens*. Direct and stepwise exposures to drought- or salt-responsive genes were screened in *R. graveolens* plantlets using the DDRT technique. Gene expression was investigated both in the control and in the salt or drought-stressed plantlets and differential banding patterns with different molecular sizes were observed using the primers OPA-01 (646,770 and 983 pb), OPA-08 (593 and 988 pb), OPA-11 (674 and 831 pb), OPA-17 (638,765 and 1000 pb), and OPA- 15 (645 and 900 pb) indicating the expression of new genes amplified under stress conditions or of genes that already exist. Accordingly, DDRT-PCR seems to be a versatile and sensitive method, capable of detecting transcriptional changes at the mRNA level in plants.

**Keywords:** Gene expression, Drought and salinity stress, Callus culture, *Ruta graveolens*

## 1. Introduction

Differential display reverse transcriptase DDRT is one of the methods designed for analyzing differences in gene expression level. It has been successfully used to identify new genes in various tissues or cells. This technique is considered simple, quick, sensitive, and powerful for screening cDNA (Alves *et al.*, 1998; Rodriguez *et al.*, 2005). *Ruta graveolens* (Rutaceae), commonly known as the rue plant is an odorous medicinal and aromatic plant, grown in the Mediterranean region for outdoor decoration due to its beautiful yellow flowers. Rue contains many secondary metabolites such as flavonoids, furocoumarins, acridonealkaloids, furoquinolines, and coumarins which are used to treat many diseases such as anthelmintic, vitiligo, antispasmodic, multiple sclerosis, and emmenagogue in veterinary medicine (Ahmad *et al.*, 2010; Zuraida *et al.*, 2014). Abiotic stresses negatively affect plant growth, and reduce crop productivity worldwide including salinity and drought. When plants are under salt stress, the result is an ionic imbalance and hyper osmotic stress (Munns and Tester, 2008). Imbalance in homeostasis usually occurs at the cell and whole plant levels (Rodriguez *et al.*, 2005). Tolerance depends on the ability of a plant to sustain growth even when conditions are unfavorable for basic plant developmental processes. This strategy involves certainly physiological and biochemical modification at the cellular and molecular levels (Xiong and Ishitani, 2006; Peleg *et al.*, 2011). Tolerance level differs from one plant to another and from one species to another species, but the mechanism starts

with stress tolerance followed by gene products that are involved in cellular protection and may be a repair mechanism (Rao *et al.*, 2006). A gradual salt built up in the soil increases the osmosis in soil solution leading to accumulative decline in nutrients' absorption and thereafter a growth inhibition. The duration and severity of the stress (acute vs. chronic) influence the developmental stage of the plant, particularly when salinity is accompanied by drought stress (Cramer *et al.*, 2011; Peleg *et al.*, 2011; Leva *et al.*, 2012). This study is aimed at examining the response of *Ruta* callus cultures to varying levels of mannitol and saline water using two types of selection: (a) shock treatment, in which cultures are directly subjected to different concentrations for the stress agent, (b) stepwise long-term treatment, in which the cultures are exposed to stress with a gradual increase in the concentrations of the selected agent. It has been reported in this work that RNA, isolated from plantlets under stress conditions, then compared to the RNA isolated from the control plantlets and the DNA of intact plant, permits an increase in the gene expression level in the plantlets under stress.

## 2. Materials and Methods

*Ruta graveolens* plants were purchased from one of Baghdad nurseries. The plant stems were first washed under running tap water for thirty minutes, and were then subjected to surface sterilization using 1.5 % (v/v) NaOCL (Clorox) for twenty minutes with vigorous shaking. Stem segments (1.0 cm in length) were excised aseptically and transferred to Petri dishes (20 mL/dish) containing agar

\* Corresponding author e-mail: sabahtech2013@gmail.com.

solidified MS medium (Murashige and Skoog, 1962) supplemented with 1.0 mg/L 2,4-D and 1.0 mg/L Kin. All cultures were incubated at  $25 \pm 2$  °C, 16/8 h (light/dark) photoperiod under a light intensity of 1000 lux. (Ahmed *et al.*, 2010).

#### 2.1. Treatments with Salinity and Drought Stress Agents

Small pieces of calli weighing 100 mg each were re-cultured onto a callus maintenance medium containing 1.0 mg/L 2,4-D and 0.5 mg/L Kin, supplemented with different concentrations (0.0, 6, 12, 18, 24 or 30 %) of mannitol as osmoticum or (5.0, 10.0, 15.0, 20.0, 25.0, 30.0 dS/m<sup>-1</sup>) of saline water collected from drainage channels for direct screening and selection method. Callus cultures were recultured three times onto the same medium. For a gradual exposure to stress agents, callus pieces weighing 100 mg were re-cultured onto the maintenance medium containing 1.0 mg/L 2,4-D; 0.5 mg/L Kin, and were subjected to a gradual increase in mannitol concentrations (0.0, 6, 12, 18, 24 or 30 %) or (5.0, 10.0, 15.0, 20.0, 25.0, 30.0 dS/m<sup>-1</sup>) of saline water. All stressed callus pieces were transferred into MS regeneration medium supplemented with 1.5 mg/L BA and 0.5 mg/L NAA after screening cycles.

#### 2.2. Extraction of Genomic DNA and Total RNA

The method of Ahmad *et al.*, (2010) was followed; briefly approximately 50 mg of dried leaves were ground with a mortar and pestle. The homogenized tissues were transferred to 600 µL of 2 % CTAB DNA extraction buffer mixed with 1.25 µL of β-mercaptoethanol in 1.5 mL Eppendorf tubes, and were incubated at 65°C for thirty minutes in a water bath. Three microliters of RNase were added and incubated at 37 °C for one hour. Then, aliquot of 200 µL chloroform: isoamyl alcohol (24:1) was added to the solution, and was mixed well. The emulsified mixture was centrifuged at 13000 rpm for fifteen minutes, and then the aqueous phase was placed into a new sterilized Eppendorf tube. Aliquots of 600 µL isopropanol and 150 µL of sodium acetate were added, and then centrifuged at 13,000 rpm for ten minutes. The supernatant was discarded, the precipitated DNA was washed with 600 µL of 70 % ethanol, centrifuged at 13,000 rpm for five minutes, and then the supernatant was discarded. DNA was air-dried for two minutes and was dissolved in 150 µL of TE buffer and incubated at 65°C for one hour in a water bath. DNA concentrations were then measured. Total RNA (in 100 mg of leaf samples) was isolated from plantlets exposed previously to abiotic stresses and from control regenerated plantlets using Geneaid total RNA Mini Kit (Vogelstein and Gillespie, 1979).

#### 2.3. Synthesis of cDNA

The total RNA extracted from different calli samples (stressed and control) was used as a template to synthesize cDNA by AccuPower® RT Premix. The primer Oligo-dt (promega, USA) was prepared to obtain 100 pmol, which was mixed with DEPC 0.1 %. It was mixed well with 5 µL of template 0.5 – 1.0 µg RNA and Oligo dt<sub>15</sub> primer 100 pmol, and was incubated at 70°C for five minutes, and was placed on ice. The incubated mixture was transferred into 5 µL AccuPower® RT Premix tube, then the volume was completed with 5 µL DEPC water. The cDNA synthesis was performed using a thermocycler reaction at 42°C, for

sixty minutes (cDNA synthesis) then 95°C, for five minutes (RTase inactivation).

#### 2.4. Differential cDNA Display

AccuPower® PCR PreMix (Bioneer, Korea) ready to use, master mix (20 µL reaction) was used; it contained 250 µM of deoxyribonucleoside triphosphate (dNTPs), 30 mM of KCl, 10 mM of Tris- HCl (pH 9.0), 1.5 mM of MgCl<sub>2</sub>, 1 Unit of Top DNA polymerase and a tracking dye. Random primers OPA-01, OPA-05, OPA-08, OPA-10, OPA-11, OPA-15, OPA-17, OPB-05, OPC-04, OPE-08 were provided (Operon model - Promega, USA). The sequences of the polymorphic primers are presented in Table 1. The primers were purchased in a lyophilized form, and were dissolved in sterile distilled water to give a final concentration of 100 ng/µL as recommended by the supplier. RAPD-PCR conditions were 94°C for four minutes, 40 PCR cycles PCR products, and 100 bp DNA ladder (i.e., the cycles were performed at 94°C for one minute, 36°C for one minute and 72°C for one minute) and were followed by a ten-minute extension step at 72°C.

**Table 1.** Random primers used for the amplification of cDNA and genomic DNA.

Primer's name	Sequence 5'----- 3'
OPA-01	CAGGCCCTTC
OPA-05	AGGGGTCTTG
OPA-08	GTGACGTAGG
OPA-10	GTGATCGCAG
OPA-11	CAATCGCCGT
OPA-15	TTCCGAACCC
OPA-17	GACCGCTTGT
OPB-05	TGCGCCCTTC
OPC-04	CCGCATCTAC
OPE-08	TCACCACGGT

The optimization of the PCR reaction was accomplished after several trials, then, the mixture listed below was adopted as PCR products and 100 pb DNA ladder was determined by electrophoresis. Aliquot of 10 µL of the product was loaded on 1.0 % agarose gel and run at 80 volt for one hour. Bands were visualized on UV trans-illuminator and were photographed. The molecular weight of the bands was determined using the photo Capt MW program.

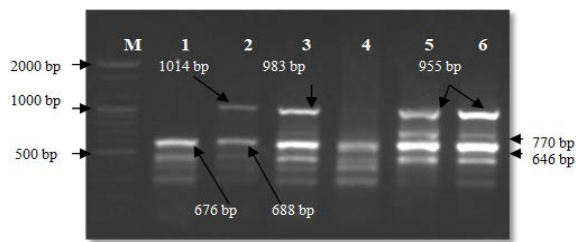
Component	Concentration	Volume (µL)
ddH <sub>2</sub> O	-----	12.0
AccuPower®PCR PreMix	1X	5.0
Primer	10 pmol	1.0
DNA sample	100 ng/ µL	2.0
Final volume		20.0

### 3. Results

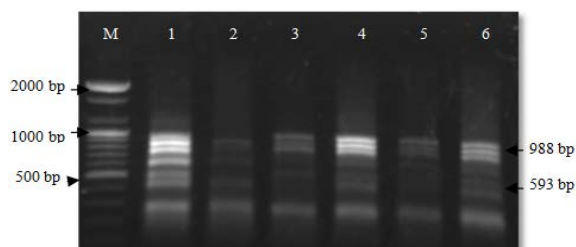
Polymorphisms at cDNAs levels in assuming drought and salinity tolerant *R. graveolens* regenerated plantlets were compared with cDNA control plantlets (regenerated plantlets which are not subjected to stress) and DNA isolated from intact plants. The cDNA was amplified with ten base arbitrary primers. The polymorphic fragments capable of differentiating the tolerant lines from the



stressed regenerated plantlets were generated by most primers. New bands were observed in salinity- and drought-stressed regenerated plantlets which were not detected in cDNA obtained from the control treatments. The primer OPA-01 generated a profile distinguished between tolerant lines in stressed regenerated plantlets and the control ones (Figure 1). The intensity of the bands increased in the regenerated stressed plantlets. The amplification by with this primer revealed the presence of a 646 bp fragments in the tolerant lines (lanes 3, 4, 5, and 6) compared with the control. On the other hand, fragments at 676 bp in the DNA extracted from intact plants (lane 1) and at 688 and 1014 bp in cDNA from control plant (lane 2) were not detected in the tolerant lines. A new band with a molecular size of about 770 bp was observed in plants produced from direct salt-screening method (lane 3) and plantlets produced from direct and stepwise drought-screening methods (lanes 5 and 6). A band at a size of 983 bp was detected in plantlets which resulted from the direct salt-screening method (lane 3) and plantlets regenerated from direct drought screening method (lane 5), while a band at 955 bp was detected in plantlets obtained from stepwise drought-screening method (lane 6). However these bands were not found in plantlets regenerated from control treatment (lanes 1 and 2). The marker OPA-08 amplified seven bands, of which five were polymorphic and two were monomorphic. The primer has an amplification product with molecular sizes about 988 and 593 bp fragments visualized in all tolerant plantlets (lanes 3, 4, 5 and 6) and in DNA from the intact plant (lane 1), but they were absent in the cDNA control plantlets (lane 2) as shown in Figure 2.

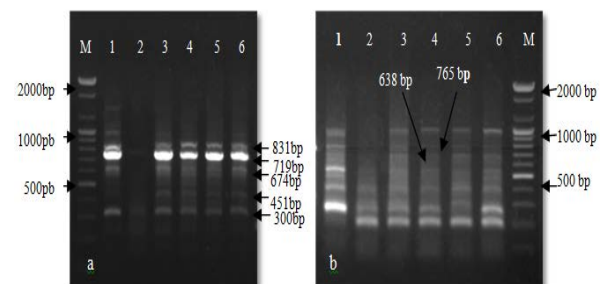


**Figure 1.** Amplification profile of differential display obtained using the primer OPA-01, lane (1): DNA from intact plant, lane (2): cDNA from regenerated non-stressed plantlet, lanes (3, 4): cDNA from regenerated plantlets subjected to direct or gradual exposure to saline water, lanes (5, 6): cDNA from regenerated plantlets subjected to direct or gradual exposure to mannitol, M: DNA ladder.



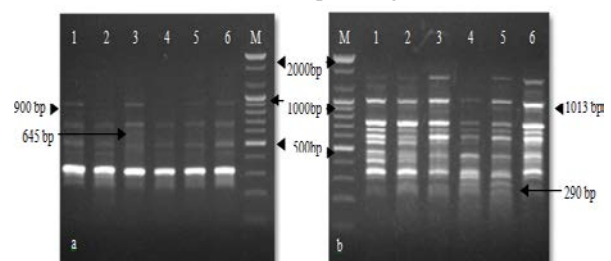
**Figure 2.** Amplification profile of differential display obtained using the primer OPA-08, lane (1): DNA from intact plant, lane (2): cDNA from regenerated non-stressed plantlet, lanes (3, 4): cDNA from regenerated plantlets subjected to direct or gradual exposure to saline water, lanes (5, 6): cDNA from regenerated plantlets subjected to direct or gradual mannitol, M: DNA ladder.

Amplification products using the primer OPA-11 (Figure 3a) which showed the presence of new bands with molecular sizes of 831 and 674 bp in the lanes 3, 4, 5, 6, and in lane 1 of the control, but they were missing in lane 2 in the control. The primer amplified a band with a molecular size of 719 bp which showed high intensity as visualized in lanes 3, 4, 5, 6, and 1, but it exhibited very low intensity in lane 2. Two bands with the molecular sizes of 541 and 300 bp were visualized in all tolerant lines, but not in control plantlets (lanes 1 and 2). Amplification with the primer OPA-17 revealed the presence of 1000, 765, and 638 bp fragments in the tolerant plantlets with a molecular size of 900 bp as visualized in the plantlets which resulted from the direct salt-screening method (lane 3) and those produced from the direct and stepwise drought-screening method (lanes 5 and 6) in the control plant (lane 1), but this band was absent in the plantlets regenerated from stepwise salt-screening method (lane 4), and in the cDNA control plantlets (lane 2). Lanes 3, 4, 5, and 6 compared with the control in lane 1, but those were absent in the cDNA of the control regenerated plants in lane 2 (Figure 3b).



**Figure 3.** Amplification profile of differential display obtained using the primer OPA-11 (a) and OPA-17 (b), lane (1): DNA from intact plant, lane (2): cDNA from regenerated non-stressed plantlet, lanes (3, 4): cDNA from regenerated plantlets subjected to direct or gradual exposure to saline water, lanes (5, 6): cDNA from regenerated plantlets subjected to direct or gradual exposure to mannitol, M: ladder 200bp.

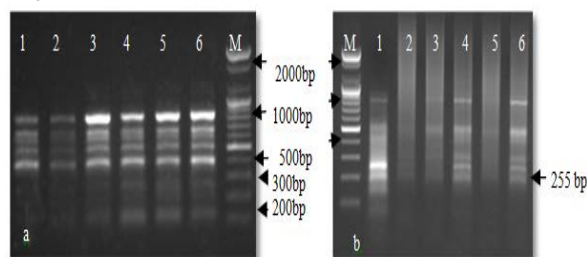
The primer OPA-15 amplified three monomorphic bands detected in all of the samples (Figure 4a).



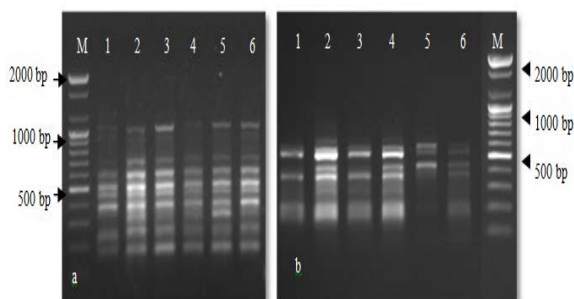
**Figure 4.** Amplification profile of differential display obtained using the primer OPA-15 (a) and OPB-05 (b), lane (1): DNA from intact plant, lane (2): cDNA from regenerated non-stressed plantlet, lanes (3, 4): cDNA from regenerated plantlets subjected to direct or gradual exposure to saline water, lanes (5, 6): cDNA from regenerated plantlets subjected to direct or gradual exposure to mannitol, M: DNA ladder.

Another band was detected in lane 3 only with a molecular size 645 bp. amplification with the primer OPB-05 (Figure 4b) confirmed the presence of a band at size 290 bp only in plantlets regenerated from stepwise salt and direct drought-screening methods (lanes 4 and 5). Meanwhile, a band with a molecular size of 1013 bp was visualized only in the plantlets produced from stepwise

drought screening method (lane 6). Many bands amplified by the primer OPA-05 with molecular sizes 100-300 bp appeared in all tolerant plantlets, but were missing in the control ones (Figure 5a). The intensity in the band at 870 bp appeared clearly in all tolerant plantlets, while a lower intensity band was exhibited in the control plantlets (lanes 1 and 2). The primer OPA-10 generated a profile differentiating the tolerant plantlets from the control ones (Figure 5b). Amplification products with this primer illustrated the presence of 1000 and 500 bp bands visualized in salt tolerant plantlets (lanes 3 and 4) and in those regenerated from stepwise drought-screening method (lane 6), while 255 bp band was clear in lanes 4 and 6 only. These bands were absent in the control ones. The two primers OPC-04 and OPE-08 showed many amplification products in all of the tested samples; however, no new bands appeared in the regenerated tolerant plantlets (Figure 6a and b).



**Figure 5.** Amplification profile of differential display obtained using the primer OPA-05 (a) and OPA-10 (b), lane (1): DNA from intact plant, lane (2): cDNA from regenerated non-stressed plantlet, lanes (3, 4): cDNA from regenerated plantlets subjected to direct or gradual exposure to saline water, lanes (5, 6): cDNA from regenerated plantlets subjected to direct or gradual exposure to mannitol, M: DNA ladder.



**Figure 6.** Amplification profile of differential display obtained using the primer OPC-04 (a) and OPE-08 (b), lane (1): DNA from intact plant, lane (2): cDNA from regenerated non-stressed plantlet, lanes (3,4): cDNA from regenerated plantlets subjected to direct or gradual exposure to saline water, lanes (5,6): cDNA from regenerated plantlets subjected to direct or gradual exposure to mannitol, M: DNA ladder.

#### 4. Discussion

DDRT-PCR and RAPD techniques confirmed that the tolerant regenerated plantlets differed genotypically from the control ones conferring genetic polymorphism among the salt-selected and drought-tolerant lines. At annealing PCR conditions, even a slight base change at the primer-annealing site was clear in the presence or absence of bands produced by RAPD. It can be, therefore, concluded that under tissue culture conditions and the presence of stress selective agents, somaclonal variation may be generating genetic changes expressed among the selected

plantlets as has been hypothesized by Larkin and Scowcroft (1981). This in turn plays an important role in varietal improvement. It is proven previously that some tissue culture variants can be superior to the donor clones in terms of abiotic tolerance (Shomeli *et al.*, 2011; Balkrishna and Shankarrao, 2013; Hadi *et al.*, 2014; Rastogi *et al.*, 2015). *In vitro*, cultures may exhibit somaclonal variation, gene inactivation, or reactivation of silent genes, and gene over expression (Muller *et al.*, 1990; Kaeppler *et al.*, 2000; Leva *et al.*, 2012; Mohammad. and Ibrahim, 2017). Activation of complex signaling pathway(s) may cause changes in the cellular gene expression which is a prerequisite for plants to adapt to extreme conditions (Tong *et al.*, 2007; Tamirisa *et al.*, 2014). DDRT-PCR has been widely used to identify the expression patterns of uncharacterized genes in many different plant species. A large number of differentially expressed genes can be identified, particularly those expressed in plants under stress (Alves *et al.*, 1998). In the present study, the total amplification products generated by these primers ranged from 200 bp in the primer OPC-04 (Figure 6a) to approximately 1400 bp in the primer OPB-05 (Figure 4b). Results confirmed that cDNAs are differentially expressed in response to both drought and salinity stresses. Drought and salinity may activate certain sets of common genes in plant cells as has been proposed by Said *et al.*, (2015). Genes that are overexpressed under stress conditions are classified into two groups; the first group includes classes of proteins such as enzymes required for biosynthesis of various osmoprotectants, LEA proteins, chaperones, and detoxification enzymes, which protect plant cells. The second group includes signaling molecules, transcription factors, and protein kinases (Rai *et al.*, 2011; Lokhande and Suprasanna, 2012). Mahajan and Tuteja (2005) reported that each stress is controlled by many genes, therefore, the exposure of plant cells to stress agents may result in the alteration of a large number of genes as well as their products. This may explain the differences which occurred in the number and intensity of cDNA bands at different concentrations of salinity and drought compared with those bands visualized in the control plantlets. The current work confirms the findings of Tamirisa *et al.*, (2014) who proposed an evidence that the enhanced abiotic stress tolerance in *Arabidopsis* transgenic plants is due to a significant increase in the expression gene levels which agrees with the results of Kamal *et al.*, (2010) who reported on the function of proteins expressed by genes in stress- tolerant plants.

#### 5. Conclusion

The findings of the present study indicate that the DDRT-PCR technique is suitable for detecting the expression of salt and drought genes in the tolerant regenerated plantlets of *R. graveolens*. This may apply to other members of Rutacea family.

#### Acknowledgements

The authors acknowledge the Central Environmental Laboratory, College of Science at the University of Baghdad, and the Department of Plant Biotechnology, College of Biotechnology, AL-Nahrain University, as well

as the Agricultural Research Directorate of the Ministry of Science and Technology.

## References

- Ahmad A, Faisal M, Anis M, Aref I. 2010. *In vitro* callus induction and plant regeneration from leaf explants of *Ruta graveolens* L. *South Afric J Bot.*, **76**: 597-600.
- Alves JD, VanToai T, and Kaya N. 1998. Differential display: A novel PCR – based method for gene isolation and cloning. *Revista Brasileira de Fisiologia Vegetal.*, **10**: 161-164.
- Balkrishna R, Shankarrao S. 2013. *In vitro* screening and molecular genetic markers associated with salt tolerance in maize. *Afric J Biotech.*, **12**: 4251-4255.
- Cramer GR, Urano K., Delort S, Pezzotti M, Shinozak K.. 2011. Effect of abiotic stress on plants: a systems biology perspective *BMC Plant Biol.*, **11**: 163.
- Kaeppeler SM, Kaeppeler HF and Rhee Y. 2000. Epigenetic aspects of somaclonal variation in plants. *Plant Mol Biol.*, **43**: 179-188.
- Kamal AHM, Kim K., Shin KH, Choi JS, Baik BK., Tsujimoto H, Heo H, Park C and Woo SH. 2010. Abiotic stress responsive proteins of wheat grain determined using proteomics technique. *Aust J of Crop Sci.*, **4**: 196-208.
- Larkin PJ and Scowcroft WR. 1981. Somaclonal variation – a novel source of variability from cell cultures for plant improvement. *Theor Appl Genet.*, **60**: 197-214.
- Leva AR, Petruccielli R and Rinaldi MR. 2012. Somaclonal variation in tissue culture: A case study with olive. **Recent Advances in plant in vitro culture**. INTECH chapter 7.
- Lokhande VH and Suprasanna P. 2012. Prospects of halophytes in understanding and managing abiotic stress tolerance. In: Ahmed P and Prasad M (Eds.), **Environmental Adaptation and Stress Tolerance of Plants in the Era of Climate Changes**. Springer Science & Business Media, LLC, pp: 29-56.
- Mahajan S and Tuteja N. 2005. Cold, salinity and drought stresses: An overview. *Arch Biochem Biophys.*, **444**: 139-158.
- Mohammad RK. and Ibrahim K.M. 2017. Cytological effects of mutagenic agents and NaCl on mitotic division in two Iraqi rice (*Oryza sativa* L.) genotypes. *J of Al-Nahrain University Sci.*, **20**: 114-119.
- Muller E, Brown PTH, Hartke S and Lorz H. 1990. DNA variation in tissue-culture-derived rice plants. *Theor Appl Genet.*, **80**: 673-679.
- Munns R and Tester M. 2008. Mechanisms of salinity tolerance. *Annu Rev Plant Biol.*, **59**: 651–681.
- Murashige T and Skoog F. 1962. A revised medium for rapid growth and bioassays with Tobacco tissue culture. *Physiol Plant*, **15**: 473-497.
- Peleg Z, Apse MP and Blumwald E. 2011. Engineering salinity and water – stress tolerance in crop plants. *Adv Bot Res.*, **57**: 407-432.
- Rai MK., Kalia RK., Singh R, Gangola M and Dhawan AK.. 2011. Developing stress tolerant plants through *in vitro* selection – An overview of the recent progress. *Environ Exp Botany*, **71**: 89-98.
- Rajeswari S, Krishnamurthi M, Shinisekar S, Prem A and Thirugnana KS. 2009. Performance of somaclones developed from intergeneric hybrids of sugarcane. *Sugar Tech.*, **11**: 258-261.
- Rao MK., Raghavendra AS and Reddy KJ. 2006. **Physiology and Molecular Biology of Stress Tolerance in Plants**. Springer, Netherlands.
- Rastogi J, Siddhant BP and Sharma BL. 2015. Somaclonal variation: A new dimension for sugarcane improvement. *GERE Bulletin of Biol.*, **6**: 5-10.
- Rodríguez M, Canales E and Borrás-Hidalgo O. 2005. *Molecular aspects of abiotic stress in plants*. *Biotechnol Aplicada*, **22**: 1-10.
- Hadi SM, Ibrahim KM and Yousif SA. 2014. Effect of shock and elevated levels of mannitol on callus growth, regeneration and proline accumulation in *Ruta graveolens* cultures. *Inter J Current Microbiol Appl Sci.*, **3**:479-488.
- Said EM, Mahmoud RA, AL-Akshar R and Safwat G. 2015. Drought stress tolerance and enhancement of banana plantlets *in vitro*. *Austin Biotechnol Bioeng.*, **2**: 1-7.
- Shomeli M, Nabipour M, Meskarbashee M and Memari H. 2011. Evaluation of sugarcane (*Saccharum officinarum* L.) somaclonals tolerance to salinity via *in vitro* and *in vivo*. *Hayati J Biosci.*, **18**: 91-96.
- Tamirisa S, Vudem DR and Khareedu VR. 2014. Overexpression of pigeonpea stress-induced cold and drought regulatory gene (*CcCCR*) confers drought, salt, and cold tolerance in *Arabidopsis*. *J Exp Botany*, **65**: 4769-4781.
- Tong S, Ni Z, Peng H, Dong G and Sun Q. 2007. Ectopic overexpression of wheat *TaSrg6* gene confers water stress tolerance in *Arabidopsis*. *Plant Sci.*, **172**: 1079–1086.
- Vogelstein B and Gillespie D. 1979. Preparative and analytical purification of DNA from agarose. *Proc Natl Acad Sci USA*, **76**: 615-619.
- Xiong L and Ishitani M. 2006. Stress signal transduction components , pathways and network integration. In: Rai A and Takabe T ( Eds): **Abiotic Stress Tolerance in Plants Toward the Improvement of Global Environment and Food**, Springer, Netherlands, pp. 3-29.
- Zuraida AR, Mohd MA, Erny MN, Fatin LI, Aya NO, Juhazliana J, Wan ZW. 2014. Improved plant regeneration and *in vitro* somatic embryogenesis in *Ruta graveolens*. *J of Exp Biol Agric Sci.*, **2**: 328-366.



# A Thermodynamic Study of Partially-Purified *Penicillium humicola* $\beta$ -mannanase Produced by Statistical Optimization

Siham A. Ismail, Om Kalthoum H. Khattab, Shaimaa A. Nour, Ghada E. A. Awad, Amany A. Abo-Elnasr and Amal M. Hashem\*

Department of Chemistry of Natural and Microbial Products, Pharmaceutical and Drug Industries Research Division, National Research Centre, El Buhouth St., Dokki, Giza, Egypt.

Received July 7, 2018; Revised August 6, 2018; Accepted August 30, 2018

## Abstract

A sequential optimization strategy, based on statistical experimental designs, is employed in this study to enhance the  $\beta$ -mannanase production from *Penicillium humicola* in a medium containing coffee waste as a carbon source. A two-level Plackett–Burman design was applied to differentiate between the bioprocess parameters that significantly influence the  $\beta$ -mannanase production followed by fractional factorial design (FFD) to optimize the most significant variables for the highest yield of  $\beta$ -mannanase. Overall, more than a 3.4-fold improvement in enzyme production was achieved due to the statistical optimization. Partially, the purification of  $\beta$ -mannanase was achieved by a 60-70 % saturation of ammonium sulfate with specific activity 27.83IU/mg protein. The partially-purified  $\beta$ -mannanase showed an optimum activity at pH5.5 and retained 80-86 % of its original activity at pH ranging from 4.5 to 6 after 120 minutes. The optimum temperature for the *Penicillium humicola*  $\beta$ -mannanase was 60°C, and the activation energy ( $E_a$ ) was 16.71kJmol<sup>-1</sup>. Thermal stability and the thermodynamic parameters of  $\beta$ -mannanase are studied at temperatures ranging between 40 and 60°C.

**Keywords:**  $\beta$ -mannanase, *Penicillium humicola*, Coffee residues, Statistical designs, Partial purification, Characterization.

## 1. Introduction

$\beta$ -Mannan and its heteropolysaccharides are found in many natural products such as copra, guar beans, ivory nuts, locust beans, roots of konjak, palm kernel, aloe vera, coffee beans, wheat bran, and the hemicelluloses of soft and hard woods (Kurakake and Komaki., 2001; Keawsompong., 2016).

A large amount of by-products are generated from the industrial use of these natural products. For example, the coffee industry is responsible for the generation of a large amount of wastes represented mainly in spent coffee ground (SCG); (Mussatto *et al.*, 2011; Obruca *et al.*, 2015). Thus, taking into consideration that the annual production of coffee beans exceeds eight million tons (Murthy *et al.*, 2012) and that one ton of green coffee generates about 650 Kg of SCG (Obruca *et al.*, 2015), one becomes well aware of the highly polluting residues of SCG. All of these wastes, arising from agricultural and industrial applications, contain around 30-35 % of polysaccharides (mainly mannan) (Chiyanzu *et al.*, 2014 and Ahirwar *et al.*, 2016) which may support pathogenic bacteria growth, and cause massive environmental pollution. Therefore, the safe disposal of these wastes or the proper utilization of them are practical methods to be worked on. The application of innovative methods such as enzymatic treatments may also be a promising strategy to

transfer these wastes into raw materials for other processes. Moreover, the usage of these wastes to produce valuable products such as enzymes was reported by many researchers (Regalado *et al.*, 2000; De Marco *et al.*, 2015; Ahirwar *et al.*, 2016 and Soni *et al.*, 2016).

$\beta$ -Mannanase (1,4-  $\beta$ -D-mannan mannanohydrolase; 3.2.1.78) is the enzyme that cleaves the  $\beta$ -1, 4-mannosidic linkages in mannans, galactomannans, glucomannans, and galactoglucomannans (El-Naggar *et al.*, 2006, Abdel-Fattah *et al.*, 2009). Therefore, due to its broad substrate specificity,  $\beta$ -mannanase has a great potential in many industrial applications including foods, feed for animals and plants, pulp and paper, pharmaceuticals and cosmetics, the production of mannan and manooligosaccharids, bioethanol and biodiesel productions, and oil and textile industries (Keawsompong., 2016; Obruca *et al.*, 2015; Chiyanzu *et al.*, 2014; Ahirwar *et al.*, 2016; Soni *et al.*, 2016; Kwon *et al.*, 2013; and Soni *et al.*, 2017). Moreover,  $\beta$ -Mannanase is produced by different microorganisms (Ahirwar *et al.*, 2016; Soni *et al.*, 2016; Soni *et al.*, 2017; Chauhan *et al.*, 2012; El-Refai *et al.*, 2014; Germec *et al.*, 2017).

The goal of the current research is to produce economical  $\beta$ -mannanase from a non-costly production medium using coffee waste. The statistical optimization of the production medium is a promising strategy to increase the yield of enzymes. The Plackett-Burman design and Fractional Factorial design are applied in this research to

\* Corresponding author e-mail: amal\_mhashem@yahoo.com.



optimize the production of  $\beta$ -mannanase from *Penicillium humicola*. A partial purification and characterization of *Penicillium humicola*  $\beta$ -mannanase were also carried out to increase the specific activity of the enzyme.

## 2. Materials and Methods

### 2.1. Materials

For this research, locust bean gums (LBG) were purchased from Sigma Chemical, and the Brazilian coffee waste was obtained from a local market. All other chemicals used in this study are analytical grade chemicals.

### 2.2. Microorganism

The fungal strain *Penicillium humicola* was obtained from the culture collection of the National Research Center in Dokki, Cairo, Egypt, and was morphologically identified by the Micro Analytical center. The culture was maintained on potato dextrose agar and incubated at 30°C for seven days before storage at 4°C with a monthly sub-culturing. The fungal cells were preserved at -80°C in a solution containing 50 % glycerol.

### 2.3. Cultivation Conditions and Enzyme Production

Inoculum preparation was carried out by transferring the spore suspensions of the well growth slant of the *P. humicola* into a 250 mL Erlenmeyer flask containing 50 mL sterilized medium which consisted of (g/L): locust bean gum, 10.0; peptone, 2.0; urea, 0.3;  $(\text{NH}_4)_2\text{SO}_4$ , 1.5;  $\text{MgSO}_4 \cdot 7\text{H}_2\text{O}$ , 0.5;  $\text{KH}_2\text{PO}_4$ , 10.0, the pH was adjusted to 5.3 before autoclaving. The inoculated flasks were incubated at 30°C for forty-eight hours in a rotary shaker adjusted at 120 rpm. The culture medium for the enzyme production had the same constituents as the inoculum medium except that the locust bean gums were replaced by coffee residues (El-Refai *et al.*, 2014). The culture flasks (50 mL) were inoculated with 10 % (v/v), and were incubated for ten days at 30°C in a rotary shaker at 150 rpm. At the end of the incubation period, the fermented medium was centrifuged at 4000 rpm for fifteen minutes in a cooling centrifuge. The clear supernatant was used as the crude enzyme solution.

### 2.4. Enzyme Assay and Protein Content

Enzyme assay was performed by incubating 0.5 mL of an appropriately-diluted culture filtrate with 1 mL of 1 %

(w/v) locust bean gum (in 50 mM sodium citrate buffer at pH 5.0) for ten minutes at 50°C (Hashem *et al.*, 2001). The reducing sugars produced were determined using the Nelson–Smogi reagent (Smogi *et al.*, 1952). One unit of enzyme activity (IU) was defined as the amount of enzyme that released 1  $\mu\text{M}$  of mannose/ml/min under the assay conditions. The protein content was determined according to Lowry *et al.*, (1951) with bovine serum albumin as a standard.

### 2.5. Optimization of *P. humicola* $\beta$ -mannanase Production

#### 2.5.1. Plackett–Burman Experimental Design

Plackett–Burman experimental design (PB) (Plackett *et al.*, 1946) is used in this study to evaluate the relative importance of culture conditions and medium components for the production of  $\beta$ -mannanase from *Penicillium humicola* in submerged fermentation. Nine different factors were chosen to perform this optimization; these include coffee residues as a carbon source, nitrogen complex (ammonium sulfate: peptone: urea in the ratio of 1:1:1), NaCl,  $\text{KH}_2\text{PO}_4$ ,  $\text{MgSO}_4$ , incubation time, initial pH of the culture medium, inoculum size, and agitation speed (rpm) culture. The variables were represented at two levels, high concentration (+1) and low concentration (-1) in eleven trials as shown in Table 1. Each row represents a trial run, and each column represents an independent variable concentration. The Plackett–Burman experimental design is based on the first order linear model:

$$Y = B_0 + \sum B_i X_i \quad \text{Eq. (1)}$$

Where Y is the response ( $\beta$ -mannanase biosynthesis),  $B_0$  is the model intercept, and  $B_i$  is the variables' estimates. The effect of each variable was determined by the following equation:

$$E(X_i) = 2(\sum M_i^+ - \sum M_i^-)/N \quad \text{Eq. (2)}$$

Where  $E(X_i)$  is the effect of the tested variable.  $M_i^+$  and  $M_i^-$  represent the  $\beta$ -mannanase production from the trials where the variable ( $X_i$ ) measured was present at high and low concentrations, respectively and N is the number of trials.

The standard error (SE) of the concentration effect was the square root of the variance of an effect, and the significance level (*p*-value) of each concentration effect was determined using student's t-test:

$$t(X_i) = E(X_i)/SE \quad \text{Eq. (3)}$$

Where  $E(X_i)$  is the effect of variable  $X_i$ .

**Table 1.** Coded levels and real values for the Plackett–Burman experiment.

Trial No.	$X_1$	$X_2$	$X_3$	$X_4$	$X_5$	$X_6$	$X_7$	$X_8$	$X_9$	$\beta$ -mannanase activity (IU/mL)
1	-1(1.8)	-1(0.329)	-1(0.375)	+1(0.06)	+1(12)	+1(6.5)	-1(120)	-1(8)	-1(0.5)	5.46
2	+1(3.8)	-1(0.329)	-1(0.375)	-1(0.02)	-1(8)	+1(6.5)	+1(180)	+1(12)	+1(1.0)	13.61
3	-1(1.8)	+1(0.862)	-1(0.375)	-1(0.02)	+1(12)	-1(4.5)	+1(180)	+1(12)	+1(1.0)	2.44
4	+1(3.8)	+1(0.862)	-1(0.375)	+1(0.06)	-1(8)	-1(4.5)	-1(120)	-1(8)	-1(0.5)	23.31
5	-1(1.8)	-1(0.329)	+1(1.25)	+1(0.06)	-1(8)	-1(4.5)	+1(180)	+1(12)	-1(0.5)	7.86
6	+1(3.8)	-1(0.329)	+1(1.25)	-1(0.02)	+1(12)	-1(4.5)	-1(120)	-1(8)	+1(1.0)	7.84
7	-1(1.8)	+1(0.862)	+1(1.25)	-1(0.02)	-1(8)	+1(6.5)	-1(120)	-1(8)	-1(0.5)	7.86
8	-1(1.8)	+1(0.862)	-1(0.375)	+1(0.06)	-1(8)	+1(6.5)	-1(120)	+1(12)	-1(0.5)	3.6
9	+1(3.8)	-1(0.329)	+1(1.25)	-1(0.02)	+1(12)	-1(4.5)	+1(180)	-1(8)	+1(1.0)	5.4
10	+1(3.8)	+1(0.862)	+1(1.25)	+1(0.06)	+1(12)	+1(6.5)	+1(180)	+1(12)	+1(1.0)	7.28

Real values (given in parentheses) are in w/v %.  $X_1$ , is coffee residues;  $X_2$ , is nitrogen complex [peptone : ammonium sulfate : urea (1:1:1)];  $X_3$ ,  $\text{KH}_2\text{PO}_4$ ;  $X_4$ ,  $\text{MgSO}_4$ ;  $X_5$ , Incubation time (days);  $X_6$ , pH;  $X_7$ , shaking speed (rpm);  $X_8$ , Inoculum size(v/v);  $X_9$ , NaCl.

### 2.5.2. Fractional Factorial Design (FFD)

Based on the results obtained from PB design, the fractional factorial design (FFD) was conducted to gain the optimized levels of the main affecting factors (Rosa *et al.*, 2010 and Farid *et al.*, 2013). The FFD design of nineteen experiments and the coded and un-coded levels of the four investigated independent variables are listed in Table 3. The second-order empirical model can be obtained from the experimental data, the relationship between the response yield ( $\beta$ -mannanase activity) and the variables through polynomial regression analysis. The form of the second-order polynomial model is as follows:

$$Y_{\text{Activity}} = \beta_0 + \beta_1 X_1 + \beta_2 X_2 + \beta_3 X_3 + \beta_4 X_4 + \beta_{11} X_1^2 + \beta_{22} X_2^2 + \beta_{33} X_3^2 + \beta_{44} X_4^2 + \beta_{12} X_1 X_2 + \beta_{13} X_1 X_3 + \beta_{14} X_1 X_4 + \beta_{23} X_2 X_3 + \beta_{24} X_2 X_4 + \beta_{34} X_3 X_4$$

Eq. (4)

Where  $Y_{\text{Activity}}$  is the predicted production of  $\beta$ -mannanase (IU/ml) and  $X_1$ ,  $X_2$ ,  $X_3$  and  $X_4$  are the independent variables corresponding to the chosen affecting factors.  $\beta_0$  is the intercept;  $\beta_1$ ,  $\beta_2$ ,  $\beta_3$ , and  $\beta_4$  are linear coefficients;  $\beta_{11}$ ,  $\beta_{22}$ ,  $\beta_{33}$  and  $\beta_{44}$  are quadratic coefficients;  $\beta_{12}$ ,  $\beta_{13}$ ,  $\beta_{14}$ ,  $\beta_{23}$ ,  $\beta_{24}$  and  $\beta_{34}$  are cross-product coefficients.

### 2.5.3. Statistical Analysis

Statistical analysis of the model was performed to evaluate the analysis of variance (ANOVA). Statistical significance of the model equation was determined by Fisher's test value, and the proportion of variance explained by the model was given by the determination of multiple coefficients for each variable. The quadratic models were represented as contour plots (3D), and the response surface curves were generated by using STATISTICA (0.6).

### 2.6. Partial Purification of *P. humicola* $\beta$ -mannanase

All of the purification steps were carried out at 4°C. The crude enzyme solution of *P. humicola* (100 mL) was partially-purified by fractional precipitations with ammonium sulfate (20–100 %, w/v), acetone and ethanol (20–100 %, v/v). The precipitated protein was obtained by centrifugation (5,000 rpm for twenty minutes) and was re-suspended in a minimum volume of 50mM sodium citrate buffer (pH 5.5). All the fractions of ammonium sulfate were dialyzed against the same buffer overnight. The enzyme activity and the protein content were estimated for each fraction.

### 2.7. Biochemical Characterization of Partially-Purified *P. humicola* $\beta$ -mannanase

#### 2.7.1. Effect of pH on Enzyme Activity and Stability

The effect of pH on the activity of partially-purified *P. humicola*  $\beta$ -mannanase, was detected at pH ranging between 4 and 6 with sodium citrate buffer (50mM). The pH stability was determined by incubating the enzyme in the abovementioned buffer at pH ranging between 4 and 6, without the substrate, at room temperature and for different periods of time. The residual enzyme activity was estimated under the standard assay condition.

#### 2.7.2. Effect of Temperature on Enzyme Activity

The effect of temperature on the activity and stability of the partially-purified *P. humicola*  $\beta$ -mannanase was studied at temperatures ranging from 40 to 60 °C. The activation energy ( $E_a$ ) for  $\beta$ -mannanase was calculated by

Arrhenius plot (log V (logarithm of % residual activity) versus reciprocal of temperature in Kelvin (1000/T)), as given in the following equation:

$$\text{Slope} = -E_a/R \quad \text{Eq. (5)}$$

#### 2.7.3. Thermal Stability and the Thermodynamic Parameters

The partially-purified enzyme solution was incubated with sodium citrate buffer (50mM) with pH at 5.5 with the temperature ranging from 40 to 60 °C for different periods of time. The residual enzyme activity was estimated under the standard assay condition. Results were expressed as first-order plot. Thermal deactivation rate constants ( $k_d$ ), half-lives ( $T_{1/2}$ ) and  $D$ -values (decimal reduction time or time required to pre-incubate the enzyme at a given temperature to maintain 10 % residual activity) at each temperature were determined. The  $k_d$  was determined by regression plot of log relative residual activity (%) versus time (min). The  $T_{1/2}$  and  $D$ -value of the partially-purified  $\beta$ -mannanase were determined by the following equations:

$$T_{1/2} = \ln 2/k_d \quad \text{Eq. (6)}$$

$$D\text{-value} = \ln 10/k_d \quad \text{Eq. (7)}$$

The increase in the temperature necessary to reduce  $D$ -value by one logarithmic cycle ( $z$  value) was calculated from the slope of graph between log D versus T (°C) using the equation:

$$\text{Slope} = -1/z \quad \text{Eq. (8)}$$

The denaturation energy ( $E_d$ ) for  $\beta$ -mannanase was determined by a plot of log denaturation rate constants ( $\ln k_d$ ) versus the reciprocal of the absolute temperature ( $K$ ) using the equation:

$$\text{Slope} = -E_d/R \quad \text{Eq. (9)}$$

The change in enthalpy ( $\Delta H^\circ$ , kJ mol<sup>-1</sup>), free energy ( $\Delta G^\circ$ , kJ mol<sup>-1</sup>), and entropy ( $\Delta S^\circ$ , J mol<sup>-1</sup> K<sup>-1</sup>) for the thermal denaturation of  $\beta$ -mannanase were determined using the following equation:

$$\Delta H^\circ = E_d - RT \quad \text{Eq. (10)}$$

$$\Delta G^\circ = -RT \ln ((k_d X h)) / ((k_b \cdot \square)) \quad \text{Eq. (11)}$$

$$\Delta S^\circ = \frac{\Delta H^\circ - \Delta G^\circ}{T} \quad \text{Eq. (12)}$$

Where  $T$  is the corresponding absolute temperature in Kelvin, ( $K$ ),  $R$  is the gas constant (8.314 J mol<sup>-1</sup> K<sup>-1</sup>),  $h$  is the Planck constant (11.04 × 10<sup>-36</sup> J min), and  $k_B$  is the Boltzman constant (1.38 × 10<sup>-23</sup> J K<sup>-1</sup>).

## 3. Results and Discussion

### 3.1. Statistical Optimization of $\beta$ -mannanase Production

For multivariable processes such as biochemical systems, in which numerous potentially influential factors are involved, it is necessary to analyze the process with an initial screening design prior to optimization. A sequential optimization approaches were applied in this study. The first approach deals with screening for nutritional factors affecting the growth of *P. humicola* with respect to  $\beta$ -mannanase production. The second approach is to optimize the factors mostly affecting the enzyme-production process.

#### 3.1.1. Plackett–Burman Design

In the first approach, the Plackett–Burman design was applied to reflect the relative importance of nine different

factors. The averages of  $\beta$ -mannanase activity for the different trials were given in IU/mL and shown in Table 1.

Data indicated a wide variation from 2.44 to 23.31 IU/mL for the  $\beta$ -mannanase activity. The main effects of the examined factors on the enzyme activity were calculated and presented graphically in Figure 1. It was offered the view for the ranking of factor estimates obtained by Plackett–Burman design. This variation reflected the importance of medium optimization to attain high productivity. The data analysis from the Plackett–Burman experiments involved a first-order (main effects) model.

The regression coefficients analyses of the tested variables for the  $\beta$ -mannanase were: coffee residues,  $\text{MgSO}_4$ , Nitrogen complex, and NaCl which all showed a positive effect on the  $\beta$ -mannanase activity. On the other hand, medium initial pH,  $\text{KH}_2\text{PO}_4$ , incubation time, inoculums size, and the shaking speed contributed negatively. The first-order model describing the correlation of the nine factors and the  $\beta$ -mannanase activity can be presented as follows:

$$Y_{\text{Activity}} = 18.460 + 4.971X_1 - 5.792X_2 + 550.850X_3 + 1.45X_4 - 2.314X_5 - 0.0044.733X_6 - 0.09X_7 + 0.180X_8 + 18.460X_9$$

Table 2 shows the *t* test, *p* effect, and confidence level. The variables showed a high confidence level that was above 90 % (Coffee residues, incubation period, agitation speed (rpm) and inoculum size) were selected for further optimization (Farid *et al.*, 2013).

**Table 2.** Statistical analysis of Plackett-Burman design showing coefficient values, effect, *t*- and *P*- values for each variable on  $\beta$ -mannanase analysis.

Variables	$\beta$ - mannanase analysis				
	Coefficient	Effect	<i>t</i> -test	<i>P</i> -value	Confidence Level (%)
Intercept	18.460				
Coffee residue	4.971	7.6575	3.160751	0.008	99.2
Nitrogen complex	-5.792	1.6925	0.698605	0.2537	74.63
$\text{KH}_2\text{PO}_4$	550.850	-3.386	-1.3762	0.0574	84.26
$\text{MgSO}_4 \cdot 7\text{H}_2\text{O}$	-2.314	2.15525	0.889613	0.2016	79.84
NaCl	1.45	1.234	0.4356	0.2145	68.87
Incubation time	0.004	-6.9475	-2.86769	0.012	98.8
pH	-0.092	-2.3025	-0.95039	0.1868	81.32
Rpm	0.180	-3.54225	-1.46212	0.0936	90.64
Inoculum size	18.460	-3.54225	-1.46212	0.0936	90.64

Nitrogen complex: (peptone+ ammonium sulfate+ urea).

### 3.1.2. Fractional Factorial Design (FFD)

Fractional factorial design (FFD) for four independent variables was applied to reach to the optimum concentration for the most significant medium components obtained from the PB design (shown above). Table 3 shows the observed and the predicted values of the produced  $\beta$ -mannanase. Multiple regression analysis of the experimental data gave the following second- order polynomial equation:

$$Y_{\text{activity}} = -3.405 + 6.432X_1 + 0.932X_1^2 + 0.116X_2^2 + 0.012X_3^2 + 0.099X_4^2 - 0.352X_1X_2 - 0.104X_1X_3 + 1.256X_1X_4 + 0.015X_1X_4 - 0.370X_1X_4 - 0.005X_1X_4$$

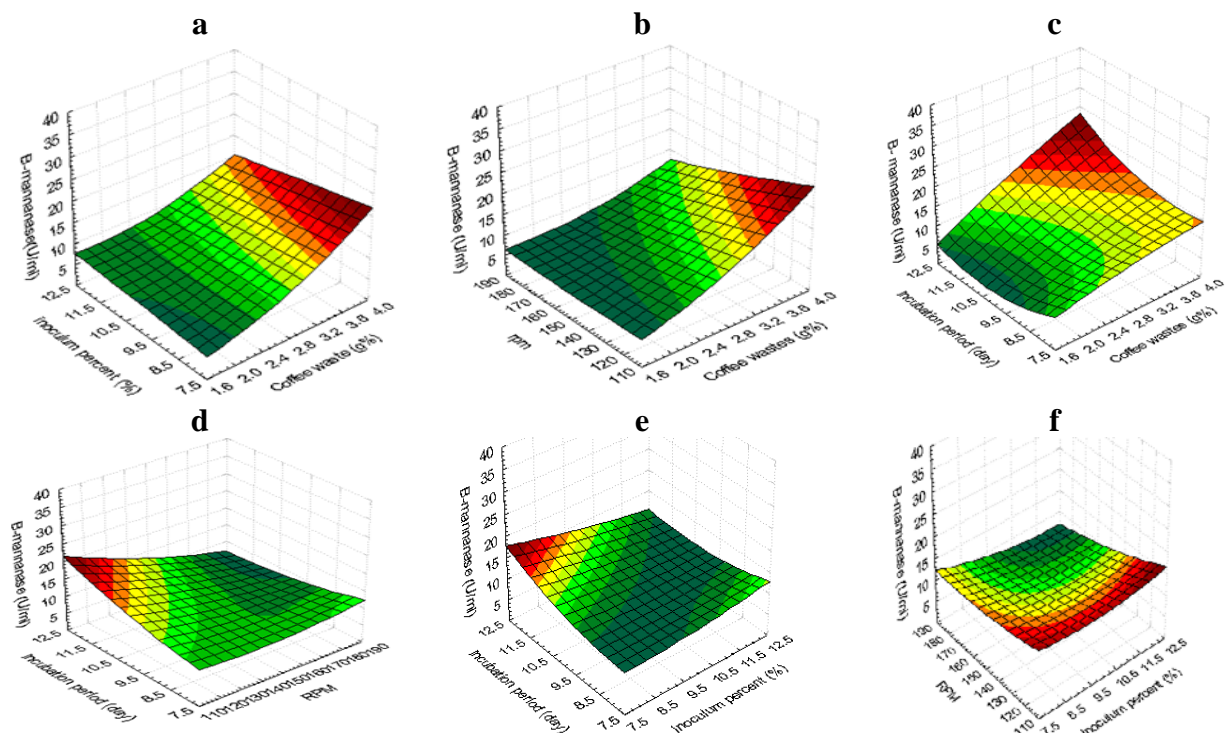
The results obtained by ANOVA analysis (Tables 4 and 5) show a significant *F*-value (11.106) which indicates the significance of the model. Model terms having values of prob > *F* (0.002) being less than 0.05 are considered significant. The determination of coefficient ( $R^2$ ) was calculated as 0.946 for  $\beta$ -mannanase (value of  $R^2 > 0.75$  indicates the aptness of the model) which shows that the statistical model explains 94.6 % of the variability in the response. The efficient of the model can be checked by the determination of  $R^2$ ; the closer  $R^2$  is to 1; the more suitable the model will be, and the better the predicted response will become. The value of *R* (0.973) being close to 1 indicates a close agreement between the experimental results and the theoretical value predicated by the model equation.

The highest value of  $\beta$ -mannanase (35.2 IU/mL), which is higher than the predicated value (32.66), was produced with a 3.8 % coffee residue, and inoculum size of 8 % at 120 rpm for twelve days. The results indicated that the statistical optimization increased the biosynthesis of  $\beta$ -mannanase about 3.4 fold of that of the basal medium (10.3 IU/mL). The influence on the yield of  $\beta$ -mannanase imposed by the factors and reciprocity between them is represented in Figure 2 A-F. It was reported by many researchers that the statistical optimization model for the fermentation process could overcome the limitations of classic empirical methods. Moreover, it was proved to be more significant for the optimization production of  $\beta$ -mannanase (Mohamad *et al.*, 2011; Rashid *et al.*, 2011; Ahirwar *et al.*, 2016; Janveja *et al.*, 2016; Soni *et al.*, 2017).



**Table 3.** Fractional factorial design (FFD) and response of  $\beta$ -mannanase activity from *Penicillium humicola*.

Trials	Independent variable				Observed response				
	X <sub>1</sub>	X <sub>2</sub>	X <sub>3</sub>	X <sub>4</sub>	Final pH	Dry wt (g/flask)	Protein (mg/mL)	$\beta$ -mannanase (IU/mL)	
	Coffee residue (g/l)	Inoculum (%)	rpm Cycle	Incubation period (Days)				Observed	Predicted
1	(+1)3.8	(+1)12	(-1)120	(-1)8	5.85	2.15	7.52	19.47	14.18
2	(+1)3.8	(+1)12	(+1)180	(-1)8	5.59	1.2	8.54	10.43	11.4
3	(-1)1.8	(+1)12	(-1)120	(-1)8	6.2	1.07	6.1	8.43	6.4
4	(0)2.8	(0)10	(0)150	(0)10	6.9	1.86	7.38	10.3	13.65
5	(-1)1.8	(+1)12	(+1)180	(-1)8	6.26	1.02	6.39	7.92	7.23
6	(+1)3.8	(+1)12	(+1)180	(+1)12	5.46	2.24	11.49	14.14	14.6
7	(-1)1.8	(-1)8	(+1)180	(+1)12	6.33	1.22	6.78	6.04	4.96
8	(+1)3.8	(-1)8	(+1)180	(-1)8	5.56	1.71	7.32	15.19	4.18
9	(+1)3.8	(-1)8	(-1)120	(-1)8	5.72	1.52	8.1	17.47	14.74
10	(-1)1.8	(+1)12	(+1)180	(+1)12	6.31	1.69	6.32	7.68	7.68
11	(-1)1.8	(-1)8	(-1)120	(-1)8	6.25	1.06	6.09	6.44	7.44
12	(-1)1.8	(-1)8	(-1)120	(+1)12	6.37	1.13	6.63	6.44	6.68
13	(+1)3.8	(-1)8	(+1)180	(+1)12	5.4	1.75	12.08	16.55	7.55
14	(0)2.8	(0)10	(0)150	(0)10	6.9	1.86	7.38	10.3	13.65
15	(+1)3.8	(-1)8	(-1)120	(+1)12	5.52	2.05	12.6	35.2	32.66
16	(-1)1.8	(-1)8	(+1)180	(-1)8	6.13	1.92	6.42	7.42	4.69
17	(-1)1.8	(+1)12	(-1)120	(+1)12	6.3	1.14	6.6	7.22	7.01
18	(0)2.8	(0)10	(0)150	(0)10	6.9	1.86	7.38	10.3	13.65
19	(+1)3.8	(+1)12	(-1)120	(+1)12	5.63	2.01	9.63	23.2	21.11

**Figure 2A-F.** Effect of culture conditions and medium composition on  $\beta$ -mannanase (IU/mL) Produced from *Penicillium humicola*.

**Table 4.** Analysis of Fractional factorial design for  $\beta$ -mannanase activity from *P. humicola*.

Term	Regression coefficient	Standard error	t- test	P-value
Intercept	-3.405	19.809	- 0.172	0.868
$X_1$	6.432	14.520	0.443	0.671
$X_1^2$	0.932	2.185	0.426	0.683
$X_2^2$	0.116	0.135	0.860	0.418
$X_3^2$	0.012	0.001	0.459	0.660
$X_4^2$	0.099	0.135	0.735	0.486
$X_1X_2$	-0.352	0.353	-0.998	0.352
$X_1X_3$	-0.104	0.024	-4.410	0.003
$X_1X_4$	1.256	0.353	3.562	0.009
$X_2X_3$	0.015	0.012	1.309	0.232
$X_2X_4$	-0.370	0.176	-2.097	0.074
$X_3X_4$	-0.005	0.012	-0.412	0.693

**Table 5.** ANOVA's Analysis of Fractional Factorial design for *P. humicola*  $\beta$ -mannanase activity.

ANOVAs					
	Df	SS	SM	F test	P
Regression	11	971.907	88.355	11.106	0.002
Residual	7	55.687	7.9551		
Total	18	91027.594			

df Degree of freedom; SS Sum of squares; MS Mean sum of squares; F Fishers's function; P corresponding level of significance,  $R^2 = 0.946$ . The value of adjusted  $R^2$  was 0.861.

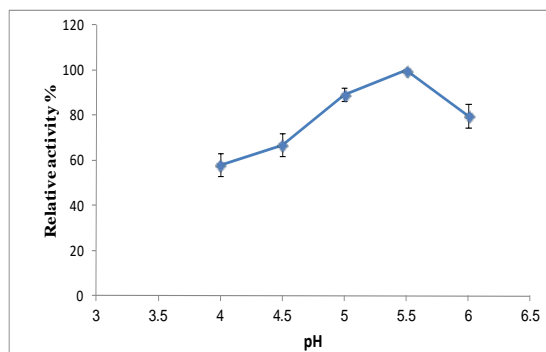
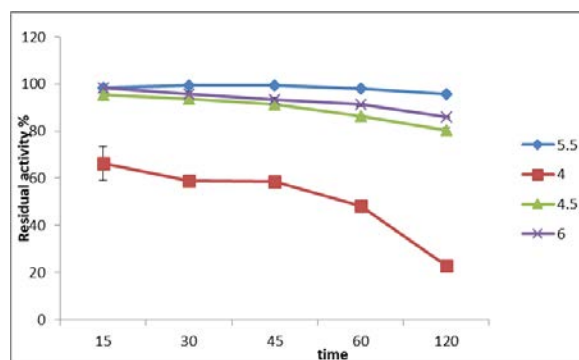
### 3.2. Partial Purification of *P. humicola* $\beta$ -mannanase

Of all the fractions obtained by the three precipitants, the fraction obtained with ammonium sulphate (60-70 % w/v) displayed the highest specific  $\beta$ -mannanase activity (27.83 IU/mg protein) which represented 60.7 % of the recovered activity. The results of the present study agree with those obtained by Mudau and Setati, (2008) who found that  $\beta$ -mannanase from *Scopulariopsis candida* was partially-purified by ammonium sulfate.

### 3.3. Biochemical Characterization of Partially-purified *P. humicola* $\beta$ -mannanase

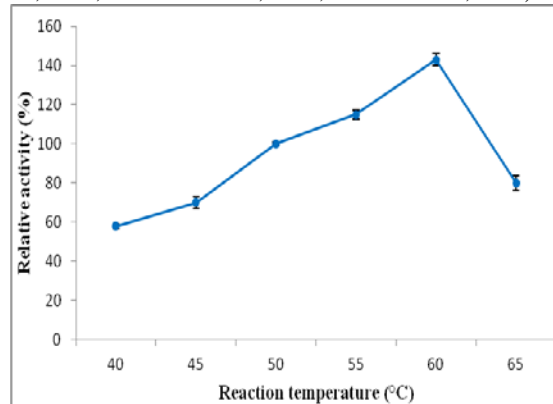
#### 3.3.1. pH Optima and Stability

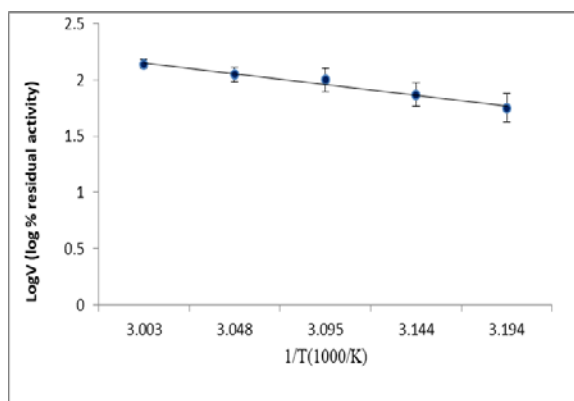
The results in Figure 3 indicate that the optimum pH of the partially-purified *P. humicola*  $\beta$ -mannanase was 5.5 similar to that of the crude enzyme in an earlier work by the same authors (El-Refai *et al.*, 2014). It was noted by some researchers that the fungal  $\beta$ -mannanase was active at acidic pH (Ahrwar *et al.*, 2016; De Marco *et al.*, 2015; Abdel-Fattah *et al.*, 2009; Blibech *et al.*, 2010). The pH stability of the tested enzyme is represented in Figure 4. It indicates that the enzyme was almost stable for two hours at pH 6. Moreover, the enzyme had a great stability at the pH range of 4.5 to 5.5, and lost only 20 % of its activity after a two-hour incubation in buffer within this pH range. The tested enzyme had a half-life-time of fifty minutes at pH 4. Abdel-Fattah *et al.*, 2009 showed that the high pH stability was at pH ranging between 4 and 6 for two hours.

**Figure 3.** Effect of the pH value of the reaction mixture on the activity of the partial pure *P. humicola*  $\beta$ -mannanase. Reaction was carried out at 50°C with 1% (w/v) locust bean gum.**Figure 4.** pH stability of partially pure *P. humicola*  $\beta$ -mannanase. The enzyme solution was incubated at different pHs for different periods of times, and the residual activity was determined under the optimum conditions.

#### 3.3.2. Effects of temperature on the Enzyme Activity

Figure 5-A represents temperature dependence of the activity of the partially-purified *P. humicola*  $\beta$ -mannanase at temperatures ranging from 40 to 65°C at pH 5.5. The results indicate that the optimum temperature for  $\beta$ -mannanase is 60°C. From a biotechnological point of view, high temperature is preferred to improve conversion rates, decrease microbial contamination, and allow greater solubility of the substrate. In this study, the optimum temperature of *P. humicola*  $\beta$ -mannanase is within the range recorded for other fungal  $\beta$ -mannanase (Howard *et al.*, 2003; De Marco *et al.*, 2015; Ahrwar *et al.*, 2016).

**Figure 5 A.** Effect of temperature of the reaction on the activity of the partial pure *P. humicola*  $\beta$ -mannanase. Reactions were carried out at pH 5.5 with 1% (w/v) locust bean gum at different temperatures.



**Figure 5 B.:** Arrhenius plots to calculate activation energy ( $E_a$ ) for partially pure *P. humicola*  $\beta$ -mannanase.

### 3.3.3. Thermal Stability and Thermodynamic Parameters

The Arrhenius equation has an important application in the calculation of the energy of activation and for the determination of the rate of chemical reactions. When a reaction has a rate constant which obeys Arrhenius' equation, a plot of  $\ln(k)$  versus  $T^{-1}(\text{K})$  gives a straight line, whose gradient and intercept can be used to determine the energy of activation ( $E_a$ ).

The apparent activation energy ( $E_a$ ) of catalysis for the partially-purified  $\beta$ -mannanase was calculated using Arrhenius plot (Figure 5 B). The regression equation for Arrhenius plots of  $\beta$ -mannanase was:  $y = -2.010 + 8.1893$ .

$E_a$  of the *Penicillium humicola*  $\beta$ -mannanase was calculated to be 16.71114 kJmol<sup>-1</sup> which is less than the  $E_a$  recorded by Regmi *et al.* (2016) for the *Bacillus* sp.CSB39  $\beta$ -mannanase (26.85 kJmol<sup>-1</sup>). The lower value of  $E_a$  indicates that the conformation of the active site for the enzyme substrate complex requires less energy. These criteria make *P. humicola*  $\beta$ -mannanase more suitable for industrial applications; hence it needs a low value of activation energy which will be reflected on the total cost of industrial processing.

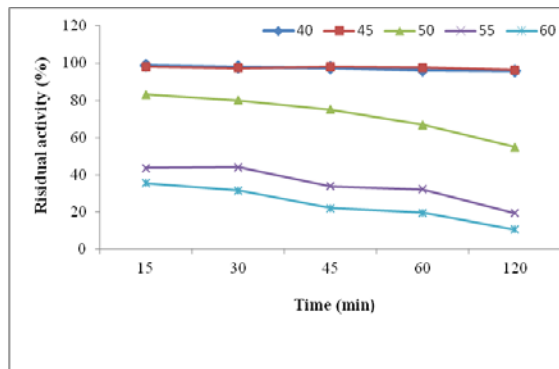
Thermostability of the enzymes increases their economic values, and provides potential benefits to different industrial processes; hence they are gaining more biotechnological attention. The results represented in Figure 6-A show that the enzyme retained 96 % of its activity when sustained in 45°C for 120 minutes and retained 66.8 % of its activity when incubated at 50°C for sixty minutes, but lost about 80 % of its activity when incubated at 60°C for sixty minutes. Blichech *et al.*, (2010, 2011) found that *P. occitanis*  $\beta$ -mannanase retained 80 % of its original activity for thirty minutes when incubated at 50°C.

Temperature enhances the rate of catalytic reaction of the enzyme, and it also affects its stability and may even lead to a complete deactivation. The thermodynamic data interpret the relation between the thermo parameter and the catalytic and other physical parameters of the enzyme. The thermostability parameters of the enzyme are summarized in Table 6. The rate of the heat of inactivation of *P. humicola*  $\beta$ -mannanase was investigated in the temperature range between 40°C and 60°C. The plots of log % residual activity versus time were linear, indicating the first-order kinetics of the enzyme (Figure 6-B). The half-lives and D-values of  $\beta$ -mannanase prolonged stability remarkably at temperatures between 40 and 45 °C. The half-life time

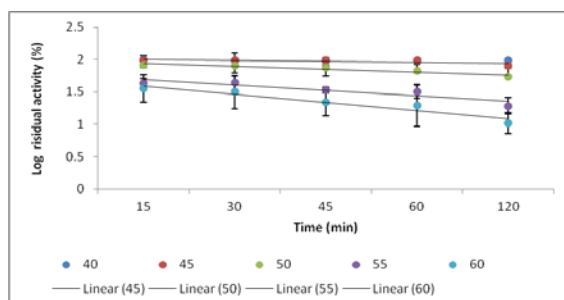
( $T_{1/2}$ ) and the calculated  $D$  value of the  $\beta$ -mannanase were found to be 6931.4–135.9 min and 23025.85–451.48 min respectively at the temperature range between 40 and 60°C. The higher values of  $T_{1/2}$  and  $D$  were very important in industrial applications. The denaturation energy ( $E_d$ ) was determined by applying the Arrhenius plot (Figure 6-C). The  $E_d$  for the partially-purified enzyme was 109.277 kJmol<sup>-1</sup>, which means that the energy required for denaturing the tested enzyme was high (Arrhenius *et al.*, 1889). The catalytic efficiency of the tested enzyme under different conditions was evaluated by the investigation of the thermodynamic parameters as:  $\Delta H^\circ$ ,  $\Delta G^\circ$ , and  $\Delta S^\circ$ . The enthalpy change ( $\Delta H^\circ$ ) of the partial-purified mannanase was 69.5669–68.18 kJ mol<sup>-1</sup> (at the tested temperature range of 40°C –60°C) which is higher than that reported for  $\beta$ -mannanase by Regmi *et al.* (2016) (24 kJ mol<sup>-1</sup>) and Panwar *et al.*, (2017) (29.9– 48.9 kJ mol<sup>-1</sup>), but is lower than that reported by Srivastava *et al.* (2016) (86.7 kJ mol<sup>-1</sup>). The observed change in  $\Delta H^\circ$  indicates that  $\beta$ -mannanase exhibits considerable conformational change at higher temperatures (Ortega *et al.*, 2009). The Gibbs free energy ( $\Delta G^\circ$ ) is related to the enzyme stability and reveals the thermal unfolding of the enzyme structure, and apparently increases with the increase of temperature.  $\Delta G^\circ$  of  $\beta$ -mannanase was slightly decreasing (111.41 kJ mol<sup>-1</sup>– 107.8 kJ mol<sup>-1</sup>) with the increase of the temperature (40– 60°C) which means that the enzyme was stable over the tested temperatures. The changes in entropy ( $\Delta S^\circ$ ) measure the extent of the disorder (Blichech *et al.*, 2011). So it represents the variation between the disorder in the ground and the transition state.  $\beta$ -mannanase had a negative entropy (–133.67 J mol<sup>-1</sup>k<sup>-1</sup> to –118.996 J mol<sup>-1</sup>k<sup>-1</sup>) which indicates that the entropy decreases upon forming the transition state (Regmi *et al.*, 2016) (Table 6). In general, the higher values of  $\Delta G^\circ$ ,  $\Delta H^\circ$  and  $\Delta S^\circ$  reflect the higher thermostability of the tested enzyme. The  $z$ -value of  $\beta$ -mannanase, which represents the increase in the temperature necessary to reduce  $D$  –value by one logarithmic cycle, was 12.33°C (Figure 6-D).

**Table 6.** Kinetic and thermodynamic parameters for thermal inactivation of purified *Penicillium humicola*  $\beta$ -mannanase.

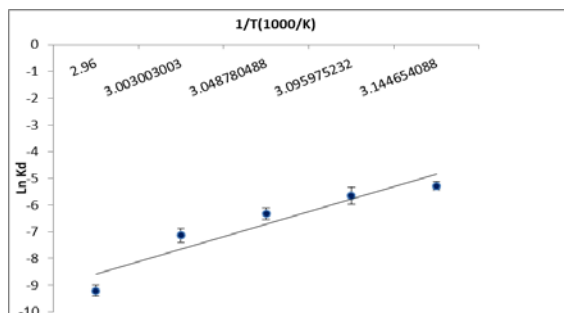
		Temperatures				
Parameters		40°C	45°C	50°C	55°C	60°C
Deactivation rate constant	$K_d \cdot 10^3$	0.1	0.8	1.8	3.5	5.1
Half-life time (min)	$T_{1/2}$	6931.472	866.434	385.0818	198.0421	135.9112
Decimal reduction time (min)	$D$ Value	23025.85	2878.231	1279.214	657.8815	451.4873
The change in enthalpy	$\Delta H^\circ$	69.5669	69.22128	68.87567	68.53006	68.18444
Free energy	$\Delta G^\circ$	111.4055	107.7293	107.2874	107.1767	107.8101
Entropy	$\Delta S^\circ$	-133.67	-121.095	-118.92	-117.825	-118.996



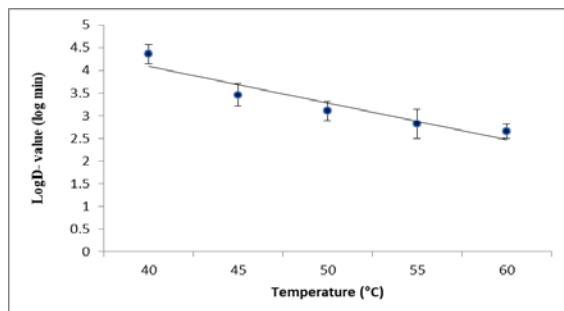
**Figure 6 A.** Thermal stability of partially pure *P. humicola*  $\beta$ -mannanase. The enzyme solution was held at different temperatures for different periods of times, and the residual activity was determined under the optimum conditions.



**Figure 6 B.** Effect of different temperatures on the rate of denaturation of the partially pure *P. humicola*  $\beta$ -mannanase.



**Figure 6 C.** Arrhenius plot to calculate deactivation energy ( $E_d$ ) for denaturation of the partially pure *P. humicola*  $\beta$ -mannanase.



**Figure 6 D.** Temperature dependence of the decimal reduction of partial purified  $\beta$ -mannanase to calculate z-values.

#### 4. Conclusion

This research evaluates the application of the statistical optimization strategy based on Plackett- Burman and Fractional Factorial designs to maximize the production of *P. humicola*  $\beta$ -mannanase using coffee waste. The current

study improved the enzyme production by 3.4 fold. *P. humicola*  $\beta$ -mannanase was fractionally purified with ammonium sulfate. The fraction obtained at 60 –70 % ammonium sulphate saturation displayed the highest specific activity of  $\beta$ -mannanase (27.83 IU/mg protein) and was stable at pH ranging from 4.5 to 6 for more than two hours. The partially- purified enzyme has optimal activity at pH 5.5 and 60°C. The thermodynamic study proved that this enzyme has future prospects for bioremediation in many industrial applications.

#### References

- Abdel-Fattah AAF, Hashem AM, Ismail AMS and Refai EMA. 2009. Purification and some properties of  $\beta$ -mannanase from *Aspergillus oryzae* NRRL 3448. *J App Sci Res.*, **5**(12): 2067-2073.
- Ahirwar S, Soni H, Rawat HK, Prajapati BP and Kango N. 2016. Experimental design of response surface methodology used for utilisation of palm kernel cake as solid substrate for optimised production of fungal mannanase. *Mycol.*, **7**(3): 143-153.
- Arrhenius S. 1889. Über die reaktionsgeschwindigkeit bei der inversion von rohrzucker durch sauren. *Zeitschrift für Physikalische Chemie.*, **4**: 226–248.
- Blibech M, Ghorbel RE, Fakhfakh I, Ntarima P, Piens K, Bacha AB and Chaabouni SE. 2010. Purification and characterization of a low molecular weight of  $\beta$ -mannanases from *Penicillium occitanis* Pol6. *App Biochem Biotechnol.*, **160**: 1227–1240.
- Blibech M, Ghorbel RE, Chaari F, Dammak I, Bhiri F, Neifar M, and Chaabouni SE. 2011. Improved mannanase production from *Penicillium occitanis* by fed-batch fermentation using Acacia seeds. *ISRN Microbiol.* **2011**:1-5
- Chauhan PS, Puri N, Sharma P and Gupta N. 2012. Mannanases: microbial sources, production, properties and potential biotechnological applications. *Appl Microbiol Biotechnol.*, **93**(5): 1817-1830.
- Chiyanzu I, Brienzo M, García-Aparicio MP and Görgens JF. 2014. Application of endo- $\beta$ -1,4-D-mannanase and cellulase for the release of mannoooligosaccharides from steam-pretreated spent coffee ground. *Appl Biochem Biotechnol.*, **172**(7):3538-3557.
- De Marco JDCI, Neto GPDS, Castro CFDS, Michelin M, and Polizeli MDL. 2015. Partial purification and characterization of a thermostable  $\beta$ -mannanase from *Aspergillus foetidus*. *Appl Sci.*, **5**(4): 881-893.
- El-Naggar MY, Youssef SA, El-Assar SA, Beltagy EA. 2006. Optimization of cultural conditions for  $\beta$ -mannanase production by a local *Aspergillus niger* isolate. *Inter J Agric Biol.*, **8**(4):539-545.
- El-Refai MA, Khattabk OH, Ismail SA, Hashem AM, Abo-Elnasr AA, and Nour SA. 2014. Improved mannanase production from *Penicillium humicola* and application for hydrolysis property. *Egyptian Pharm J.*, **13**:160–167.
- Farid MA, Ghoneimy GA, El-Khawaga MA, Negm-Eldein A and Awad GEA. 2013. Statistical optimization of glucose oxidase production from *Aspergillus niger* NRC9 under submerged fermentation using response surface methodology. *Ann Microbiol.*, **63**: 523-531.
- Germec M, Yatmaz E, Karahalil E and Turhan I. 2017. Effect of different fermentation strategies on  $\beta$ -mannanase production in fed-batch bioreactor system. *Biotech.*, **1**:7(1):77.
- Hashem AM, Ismail AMS, El-Refai MA and Abdel-Fattah AF. 2001. Production and properties of  $\beta$ -Mannanase by free and immobilized cells of *Aspergillus oryzae* NRRL 3488. *Cytobios.*, **105**: 115-130.

- Howard RL, Abotsi E, van Rensburg JEL and Howard S. 2003. Lignocellulose biotechnology: issue of bioconversion and enzyme production. *Afri J Biotechnol.*, **2**: 602-619.
- Janveja C, Rana SSA and Soni SK. 2016. Statistical optimization of media components for the enhanced B-xylanase and B-mannanase production from *Aspergillus niger* C-5 via solid state fermentation of wheat bran. *Int J Pharm Bio Sci.*, **7(1)**: 89-102.
- keawsompong S. 2016.** Mannanase. Microbial Enzymes in Bioconversions of Biomass. **Department of Biotechnology, Faculty of Agro-Industry, Kasetsart University, Bangkok, Thailand, pp.215-229.**
- Kurakake M. and Komaki T. 2001. Production of b-Mannanase and b-Mannosidase from *Aspergillus awamori* K4 and Their Properties. *Current Microbiol.*, **42**: 377-380.
- Kwon EE, Yi H and Jeon Y. J. 2013. Sequential co-production of biodiesel and bioethanol with spent coffee grounds. *Bioresour Technol.*, **136**: 475-480.
- Lowry OH, Rosebrough NH, Farr A L and Randall R. 1951. Protein measurement with the Folin phenol reagent. *J Biol Chem.*, **193**: 265-275.
- Mohamad SN, Ramanan RN, Mohamad R and Ariff AB. 2011. Improved mannan degrading enzymes production by *Aspergillus niger* through medium optimization. *New Biotechnol.*, **28**: 146-152.
- Mudau MM, Setati M.E. 2008. Partial purification and characterization of endo- $\beta$ -1,4 mannanases from *Scopulariopsis candida* strains isolated from solar salterns. *Afri J Biotechnol.*, **7(13)**: 2279-2285.
- Murthy PS and Naidu MM. 2012. Sustainable management of coffee industry by-products and value addition- A review. *Resour Conserv Recycle*, **66**: 45-58.
- Mussatto SI, Machado EM, Martins S, and Teixeira JA. 2011. Production, composition, and application of coffee and its industrial residues. *Food and Bioprocess Technology.*, **4(5)**: 661-672.
- Obruca S, Benesova P, Kucera D, Petrik S and Marova I. 2015. Biotechnological conversion of spent coffee grounds into polyhydroxyalkanoates and carotenoids. *N Biotechnol.*, **32(6)**: 569-574.
- Ortega N, Perez-Mateos M, Pilar MC, Busto MD. 2009. Neutrase immobilization on alginate-glutataldehyde beads by covalent attachment. *J Agric Food Chem.*, **57**: 109-115.
- Panwar D, Kaira GS and Kapoor M. 2017. Cross-linked enzyme aggregates (CLEAs) and magnetic nanocomposite grafted CLEAs of GH26 endo- $\beta$ -1, 4-mannanase: Improved activity, stability and reusability. *Inter J Biol Macromol.*, **105**: 1289-1299.
- Plackett Rland Burman JP. 1946. The design of optimum multifactorial experiments. *Biometrika.*, **37**: 305-325.
- Rashid JIA, Samat N and Yusoff WMW. 2011. Optimization of temperature, moisture content and inoculum size in solid state fermentation to enhance mannanase production by *Aspergillus terreus* SUK-1 using RSM. *Pak J Bio Sci.*, **14**: 533-539.
- Regalado C, García-Almendárez BE, Venegas-Barrera LM, Téllez-Jurado A, Rodríguez-Serrano G, Huerta-Ochoa S and Whitaker JR. 2000. Production, partial purification and properties of  $\beta$ -mannanases obtained by solid substrate fermentation of spent soluble coffee wastes and copra paste using *Aspergillus oryzae* and *Aspergillus niger*. *J Sci Food Agri.*, **80(9)**: 1343-1350.
- Regmi S, Pradeep GC, Choi YH, Choi YS, Choi JE, Cho SS, Yoo JC. 2016. A Multi-tolerant low molecular weight mannanase from *Bacillus* sp. CSB39 and its compatibility as an industrial biocatalyst. *Enzyme Microb Technol.*, **92**: 76-85.
- Rosa SM, Abel Soria M, Vélez CG and Galvagno MA. 2010. Improvement of a two-stage fermentation process for docosahexaenoic acid production by *Aurantiochytrium limacinum* SR21 applying statistical experimental designs and data analysis. *Bioresour Technol.*, **101**: 2367-2374.
- Smogi M. 1952. Notes on sugar determination. *J Biol Chem.*, **195**: 19-23.
- Soni H, Rawat HK, Pletschke BI and Kango N. 2016. Purification and characterization of  $\beta$ -mannanase from *Aspergillus terreus* and its applicability in depolymerization of mannans and saccharification of lignocellulosic biomass. *Biotech.*, **6(2)**: 136.
- Soni H, Rawat HK, Ahirwar S. and Kango N. 2017. Screening, statistical optimized production, and application of  $\beta$ -mannanase from some newly isolated fungi. *Engin Life Sci.*, **17(4)**: 392-401.
- Srivastava PK. and Kapoor M. 2016. Metal-dependent thermal stability of recombinant endo-mannanase (ManB-1601) belonging to family GH 26 from *Bacillus* sp. CFR1601. *Enzyme Microbial Technol.*, **84**: 41-49.





# Biological Control of *Macrophomina phaseolina* in *Vigna mungo* L. by Endophytic *Klebsiella pneumoniae* HR1

Sampad Dey, Prajesh Dutta and Sukanta Majumdar\*

Microbiology and Microbial Biotechnology Laboratory, Department of Botany, University of Gour Banga, Malda, West Bengal-732 103, India

Received July 18, 2018; Revised August 14, 2018; Accepted August 30, 2018

## Abstract

An endophytic isolate HR1 from the root nodules of *Vigna mungo* L. was isolated and identified as *Klebsiella pneumoniae* by 16S rDNA sequencing. The isolate can solubilize phosphate, zinc and produce siderophore, IAA, and HCN. Moreover, the isolate can tolerate heavy metal cadmium and produce hydrolytic enzymes protease, amylase and chitinase. *K. pneumoniae* inhibited the growth of *Macrophomina phaseolina* strongly in a paired culture study. The greenhouse study revealed that HR1 significantly increased the germination percentage, shoot and root length, shoot and root dry weight in the treated plants compared to the healthy control and the *M. phaseolina* infected plant. *K. pneumoniae* reduced the occurrence of *M. phaseolina* which induced the root rot disease in *Vigna*. The lowest percentage of disease incidence (18.2 %) was observed when *K. pneumoniae* was applied in dual-mode (seed bacterization + soil drench application) in the *M. phaseolina*-infested soil. Activities of defense-related enzymes such as, chitinase, phenylalanine ammonia lyase, peroxidase and  $\beta$ -1, 3-glucanase increased significantly following the application of *K. pneumoniae*, and challenged inoculation with *M. phaseolina*. Results clearly indicate that the isolate may be used as biocontrol agent to induce systemic resistance to *M. phaseolina*.

**Keywords:** Endophytic, *Klebsiella pneumoniae*, Root rot, *Macrophomina phaseolina*, Induced systemic resistance

## 1. Introduction

*Vigna mungo* (L.) (Black gram), is an important pulse crop occupying a unique position in Indian agriculture and is a major source of protein (24 %) for humans as well as animals (Satyanandam *et al.*, 2013). Most often, for its nutritional values it has been recommended for diabetes. However, the plant is severely affected by charcoal rot, a devastating root rot disease distributed over arid to tropical regions (Cottingham, 1981; Abawi and Pastor-Corrales, 1990). The pathogenic fungus, *Macrophomina phaseolina* (Tassi) Goid (Dothideomycetes, Botryosphaerales) is responsible for this devastating root rot disease leading to seedling blight in the initial stage, and brown lesions on roots and stems are found later in the mature stages of the plant (Iqbal *et al.*, 2010b). *M. phaseolina* is a soil and seed-borne fungal pathogen, which produces cushion-like black microsclerotia (Wheeler, 1975). Thus, the management of the root rot disease is essential to meet the enhanced requirements of the crop productivity by an actively growing population. To cope with this problem, farmers generally use chemical fungicides mostly non-judicially. Moreover, the prolonged use of chemical fungicides is environmentally not suited because they could generate resistant pathogen (McMullen and Bergstrom, 1999). So, an alternative method needs to be developed for a sustainable and eco-friendly cultivation of black gram.

In this milieu, plant-associated bacteria can play an important role in the biological control of many plant diseases. Recently, lot of attention has been given to the use of these organisms as biocontrol agents as well as plant-growth promoters to reduce the detrimental effects resulting from using chemical fungicides. Bacterial endophytes can be suitable biocontrol agents as they colonize the same ecological niche, which is inhabited by phytopathogens (Berg *et al.*, 2005). After the colonization in inter tissues, these microorganisms produce some important biochemical compounds, and can alter the plant cell metabolism to enhance host resistance to diseases (Krishnamurthy and Gnanamanickam, 1997; Bloembergen and Lugtenberg, 2001; Lugtenberg and Kamilova, 2009). Several endophytic bacteria such as *Pseudomonas*, *Bacillus*, and *Paenibacillus* have been reported for their antagonism against *M. phaseolina* (Atef, 2000; Senthilkumar *et al.*, 2009).

Endophytic *Klebsiella* spp. was reported earlier by authors to possess plant growth- promoting activities (Sharma *et al.*, 2014; Yamina *et al.*, 2014). Reports on heavy-metal resistant strains of *K. pneumoniae*, *Pseudomonas aeruginosa* and *Pantoea agglomerans* were mentioned earlier by researchers (Nath *et al.*, 2012; Yamina *et al.*, 2014; Bhagat *et al.*, 2016). There have been several reports which emphasized the antagonistic activity of *Klebsiella* sp. and *Pseudomonas* sp. against some pathogenic fungi including *M. phaseolina* (Das *et al.*, 2015; Kumar *et al.*, 2007).

\* Corresponding author e-mail: smajumdarwbbs@gmail.com.



The current study is conducted to investigate the effectiveness of the endophytic bacteria *Klebsiella pneumoniae* HR1 (Gamma proteobacteria, Enterobacteriales) in controlling *M. phaseolina* root rot disease in *Vigna*, and to determine the role of the isolate in the induction of plant defence-enzymes in response to the *M. phaseolina* infection.

## 2. Material and Methods

### 2.1. Isolation of Endophytic Strain from Root nodule of *V. mungo* L.

Healthy root nodules of *V. mungo* were collected from different agricultural fields of three districts in North Bengal -Malda, Uttar Dinajpur and Dakshin Dinajpur. The samples were washed with sterile distilled water, and were then surface sterilized using 95 % ethanol for one minute, followed by 0.1 % mercuric chloride (HgCl<sub>2</sub>) for three minutes. They were finally rinsed six times with sterile distilled water. Then, 1g of nodules was crushed in 5 mL of sterile water resulting in a milky suspension, which was serially diluted up to 10<sup>-6</sup> dilution. 0.1 mL of each dilution was spread on sterile yeast extract mannitol agar (YEMA) plates containing 0.1 % Congo red. The plates were incubated for forty-eight hours at 28 ± 1°C. The colonies were picked and maintained in YEMA slant at 4°C for further study.

### 2.2. Characterization and Identification of the Bacterial Strain

The isolates were characterized morphologically on the basis of the colony colour, shape, appearance, diameter, transparency, and gram staining. For the biochemical characterization, oxidase test, production of acid and gas from carbohydrate, citrate utilization, nitrate reduction, gelatin liquefaction, urease, methyl red and Voges Proskauer tests were performed by following the standard protocols (Cappuccino and Sherman, 1992).

For identification, genomic DNA was extracted from the twenty-four-hour-old culture following the method of Stafford *et al.*, (2005). DNA was precipitated from the aqueous phase with chilled ethanol (100 %) and was pelleted by centrifuging at 12000 rpm for fifteen minutes, followed by washing in 70 % ethanol and centrifugation. The pellet was, then, air- dried and suspended in TE buffer pH 8. For ITS-PCR amplification, DNA was amplified by mixing the template DNA (50 ng) with the polymerase reaction buffer, dNTP mix, primers and Taq polymerase. The polymerase chain reaction was performed in a total volume of 100 µL containing 78 µL of deionized water, 10 µL 10× Taq polymerase buffer, 1 µL of 1U Taq polymerase, 6 µL 2 mM dNTPs, 1.5 µL of 100 mM reverse and forward primers and 3.5 µL of 50 ng template DNA. The amplification of 16S rRNA gene was carried out by PCR using the forward (27f 5' GAGTTTGATCACTGGCTCAG 3') and reverse (1492r 5' TACGGCTACCTTGTTACGACTT 3') primers (Byers *et al.*, 1998). The PCR was programmed with an initial denaturing at 94 °C for five minutes, followed by thirty cycles of denaturation at 94 °C for thirty seconds, annealing at 61°C for thirty seconds and an extension at 70°C for two minutes and with a final extension at 72°C for seven minutes in a Thermocycler (Applied Biosystems, 2720). The amplified products were resolved by

electrophoresis in 0.8 % agarose gel and PCR amplicons were purified. The purified DNA sequenced from Xcelris laboratory, Ahmadabad, India, and the 16S rDNA sequence obtained from PCR products were subjected to BLAST analyses. After complete annotation, the DNA sequences were deposited to NCBI GenBank through BankIt to get accession number. A phylogenetic analysis was conducted in MEGA - 4.0.2 software (Tamura *et al.*, 2007). The evolutionary history was inferred by Neighbor-Joining Method (Saitou and Nei, 1987).

### 2.3. In vitro Screening for Plant Growth Promoting Activity

#### 2.3.1. Phosphate Solubilization

The phosphate solubilization efficacy of the isolate was determined using both Pikovskaya's and National Botanical Research Institute's phosphate (NBRIP) medium (Pikovskaya, 1948; Nautiyal, 1999). The isolate was spot-inoculated at the center of the plate and was incubated for seven days at 28°C. The clear zone around the colony indicated phosphate solubilization activity.

#### 2.3.2. Zinc Solubilizing Activity

A modified Pikovskaya medium supplemented with zinc oxide (Glucose 10g, MgSO<sub>4</sub>·7H<sub>2</sub>O 0.1g, (NH<sub>4</sub>)<sub>2</sub>SO<sub>4</sub> 1g, KCl 0.2g, K<sub>2</sub>HPO<sub>4</sub> 2g, yeast extract 5g, ZnO 1g and Agar 20g in 1000 mL dH<sub>2</sub>O) was used for determining the zinc-solubilizing activity of the isolate. The plate was streaked and incubated for seven days at 30°C. The clear zone around the colony was considered as a positive result (Pikovskaya, 1948).

#### 2.3.3. Indole Acetic Acid (IAA) Production

IAA production was determined by inoculating the bacterial suspension (100 µL) in a YEM broth supplemented with tryptophan (0.01 %), and was incubated for three days. After centrifugation at 10000 rpm for twenty minutes, the supernatant was collected. A few drops of the orthophosphoric acid and 4 ml of the Salkowski reagent (1 mL of 0.5 M FeCl<sub>3</sub> solution in 50 mL of perchloric acid) were added to 2 mL of the supernatant and were kept in the dark for thirty minutes at room temperature. The appearance of the pink colour confirmed the IAA production (Brick *et al.*, 1991).

#### 2.3.4. Production of Ammonia

For ammonia production, a freshly-grown culture was inoculated in 10 mL peptone water and was incubated for forty-eight hours at 28 ± 2°C. Then, Nessler's reagent (0.5 mL) was added. The development of the brown to yellow colour represents positive results for ammonia production (Cappuccino and Sherman, 1992).

#### 2.3.5. Hydrogen Cyanide (HCN) production

The evaluation of hydrogen cyanide (HCN) production was done by inoculating the bacterial isolate on a YEMA medium amended with glycine. A Whatman No. 1 filter paper previously soaked in picric acid solution (0.05% solution in 2% sodium carbonate) was placed at the inner side of the Petri plate. Then the plate was sealed and incubated for forty-eight hours at 30°C. The change in colour of the filter paper from deep yellow to reddish brown was considered as an indication of the HCN production (Bakker and Schippers, 1987).

### 2.3.6. Siderophore Production

Siderophore production was detected on a Chrome-azurool S (CAS) medium following the method of Schwyn and Neilands, (1987). The isolate (24-hour-old culture) was spotted on a CAS medium, and all plates were incubated at  $28 \pm 1^\circ\text{C}$  for forty-eight hours. The formation of yellow or orange halos around the colonies was considered as the positive response to the production.

### 2.3.7. Heavy Metal Tolerance

Heavy-metal tolerance of the isolate was determined using cadmium (Cd) as a heavy metal source. The dilution plate method was used to determine the lowest concentration of Cd that absolutely prevented the growth of the bacterial strain. The YEM agar plate supplemented with 25, 50, 75 and 100  $\mu\text{g/mL}$   $\text{CdCl}_2$  was used. The inoculated plates were incubated for seven days at  $28^\circ\text{C}$ .

## 2.4. Production of Extracellular Hydrolytic Enzymes

### 2.4.1. Protease Production

The assay of protease production was performed on sterile skim milk agar plates. The isolate was spot-inoculated and incubated at  $30^\circ\text{C}$ . The zone of clearance around the colony indicated the production of protease (Chaiham *et al.*, 2008).

### 2.4.2. Amylase Production

For amylase production, the bacterial isolate was spot-inoculated on starch agar medium and was incubated for forty-eight hours at  $30^\circ\text{C}$ . After the incubation period, the plate was flooded with Lugol's iodine solution, and was kept for a minute. The colorless zone around the colonies indicated the production of amylase (Shaw *et al.*, 1995).

### 2.4.3. Cellulase Production

The production of cellulase was assessed by following the method of Rangel-Castro *et al.*, (2002) with some modifications. The isolate was inoculated on a modified YEMA medium supplemented with CMC (Carboxymethyl cellulose) instead of mannitol. The plate was incubated at  $30^\circ\text{C}$  for five days. After incubation, the media was flooded with an aqueous solution of Congo red (1% w/v), and the formation of a clear zone was considered as a positive response in the production of cellulase by the bacterial isolate.

### 2.4.4. Chitinase Production

Chitinase production efficacy of the isolate was determined by following the method of Roberts and Selitrennikoff, (1988) with some modifications. The chitinase-detection agar (CDA) plate was prepared by replacing mannitol with 1% colloidal chitin in modified YEMA, and the strain was spot-inoculated at the center of the plate. The plate was then incubated at  $28^\circ\text{C}$  for seven to ten days. The formation of a clear zone indicated the production of chitinase.

## 2.5. In-vitro Antagonistic Activity

The *in-vitro* antagonistic activity of the isolate was assessed by a dual culture method against the fungal pathogens: *M. phaseolina*, *Fusarium oxysporum* Smith & Swingle (Sordariomycetes, Hypocreales), *F. semitectum* Berk. and Ravenel (Sordariomycetes, Hypocreales), *Colletotrichum* sp, *Alternaria alternata* (Fr.) Keissl (Dothideomycetes, Pleosporales), and *Aspergillus* sp. in

modified PDA supplemented with 2 % sucrose instead of dextrose (Kumar *et al.*, 2012). The inoculated plates were incubated at  $28 \pm 1^\circ\text{C}$  for five days, and the inhibition of the colony growth was measured. The percentage of inhibition was calculated using the following formula –

$$PI = \left( \frac{C - T}{C} \right) \times 100$$

PI = Percentage of inhibition, T = Radial growth of the fungal colony opposite the bacterial colony, and C = radial growth of the pathogen in the control plate.

All the plant pathogenic cultures were obtained from the culture collection of Microbiology and Microbial Biotechnology laboratory at the University of Gour Banga, Malda.

## 2.6. Assessments of Strain HR1 as a Biocontrol Agent against Root Rot Disease of *V. mungo* under Greenhouse Conditions

The efficacy of the strain HR1 to control the root rot disease of *V. mungo*, caused by *M. phaseolina* was determined under greenhouse conditions. The seeds of *V. mungo* var. sarada were collected from the 'Pulse and Oil seeds Research Station' Rani Bagan, Behrampur, West Bengal, India. For seed bacterization, the isolate was grown in a YEM broth at  $30^\circ\text{C}$  and 140 rpm on a rotary shaker for three days. After centrifugation at 6000 rpm for fifteen minutes, the bacterial suspension was diluted to attain the concentration of  $10^8$  CFU/mL.

The surface-sterilized seeds were soaked in a bacterial suspension supplemented with 1 % CMC overnight, and were sown (6 seeds/bag) in black polythene bags containing 2 kg of sterilized soil. The bacterium was also applied as soil drench (100 mL/Kg soil, concentration of  $10^8$  CFU/mL) to the rhizosphere of potted plants after seven days of growth.

The mass inocula of *M. phaseolina* was prepared by inoculating mycelial block in a pre-sterilized 30g moist oat meal medium, and was incubated at  $30^\circ\text{C}$  for five days for soil infestation. The inoculum (0.1 % w/w) was mixed thoroughly in the double autoclaved soil.

Growth promotion of *Vigna* plants was measured in terms of increase in the percentage of seed germination, shoot and root length, shoot and root dry weight following the application of the bacterial isolate. The vigor index was calculated as described by Abdul-Baki and Anderson, (1973).

The root rot disease caused by *M. phaseolina* was assessed, after fifteen days of growth by measuring the percentage of disease incidence (PDI) as follows:

$$PDI = \left( \frac{\text{Number of diseased plants}}{\text{Total number of plants}} \right) \times 100$$

The sets of treatments were: I – sterilized soil and unbacterized seed (healthy control), II – *M. phaseolina* inoculated sterilized soil (diseased control), III – bacterized seeds of black gram with *K. pneumoniae* and challenge inoculation with *M. phaseolina* and IV – dual-mode of application (seed bacterization + soil drench) of *K. pneumoniae*, challenge inoculation with *M. phaseolina*. The plants were maintained in a normal daylight condition. Ten replicates were taken for each treatment, and the average of the ten replicate plants were analyzed.

## 2.7. Biochemical Analysis

Leaves of *V. mungo* were grown in treated or control soil used for all the biochemical analysis. The leaves were collected for assay after fifteen days of germination.

## 2.8. Enzyme Assay

### 2.8.1. Peroxidase (EC 1.11.1.7)

The extraction and assay of peroxidase (POX) were conducted by following the method of Chakraborty *et al.*, (1993). Activity was assayed at 465 nm by monitoring the oxidation of O-dianisidine in the presence of H<sub>2</sub>O<sub>2</sub>. Specific activity was expressed as the increase in ΔA 465/min/ g tissue.

### 2.8.2. Chitinase (EC 3.2.1.39)

The extraction of chitinase (CHT) and measurement of its activity were conducted by following the method described by Boller and Mauch, (1998) with modifications. 1g of the leaf samples was crushed in 5 mL of 0.1 M chilled sodium citrate buffer (pH 5.0). The homogenate was centrifuged at 12000 rpm for ten minutes at 4°C. The supernatant was used as the enzyme source.

In the assay mixture, colloidal chitin was used for the detection of chitinase activity, and the activity was determined by measuring the released N-acetyl glucosamine (Glc-Nac). The colloidal chitin was prepared according to the method of Roberts and Selitrennikoff, (1988). The activity was expressed as mg Glc-Nac released/ g tissue /hour.

### 2.8.3. Phenylalanine Ammonia Lyase (EC 4.3.1.5)

The enzyme phenylalanine ammonia lyase (PAL) was extracted, and its activity was measured by following the method of Chakraborty *et al.*, (1993). PAL activity was determined by measuring the production of cinnamic acid from L-phenylalanine spectrophotometrically at 290 nm. The enzyme activity was expressed as μg cinnamic acid/min/ g tissue.

### 2.8.4. β-1, 3-Glucanase (EC 3.2.1.39)

β-1, 3-glucanase (GLU) was extracted and assayed from the leaf samples following the method of Pan *et al.*, (1991). The reaction mixture consisted of 62.5 μL of the leaf enzyme extract and 62.5 μL of laminarin (4%). The mixture was incubated at 40°C for ten minutes and 375 μL of DNSA (dinitro salicylic acid) was added to the mixture following incubation for five minutes on a boiling water bath. Finally, the coloured solution was diluted with 4.5 mL of water, and the amount of glucose liberated was determined spectrophotometrically using a standard curve. The enzyme activity was expressed as μg glucose released/min/g tissue.

## 2.9. Statistical Analyses

The results were analysed statistically using one-way ANOVA, SPSS version 22 software. Duncan's Multiple Range Test (DMRT) was used for mean separation wherever appropriate.

## 3. Results

### 3.1. Characterization and Identification of HR1

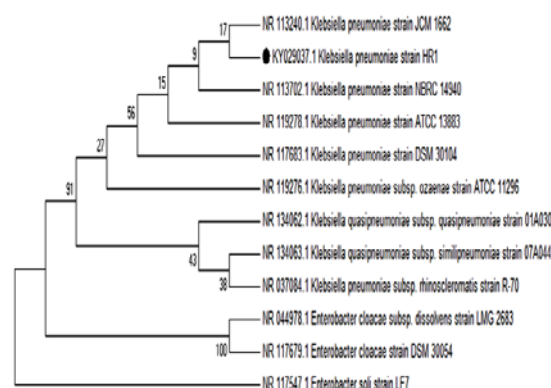
The morphological study revealed that the isolate HR1 is rod-shaped, gram-negative bacterium and showed positive response in the Voges- Proskauer test, acid-gas production test, nitrate reduction test, urease test, as well as the citrate-production test during the biochemical characterization (Table 1).

**Table 1.** *In vitro* Morphological and Biochemical characterization of the endophytic isolate HR1.

Morphological and Biochemical tests	Bacterial Isolate HR1
Gram stain	-
Shape	Rod
Indole Production	-
Oxidase	-
Citrate	+
Gelatin Hydrolysis	-
Urease	+
Methyl red	-
Voges Proskauer	+
Acid- gas production	+
Nitrate	+

'+' = Activity Present; '-' = Activity Absent.

A continuous stretch of the 1420 16S rRNA gene sequence was obtained from the isolate HR1. The BLAST query of the sequence against GenBank database confirmed the identity of the isolate as *K. pneumoniae* with 99 % similarity with the sequences of other isolates of the same genus deposited in NCBI database. This was confirmed with the phylogenetic analysis, in which the HR1 isolate clustered with other *K. pneumoniae* isolates (Figure 1). The sequence has been deposited in NCBI, GenBank database under the accession No. KY029037.



**Figure 1.** The phylogenetic relationships of the strain *K. pneumoniae* HR1 based on 16S rRNA gene analysis. Evolutionary distances were calculated using the Neighbor – joining method. The level of bootstrap support (1,000 repetitions) is indicated at all nodes

### 3.2. Evaluation of PGP Activities and Excretion of Extracellular Hydrolytic Enzymes

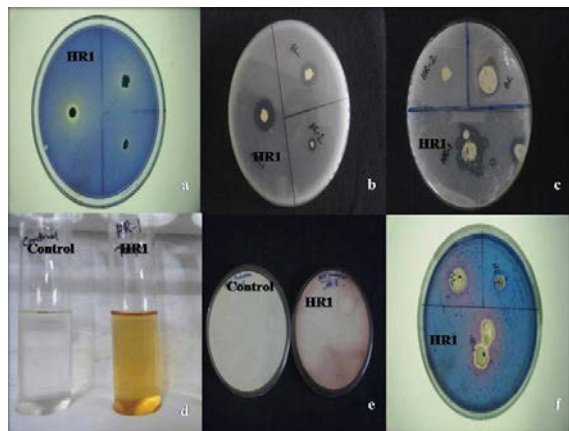
The isolate was evaluated for *in-vitro* plant growth-promoting (PGP) activities. The phosphate-solubilising activity was assessed both with PKV and NBRIP medium, and the isolate HR1 showed positive results in both cases. The isolate also produced a clear zone on the modified PKV medium containing ZnO, which indicated its efficacy as a zinc-solubilizer. The isolate also produced siderophore, IAA and HCN (Table 2, Figure 2). The *K. pneumoniae* HR1 showed a transparent zone on the chitinase-detection agar plate which clearly indicated the

ability of HR1 to produce chitinase. The halo zones around the bacterial spot on the starch agar and skim milk agar revealed that the strain produced amylase and protease, respectively. However, the isolate could not show positive results on the CMC agar plate (Table 2). The bacterial isolate showed its active growth on the YEM agar plates containing 25, 50, 75 and 100 µg / mL of CdCl<sub>2</sub> concentration which shows that the isolate could tolerate cadmium.

**Table 2.** *In vitro* tests of endophytic isolate HR1 for the determination of PGP activities and production of extracellular hydrolytic enzymes by the isolate.

PGP Activities		Extracellular Hydrolytic Enzymes	
Traits	Response of isolate HR1	Hydrolytic Enzymes	Production by Isolate HR1
Phosphate solubilization	+	Protease	+
Zinc solubilization	+	Amylase	+
IAA production	+	Cellulase	-
Ammonia production	-	Chitinase	+
HCN production	+		
Siderophore production			

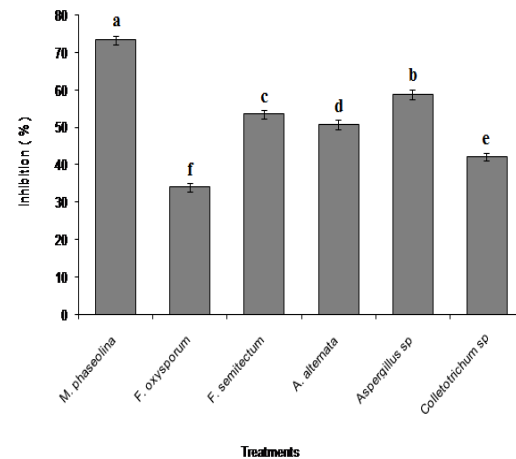
'+' = Positive activity/ presence of hydrolytic enzymes; '-' = Negative activity / absence of hydrolytic enzymes



**Figure 2.** *In vitro* PGP activity of *K. pneumoniae* HR1. a. Phosphate solubilization in NBRIP media, b. Phosphate solubilization in PKV media, c. Zinc solubilization, d. IAA production, e. HCN production, f. Siderophore production

### 3.3. *In vitro* Antagonistic Activity of *K. pneumoniae* against Fungal Pathogens

*In vitro* antagonism of *K. pneumoniae* was tested against *M. phaseolina*, *F. oxysporum*, *F. semitectum*, *A. alternata*, *Aspergillus* sp. and *Colletotrichum* sp. The results revealed that *K. pneumoniae* inhibited the tested pathogens significantly ( $F=381.662$ ;  $df=5$ ;  $P=0.05$ ). The highest inhibition observed against *M. phaseolina* was (73.3 %), followed by *Aspergillus* sp. (58.8 %), *F. semitectum* (53.5 %), *A. alternata* (50.8 %) and *Colletotrichum* sp. (42.26 %). However, *K. pneumoniae* showed the lowest percentage of inhibition against *F. oxysporum* (34.12 %) (Figure 3).



**Figure 3.** Inhibition of the growth of fungal pathogens by *K. pneumoniae* HR1 expressed in terms of percentage of inhibition. Data represent mean  $\pm$  SD. Bars not sharing the same letter are different at the  $P<0.05$  level by one-way ANOVA with DMRT

### 3.4. Assessments of Root Rot Disease of *V. mungo*

The greenhouse study revealed that the application of *K. pneumoniae* reduced the disease incidence significantly ( $F=766.697$ ;  $df=2$ ;  $P=0.05$ ) in comparison to the control plants in the presence of *M. phaseolina*. It was observed that the percentage of disease incidence was quite high (78.2 %) in the diseased control plants. PDI decreased when the plants were inoculated (seed bacterization) with the isolate; however, the lowest PDI (18.2 %) was achieved when *K. pneumoniae* was applied in a dual-mode (seed bacterization + soil drench application at  $10^8$  CFU/mL concentration) (Table 3).

**Table 3.** Assessment of root rot disease of *V. mungo*, caused by *M. phaseolina* in terms of the percentage of disease incidence (PDI) and the percentage of decrease over control (PDOC) following treatment with *K. pneumoniae* HR1 and pathogen challenge.

Days of inoculation	Treatments	Disease assessment	
		PDI	PDOC
15	Control	78.2 $\pm$ 3.4 <sup>a</sup>	-
	T1	27.3 $\pm$ 0.5 <sup>b</sup>	65.02 $\pm$ 0.9
	T2	18.2 $\pm$ 0.9 <sup>c</sup>	76.73 $\pm$ 0.2

Results represented as mean  $\pm$  SD, T1 = Seeds of *V. mungo* bacterized with *K. pneumoniae* and challenge inoculation with *M. phaseolina*; T2= Dual-mode of application (seed bacterization + soil drench at  $1 \times 10^8$  CFU/mL) of *K. pneumoniae*, challenge inoculation with *M. phaseolina*. Values in rows not sharing the same letter are different at the  $P<0.05$  level by one-way ANOVA with DMRT ( $n=10$ )

### 3.5. Effect of *K. pneumoniae* on the Growth of *V. mungo* in a *M. phaseolina*-infested soil

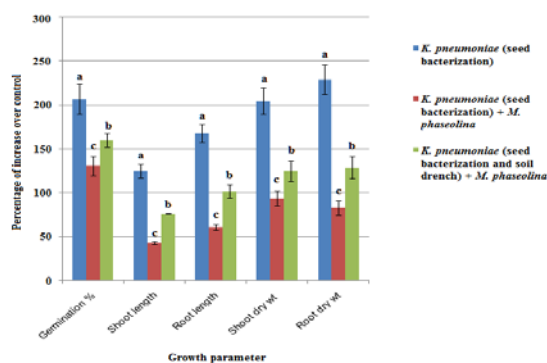
The dual application of *K. pneumoniae* led to a significant increase in the growth of *Vigna* in terms of increase in the germination percentage, shoot and root length, shoot and root dry weight in comparison to the healthy control and the *M. phaseolina*-infested plants (diseased control). A significant decrease in the germination percentage ( $F=578.569$ ;  $df=4$ ;  $P=0.05$ ), shoot length ( $F=187.688$ ;  $df=4$ ;  $P=0.05$ ) and dry weight ( $F=466.831$ ;  $df=4$ ;  $P=0.05$ ), root length ( $F=112.143$ ;  $df=$

4;  $P=0.05$ ), dry weight ( $F=969.355$ ;  $df=4$ ;  $P=0.05$ ) and vigour index ( $F=1443.915$ ;  $df=4$ ;  $P=0.05$ ) were observed in the presence of *M. phaseolina*. As for the percentage of increase over control (PIOC), a statistically-significant increase in seed germination, shoot length, root length and

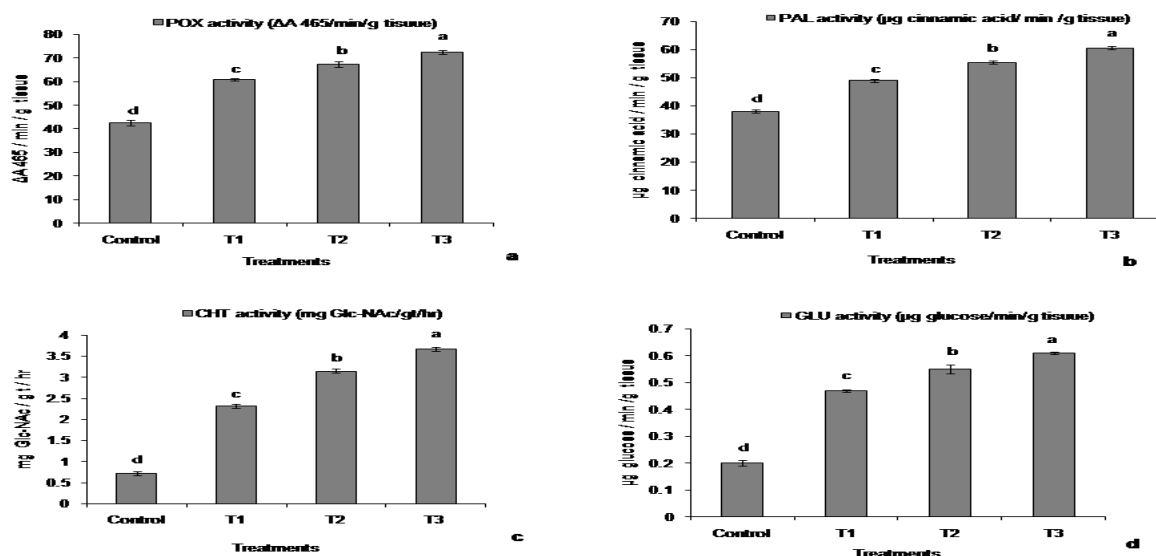
**Table 4.** Effect of *K. pneumoniae* HR1 on the growth of *V. mungo* in a *M. phaseolina*-infested soil.

Growth Parameters	Treatments				
	Untreated Healthy	Untreated Inoculated ( <i>M. phaseolina</i> )	Treated Healthy ( <i>K. pneumoniae</i> HR1)	Treated Inoculated [ <i>K. pneumoniae</i> HR1 (Seed treatment) + <i>M. phaseolina</i> ]	Treated Inoculated [ <i>K. pneumoniae</i> HR1 (Seed treatment + Drench Application) + <i>M. phaseolina</i> ]
Germination (%)	88.27±1.38 <sup>u</sup>	30.4±1.73 <sup>e</sup>	93.3±0.70 <sup>a</sup>	70.2±0.72 <sup>u</sup>	79.1±0.3.20 <sup>c</sup>
Shoot length (cm)	14.3±0.50 <sup>u</sup>	7.2±0.35 <sup>e</sup>	16.1±0.24 <sup>a</sup>	10.3±0.42 <sup>u</sup>	12.6±0.61 <sup>c</sup>
Root length (cm)	3.3±0.17 <sup>u</sup>	1.4±0.11 <sup>e</sup>	3.8±0.19 <sup>a</sup>	2.3±0.14 <sup>u</sup>	2.9±0.13 <sup>c</sup>
Shoot Dry weight (g)	0.23±0.01 <sup>u</sup>	0.09±0.004 <sup>e</sup>	0.29±0.003 <sup>a</sup>	0.18±0.003 <sup>u</sup>	0.21±0.006 <sup>c</sup>
Root Dry weight (g)	0.06±0.002 <sup>u</sup>	0.02±0.001 <sup>e</sup>	0.07±0.001 <sup>a</sup>	0.04±0.0002 <sup>u</sup>	0.05±0.0007 <sup>c</sup>
Vigour Index	1554.9±52.23 <sup>u</sup>	262.0±19.01 <sup>e</sup>	1862.2±16.13 <sup>a</sup>	880.8±21.39 <sup>u</sup>	1225.9±13.66 <sup>c</sup>

Results represented as mean  $\pm$  SD, values in rows not sharing the same letter are different at the  $P<0.05$  level by one-way ANOVA with DMRT (n=10)



**Figure 4.** Effect of *K. pneumoniae* HR1 on the growth of *V. mungo*. Control refers to the plants inoculated with *M. phaseolina* only. Data represent mean  $\pm$  SD. Bars not sharing the same letter are different at the  $P<0.05$  level by one-way ANOVA with DMRT.



**Figure 5.** Activities of Peroxidase (a), Phenylalanine ammonia lyase (b), Chitinase (c) and  $\beta$ -1, 3 glucanase (d) in leaves of *V. mungo* after 15 days of growth and challenged inoculation with *M. phaseolina*. T1- *M. phaseolina* inoculated, T2- Bacterized Seeds of black gram with *K. pneumoniae* and challenge inoculation with *M. phaseolina*, T3 – Dual-mode of application (seed bacterization + soil drench) of *K. pneumoniae*, challenge inoculation with *M. phaseolina*. Bars with different letter are significantly different at  $P<0.05$  according to DMRT.

dry weight was observed in the plants in the presence of *K. pneumoniae* alone, in comparison to other treatments (Table 4, figure 4).

### 3.6. Activities of Defence Enzymes during Disease Suppression by *K. pneumoniae*

Activities of defence enzymes were assayed in leaves subjected to various treatments. The activities of defence enzymes increased significantly after the application of *K. pneumoniae* and challenged inoculation with *M. phaseolina*. However, the most significant increase observed was when the isolate was applied in a dual-mode following the challenge inoculation with the pathogen [POX ( $F=334.694$ ;  $df=3$ ;  $P=0.05$ ), PAL ( $F=257.825$ ;  $df=3$ ;  $P=0.05$ ), CHT ( $F=3439.517$ ;  $df=3$ ;  $P=0.05$ ), GLU ( $F=262.067$ ;  $df=3$ ;  $P=0.05$ )] (Figure 5).



#### 4. Discussion

*M. phaseolina* is the causal agent of charcoal root rot disease. It is a devastating pathogen affecting agricultural and forest crops, with more than five-hundred susceptible host's worldwide (Wyllie *et al.*, 1984). In the present study, the researchers have isolated and characterized one endophytic isolate from *K. pneumoniae* HR1 for its antagonistic and biocontrol efficacy against *M. phaseolina*.

The endophytic gram-negative and rod-shaped bacterium *K. pneumoniae* HR1 was isolated from the root nodules of the leguminous plant, *V. mungo*, on yeast extract mannitol agar medium, and was preliminarily characterized morphologically and biochemically. The HR1 isolate exhibited a phosphate-solubilising activity by producing halos zone on the Pikovskaya's (PKV) and National Botanical Research Institute's phosphate (NBRIP) media. The bacterium could solubilize zinc oxide (insoluble) supplemented in a modified PKV medium. Both phosphate and zinc are essential nutrients and play a crucial role in the promotion of plant growth. Enhancement of growth in *V. radiata* by the zinc-phosphate-solubilizing bacterial isolates was reported previously (Iqbal *et al.*, 2010a). Vaid *et al.*, (2014) also reported that about the Zn-solubilising and IAA-producing *Burkholderia* and *Acinetobacter* strains which increased the uptake of Zn and promoted the growth of rice plant. Plant growth-promoting rhizobacterial strains actively colonize plant roots and exert beneficial effects on the host. Endophytes, residing inside the plants, with plant growth-promoting activities are considered more effective in promoting growth in host plants. In their study, Sharma *et al.*, (2014) isolated endophytic *Klebsiella* spp. which could solubilise ZnO. In the present study, it was also observed that the endophytic isolate HR1 solubilized ZnO quite efficiently. Heavy-metal tolerance is considered one of the crucial attributes of PGPRs. Bacterial isolates with this capacity are considered effective to induce systemic tolerance in plants against heavy-metal stress. Several reports suggested that *Klebsiella* sp. has greater cadmium and other heavy-metal tolerance efficiency (Nath *et al.*, 2012; Yamina *et al.*, 2014). In the present study, the isolate *K. pneumoniae* HR1 could tolerate even up to 100 µg/mL of CdCl<sub>2</sub>. Furthermore, the isolate-HR1 was found to be the producer of IAA, siderophore, hydrogen cyanide, chitinase, amylase and protease. The production of several hydrolytic enzymes such as protease, chitinase, cellulase, lipase and amylase by *Klebsiella* sp. was demonstrated by Mazzucotelli *et al.*, (2013), which showed similar results to the observations of the current study. The production of hydrolytic enzymes, hydrogen cyanide, and siderophore by the isolate HR1 may be the probable mechanisms responsible for the antagonistic activity against phytopathogens. IAA-producing bacteria are believed to influence the endogenous auxin pool of plants, and thus can promote root elongation and plant growth (Patten and Glick, 2002; Ahemad and Khan, 2011a; Ahemad and Khan, 2011b). Jha and Kumar, (2007) also stressed the plant growth promoting traits- phosphate solubilization, IAA production, and nitrogenase activity of *K. oxytoca*. *In vitro* PGP traits such as IAA, siderophore, HCN production, and phosphate solubilization of endophytic

PGP bacteria inside the roots of *Brassica napus* were reported by Etesami *et al.*, (2014).

The isolate showed commendable antagonistic activity against phytopathogens used in the present study. The highest inhibition percentage against *M. phaseolina* (73.3 %) and the lowest inhibition against *F. oxysporum* (34.12 %) were observed by *K. pneumoniae* in the paired culture. The inhibition of fungal pathogens by the isolate may be attributed to the production of antifungal enzymes- chitinase, protease, amylase as well as HCN. Simonetti *et al.*, (2015) reported antagonistic activities of eleven bacterial isolates against *M. phaseolina*. Among the isolates *Pseudomonas fluorescens* 9 showed the highest percentage of inhibition (62 %) *in vitro*. Their study is consistent with the results of the current work. Moreover, this study showed that the isolate HR1 exhibited a much more inhibition efficiency against *M. phaseolina*.

In the present study, the application of *K. pneumoniae* both in a single and a dual-mode, in the presence of *M. phaseolina* resulted in a significant increase in growth, measured in terms of increase in shoot and root length, shoot and root dry weight, and vigour index of black gram. However, a significant decrease in the growth parameters was found in the presence of *M. phaseolina* compared to the untreated healthy black gram. During the assessment of the root rot disease, the highest percentage of decrease over control (76.73 %) was observed when *K. pneumoniae* was applied two times (as seed bacterization + soil drench application at 10<sup>8</sup> CFU/mL) in the of *M. phaseolina*. Plants subjected to a dual application with the bacterium in the presence of the pathogen also showed a significantly higher percentage of increase than the control (PIOC) in comparison to the other treatments. It is quite apparent that *K. pneumoniae* not only promoted growth but effectively reduced the root rot disease of *V. mungo* as a potent antagonistic endophytic PGPR strain. Previously, *K. pneumoniae* was reported as disease suppressive and as a plant growth-promoting strain, which reduced 72 % of stem rot severity caused by *Sclerotinia* increasing the plant height by 52–67 % (Abdeljalil *et al.*, 2016).

The role of potential bacterial antagonists in reducing the severity of *M. phaseolina* root rot disease by enhancing the activities of peroxidase, PAL, β-1, 3-glucanase and chitinase was also highlighted by many other authors (Govindappa *et al.*, 2011). Kumar *et al.*, (2007) focused on the control of charcoal rot of chickpeas caused by *M. phaseolina* via the application of a potent antagonistic isolate Pf4-99. Feng *et al.*, (2006) also reported that the rice endophytic strain YS19 promoted growth and increased root biomass. In the current study, it was observed that the activities of defence-related enzymes peroxidase, chitinase, phenylalanine ammonia lyase and β-1, 3-glucanase increased significantly after the application of *K. pneumoniae* and challenge inoculation with *M. phaseolina*. The increased activities of peroxidase (PR9), chitinase (PR3) and β-1, 3-glucanase (PR2) indicate the activation of PR proteins during defence. Since the application of *K. pneumoniae* in the *M. phaseolina*-infested soil increased the accumulation of defence-related enzymes in leaves, it is quite apparent that *K. pneumoniae* HR1 endophytic strain induces a systemic response. Bruce and West, (1989) reported the role of peroxidase in the biosynthesis of lignin which limited the extent of pathogen spread because of antifungal activity. The accumulation of

PR proteins during the induction of resistance in crops against pathogens by biocontrol agents was also reported earlier by some researchers (Bargabus *et al.*, 2004; Bharati *et al.*, 2004). Resistance in *V. mungo* against *M. phaseolina* was induced through the accumulation of phenolics, PR proteins and the induction of defence enzymes by the two potent endophytic strains of *P. fluorescens* – Endo2 and Endo35 (Karthikeyan *et al.*, 2005). Govindappa *et al.*, (2010) reported that higher activities of peroxidase, phenylalanine ammonia lyase, chitinase, polyphenol oxidase and  $\beta$ -1, 3-glucanase involved in phenyl propanoid pathways were observed in the potent antagonistic strain *Bacillus subtilis* which treated safflower plants after challenge inoculation with *M. phaseolina*. The induction of systemic resistance in legumes (*V. mungo*, *V. radiata*) against *F. oxysporum* and *A. alternata* was also highlighted by Rao *et al.*, (2015).

## 5. Conclusion

The endophytic isolate *K. pneumoniae* HR1 showed strong antagonistic activity and suppression of the root rot disease, caused by *M. phaseolina*. While determining the mechanism of action, it was found to promote plant growth-promotion and induce resistance in the host plants by elevating the synthesis of defence-related enzymes. The results of the current study provide strong evidence that the endophytic *K. pneumoniae* HR1 has a great potential as a candidate for the biocontrol of the soil-borne fungal pathogen, *M. phaseolina*, and as a plant-growth promoter. The use of such beneficial endophytes, which can induce resistance to diseases in the host plants, is a boon to agriculture for a better crop production and a healthy soil.

## Acknowledgments

Xcelris laboratory, Ahmadabad and Pulse and Oilseeds Research Station, Rani Bagan, Behrampore, West Bengal, India are thankfully acknowledged for the molecular identification of endophytic strain on the basis of 16S rDNA partial sequencing and for supplying the seeds of *Vigna mungo* var. sarada which helped carry out this research.

## Conflict of interest

The authors declare that they have no conflict of interest.

## References

Abawi GS and Pastor-Corrales MA. 1990. Root rots of beans in Latin America and Africa: Diagnosis, Research Methodologies, and Management Strategies, Centro Internacional de Agricultura Tropical (CIAT), Cali, Colombia, pp. 114.

Abdeljalil NOB, Vallance J, Gerbore J, Rey P and Daami-Remadi M. 2016. Bio-suppression of *Sclerotinia* stem rot of tomato and biostimulation of plant growth using tomato associated rhizobacteria. *J Plant Pathol Microbiol*, **7**: 331.

Abdul-Baki A and Anderson JD. 1973. Vigor determination in soybean seed by multiple criteria. *Crop Sci*, **13**: 630–633.

Ahemad M and Khan MS. 2011a. Effects of insecticides on plant-growth-promoting activities of phosphate solubilizing

rhizobacterium *Klebsiella* sp strain PS19. *Pestic Biochem Physiol*, **100**: 51–56.

Ahemad M and Khan MS. 2011b. Biotoxic impact of fungicides on plant growth promoting activities of phosphate-solubilizing *Klebsiella* sp isolated from mustard (*Brassica campestris*) rhizosphere. *J Pest Sci.*, **85**: 29–36.

Atef NM. 2000. *In vitro* antagonistic action of eggplant and sweet potato phylloplane bacteria to some parasitic fungi. *Phytopathol Mediter.*, **39**: 366–375.

Bakker AW and Schippers B. 1987. Microbial cyanide production in the rhizosphere in relation to potato yield reduction and *Pseudomonas* spp. mediated plant growth stimulation. *Soil Biol Biochem.*, **19**: 451–457.

Bargabus RL, Zidack NK, Sherwood JE and Jacobsen BJ. 2004. Screening for the identification of potential biological control agents that induce systemic acquired resistance in sugar beet. *Biol Control*, **30**: 342–350.

Berg G, Eberl L and Hartmann A. 2005. The rhizosphere as a reservoir for opportunistic human pathogenic bacteria. *Environ Microbiol.*, **7**: 1673–1685.

Bhagat N, Vermani M and Bajwa HS. 2016. Characterization of heavy metal (cadmium and nickel) tolerant Gram negative enteric bacteria from polluted Yamuna river, Delhi. *Afr J Microbiol Res.*, **10**: 127–137.

Bharati R, Vivekananthan R, Harish S, Ramanathan A, Samaiyappan R (2004) Rhizobacteria based bioformulations for the management of fruit rot infection in chillies. *Crop Prot.*, **23**: 835–843.

Bloemberg GV and Lugtenberg BJJ. 2001. Molecular basis of plant growth promotion and biocontrol by rhizobacteria. *Curr Opin Plant Biol.*, **4**(4): 343–350.

Boller T and Mauch F. 1998. Colorimetric assay for chitinase. *Meth Enzymol.*, **161**: 430–435.

Brick JM and Bostock RM, Silverstone SE. 1991. Rapid in situ assay for indole acetic acid production by bacteria immobilized on nitrocellulose membrane. *Appl Environ Microbiol.*, **57**: 535–538.

Bruce RJ and West CA. 1989. Elicitation of lignin biosynthesis and isoperoxidase activity by pectic fragments in suspension cultures of castor bean. *Plant Physiol.*, **91**: 889–897.

Byers HK, Stackebrandt E, Hayward C and Blackall LL. 1998. Molecular investigation of a microbial mat associated with the great artesian basin. *FEMS Microbiol Ecol.*, **25**: 391–403.

Cappuccino JC and Sherman N. 1992. **Microbiology a Laboratory Manual**, third ed. Benjamin/Cummings Pub Co, New York, pp. 125–179.

Chaiham M, Chunhaleuchanon S, Kozo A and Lumyong S. 2008. Screening of rhizobacteria for their plant growth promoting activities. *KMITL Sci Tech J.*, **8**: 18–23.

Chakraborty U, Chakraborty BN and Kapoor M. 1993. Changes in levels of peroxidase and phenylalanine ammonia lyase *Brassica napus* cultivars showing variable resistance to *Leptosphaeria maculans*. *Folia Microbiol.*, **38**: 491–496.

Cottingham C. 1981. Numbers and distribution of sclerotia of *Macrophomina phaseolina* in soils of South Carolina. *Plant Disease Reporter.*, **65**: 355–356.

Das MP, Devi PV and Yasmine Y. 2015. A study on antagonistic potential of bacteria against phytopathogenic fungi. *Int J Pharm Sci Rev Res.*, **34**: 191–193.

Etesami H, Hosseini M and Alikhani HA. 2014. *In planta* selection of plant growth promoting endophytic bacteria for rice (*Oryza sativa* L.). *J Soil Sci Plant Nutr.*, **14**: 491–503.

Feng Y, Shen D and Song W. 2006. Rice endophyte *Pantoea agglomerans* YS19 promotes host plant growth and affects



- allocations of host photosynthates. *J Appl Microbiol.*, **100**: 938–945.
- Govindappa M, Lokesh S, Rai VR, Naik VR and Raju SG. 2010. Induction of systemic resistance and management of safflower *Macrophomina phaseolina* root rot disease by biocontrol agents. *Arch Phytopathology Plant Protect*, **43**: 26–40.
- Govindappa M, Rai VR and Lokesh S. 2011. Screening of *Pseudomonas fluorescens* isolates for biological control of *Macrophomina phaseolina* root-rot of safflower. *Afr J Agric Res.*, **6**: 6256–6266.
- Iqbal U, Jamil N, Ali I and Hasnain S. 2010a. Effect of zinc-phosphate solubilizing bacterial isolates on growth of *Vigna radiata*. *Ann Microbiol.*, **60**: 243–248.
- Iqbal U, Mukhtar T, Muhammad S, Iqbal, Ul Haque I and Malik SR. 2010b. Host plant resistance in black gram against charcoal rot (*Macrophomina phaseolina* (tassi) goid). *Pak J Phytopathol.*, **22(2)**: 126–129.
- Jha PN and Kumar A. 2007. Endophytic colonization of *Typha australis* by a plant growth-promoting bacterium *Klebsiella oxytoca* strain GR-3. *J Appl Microbiol.*, **103**: 1311–1320.
- Karthikeyan M, Bhaskaran R, Radhika K, Mathiyazhagan S, Jayakumar V, Sandosskumar R and Velazhahan R. 2005. Endophytic *Pseudomonas fluorescens* Endo2 and Endo35 induce resistance in black gram (*Vigna mungo* L. Hepper) to the pathogen *Macrophomina phaseolina*. *J Plant Interact.*, **1**: 135–143.
- Krishnamurthy K and Gnanamanickam SS. 1997. Biological control of sheath blight of rice: induction of systemic resistance in rice by plant-associated *Pseudomonas* spp. *Curr Sci.*, **72**: 331–334.
- Kumar P, Dubey RC and Maheshwari DK. 2012. *Bacillus* strains isolated from rhizosphere showed plant growth promoting and antagonistic activity against phytopathogens. *Microbiol Res.*, **167**: 493–499.
- Kumar V, Kumar A and Kharwar RN. 2007. Antagonistic potential of fluorescent pseudomonads and control of charcoal rot of chickpea caused by *Macrophomina phaseolina*. *J Environ Biol.*, **28**: 15–20.
- Lugtenberg B and Kamilova F. 2009. Plant growth-promoting rhizobacteria. *Annu Rev Microbiol.*, **63**: 541–556.
- Mazzucotelli CA, Ponce AG, Kotlar CE and Moreira MR. 2013. Isolation and characterization of bacterial strains with a hydrolytic profile with potential use in bioconversion of agro industrial by-products and waste. *Food Sci Technol.*, **33**: 295–303.
- McMullen M and Bergstrom G. 1999. Chemical and biological control of *Fusarium* head blight 1999 projects and progress. In Proceedings of the 1999 National *Fusarium* Head Blight Forum, Sioux Falls, South Dakota, pp. 61–63.
- Nath S, Deb B and Sharma I. 2012. Isolation and characterization of cadmium and lead resistant bacteria. *Global Adv Res J Microbiol.*, **1**: 194–198.
- Nautiyal CS. 1999. An efficient microbiological growth medium for screening phosphate solubilising microorganisms. *FEMS Microbiol Lett.*, **170**: 65–270.
- Pan SQ, Ye XS and Kuc J. 1991. A technique for detection of chitinase,  $\beta$ -1, 3-glucanase and protein patterns after a single separation using polyacrylamide gel electrophoresis or isoelectric focussing. *Phytopathol.*, **81**: 970–974.
- Patten C and Glick CR. 2002. Role of *Pseudomonas putida* indoleacetic acid in development of host plant root system. *Appl Environ Microbiol.*, **68**: 3795–3801.
- Pikovskaya RI. 1948. Mobilization of phosphorus in soil in connection with vital activity of some microbial species. *Microbiol.*, **17**: 362–370.
- Rangel-Castro JJ, Levenfors JJ and Danell E. 2002. Physiological and genetic characterization of fluorescent *Pseudomonas* associated with *Cantharellus cibarius*. *Can J Microbiol.*, **48**: 739–748.
- Rao GS, Reddy NNR and Surekha C. 2015. Induction of plant systemic resistance in legumes *Cajanus cajan*, *Vigna radiata*, *Vigna mungo* against plant pathogens *Fusarium oxysporum* and *Alternaria alternata*—a *Trichoderma viride* mediated reprogramming of plant defense mechanism. *Int J Recent Sci Res.*, **6**: 4270–4280.
- Roberts WK and Selitrennikoff CP. 1988. Plant and bacterial chitinase differ in antifungal activity. *J Gen Microbiol.*, **134**: 169–176.
- Saitou N and Nei M. 1987. The neighbor-joining method: A new method for reconstructing phylogenetic trees. *Mol Biol Evol.*, **4**: 406–425.
- Satyanandam T, Babu K, Rosaiah G and Vijayalakshmi M. 2013. Screening of *Rhizobium* strains isolated from *Vigna mungo* native to rice fallows for the production of indole acetic acid. *Int J Pharm Biol Sci.*, **3(4)**: 56–61.
- Schwyn B and Neilands J. 1987. Universal chemical assay for the detection and determination siderophores. *Anal Biochem.*, **160**: 47–56.
- Senthilkumar M, Swarnalakshmi K, Govindasamy V, Lee YK and Annapurna K. 2009. Biocontrol potential of soybean bacterial endophytes against charcoal rot fungus, *Rhizoctonia bataticola*. *Curr Microbiol.*, **58**: 288–293.
- Sharma P, Kumawat KC, Kaur S and Kaur N. 2014. Assessment of zinc solubilization by endophytic bacteria in legume rhizosphere. *Ind J Appl Res.*, **4**: 439–441.
- Shaw FJ, Lin PF, Chen CS and Chen CH. 1995. Purification and characterization of an extracellular  $\alpha$ -amylase from thermos species. *Bot bull Acad Sin.*, **36**: 195–200.
- Simonetti E, Viso NP, Montecchia M, Zilli C, Balestrasse K and Carmona M. 2015. Evaluation of native bacteria and manganese phosphite for alternative control of charcoal root rot of soybean. *Microbiol Res.*, **180**: 40–48.
- Stafford WHL, Baker GC, Brown SA, Burton SG and Cowan DA. 2005. Bacterial diversity in the rhizosphere of Proteaceae species. *Environ Microbiol.*, **7**: 1755–1768.
- Tamura K, Dudley J, Nei M, Kumar S. 2007. MEGA4: Molecular evolutionary genetics analysis (MEGA) software version 4.0. *Mol Biol Evol.*, **24**: 1596–1599.
- Vaid SK, Kumar B, Sharma A, Shukla AK and Srivastava PC. 2014. Effect of zinc solubilizing bacteria on growth promotion and zinc nutrition of rice. *J Soil Sci Plant Nutr.*, **14**: 889–910.
- Vasebi Y, Safaie N and Alizadeh A. 2013. Biological control of soybean charcoal root rot disease using bacterial and fungal antagonists In Vitro and greenhouse condition. *J Crop Prot.*, **2(2)**: 139–150.
- Wheeler BEJ. 1969. **An Introduction to Plant Diseases**, John Wiley and Sons Ltd, London.
- Wheeler H. 1975. **Plant Pathogenesis**, Academic press, London, New York, pp. 2–3.
- Wyllie T, Gangopadhyay S, Teague W and Blanchar R. 1984. Germination and production of *Macrophomina phaseolina* microsclerotia as affected by oxygen and carbon dioxide concentration. *Plant Soil*, **81**: 195–201.
- Yamina B, Tahar B, Lila M, Hocine H and Laure FM. 2014. Study on cadmium resistant-bacteria isolated from hospital wastewaters. *Adv Biosci Biotechnol.*, **5**: 718–726.



# Effect of Temperature Constraints on Morphological and Cytogenetical Attributes in Cluster bean [*Cyamopsis tetragonoloba* (L.) Taub.]

Girjesh Kumar and Shefali Singh\*

Plant Genetics Laboratory, Department of Botany, University of Allahabad- 211002, India.

Received July 4, 2018; Revised August 15, 2018; Accepted September 3, 2018

## Abstract

The drifting climatic scenario and constant changes in temperature profiles has culminated into heavy crop losses that have set up an alarming situation across the world. A slight modification in temperature ranges results in detrimental effects on the life processes of crop plants as well as on yield attributes. To pursue the effects of temperature stress on plants, both heat and cold stresses are vital cues; hence, they are investigated in this study. *Cyamopsis tetragonoloba* (L.) Taub, has been a test model for the present study due to its restricted pervasion and environmental limitations. The experimental setup included heat stress as well as cold stress (including chilling stress and freezing stress) given at the seedling stage in three replicates. Exposure to freezing stress affected the young seedlings severely, and they eventually collapsed and could not be studied further. The seedlings exposed to the chilling and heat-stress displayed varying degrees of survivability, and were carefully monitored till maturity. Various morphological parameters were recorded at the growing stage. With the advent of the reproductive stage, young floral buds were subjected to fixation in carnoy's fixative. The degree of cytological abnormalities showed a parallel ascend to the increasing stress, where cold stress had a more severe impact on microsporogenesis than heat stress. The morphological characters also exhibited a negative correlation after the treatment, but more profound deterrent results were retrieved in the case of cold stress. In conclusion, cold stress was found to introduce serious effects on plant growth and reproduction, and turned out to be more serious on plants compared with heat stress, for which plants express a degree of diligence and adaptability at short durations.

**Keywords:** *Cyamopsis tetragonoloba*, Meiosis, Morphological attributes, Temperature stress

## 1. Introduction

Perpetuation and pervasion patterns of various life forms to variable realms are dependent on wholesome cumulative requirements in terms of abiotic factors. This implies that abiotic factors are intrinsic in dictating biotic life. For instance, living entities of tropic and temperate zones display a vast deal of morphological differences which are the visible reciprocation of differential abiotic patterns in that area. This validates that climatic factors play an intrinsic role in organic sustenance. Among these, temperature is one such limiting attribute that controls and restricts the perpetuation of living beings, is among mainstays for incinerating vitality and vigorosity to the cells. Global temperature is forecasted to continuously increase by 1–3.7°C by the end of the 21<sup>st</sup> century (IPCC, 2013). Temperature acts as a limiting factor for plants growth and their yield, and also for the geographical distributions of plants (Siddiqui *et al.*, 2015).

Any deviation below or above the optimum temporal condition generates a set of stressful responses. Low temperature is one of the major environmental factors impacting plant growth, development, and ecological

distribution (Allen and Ort, 2001). Cold stress prevents the expression of the genetic potential of plants directly through the inhibition of metabolic reactions, and indirectly through cold-induced osmotic, oxidative, and other stresses (Chinnusamy *et al.*, 2007) causing significant crop losses. A transient elevation in temperature, that is by 10–15°C above the ambient condition, is considered a heat stress, which also alleviates crop losses. It causes multifarious and often adverse alterations to the plant growth, development, physiological processes and yield (Hasanuzzaman *et al.*, 2013).

The morphological dissimilarities reflect the divergence at the cytogenetical and gene- expression level, since the different set of proteins and enzymes work synergistically and inclusively in combating stress constraints. On the genomic level, plant diversity correlates with a high degree of variation in the overall genome size, ploidy level, and chromosome number (Kellogg and Bennetzen, 2004), which results in a course of genome adaptation and change. In order to facilitate the acclimatization of the plant to a distinct niche, adaptive potentialities need to evolve within that life system. Different types of cognitive work on temperature stress have been conducted underlining a multitude of influences

\* Corresponding author e-mail: shefalisingh.910@gmail.com.

of temperature modulation on life (Barnabas *et al.*, 2008; Hedhly *et al.*, 2008; Hatfield and Preuger, 2015).

The most substantial impacts of abiotic stresses occur in the reproductive stages of plants and limit the plant productivity. According to Bione *et al.* (2000), meiosis is strongly influenced by environmental conditions, where both male and female gametogenesis gets affected; microsporogenesis dealing with pollen development is a highly stress-sensitive event. Several researches have been conducted on legumes, including *Vicia faba* (Siddiqui *et al.*, 2015), and *Cicer arietinum* (Sharma and Nayyar, 2014). The cytomorphological responses of buckwheat to temperature stress have also been studied by (Kumar and Srivastava, 2015). The current study is designed to investigate such effects on anther meiosis in cluster beans.

Sophisticated acclimation strategies are being formulated for the sake of introducing plants to novel environments. These efforts may serve as a measure for amplifying quantitative gains. However, the introduction and cultivation of new crops in a given environment require management practices and trait selections that enable the crop species to perform to their full potential (Singh *et al.*, 2008). Therefore, it is crucial to study the salient effects resulting from temperature disturbances to plants growth and metabolism. Crop production of *C. tetragonoloba* is limited to arid regions, and the plant has a curtailed range of temperature tolerance. This draws the plot for the present experimental work through which the cytogenetical and the morphological characteristics of *C. tetragonoloba* (L.) Taub., (commonly known as guar or cluster bean), is investigated in details. Cluster bean pods contain condensed tannins in addition to *p*-coumaric acid, caffeic acid, gallic acid, gentisic acid, quercetin, kaempferol and its 3-arabinoside, *p*-hydroxycinnamyl, and coniferyl alcohol (Asolkar *et al.*, 1992). Moreover, cluster beans are also valued for various ethnobotanical uses.

## 2. Material and Methods

### 2.1. Seed Procurement

Fresh seeds of *C. tetragonoloba* (L.) Taub., variety RGC-1038, were obtained from Central Arid Zone Research Institute (CAZRI), Rajasthan.

### 2.2. Treatment

The seeds were thoroughly washed for ten minutes with distilled water, and 0.1 % mercuric chloride was utilized for surface sterilization. The seeds were sown in pots (a mixture of soil and farmyard manure) provided with ambient environmental conditions for germination at the temperature  $27 \pm 2^\circ\text{C}$ , until the emergence of two cotyledonary stages. After the emergence of two cotyledons, the seedlings were subjected to temperature stress including heat and cold stress treatments in an incubator at a pre-requisite temperature for a different time durations. Cold stress was subdivided into chilling stress (at  $4^\circ\text{C}$ ) and freezing stress (at  $-4^\circ\text{C}$ ) (Miura and Frumoto, 2013); for the duration of three hours, six hours, and nine hours respectively. The seedlings were subjected to heat stress at the temperature  $50^\circ\text{C}$  for the same time durations. Following treatment, the seedlings were maintained in each set for a recovery period that was equal to the duration of treatment, and were then re-transferred to the

pots in triplicates in a completely randomized block design (CRBD).

### 2.3. Cytogenetical Study

Plant growth was carefully monitored, and after reaching the reproductive stage, young floral buds were fixed in Carnoy's fixative (3 parts Alcohol: 1 part Glacial Acetic Acid) for twenty-four hours, and were preserved in 70 % alcohol at  $4^\circ\text{C}$ . The buds were teased, and anthers were smeared in a drop of 2% acetocarmine stain for cytological investigation. The slides were observed at 40X resolution by the Nikon Phase Contrast microscope (Nikon Eclipse, E200, Japan), and the microphotography was done using the PCTV software. Based on the stainability criteria of glycerol-acetocarmine stain, pollen fertility percentage was also calculated (Marks, 1954). Fully-stained globose-nucleated pollen grains were regarded fertile, whereas light-stained enucleated pollen grains were documented as sterile. Three independent slides were prepared from which ten microscopic views were documented for the scoring of data.

### 2.4. Morphological and Yield Study

Various morphological parameters were recorded to analyze the effects of temperature stress on the morphological characteristics. The parameters included were survivability percentage, plant height and days to 50 % flowering. Certain yield parameters studied were cluster per plants, pods per cluster, pod length and seeds per pod.

### 2.5. Statistical Analysis

A statistical calibration was done using SPSS 16.0 version software. The data were statistically analyzed by one-way analysis of variance (ANOVA). The means were compared at  $P \leq 0.5$  applying the Post hoc and Duncan Multiple Range Test (DMRT). A graphical representation of data was performed using Sigma Plot 10.0 software.

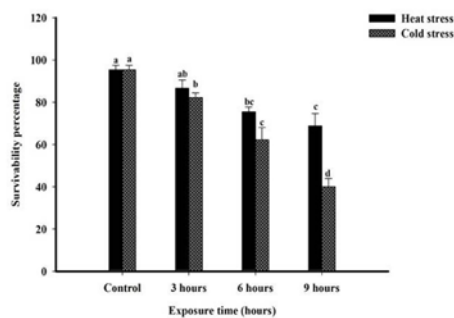
## 3. Results

### 3.1. Influence of Temperature Stress on Morphological Parameters

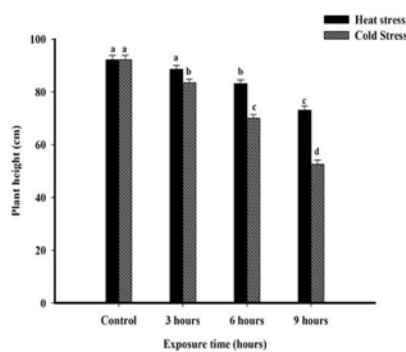
Various morphological parameters were delved to examine all adversities and effects. At the inception of the study, the seedlings showed certain morphological symptoms. In case of heat stress, scorching of seedlings was the most conspicuous symptom present. Occurrence of injuries such as surface pitting, ice formation, water soak spots, and internal discoloration of lesions were discernible in the freezing-stress sets at all of the three time durations. The seedlings were highly susceptible and eventually succumbed to die within two to three days; henceforth, the freezing stress was not monitored further. As for the surface lesions in the case of chilling stress, the injuries were comparatively less severe and included seedling shrinkage, epidermal distortion, and minor chlorotic sites.

The survivability percentage (as shown in Figure 1) was found to be highly affected in the case of chilling-stress treatment compared to the heat-stress treatment. In fact, survivability percentage was among the first hand clues for the effect on the two stresses investigated in this study. The chilling stress was comparatively more detrimental to the plant growth. Survivability percentage was recorded to be  $95.33 \pm 2.20^a$  in the case of the control.

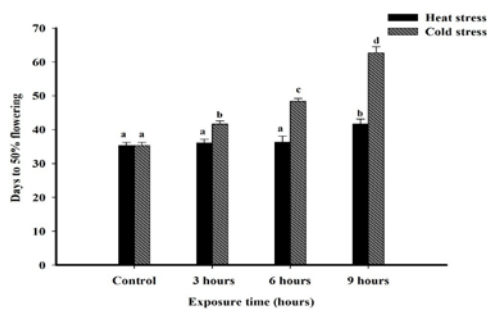
It declined down to  $68.88 \pm 5.87^c$  in the case of heat stress, and was curtailed down to a low percentage of  $39.99 \pm 3.84^d$  in the case of chilling cold stress in nine hours of treatment. Also, a similar decline was observed in the plant height trend (Figure 2). Mean plant height in the control was recorded to be  $92.16 \pm 1.69^a$  cm, which declined from  $88.60 \pm 1.40^a$  cm to  $73.06 \pm 1.55^c$  cm at the heat stress, whereas the mean plant height went down from  $83.46 \pm 1.33^b$  to  $52.53 \pm 1.63^d$  cm in the case of chilling stress after nine and three hours of treatments respectively. The cold stress resulted in a delay in the initial onset of flowering, the trend of which is documented in the graph of days to 50% flowering (Figure 3). As for the control, days to 50% flowering was recorded to be  $35.33 \pm 0.88^a$  days, whereas it occurred after  $41.66 \pm 1.45^b$  days at the heat stress, and after  $62.66 \pm 1.85^d$  days in the case of cold stress after nine hours of treatment.



**Figure 1.** Effect of temperature stress on survivability percentage in *Cyamopsis tetragonoloba* (L.) Taub.



**Figure 2.** Effect of temperature stress on plant height in *Cyamopsis tetragonoloba* (L.) Taub.



**Figure 3.** Effect of temperature stress on days to 50 % flowering in *Cyamopsis tetragonoloba* (L.) Taub.)

### 3.2. Influence of Temperature Stress on Microsporogenesis

The cytological imaging was obtained through the cytogenetical investigation of pollen mother cells. Meiotic events in the control set followed a normal course. The chromosomal morphology at various stages of meiosis I/II were examined and were found to be absolutely normal. Figure 4 shows the cytological plate representing various important meiotic stages. Metaphasic plate I displayed the presence of seven bivalents (Figure 4A) at the equatorial plate segregated synchronically at anaphase I (Figure 4B), resulting in 7:7 poleward separation. However, a large proportion of chromosomal abnormality was witnessed in the case of the stress-treated sets. Table 1 displays the effect of temperature stress on the chromosomal morphology of *Cyamopsis tetragonoloba* (L.) Taub. The total abnormality percentage (TAB %), the criteria for adjudging the extent of chromosomal abnormality, increased from  $2.65 \pm 0.25\%$  to  $11.15 \pm 0.19\%$  in the case of heat stress, whereas after the cold stress treatments, an increment from  $5.84 \pm 0.36\%$  to  $16.40 \pm 0.37\%$  was reported. In comparison, it was perceived that the cold stress had left a marked genotoxicity on the chromosomal entity of this drought-tolerant plant. The preponderant abnormalities witnessed were secondary associations: stickiness (Figure 4G), unorientation, precocious movement, multivalents (Figure 4D), disturbed polarity (Figure 4J), laggard chromosome and anaphase bridge formation etc. In the case of heat stress, precocious movement ( $0.56 \pm 0.16\%$  to  $1.56 \pm 0.07\%$ ) and unorientation ( $0.37 \pm 0.24\%$  to  $1.29 \pm 0.17\%$ ) at metaphase I/II were the most predominant abnormalities found upon increasing the duration of treatment from three to nine hours. Multivalents, bridges and laggard formation were recorded at six and nine hours of treatments in the case of heat stress. In relation to responses to cold stress, stickiness at metaphase I/II was the most pronounced abnormality reported, which increased from  $0.62 \pm 0.31\%$  to  $2.20 \pm 0.23\%$  after three and nine hours of treatments respectively. Considerable frequency of univalent formation was also seen in the cold-stress treated set. Increment from  $0.54 \pm 0.16$  to  $1.81 \pm 0.19$  in the case of multivalents and from  $0.53 \pm 0.14$  to  $1.21 \pm 0.36$  in the case of bridges was recorded in the cold-stress treated set.

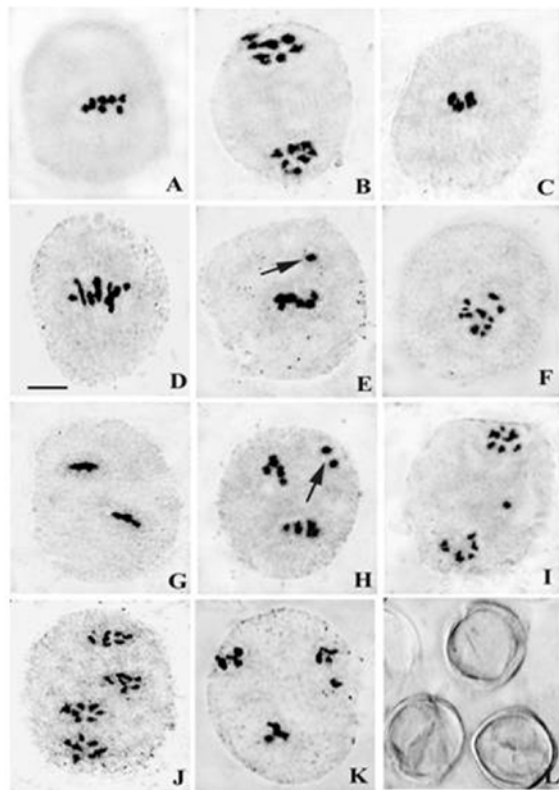
Pollen fertility is a criterion of extreme significance that governs the reproductive success. Fertile pollens were globose, nucleated and darkly-stained with proper ornamentation on the exine wall. Pollen fertility in case of the control set was calculated to be  $98 \pm 0.57^a\%$ . In the case of heat stress, it was calculated to be at  $93 \pm 1.15^b\%$  in the three-hour-treatment set, and declined to  $77.33 \pm 0.88^d\%$  after nine hours of treatment. At cold stress, it was recorded to be in  $90.33 \pm 0.88^b\%$  after three hours of treatment, and descended to  $61.33 \pm 0.88^d\%$  in the nine-hour-treatment set. A graphical representation of pollen fertility is provided in Figure 5. Sterile pollens are represented in Figure 4L.

**Table 1.** Effects of temperature stress on anther meiosis in *Cyamopsis tetragonoloba* (L.) Taub.

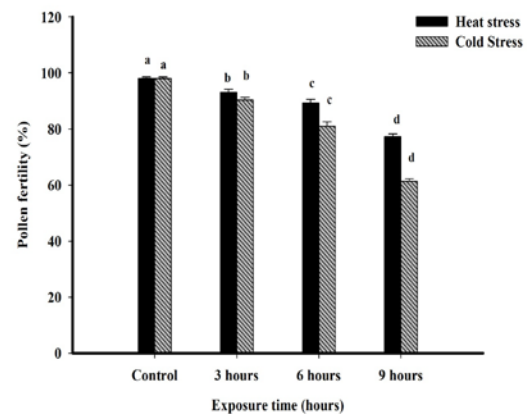
Treatment	Duration	Metaphasic Abnormality I/II (Mean ± SE)						Anaphasic Abnormality I/II (Mean ± SE)					Others	TAB%
		Sa	St	Un	Pr	Uni	Mt	St	Un	Dsp	Br	Lg		
Control	-	-	-	-	-	-	-	-	-	-	-	-	-	-
Heat stress (50°C)	3 hours	0.47± 0.2	0.09± 0.09	0.37± 0.18	0.56± 0.16	-	-	-	0.47± 0.24	0.28± 0.16	-	-	0.37± 0.25	2.65 ± 0.25
	6 hours	0.54± 0.16	0.53± 0.31	1.16± 0.22	0.89± 0.17	0.27± 0.15	0.08± 0.08	0.45± 0.9	0.62± 0.07	0.54± 0.15	0.09± 0.09	0.71± 0.08	0.62± 0.07	6.52± 0.42
	9 hours	0.73± 0.08	0.82± 0.14	1.29± 0.12	1.56± 0.07	0.63± 0.22	0.46± 0.10	0.91± 0.10	0.83± 0.17	1.00 ± 0.08	0.73± 0.10	1.09± 0.13	1.01± 0.11	11.15± 0.19
Cold stress (4°C)	3 hours	0.35± 0.08	0.62± 0.31	0.62± 0.07	0.35± 0.23	0.44± 0.08	0.54± 0.16	0.71± 0.08	0.53± 0.14	0.18± 0.18	0.53± 0.14	0.18± 0.18	0.63± 0.18	5.84 ± 0.36
	6 hours	0.75± 0.09	1.41± 0.15	0.85± 0.18	0.83± 0.14	0.95± 0.27	1.03± 0.09	1.03± 0.07	0.85± 0.18	1.03± 0.07	0.74± 0.23	0.57± 0.29	0.74± 0.08	10.88± 0.33
	9 hours	1.40± 0.18	2.20± 0.23	1.20± 0.16	1.10± 0.20	1.40± 0.20	1.81± 0.19	1.60± 0.10	1.10± 0.27	1.20± 0.31	1.21± 0.36	0.90± 0.15	0.99± 0.25	16.40± 0.37

Mean ± S.E. Values followed by the superscript differ at  $p < 0.05$  among treatments by the DMRT

Abbreviations – **Sa**: Secondary association; **St**: Stickiness; **Un**: Unorientation; **Pr**: Precocious movement; **Uni**: Univalents; **Mt**: Multivalents; **Dsp**: Disturbed polarity; **Br**: Bridge; **Lg**: Laggard formation; **TAB %**: Total Abnormality Percentage.



**Figure 4.** Cytological plate- **A**: Normal metaphase I (7 bivalents), **B**: Normal anaphase I (7:7 migration), **C**: Clumping at metaphase I, **D**: Multivalent at metaphase I, **E**: Precocious movement at metaphase I, **F**: Univalents at metaphase I, **G**: Stickiness with unorientation at metaphase II, **H**: Unoriented precocious metaphase II, **I**: Unoriented laggard formation at anaphase I, **J**: Disturbed polarity at anaphase II, **K**: Tripolarity, **L**: Sterile pollens. Scale Bar 1cm= 10.50  $\mu$ m.



**Figure 5.** Effect of temperature stress on pollen fertility in *Cyamopsis tetragonoloba* (L.) Taub.

### 3.3. Influence of Temperature Stress on Yield Parameters

Yield contributing traits were also recorded, and it was found that ambient temperature is required for high-throughput quantitative results. Yield attributes such as pods per cluster, cluster per plant, seeds per pod and pod length were all investigated (as shown in Table 2). Apparently, both heat and cold-stress responses resulted in alteration in the quantitative attributes. However, cold stress resulted in more profound losses than the heat-stress. Data of cluster per plant was calculated to be  $13.66 \pm 0.57^a$  in the control which declined to  $12.66 \pm 0.88^c$  (heat stress) and  $9.00 \pm 0.57^c$  (at cold stress) after nine hours of treatment. In the control, pod per cluster, was calculated to be  $5.00 \pm 0.57^a$ , whereas at heat stress, it was calculated to be  $4.66 \pm 0.66^a$  (after three hours of treatment) and  $3.66 \pm 0.88^a$  (after nine hours of treatment). In the case of cold stress, pod per cluster was documented to be  $4.00 \pm 0.57^b$  after three hours of treatment, and declined to  $2.33 \pm 0.33^c$  after nine hours of treatment. Pod length was also measured; the value of which was  $6.82 \pm 0.17^a$  (in the

control), whereas at the longest duration of heat-stress, it was recorded to be  $4.28 \pm 0.36^c$ . After nine hours of cold-stress treatment, it was found to be  $3.79 \pm 0.28^c$ . The number of seeds per pod in the case of the control was

$8.33 \pm 0.33^a$ , which declined to  $6.33 \pm 0.33^a$  (heat stress) and was  $4.66 \pm 0.87^b$  (cold stress) for the longest duration of time.

**Table 2.** A comparison of the impact of temperature stress on yield attributes in *Cyamopsis tetragonoloba* (L.) Taub.

Treatment	Exposure time	Cluster/ plant (Mean $\pm$ SE)	Pods/cluster (Mean $\pm$ SE)	Pod length (Mean $\pm$ SE)	Seeds/pod (Mean $\pm$ SE)
Control	-	$13.66 \pm 0.88^a$	$5.00 \pm 0.57^a$	$6.82 \pm 0.17^a$	$8.33 \pm 0.33^a$
Heat stress (50°C)	3 hours	$13.55 \pm 0.71^a$	$4.66 \pm 0.66^a$	$6.08 \pm 0.32^a$	$8.00 \pm 0.57^a$
	6 hours	$14.47 \pm 0.53^a$	$4.33 \pm 0.33^a$	$4.85 \pm 0.35^b$	$7.66 \pm 0.88^a$
	9 hours	$12.66 \pm 0.88^c$	$3.66 \pm 0.88^a$	$4.28 \pm 0.36^b$	$6.33 \pm 0.33^a$
Cold stress (4°C)	3 hours	$15.33 \pm 0.33^b$	$4.00 \pm 0.57^b$	$5.27 \pm 0.16^b$	$7.66 \pm 0.88^a$
	6 hours	$11.00 \pm 0.57^c$	$3.33 \pm 0.33^{bc}$	$4.02 \pm 0.09^c$	$6.00 \pm 0.57^{ab}$
	9 hours	$9.00 \pm 0.57^c$	$2.33 \pm 0.33^c$	$3.79 \pm 0.28^c$	$4.66 \pm 0.88^b$

Data representing Mean values followed by lowercase letters represent Standard errors that are statistically significant at  $P \leq 0.05$ .

#### 4. Discussion

Understanding how different plants cope with stress during their reproductive (gametophytic) phase is critical in managing the future of agricultural productivity (Zinn *et al.*, 2010).

##### 4.1. Impact of Temperature on Morphological Behaviour

Ambient temperature is a pre-requisite for the survivability as well as perpetuation of plants. Temperature is a critical environmental cue that influences the seedling establishment. A slight difference of only few degrees may inevitably lead to notable changes in the growth and survival rate of plants (Salisbury and Ross, 1985). Plants exposed to low temperatures had marks of injuries as a result of the chilling stress. Chilling stress has been found to cause membrane disruption; according to Steponkus (1984), the most malicious effects of chilling stress are membrane damaging and loss of fluidity and dehydration. Heat-induced chlorosis is reported in the present work; it has also been reported in mung bean (Kumar *et al.*, 2011) and chickpeas (Kumar *et al.*, 2013).

Low survivability was observed at longer durations of both stresses with respect to the control due to temporal constraints. This is the case because temperature above and below the threshold limit is tough to be endured as the inclusive metabolic cues get affected. As far as flowering is concerned, the seedlings that were subjected to low temperature, reached their blooming and flowering stages late in comparison with the control at the exposure to heat stress. Flowering is a very crucial stage in plants, since it directly affects the seed yield. It is regulated by an elaborate network of genetic pathways responsive to endogenous and environmental stimuli (Andrés and Coupland, 2012). Perhaps, the plausible reason for this is that the plant initially had a retarded metabolism which affected the growth responses. With reimbursement after the initial distortion, the plants started to flourish. Exposure to a short-term cold stress, or an overexpression of cold-responsive genes, delays flowering by activating Flowering Locus C (FLC) (Seo *et al.*, 2009), whereas the delay in flowering at the exposure to heat stress correlates

with the reduced expression of FLOWERING LOCUS T-like 3 (FTL3), an FT homologue (Nakano *et al.*, 2013)

##### 4.2. Impact of Temperature on Cytogenetical Behaviour

In this study, the reproductive stage, which is an extremely critical stage, was found to be sensitive to temperature stresses. Both heat and cold stresses had led to disturbances in the sequential cellular cascade. In the process of microsporogenesis, the effects of cold and heat stresses are expressed in the form of blockage of meiosis, abnormal meiosis, and abnormal tapetal development (Whyte, 1975). Spindle dysfunctioning and malfunctioning are often linked to temperature-stress introduced ramifications of meiosis. Callan (1942) with *Triton* showed that low temperature manipulation can be used for the joint control of spindle development, spiralization, and nucleic acid metabolism. Similar results were recorded for high temperatures (5 hours to 2 days at 30°-40° C) at mitosis and meiosis *e.g.* PMC of *Fritillaria* (Barber, 1940).

Chromosomal stickiness is characterized by chromosomal clustering during any phase of the cell cycle which may be attributed to genetic and environmental factors (Pagliarini, 2000). It may result from the defective functioning of specific nonhistone proteins involved in the chromosomes organization, which is needed for chromosome separation and segregation (Gaulden, 1987). Chromosomal pairing and synapsis is essential for the organization of bivalents. Some sorts of mutations in the cohesion proteins might lead to univalents (Kumar and Dwivedi, 2015). Cold-stress-sponsored disruption of synaptonemal complex affects the synaptic precision, and the failure to withhold the bivalents together might result in univalents. The bridges observed seem to be a result of the non-separation of chiasma due to stickiness (Kumar and Rai, 2007). The disturbed polarity and unorientation occurred as a result of the shifting of poles or because of spindle malfunctioning.

Pollen viability, an important criterion that regulates fidelity of fertilization, is a result of male meiotic events, and can assist in examining the effects communicated by temperature fluctuations on the reproductive stages. Heat stress proved to be comparatively less lethal for pollens compared with chilling stress. At low temperatures, lower levels of sucrose, glucose and fructose result in the



starvation of developing microspores which causes pollen sterility (Parish *et al.*, 2012). Heat stress can also cause pollen sterility by reducing carbohydrate deposition in pollen grains (Jain *et al.*, 2007) which induces tapetum degradation (Sakata *et al.*, 2000). High temperatures may even affect the endoplasmic reticulum structure, and block its function in the tapetum causing earlier-than-usual degeneration of the tapetum (Omae *et al.*, 2012). This degradation of the nutritive tissues of the tapetum may lead to pollen sterility. Carbohydrate mobilization of the tapetum and its genetic control may play an important role in the pollen development under stress conditions. Improvement of stress tolerance in crop species will, therefore, require a better understanding of the effects of stress on the sporophyte, as well as on the sporophyte-gametophyte communication (Pacini and Dolferus, 2016).

#### 4.3. Impact of Temperature on Yield Parameters

According to Maulana and Teso (2011), cold-temperature stress at the seedling stage reduced the seedling vigour and dry weight significantly, and also delayed the time to reach flowering and maturity; these results are similar to those obtained in the present study. Alvarado and Hernaiz (2007) also reported a delay of maturity in rice due to the impact of low temperatures. Kazan and Lyons (2016) maintained that if flowering occurs prematurely under stressful environments, seed-set and grain filling may be compromised. Longer durations of stress for both sets had hampered the floral genesis, which resulted in less flowering and in the formation of rudimentary sterile flowers. It was found that yield contributing traits were negatively affected by low temperature ranges. Heat stress also led to a decline in the yield. In comparison, cold stress was more lethal for the yield attributes; similar results were obtained by Thakur *et al.*, (2010). Temperatures below 15°C abort chickpea flowers and reduce the number of pods per plant, and seeds per pod (Nayyar *et al.*, 2005; Kaur *et al.*, 2011). Barlow *et al.*, (2015) revealed that frost led to the sterility and abortion of formed grains in wheat (*Triticum aestivum* L.), while excessive heat had caused a reduction in the grains number. Suzuki *et al.*, (2001) reported a correlation between pollen fertility and pod setting in that poor pollen fertility led to low pod and seed setting.

Studies related to heat stress revealed that plants had an intrinsic adaptability potential. Plants can alter their metabolism in various ways in response, particularly by producing compatible solutes that are able to organize proteins and cellular structures, maintain cell turgor by osmotic adjustment, and to modify the antioxidant system to re-establish the cellular redox balance and homeostasis (Valliyodan and Nguyen, 2006; Munns and Tester, 2008).

## 5. Conclusion

The examination of stress and stress-related responses in plants is critical for devising stress-amelioration measures. The cardinal stages in a life cycle are growth and morphogenesis, flowering, and seed setting. These stages are intimately interwoven in a chain. The current study concludes that plants overall growth parameters including survival, microsporogenesis, and yield attributes are significantly influenced by stress. The investigation of the cytogenetical and the morphological parameters has

shown that optimal temperature is a basic requirement for the vitalization to the living cells. Proper understanding is thus essential for stress-tolerance engineering. Sincere future attempts will enhance plants survivability and adaptation to hostile environment

## Acknowledgements

Authors are thankful to the Central Arid Zone Research Institute (CAZRI, Rajasthan) for providing the seeds of cluster beans. They also express their gratitude to the lab members of Plant Genetics Laboratory for their help and support.

## References

- Allen DJ and Ort DR. 2001. Impacts of chilling temperatures on photosynthesis in warm-climate plants. *Trends in Plant Sci*, **6**: 36–42.
- Alvarado R and Hernaiz S. 2007. Antecedentes generales sobre el arroz en Chile, in *Arroz Manejo Tecnológico*, R. Alvarado, Ed., 162 of Boletín INIA. 179, Instituto de Investigaciones Agropecuarias INIA, Centro Regional de Investigación Quilamapu, Chillán, Chile.
- Andrés F and Coupland G. 2012. The genetic basis of flowering responses to seasonal cues. *Nature Rev Genet*, **13**: 627–639.
- Asolkar LV, Kakkar KK and Chakra OJ. 1992. Glossary of Indian medicinal plants with active principles, Part I (Publications and Information Directorate, CSIR New Delhi). 245.
- Barber HN. 1940. The suppression of meiosis and the origin of diplochromosomes. *PRSB*, **128**: 170–85.
- Barlow KM, Christy BP, O'Leary GJ, Riffkin PA and Nuttall JG. 2015. Stimulating the impact of extreme heat and frost events on wheat crop production: a review. *Field Crops Res*, **171**: 109–119.
- Barnabas B, Jager Kand Feher A. 2008. The effect of drought and heat stress on reproductive processes in cereals. *Plant, Cell Environ*, **31**: 11–38.
- Bione ICP, Pagliarini MS and Toledo JFF. 2000. Meiotic behavior of several Brazilian soybean varieties. *Genet Mol Biol*, **23**: 23–631.
- Callan HG. 1942. Heterochromatiri in *Triton*. *PRSB*, **130**: 324–335.
- Chinnusamy V, Zhu J and Zhu JK. 2007. Cold stress regulation of gene expression in plants. *Trends in Plant Sci*, **12**: 444–451.
- Gaulden ME. 1987. Hypothesis: some mutagens directly alter specific chromosomal proteins (DNA topoisomerase II and peripheral proteins) to produce chromosome stickiness, which causes chromosome aberrations. *Mutagenesis*, **2**: 357–365.
- Hasanuzzaman M, Nahar K and Fujita M. 2013. Extreme temperatures, oxidative stress and antioxidant defense in plants. In: **Abiotic Stress: Plant Responses and Applications in Agriculture**; Vahdati K. and Leslie C. (Eds.), In Tech: Rijeka, Croatia; pp. 169–205.
- Hatfield JL and Prueger JH. 2015. Temperature extremes: effect on plant growth and development. *Weather and Climate Extremes*, **10**: 4–10.
- Hedhly A, Hormaza JI and Herrero M. 2008. Global warming and plant sexual reproduction. *Trends in Plant Sci*, **14**: 30–36.
- IPCC, 2013: Climate Change 2013: **The Physical Science Basis. Contribution of Working Group I to the Fifth Assessment Report of the Intergovernmental Panel on Climate Change**, Stocker TF, Qin D, Plattner G-K., Tignor M, Allen SK, Boschung J, Nauels A, Xia Y, Bex V and Midgley PM. (Eds.).

Cambridge University Press, Cambridge, United Kingdom and New York, NY, USA, 1535 pp

Jain M, Prasad PVV, Boote KJ, Hartwell AL, Chourey PS. 2007. Effects of season-long high temperature growth conditions on sugar-to-starch metabolism in developing microspores of grain sorghum (*Sorghum bicolor* L. Moench). *Planta*, **227**: 67–79.

Kaur G, Kumar S, Thakur P, Malik JA, Bhandhari K, Sharma KD and Nayyar H. 2011. Involvement of proline in response of chickpea (*Cicer arietinum* L.) to chilling stress at reproductive stage. *Sci Hortic*, **128**: 174–181.

Kazan K and Lyons R. 2016. The link between flowering time and stress tolerance. *J Exp Bot*, **67**: 47–60.

Kellogg EA and Bennetzen JL. 2004. The evolution of nuclear genome structure in seed plants. *Am J Bot*, **91**: 1709–1725.

Kumar G and Rai P. 2007 EMS Induced Karyomorphological Variations in Maize (*Zea mays* L.) Inbreds. *Turk J Biol.*, **31**: 187–195

Kumar G and Dwivedi H. 2015. Ethyl methane sulphonate induced desynaptic variants in ajwain (*Trachyspermum ammi* (L.) Sprague). *Jordan J Biol Sci*, **8**: 237–241.

Kumar G and Srivastava A. 2015. Cytomorphological and Biochemical Impact of Temperature stress in Buckwheat (*Fagopyrum esculentum* Moench). *Int J Environ Sci Toxicol Res*, **3**(8): 134–143.

Kumar S, Kaur R, Kaur N, Bhandhari K, Kaushal N, Gupta K, Bains TS and Nayyar H. 2011. Heat-stress induced inhibition in growth and chlorosis in mungbean (*Phaseolus aureus* Roxb.) is partly mitigated by ascorbic acid application and is related to reduction in oxidative stress. *Acta Physiol Plantarum*, **33**: 2091–2101.

Kumar S, Thakur P, Kaushal N, Malik JA, Gaur P and Nayyar H. 2013. Effect of varying high temperatures during reproductive growth on reproductive function, oxidative stress and seed yield in chickpea genotypes differing in heat sensitivity. *Arch Agronomy Soil Sci*, **59**: 23–843.

Marks GE. 1954. An aceto-carminic glycerol jelly for use in pollen fertility counts. *Stain Technol*, **29**: 277.

Maulana F and Teso TT. 2011. Cold temperature episode at seedling and flowering stages reduces growth and yield components in sorghum. *Crop Sci Soc Am*, **53**: 564–574.

Miura K and Frumoto T. 2013. Cold signalling and cold response in plants. *Int J Mol Sci*, **14**: 5312–5337.

Munns R and Tester M. 2008. Mechanisms of salinity tolerance. *Ann Rev Plant Biol*, **59**: 651–681.

Nakano Y, Higuchi Y, Sumitomo K and Hisamatsu T. 2013. Flowering retardation by high temperature in chrysanthemums: involvement of FLOWERING LOCUS T-like 3 gene repression. *J Exp Bot*, **64**: 909–920.

Nayyar H, Bains TS, Kumar S and Kaur G. 2005. Chilling effect during seed filling on accumulation of seed reserves and yield of chickpea. *J Sci Food Agric*, **85**: 1925–1930.

Omae H, Kumar A and Shono M. 2012. Adaptation to high temperature and water deficit in the common bean (*Phaseolus*

*vulgaris* L.) during the reproductive period. *Hindawi Publishing Corporation J Bot*, **6**.

Pacini E and Dolferus R. 2016. The trials and tribulations of the plant male gametophyte-Understanding reproductive stage stress tolerance. In: **Abiotic and Biotic Stress in Plants-Recent Advances and Future Perspectives**; Shanker AK and Shanker C. (Eds.); InTech: Rijeka, Croatia, pp. 703–754.

Pagliarini MS. 2000. Meiotic behavior of economically important plant species: the relationship between fertility and male sterility. *Gene Mol Biol*, **23**: 997–1002.

Parish RW, Phan HA, Iacuone S and Li SF. 2012. Tapetal development and abiotic stress: A centre of vulnerability. *Functional Plant Biol*, **39**: 553–559.

Sakata T, Takahashi H, Nishiyama I and Higashitani A. 2000. Effects of high temperature on the development of pollen mother cells and microspores in barley *Hordeum vulgare* L. *J Plant Res*, **11**: 395–402.

Salisbury FB and Ross CW. 1985. **Plant Physiology**. 3rd Edition. USA: Wadsworth, Inc.

Seo E, Lee H, Jeon J, Park H, Kim J, Noh YS and Lee I. 2009. Crosstalk between cold response and flowering in *Arabidopsis* is mediated through the flowering-time gene SOC1 and its upstream negative regulator FLC. *Plant Cell*, **21**: 3185–3197.

Sharma KD and Nayyar H. 2014. Cold stress alters transcription in meiotic anthers of cold tolerant chickpea (*Cicer arietinum* L.). *BMC Res Notes*, **7**: 717–729.

Siddiqui MH, Al-Khaishany MY, Al-Qutami MA, Al-Whaibi MH, Grover A, Ali HM, Al-Whaibi, MS. 2015. Morphological and physiological characterization of different genotypes of faba bean under heat stress. *Saudi J Biol Sci*, **22**: 656–663.

Singh SK, Kakani VG, Brand D, Baldwin B and Reddy KR. 2008. Assessment of cold and heat tolerance of winter-grown canola (*Brassica napus* L.) cultivars by pollen-based parameters. *J Agro Crop Sci*, **194**: 225–236.

Steponkus PL. 1984. Role of the plasma membrane in freezing injury and cold acclimation. *Annu Rev Plant Physiol*, **35**: 543–584.

Suzuki K, Tsukaguchi T, Takeda H and Egawa Y. 2001. Decrease of pollen stainability of green bean at high temperatures and relationship to heat tolerance. *J Am Soc Hortic Sci*, **126**(5): 571–574.

Thakur P, Kumar S, Malik JA, Berger JD and Nayyar H. 2010. Cold stress effects on reproductive development in grain crops: an overview. *Environ Exp Bot*, **67**: 429–443.

Valliyodan B and Nguyen HT. 2006. Understanding regulatory networks and engineering for enhanced drought tolerance in plants. *Curr Opin Plant Biol*, **9**: 189–195.

Whyte RO. 1975. The geography of abnormal meiosis in plants. *The Nucleus*, **18**: 183–203.

Zinn KE, Tunc-Ozdemir M and Harper JF. 2010. Temperature stress and plant sexual reproduction: uncovering the weakest links. *J Exp Bot*, **61**: 1959–1968



# Delta-Aminolevulinic Acid Dehydratase Inhibition and RBC Abnormalities in Relation to Blood Lead among Selected Jordanian Workers.

Ziad A. Shraideh<sup>1\*</sup>, Darwish H. Badran<sup>2</sup>, Abdelrahim A. Hunaiti<sup>3</sup> and Abdelkader Battah<sup>4</sup>

<sup>1</sup>Department of Biological Sciences, School of Science, <sup>2</sup>Department of Anatomy and Histology, School of Medicine, <sup>3</sup>Department of Clinical Laboratory Sciences, School of Science, <sup>4</sup>Department of Pathology, Microbiology and Forensic Medicine, School of Medicine, The University of Jordan, Amman, Jordan

Received June 18, 2018; Revised August 9, 2018; Accepted September 9, 2018

## Abstract

Lead toxicity is a public health hazard particularly to the occupationally exposed workers. Evidence is mounting successively regarding the adverse health effects of lead at low levels. This study is conducted to assess lead cytotoxicity and the antioxidant status of selected groups of Jordanian workers occupationally exposed to lead poisoning or automobile buffs. A total of ninety male workers were selected for the study. The workers studied included: Radiator welders, exhaust workers, automobile electronics and mechanics, metal workers, and car painters in Amman city. The control group included 20 subjects of the same age group without any occupational exposure to lead. A number of biological parameters have been studied in order to estimate the degree of lead intoxication in the selected worker groups. The groups did not significantly differ among each other in the average of age ( $34 \pm 0.9$ ) and work years ( $17.1 \pm 1.8$ ). The researchers studied the effect of exposure to lead on the activity of  $\delta$ -ALAD (a key enzyme in heme biosynthesis). A significant decrease and a negative correlation between  $\delta$ -ALAD and blood lead were observed in all the studied worker groups. The effect of exposure to lead on the morphology of RBCs was investigated. Fibrillation and particulate structures on the surface of RBCs and irregular plasma membrane evaginations were seen under scanning electron microscope. Determination of blood-lead concentration,  $\delta$ -ALAD activity as well as morphological investigations of RBCs could be beneficial in the evaluation of lead toxicity.

**KeyWords:** Blood lead, Lead toxicity,  $\delta$ -ALAD, RBC morphology, SEM.

## 1. Introduction

The exposure of humans to lead and its adverse health effects is of a global concern because of its ubiquity in the environment. Studies from different countries have revealed that lead poisoning is a problem for urban populations, and more so in developing countries, where there are no (or few) environmental regulations (Ahamed *et al.*, 2006; Ambrogi *et al.*, 1996). Although car emissions from the consumption of leaded gasoline has been the chief source of wide-spread environmental lead contamination in urban areas (Bakalli *et al.*, 1995 and Baghurst *et al.*, 1992). Other sources, such as leaded pipes for water supply, lead-based paints, the use of leaded ceramics and canned food, lead in cosmetics and folk remedies, are good sources of lead exposure, in addition to lead smelters and industrial processes (Baghurst *et al.*, 1992; Bilot, 1992) following the phasing out of leaded gasoline in 2000 in India (Boyd *et al.*, 1981).

Several antioxidant molecules, such as glutathione (GSH) and glutathione disulfide (GSSG) levels, and enzymes, glutathione peroxidase (GPx), superoxide dismutase (SOD), and catalase (CAT) activities are the most commonly used parameters to evaluate lead-induced oxidative damage in animals and occupationally-exposed

lead workers (Burns and Godwin, 1991; Burns *et al.*, 1996 and Bustos and Battle, 1989). The delta-aminolevulinic acid dehydratase ( $\delta$ -ALAD) is the second enzyme in the heme biosynthesis pathway and catalyses the condensation of two molecules of delta-aminolevulinic acid ( $\delta$ -ALA) to porphobilinogen (PBG), with the thiol (SH) group essential for its activity. Because of its affinity with the SH group, lead is known to inhibit  $\delta$ -ALAD activity (Dacie and Levis, 1984), resulting in the accumulation of d-ALA. The latter has been shown to undergo metal catalyzed autooxidation and give rise to the formation of reactive oxygen species (ROS) as superoxide ion ( $O_2^{\cdot -}$ ), hydroxyl radical ( $OH^{\cdot}$ ) and hydrogen peroxide ( $H_2O_2$ ). This possibility implies that  $\delta$ -ALAD inhibition, in addition to being a biochemical indicator of lead toxicity, might also be a promising indicator of lead-induced oxidative stress.

## 2. Material and Methods

### 2.1. Worker Groups

Blood samples were obtained from ninety male occupational workers in Amman city. The Jordanian workers were divided into six categories (fifteen workers each) including: Radiator welders, exhaust workers, automobile electronics and mechanics, metal workers and car painters. Blood samples of the control group were obtained from twenty males of non-exposed persons.

\* Corresponding author e-mail: zshraideh@ju.edu.jo.

## 2.2. Determination of Blood Lead

Blood lead levels were determined according to the method described by Shraideh *et al.* (2018). Using a graphite furnace, atomic absorption spectrophotometer and blood lead contents were expressed as  $\mu\text{g/dL}$ .

## 2.3. Determination of $\delta$ -ALAD Activity

### 2.3.1. Principle

The enzyme  $\delta$ -ALAD which is found in RBC's converts two units of  $\delta$ -ALA to one unit of PBG in peripheral blood; the reaction stops at this monopyrrole stage rather than proceeding to porphyrin. Therefore,  $\delta$ -ALAD activity in erythrocyte can be determined simply by incubating a sample of peripheral blood with ALA and measuring the PBG spectrophotometrically. The formed PBG (aromatic amine) condenses with *p*-dimethylaminobenzaldehyde to produce a cherry red- color.

### 2.3.2. Preparation of Reagent for Enzymatic Measurements

1. 0.2 g of Triton X-100 reagent were dissolved in 100 mL double deionized distilled water.
2. 16.8 mg of  $\delta$ -ALA hydrochloride substrate were dissolved in 10 mL of 0.25 M citrate-phosphate buffer of pH 6.6 using a pH meter.
3. 0.25 g of *N*-ethylmaleimide were dissolved in 40 mL of warm double deionized distilled water, then 10 g of trichloroacetic acid were added, and the final volume was completed to 100 mL in a volumetric flask to prepare the protein precipitant reagent.
4. On the day of the test, 9.33 mL of 60 % perchloric acid were completed to 50 mL with *p*-dimethylbenzaldehyde in a volumetric flask to prepare Erlich'sh reagent.

### 2.3.3. Procedure

Heparinized blood samples were drawn on the day of test and the hematocrit value was determined on aliquot. Enzyme assay was performed on freshly drawn blood samples. The procedure of Tietz (1987) was followed. It consists of the following steps:

0.2 mL of blood was added to 1.3 mL of Triton X-100 reagent causing immediate hemolysis. 1 mL of the buffered  $\delta$ -ALAD substrate was added to the mixture, and mixed well. Before incubation, 1 mL of the mixture was removed immediately for the blank, and was added to a tube containing 1 mL of protein precipitant. The remainder of the reaction mixture was covered, and incubated at 38°C for one hour. 1.5 mL of protein precipitate were added immediately at the end of the incubation period. After centrifugation, 1.5 mL of the supernatant solution (Blank and test) were removed, then 1.5 mL of the modified Ehrlich's reagent was added. Color was measured at 555 nm after fourteen minutes using PYE UNICAM SP-6-350 spectrophotometer (PYE UNICAM, Ltd-Cambridge/England). The activity of  $\delta$ -ALAD was calculated according to the formula:

Units  $\delta$ -ALAD / mL erythrocyte=

$$(A_{\text{test}} - A_{\text{blank}}) \times 100 \times 12.5 \times 1.0/0.1 \times \text{hematocrit}$$

Where: 100/hematocrit = correction for erythrocyte fraction of whole blood 12.5= dilution factor of the blood

0.1= correction for the definition of enzyme activity one unit being defined as an increase in  $A_{555}$  of 1.100 (1.0 cm light path) per h at 38°C

## 2.4. Erythrocyte Morphology (Scanning Electron Microscopy (SEM) Preparation):

Nine grams of NaCl were added to 1 L of 0.15 M isosmotic phosphate buffer solution of pH 7.4 to have phosphate-buffer saline (PBS) (Dacie and Levis, 1984).

Erythrocytes were fixed with 1.25 % (w/v) glutaraldehyde in PBS, and were kept at 4°C as described by Bilot (1992). After two washes with PBS, cells were dehydrated in a series of alcohol [from 30 to 100 % (v/v) ethanol]. First, the pellets were suspended in 30 % ethanol, mixed and kept for ten minutes, then were centrifuged for two minutes at 2000 rpm. The same procedure was repeated with 50, 70, 90 and 100 % ethanol. Finally, pellets were suspended in 100 % ethanol, and gently dropped onto a glass coverslip that had been cleaned with ethanol. The samples mounted on glass slide were gold-coated by the sputtering method at 1200v, 20 mA for 165 seconds using polaron E6100 coater. Specimens were viewed and photographed by Vega 3 TESCAN SEM, 19 Kv.

## 2.5. Statistical Tests

In all statistical analysis, 'students' *t*-test was used to compare the means of two groups. It determines whether the two means are significantly different or not at  $P < 0.05$ . In addition, analysis of variance (ANOVA) was used to determine if mean values are significantly different among different worker groups or not at  $P < 0.05$ .

Correlation coefficients (*r* values) were also calculated to determine whether the two variables are related positively (up to +1), negatively (down to -1), or not at all (0). It was used to determine the relation between Blood-Pb level and  $\delta$ -ALAD activity.

## 3. Results

### 3.1. Worker Groups

For this study, blood was collected from ninety Jordanian workers distributed over six different work groups as shown in table 1.

**Table 1.** Distribution of workers in worker groups (TRT).

TRT#	Number	Worker
1	15	Radiator Welders
2	15	Exhaust Workers
3	15	Automobile Electronics
4	15	Car painters
5	15	Mechanics
6	15	Metal workers

### 3.2. Blood- Pb Concentration in Occupational Worker

A comparison between Blood -Pb levels in different types of work groups is shown in Table 2. The blood samples were obtained from ninety males of occupational workers in Amman city. The Jordanian workers were divided into six categories (fifteen workers each) including: Radiator welders, exhaust workers, automobile electronics and mechanics, metal workers and car painters. The blood samples of the control group were obtained from twenty males of non-exposed persons.

Blood-Pb concentrations for all individuals were measured, and Table 2 shows the results obtained according to the occupation. The results indicated that there is a significant increase in the mean values of blood-

Pb concentration in the studied groups compared to the control group. Also, there was a significant difference in blood lead among the different worker groups (Group 3 showed the highest increase).

**Table 2.**  $\delta$ -ALAD activity (U/ mL) and B: blood [pb] among TRT ( $\mu$ g/dl) among workers group

TRT#	A: Mean $\pm$ S E	B: Mean $\pm$ S E
1.	170 $\pm$ 7	14.5 $\pm$ 1.4
2.	160 $\pm$ 6	16.4 $\pm$ 1.2
3.	140 $\pm$ 6	21.0 $\pm$ 1.6
4.	165 $\pm$ 6	15.0 $\pm$ 1.3
5.	160 $\pm$ 6	15.0 $\pm$ 1.7
6.	165 $\pm$ 7	15.0 $\pm$ 1.6
7. (control)	220 $\pm$ 9	4.3 $\pm$ 0.5

SE= Standard Error

### 3.3. $\delta$ -ALAD activity in occupational workers:

The researchers studied the effect of exposure to lead on the activity of  $\delta$ -ALAD (key enzyme in heme biosynthesis). A significant decrease and a negative correlation between  $\delta$ -ALAD and blood lead (Table 2) were observed in all the studied worker groups (Table 2).

$\delta$ -ALAD activity was determined for all the blood samples obtained and was calculated as shown in Table 2. The control group has the maximum  $\delta$ -ALAD activity (220  $\pm$  9 U/ mL). In the worker groups that are occupationally exposed to lead, the  $\delta$ -ALAD activity ranged from 140 U/mL to 160 U/mL with a mean value of  $\pm$  SD of 160  $\pm$  6.3U/mL. Automobile electronics, with the highest blood lead concentration, show the lowest  $\delta$ -ALAD activity (140 U/ mL). On the other hand, the control group had a maximum value of (220  $\pm$  9 U/ mL).

When the  $\delta$ -ALAD activities of the workers were compared with the control group, significant differences were observed between the mean values of the control group and each of the other study's groups. In addition, there were significant differences ( $P < 0.05$ ) in the means of  $\delta$ -ALAD activity among the groups using ANOVA test.

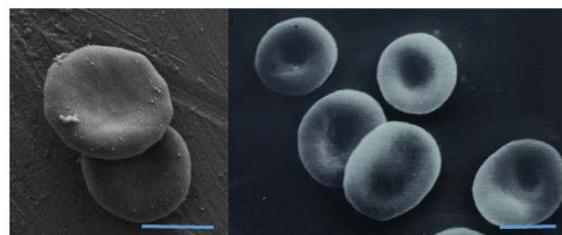
When the correlation between  $\delta$ -ALAD activity and blood-Pb level was studied, a significant negative correlation ( $r = -0.44$ ) was observed between the blood-Pb level and  $\delta$ -ALAD activity in exhaust workers at ( $P < 0.05$ ). No correlations were observed in radiator welders, automobile electronics and car painters. However, when the whole samples were studied together, there was a negative correlation ( $r = -0.41$ ) between blood-Pb level and  $\delta$ -ALAD activity at ( $P < 0.05$ ).

### 3.4. Erythrocyte Morphology:

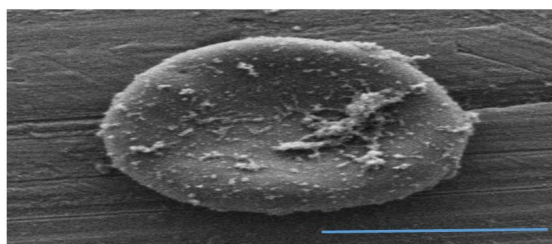
The examination of the blood samples using scanning electron microscopy (SEM) revealed shape abnormalities and morphological changes in erythrocytes. In every worker group, one or more of the following erythrocyte abnormalities was observed: fibrillar and particulate matter on the surface of RBCs, acanthocytes with irregular RBC boundary, target cell with a central membrane evagination and irregular cell shape with many membrane evaginations. Sometimes more than one abnormality was observed in the same individual.

Morphological changes in erythrocytes can be seen in SEM micrographs of representative worker cases (Figures 2-9).

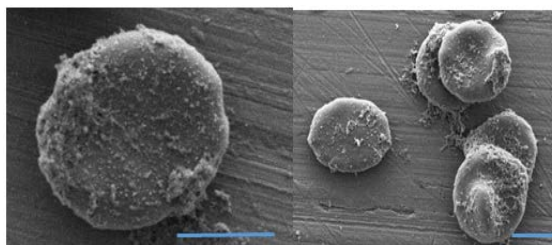
Figure 1 shows SEM of RBCs of control individuals not exposed to occupational lead contamination. Figure 2 shows RBC of radiator welders with fibrillar structures on the surface of RBCs. Figure 3 shows RBC of exhaust workers with acanthocytes, fibrillar structures and membrane evaginations. Figure 4 shows RBC of Automobile electronics workers with acanthocyte and target cell abnormalities. Figure 5 shows RBC of car painters with target cell and surface fibrillar abnormalities. Figure 6 shows RBCs of mechanics with surface fibrillar abnormalities. Figures 7 and 8 show RBC of metal workers with target cell and surface fibrillar abnormalities. These abnormalities will badly affect the normal functions of RBCs.



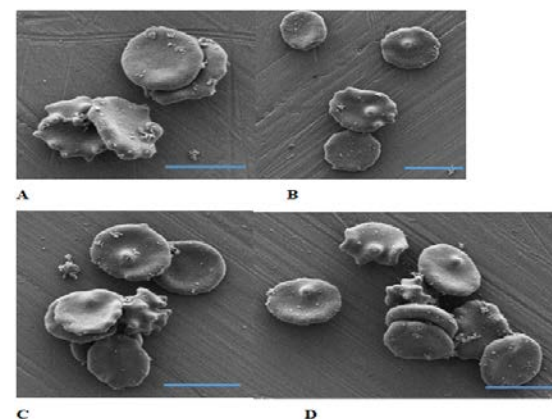
**Figure 1.** SEM of RBCs of two control individuals, not exposed to occupational lead contamination. Scale bar = 5 microns.



**Figure 2.** RBC of radiator welder with fibrillar structures on the surface of RBCs. Scale bar = 5 microns.

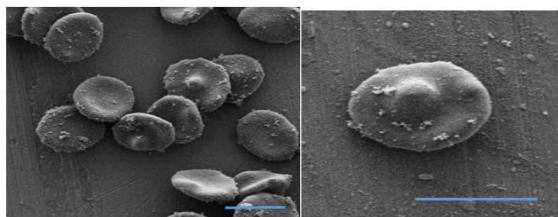


**Figure 3.** RBC of exhaust workers with acanthocytes, fibrillar structures, and membrane evaginations. Scale bar = 4 microns.

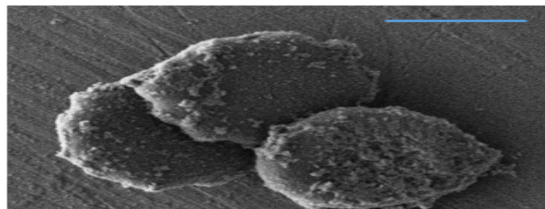


**Figure 4.** Shows RBC electronics workers with acanthocyte and target cell abnormalities. Scale bar = 7 microns.

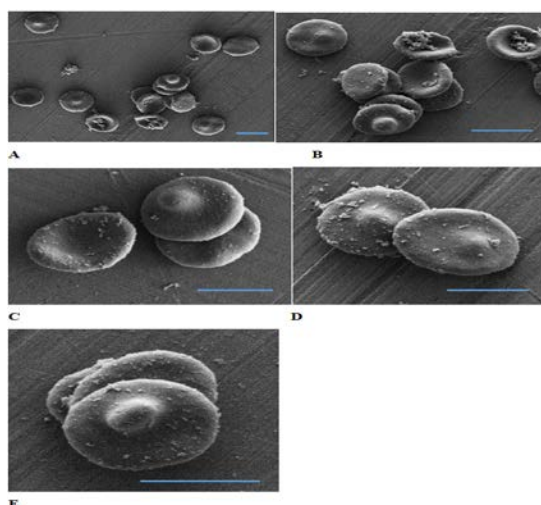




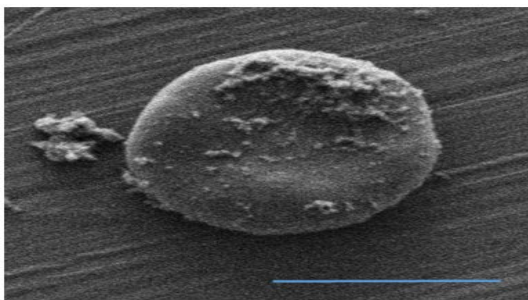
**Figure 5.** RBC of car painters with target cell and surface fibrillar abnormalities. Scale bar = 7 microns.



**Figure 6.** RBCs of mechanics with surface fibrillar abnormalities. Scale bar = 5 microns.



**Figures 7.** RBC of metal workers with target cell and surface fibrillar abnormalities. Scale bar (A and B) = 7 microns, (C, D, E) = 5 microns.



**Figure 8.** RBC of metal worker with surface fibrillar abnormalities. Scale bar = 5 microns.

## 4. Discussion

### 4.1. $\delta$ -ALAD Activity in Occupational Workers

In the present study, significant differences ( $P < 0.05$ ) were observed between the control group and each of the studied groups, as well as among groups. Automobile electronics have the lowest mean value (140 U/ml), followed by exhaust workers and mechanics (160 U/ml). Car painters and metal workers have equal mean values (165 U/ml). Radiator welders have the highest mean value (170 U/ml), whereas the control group has a mean value

of 220 U/ml. On the other hand, a significant negative correlation ( $r = -0.41$ ) was observed between blood-Pb level and  $\delta$ -ALAD activity in occupational workers at  $P < 0.05$ .

La-Llave-Leon *et al.* (2017) described an association between blood lead levels and Delta-Aminolevulinic Acid Dehydratase in pregnant women.

The inhibition of enzymes in the heme biosynthesis pathway serves as potentiality important biological indicators of chemical exposure and cell injury (Goering and Rehm, 1990). Lead plays a dual role as both pseudo substrate and inhibitor of enzyme  $\delta$ -ALAD, hence  $Pb^{+2}$  acts as a parabolic competitive inhibitor of the enzyme.

The enzyme results of the present study are consistent with what have been reported in previous studies. Inhibitors of  $\delta$ -ALAD is well-documented and the accumulation of the substrate of this enzyme (i.e.  $\delta$ -ALAD) is reported in individuals exposed to lead (Dacie and Levis, 1984). In north Australia, Burns *et al.* (1996) found significant differences between blood-Pb level and  $\delta$ -ALAD activity in the sniffers of leaded and unleaded petrol. In addition, the results could be explained in the light of molecular biology. Polymorphism in  $\delta$ -ALAD may be associated with difference in blood-Pb levels. Individuals who inherited ALAD2 allele are more susceptible to lead poisoning than individuals who inherited ALAD1 allele (Smith *et al.*, 1995).

Stanley and Resco (1996) found that elevated tissue lead concentrations and depression of  $\delta$ -ALAD activity in blood of small mammals was significant at the 0.05 level. Lead supplementation to broiler chickens caused a linear decrease in  $\delta$ -ALAD activity (Bakalli *et al.*, 1995). Chunping *et al.* (2011) demonstrated that lead exposure suppressed ALAD transcription by increasing methylation level of the promoter CpG islands. Furthermore, Baghurst *et al.* (1992), found that the activity of  $\delta$ -ALAD was negatively correlated with blood-Pb level in Granite City where a former secondary lead smelter was in operation, and the surrounding area was heavily contaminated with lead. On the other hand, Ahamed *et al.* (2006) demonstrated the inhibition of  $\delta$ -ALAD activity in relation to blood lead.

### 4.2 Erythrocyte Morphology

In lead toxicity erythropoietic cells of the bone marrow undergo morphological changes resulting in increased production of abnormal erythrocytes (i.e. stippled erythroblasts have nuclear abnormalities, variation in cell size and inadequate hemoglobin).

The inhibition of P5N brings about the intracellular accumulation of pyrimidine nucleotides with consequent metabolic changes causing an accelerated destruction of erythrocytes. The hemolytic component of the anemia of lead poisoning may be explained therefore by the basis that the excess nucleotides diverts ATP activity from important metabolic functions consequently resulting in red-cell membrane damage (Tietz, 1987).

Acanthocytosis can be attributed to alterations in the structure, contours and surface properties of the red cell-membrane, resulting from the abnormal phospholipids metabolism (Dacie and Levis, 1984).

## 5. Conclusion

- Occupational workers dealing with radiators, exhausts, electronics and car painters are at risk of developing lead poisoning; they should, therefore, take protection



steps against lead poisoning. These steps may include medical monitoring, educating the workers, and following the safety rules.

- Subclinical cases of lead poisoning may develop abnormal hematological parameters and RBC abnormalities.

### Acknowledgement

The authors are thankful to the SRSF for providing funding for this work (SRSF-Project # MPH/2/02/2014).

### References

- Ahamed M, Verma S, Kumar A and Siddiqui MKJ. 2006. Delta-aminolevulinic acid dehydratase inhibition and oxidative stress in relation to blood lead among urban adolescents. *Hum Exper Toxicol.*, **25**(9): 547-553.
- Ambrogi C, Cardini J, Baldi S B, Cini S B, Cini C C, Buzzigoli J, Quinones-Galvan A and Frannini E. 1996. Delta – aminolevulinic acid dehydratase and zinc protoporphyrin in very low lead exposed pets: a community study. *Vet Hum Toxicol.*, **38**(5):336-9.
- Bakalli R I, Pesti G M., Ragland W L, Konjufca V and Novak R. 1995. Delta – aminolevulinic acid dehydratase: a sensitive indicator of lead exposure in broiler chicks (*Gallus domesticus*). *Bull Environ Contam Toxicol.*, **55**(6):833-9.
- Baghurst P A, McMichael A J, Wigg N R, Vimpani G V, Robertson E F, Roberts R J and Tong S L. 1992. Environmental exposure to lead and children's intelligence at the age of seven years. The Port Pirie Cohort study. *N Engl J Med.*, **327**(18):1279-84.
- Baghurst P A, Tong S.L., McMichael, A.J., Robertson, E.F., Wigg, N. R. Vimpani, G. V. 1992. Determination of blood lead concentrations to age 5 years in a birth cohort study of children living in the lead smelting city of Port Pirie and surrounding areas. *Arch Environ Health.*, **47**(3):203-10.
- Bilto Y Y. 1992. Effects of cholesterol, lipostabil and gemfibrozil on erythrocyte deformability. *Dirasat.*, **20B**(4): 112-22.
- Boyd S D, Wasserman G S and Green V. A. 1981. Lead arsenate ingestion in eight children. *Clin. Toxic.*, **18**: 489-91.
- Burns C B and Godwin I. R. 1991. A comparison of the effects of inorganic and alkyl lead compounds on human erythrocytic delta-aminolevulinic acid dehydratase (ALAD) activity *in Vitro*. *J Appl Toxicol.*, **11**(2):103-10.
- Burns C B, Currie B J and Powers J R. 1996. An evaluation of unleaded petrol as harm reduction strategy for petrol sniffers in an aboriginal community. *J.Toxicol.*, **34**(1): 27-36.
- Bustos N L and Batlle A. M. 1989. Enzyme replacement therapy in porphyries- V. *In vivo* correction of delta- aminolevulinic acid dehydratase defective in erythrocytes in lead intoxicated animals by enzyme- loaded red blood cell ghosts. *Drug Des Deliv.*, **5**(2): 125-31.
- Chunping, L., Ming, Xu., Sumeng, W., Xiaolin Y., Shourong, Z., Jingping, Z., Qizhan, L., and Yujie, S. 2011. Lead exposure suppressed ALAD transcription by increasing methylation level of the promoter CpG islands. *Toxicol Lett.*, **203**(1): 48-53.
- Dacie, J. V. and Lewis, S. M. **Practical Hematology**, sixth ed. 1984. Churchill Livingstone, UK, pp. 453.
- Goering, P.I. and Rehm, S. 1990. Inhibition of liver, kidney and erythrocyte delta-aminolevulinic acid dehydratase (porphobilinogen synthase) by gallium in the rat. *Environ Res.*, **53**(2):135-51.
- La-Llave-Leon, O., Méndez-Hernández, EM., Castellanos-Juárez, FX, Esquivel-Rodríguez, E., Vázquez-Alaniz, F, Sandoval-Carrillo, A, García-Vargas, G., Duarte-Sustaita, J, Candelas-Rangel, J.L. and Salas-Pacheco, J.M. 2017. Association between Blood Lead Levels and Delta-Aminolevulinic Acid Dehydratase in Pregnant Women. *Int J Environ Res Public Health.*, **14**(4): 432-441.
- Shraideh Z, Badran D, Abdelrahim H and Battah A. 2018. Association between occupational lead exposure and plasma levels selected oxidative stress related parameters in Jordanian automobile workers. *Inter J Occupational Med Environ Health*, **31**(4): 1-9.
- Smith, C. M., Wang, X., Hu, H. and Kelsey, K. T. 1995. A polymorphism in the delta-aminolevulinic acid dehydratase gene may modify the pharmacokinetics and toxicity of lead. *Environ. Health Perspect.*, **103**(3): 248-53.
- Stansley, W. and Resco, D. E. 1996. The uptake and effects of lead in small mammals and frogs at a trap and skeet range. *Arch Environ Contam Toxicol.*, **30**(2): 220-6.
- Tietz., N. W. **Fundamentals of Clinical Chemistry**, third Ed. 1987. W. B Saunders Company, Philadelphia, pp. 1010.



# Analysis and Characterization of Purified Levan from *Leuconostoc mesenteroides* ssp. *cremoris* and its Effects on *Candida albicans* Virulence Factors

Jehan A.S. Salman<sup>\*</sup>, Hamzia A. Ajah and Adnan Y. Khudair

Department of Biology, College of Science, Mustansiriyah University, Baghdad-Iraq

Received July 8, 2018; Revised August 14, 2018; Accepted September 26, 2018

## Abstract

The objective of the current study is to characterize levan purified from *Leuconostoc mesenteroides* ssp. *cremoris* and the detection of its effects against the growth and virulence factors of *C. albicans*. The purification and characterization of levan produced by local isolates was done using thin layer chromatography (TLC) and High performance liquid chromatography (HPLC) analysis which determined and proved that purified levan is a homopolysaccharide consisting only of fructose. The determination of functional group analysis of levan was studied using Fourier transform infrared spectroscopy (FTIR). The results showed that the bond region in 857.60 cm<sup>-1</sup> is typical to carbohydrates (identification of polysaccharides). The melting point was also determined. Levan began to liquefy at 224 °C, and was completely melting at 330 °C. The antifungal activity of levan was determined against fourteen isolates of *Candida albicans* taken from oral and vaginal specimens. The MIC for all of the *C. albicans* isolates was between (50 –100) mg/mL. The effects of purified levan (at sub MIC) on *C. albicans* virulence factors which included phospholipase, haemolysin production, biofilm formation and hyphal transition were determined. The results showed that purified levan had the ability to inhibit the virulence factors of *C. albicans* with significant differences compared with the control. The change in the P<sub>z</sub> value of most isolates was recorded and turned from strong isolates to moderate isolates. On the other hand, the inhibition of haemolysin production was recorded. The highest inhibition percentage was 58.53 %, while the lowest percentage was 53.84 %. The purified levan showed inhibitory effects on *C. albicans* biofilm formation in microtiter plates and acrylic denture resin specimens at different incubation times of 24, 48, and 72 hours. In the microtiter plates, the highest inhibition percentage of biofilm formation was 70.58 % at a seventy-two- hour incubation time, whereas for the acrylic denture resin specimens, the highest inhibition percentage of biofilm formation was 68 % at a seventy-two-hour incubation time. Also, the inhibition of hyphal transition was recorded, and the highest inhibition percentage of hyphal transition was 59.26 %. In conclusion, purified levan showed inhibitory effects on the growth and virulence factors of *C. albicans*.

**Keywords:** Levan, *Leuconostoc mesenteroides*, Inhibitory effect, *Candida albicans*, Virulence factors

## 1. Introduction

Levan is a fructose polymer synthesized from sucrose by a wide range of microorganisms, and it is a non-toxic, biologically-active, extracellular polysaccharide (Franken *et al.*, 2013). Bacterial levans often have molecular weights over 500,000 Da, and are commonly branched which results in offering a broad spectrum of applications (Öner *et al.*, 2016). Levan belongs to a larger group of commercially-important polymers referred to as fructans, which are used as a source of prebiotics. The synthesis of levan is catalyzed by a group of enzymes referred to as levansucrases using sucrose as substrate (Hill *et al.*, 2017). Some microbial levans exhibit biological activities such as antitumor, antidiabetic, and immune-stimulating activities (Lu *et al.*, 2014). In medicine, levan is used as a blood and plasma volume expander and drug delivery. In blood and plasma volume expansion, levan

can replace the normal blood protein in providing osmotic pressure which is useful for preventing hemorrhagic shocks, as well as burn and surgery shocks (Rehm, 2009).

*Candida albicans* is a member of the normal human microbiota (Jabra-Rizk *et al.*, 2016). The ability of *C. albicans* to infect such diverse host niches is supported by a wide range of virulence factors which include biofilm formation, phenotypic switching, and the secretion of hydrolytic enzymes (Brunke *et al.*, 2016). The effect of levan on yeast-hyphal transition associated with tissue invasion and the escape from phagocyte cells after host internalization was estimated, and it is considered as an important virulence factor (Jacobsen *et al.*, 2012). This study is conducted with the objective of characterizing levan purified from local *L. mesenteroides* ssp. *cremoris*, and for the detection of its activity against the growth and virulence factors of *C. albicans*.

<sup>\*</sup> Corresponding author e-mail: jehanmmd.ja@gmail.com ; Dr.jehan@uomustansiriyah.edu.iq.

## 2. Materials and Methods

### 2.1. Microorganisms

#### 2.1.1. *Leuconostoc mesenteroides* ssp. *cremoris* Isolates

*Leuconostoc mesenteroides* sp. *cremoris* was isolated from local fish intestines and was identified using cultural, microscopical, and biochemical test as well as the Vitek 2 system.

#### 2.1.2. *Candida albicans* Isolates

Fourteen *C. albicans* isolates were taken from oral and vaginal specimens. All isolates were subjected to the cultural, microscopical, and biochemical tests as well as the Vitek 2 system.

### 2.2. Levan Production

This process was done according to the procedure described by (Abou-Taleb, *et al.*, 2015). 250 mL Erlenmeyer flasks, containing 100 mL of a levan production medium (2.5g Yeast extract, 200g Sucrose, 0.2g  $MgSO_4 \cdot 7H_2O$ , 5.5 g  $K_2HPO_4$  added to one liter of distilled water, with the pH adjusted to seven then autoclaved), were inoculated with 2% of *L. mesenteroides* ssp *cremoris* suspension containing ( $9 \times 10^8$  CFU/mL), and was incubated at 30°C for twenty-four hours.

### 2.3. Precipitation of Levan

After twenty-four hours of incubation, the culture was centrifuged at 10000 rpm for ten minutes to obtain the pellets which are used as source for cell dry weight. The pellets were washed twice with distilled water, and dried at 80°C. The supernatant was used for the precipitation of levan by adding 1.5 volumes of ice - cold absolute ethanol for levan precipitation. The precipitated pellets were washed twice by distilled water, and were collected by centrifugation at 10000 rpm for ten minutes. The levan dry weight was determined after oven-drying at 110°C for twenty-four hours (Abou-Taleb, *et al.*, 2015).

### 2.4. Purification of Levan Produced by *L. mesenteroides* ssp. *cremoris*

The precipitated levan polymer at optimum conditions was re-suspended in demineralized water at 4°C over the duration of sixteen hours, and was then dialyzed (MWCO 14,000 Da) overnight against demineralized water. The polymer was precipitated with two volumes of 96 % ice – cold ethanol, centrifuged for ten minutes at 10.000 rpm (Abou-Taleb, *et al.*, 2015). The O.D was measured at 400 nm to estimate levan concentration at each step of the purification according to the equation described by González - Garcinuño *et al.* (2017):

$$y = 0.1645x - 0.035$$

where y is the absorbance at 400 nm, and x is the levan concentration expressed in mg / mL. The purified levan was dried at (40-45) °C., and was kept for further analysis .

### 2.5. Characterization of Levan Purified from *L. mesenteroides* ssp. *Cremoris*

#### 2.5.1. Thin-Layer Chromatography (TLC)

Levan (0.01 gm.) purified from *L. mesenteroides* ssp. *cremoris*, was hydrolyzed in 5 % HCl (v/v) and

was heated for an hour in a water bath at 100°C. Equal weights (0.01gm) of glucose, sucrose, and fructose were dissolved in 1mL of 1% ethanol. Thin-Layer Chromatography (TLC) has been performed by using silica. The position and distance of the spots were determined, and the relative flow ( $R_f$ ) had been calculated as described by (Radhi *et al.*, 2013):

$$R_f = \frac{\text{Distance moved by substance}}{\text{Distance moved by the solvent front}}$$

#### 2.5.2. High Performance Liquid Chromatography (HPLC)

The analysis of Levan by high performance liquid chromatography (HPLC) has been carried out at the Ministry of Science and Technology in Baghdad, Iraq. The instrument operates using mobile phase containing 15 mM NaOH spiked with 1 mM barium acetate; the flow rate was 1.5 mL/min, temperature was 40 °C, and the injection volume was 20 µL .

#### 2.5.3. Fourier Transform Infrared Spectroscopy (FTIR)

Fourier transform infrared spectroscopy (FTIR) has been carried out using (Bruker – Tensor 27 with ATR unit) in the Physics Department at the Collage of Sciences of Mustansiriyah University in Baghdad, Iraq. The instrument operates in the wavenumber range of (400 – 4000  $cm^{-1}$ ) that measures the amount of IR radiation reflected or transmitted through a sample. The results obtained are in the form of a graphical chart, in which the X – axis represents the wave number, while the Y-axis represents the transmittance % .

#### 2.5.4. Melting Point

A melting-point test has been carried out using (Melting Point, Digital, Advanced, SMP30). The capillary tube that was sealed at one end was filled with levan up to 2-3 mm, and was then inserted into a melting point apparatus and heated. At this point, two temperatures were recorded: the temperature at which the substance began to liquefy, and the temperature at which it became completely liquefied.

### 2.6. Antifungal Activity of Levan Purified from *L. mesenteroides* sp. *cremoris* against *Candida albicans* Isolates

The antifungal activity of levan purified from *L. mesenteroides* ssp. *cremoris* against *C. albicans* isolates was determined by the microdilution method in 96 – well flat-bottom microplate titer on the basis of minimum inhibitory concentration (MIC) values. The experiment was done according to the procedures described by Salman *et al.* (2018) with slight modification.

### 2.7. Effect of Levan Purified from *L. mesenteroides* sp. *Cremoris* on *Candida albicans* Virulence Factors

#### 2.7.1. Inhibition of Phospholipase Production

The inhibition of Phospholipase production by levan was detected. The *C. albicans* isolates were grown in the presence and absence of levan at the sub MIC concentration; 20 µL of *C. albicans* suspension compared to 0.5 McFarland was added to 80 µL of a Sabouraud dextrose broth (SDB) and mixed with 100 µL of levan; while the control contained only 180 µL of broth and 20 µL of *Candida* suspension. Then 10 µL from all of the isolates was placed on the surface of the egg yolk medium, and was left to dry at room temperature. The plates were

then incubated at 37°C for twenty-four hours; after incubation, the  $P_z$  value was calculated as follows (Zarei *et al.*, 2010):

$$\text{Phospholipase activity } P_z = \frac{\text{Diameter of colonies (mm)}}{\text{Diameter of the zone of opacity + colonies}}$$

### 2.7.2. Inhibition of Haemolysin Production

The inhibition of haemolysin production by levan was detected using the procedure described by (Lee *et al.*, 2014), and the experiment was done in triplicate. *C. albicans* isolates were grown in the presence and absence of levan at the sub MIC concentration; 20  $\mu$ L of *C. albicans* suspension compared to 0.5 McFarland was added to 80  $\mu$ L of SDB and mixed with 100  $\mu$ L of levan, while the control contained only 180  $\mu$ L of SDB and 20  $\mu$ L of the *C. albicans* suspension without levan, incubated at 37 °C for twenty-four hours.

Candidal cultures (treatment and control) at 100  $\mu$ L were added to 10 mL of red-blood cells that were previously prepared and were incubated at 37 °C for one hour. Centrifugation was applied after incubation at 12,000 rpm for ten minutes to collect the supernatants. The optical densities of the supernatants were then measured at 543 nm. Inhibition of haemolysin production percentage was calculated according to the equation described by Chevalier *et al.* (2012) with slight modification.

$$\% \text{ Inhibition of haemolysin production} = \frac{\text{O.D control} - \text{O.D treatment}}{\text{O.D control}} \times 100$$

### 2.7.3. Inhibition of Biofilm Formation in Microtiter Plates

The effect of levan on the biofilm formation of *C. albicans* was studied using 96 flat-bottom well microtiter plates. The *C. albicans* isolates were grown at 37 °C for 24, 48, and 72 hours in the presence and absence of levan at the sub MIC concentration (the experiment was done in triplicate). Inhibition of the biofilm formation percentage was calculated according to the equation described by Chevalier *et al.* (2012).

$$\% \text{ Inhibition of hyphal transition} = \frac{\text{No. of hyphae in control} - \text{No. of hyphae in treatment}}{\text{No. of hyphae in control}} \times 100$$

### 2.7.4. Inhibition in Acrylic Denture Resin Specimens

The effect of levan on the biofilm formation of *C. albicans* was studied using acrylic denture resin specimens (obtained from Dentistry College at Mustansiriyah University in Baghdad, Iraq); the experiment was done in triplicate. The acrylic denture resin specimens were kept for twenty-four hours in the levan solution at sub MIC concentration. The control acrylic specimens were kept in water according to the procedure described by Salman (2018) with modification. Inhibition of the biofilm formation percentage was calculated according to the abovementioned equation described by Chevalier *et al.* (2012).

### 2.8. Inhibition of Hyphal Transition

The effect of levan on yeast- hyphal transition was estimated by the cultivation of *C. albicans* in the hyphal transition medium (YEP broth). The experiment was done in triplicate. *C. albicans* isolates were grown at 37 °C for twenty-four hours in the presence and absence of levan at sub MIC concentration. 20  $\mu$ L of *Candida* suspension compared to 0.5 McFarland was added to 80  $\mu$ L of YEP broth, and mixed with 100  $\mu$ L of levan,

while the control contained only 180  $\mu$ L of YEP broth and 20  $\mu$ L of the candidal suspension. Yeast and hyphae were counted using a hemocytometer slide by observation under an optic microscope. The numbers of hyphae were determined, and the inhibition of the hyphal transition was calculated by comparing it with the control. The inhibition of the hyphal transition was calculated according to the equation described by kumar, *et al.*, (2011) with modification.

$$\% \text{ Inhibition of hyphal transition} = \frac{\text{No. of hyphae in control} - \text{No. of hyphae in treatment}}{\text{No. of hyphae in control}} \times 100$$

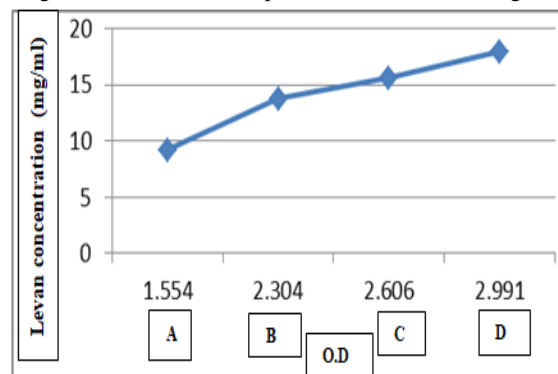
### 2.9. Statistical Analysis

SPSS software version 21/ France was used for data analysis by one-way ANOVA- test to calculate the *P*- value between the test groups' means in the study.

## 3. Results

### 3.1. Purification of Levan Produced by *L. mesenteroides ssp. cremoris*

The purification of levan produced by *L. mesenteroides ssp. cremoris* was done for the sake of this study. After production under optimum conditions, the concentration of levan was estimated at each of the purification steps. The results showed that levan concentration increased at each step of the purification process. The concentrations recorded were: (9.234, 13.7933, 15.6291, 17.9696) mg /mL before precipitation, after precipitation, after dialysis, and at the last precipitation respectively (Figure 1). The total dry weight of levan after purification was 7.621 g /L.

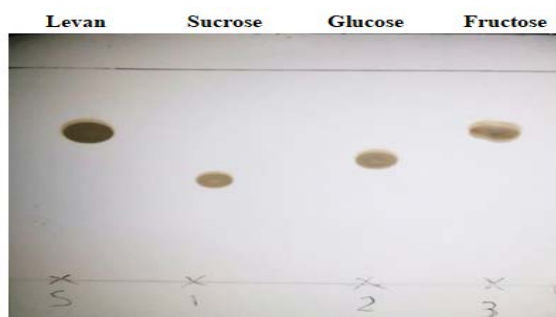


**Figure 1.** Concentration of levan produced by *L. mesenteroides ssp. cremoris* at different steps of purification, A: before precipitation, B: after precipitation, C: after dialysis, D: after last precipitation.

### 3.2. Characterization of Levan Purified from *L. mesenteroides ssp. cremoris*

#### 3.2.1. Thin-Layer Chromatography (TLC)

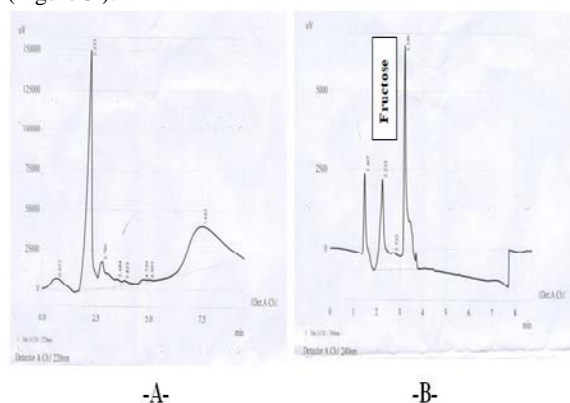
Levan contents produced by *L. mesenteroides ssp. cremoris* were analyzed by TLC to determine their components of monosaccharides. The  $R_f$  values of fructose were identical or so close to the acid hydrolyzed levan. The  $R_f$  value of levan was 0.42, while the  $R_f$  values of sucrose, fructose, and glucose were 0.32, 0.42 and 0.37, respectively. This result indicates that the purified levan from *L. mesenteroides ssp. cremoris* consisted solely of fructose (Figure 2).



**Figure 2.** Thin - Layer Chromatography analysis of levan purified from *L. mesenteroides* ssp. *cremoris*

### 3.2.2. High Performance Liquid Chromatography (HPLC)

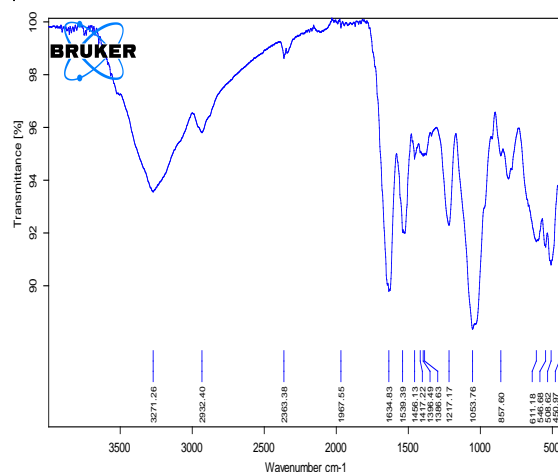
High performance liquid chromatography (HPLC) was used to separate, identify, and quantify each component in the mixture. The results revealed that the levan consisted solely of fructose, which indicates that the purified levan was of the homopolysaccharide type (Figure 3).



**Figure 3.** A: HPLC analysis of levan produced by *L. mesenteroides* ssp. *cremoris*; B: HPLC analysis of standard sugar

### 3.2.3. Fourier Transform Infrared Spectroscopy (FTIR)

Fourier transform infrared spectroscopy (FTIR) spectra analysis was used to detect the functional groups of purified levan from *L. mesenteroides* ssp. *cremoris*. The characteristic peaks of levan indicated that the purified levan was of the polysaccharide type. The band in the region of  $3271.26\text{ cm}^{-1}$  represents hydroxyl (O-H) stretching, while the band in region of  $2932.40\text{ cm}^{-1}$  is for (C-H) stretching vibration. The band region of  $1634.83\text{ cm}^{-1}$  is typical for C=O stretching, while the band region found in the  $1417.22\text{ cm}^{-1}$  and  $1217.17\text{ cm}^{-1}$  are due to C-H plan deformation and aromatic skeletal stretching. The bond region in  $857.60\text{ cm}^{-1}$  is typical for carbohydrates (identification of polysaccharides) (Figure 4).



**Figure 4.** FTIR spectra of levan produced by *Leuconostoc mesenteroides* ssp. *cremoris*.

### 3.2.4. Melting Point

Melting point analysis was used to detect the temperature at which the compound began to liquefy. Also it can provide the information about the purity of the sample. The results showed that the purified levan from *L. mesenteroides* ssp. *cremoris* began to liquefy at  $224\text{ }^{\circ}\text{C}$ , and at  $330\text{ }^{\circ}\text{C}$  levan was completely melting. Purified levan was characterized as a white crystalline powder highly soluble in water.

### 3.3. Antifungal Activity of Levan Purified from *L. mesenteroides* ssp. *cremoris* against *Candida albicans* Isolates

The Antifungal activity of the biopolymer levan was determined on the basis of minimum inhibitory concentration (MIC) values. MIC at concentrations ranging between 200 and  $0.09\text{ mg/mL}$  was determined for all of the *C. albicans* isolates. The results showed that the MIC for all *C. albicans* isolates was between (50 – 100)  $\text{mg/mL}$ .

### 3.4. Effect of Levan Purified from *L. mesenteroides* ssp. *cremoris* on *Candida albicans* Virulence Factors

#### 3.4.1. Inhibition of Phospholipase Production

In the current study, levan had a high effect on the phospholipase production of all *C. albicans* isolated from both oral and vaginal candidiasis. Phospholipase activity decreased in all of the *C. albicans* isolates. The  $P_z$  value reached 0.81 compared to the control. The results of the statistical analysis showed significant differences ( $P = 0.001$ ) between the treatment and control groups of all the isolates (Table 1).



**Table 1.** Inhibition of phospholipase production by levan purified from *L.mesenteroides ssp.cremoris*.

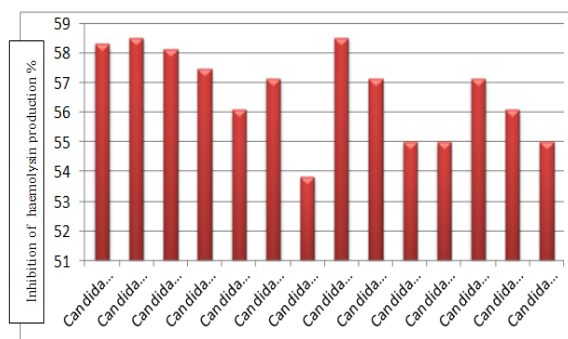
Candidal isolates	P <sub>z</sub> value		P Value
	Control Mean ± SD	Treatment Mean ± SD	
<i>C. albicans</i> (CO <sub>1</sub> )	0.68 ± 0.01	0.73 ± 0.02	0.001
<i>C. albicans</i> (CO <sub>2</sub> )	0.68 ± 0.03	0.74 ± 0.02	0.001
<i>C. albicans</i> (CO <sub>3</sub> )	0.65 ± 0.03	0.72 ± 0.03	0.001
<i>C. albicans</i> (CO <sub>4</sub> )	0.70 ± 0.03	0.73 ± 0.02	0.001
<i>C. albicans</i> (CO <sub>5</sub> )	0.69 ± 0.03	0.76 ± 0.05	0.001
<i>C. albicans</i> (CO <sub>6</sub> )	0.69 ± 0.05	0.77 ± 0.05	0.001
<i>C. albicans</i> (CO <sub>7</sub> )	0.71 ± 0.08	0.75 ± 0.03	0.001
<i>C. albicans</i> (CO <sub>8</sub> )	0.79 ± 0.04	0.81 ± 0.02	0.001
<i>C. albicans</i> (CO <sub>9</sub> )	0.70 ± 0.01	0.74 ± 0.06	0.001
<i>C. albicans</i> (CV <sub>1</sub> )	0.69 ± 0.04	0.72 ± 0.04	0.001
<i>C. albicans</i> (CV <sub>2</sub> )	0.70 ± 0.05	0.73 ± 0.02	0.001
<i>C. albicans</i> (CV <sub>3</sub> )	0.70 ± 0.02	0.77 ± 0.04	0.001
<i>C. albicans</i> (CV <sub>4</sub> )	0.70 ± 0.02	0.77 ± 0.03	0.001
<i>C. albicans</i> (CV <sub>5</sub> )	0.69 ± 0.02	0.72 ± 0.03	0.001

CO: Oral isolates; CV: vaginal isolates;  $P = 0.001$ : significant differences

$P_z = 1$  → Negative for phospholipase  
 $P_z = 0.80-0.89$  → Weak phospholipase  
 $P_z = 0.70 - 0.79$  → Moderate phospholipase  
 $P_z = <0.70$  → Strong phospholipase

### 3.4.2. Inhibition of Haemolysin Production

The inhibitory effect of levan purified from *L. mesenteroides ssp. cremoris* on haemolysin production from *C. albicans* isolated from oral and vaginal candidiasis was observed in this study. The haemolysin activity decreased in all the *C. albicans* isolates, and the optical density of hemoglobin released from lysed erythrocytes ranged between (0.17 and 0.18) compared with the control (0.39 and 0.43). The results of statistical analysis showed significant differences ( $P \leq 0.01$ ) between the treatment and control groups of all the isolates. The highest inhibition percentage for haemolysin production was 58.53 %, while the lowest inhibition percentage was 53.84 % (Figure 5).

**Figure 5.** Inhibition percentage of haemolysin production of *C. albicans* by levan purified from *L. mesenteroides sp. cremoris*

### 3.4.3. Inhibition of Biofilm Formation in Microtiter Plates

In this study, levan is shown to have an inhibitory effect on the biofilm formation of all *C. albicans* isolated

from both oral and vaginal candidiasis. The biofilm formation decreased in all of the *C. albicans* isolates at different incubation times of 24, 48, 72 hours compared to the control. The highest inhibition percentage for biofilm formation was 70.58%, while the lowest percentage was 50 % at seventy-two-hour incubation time for *C. albicans* isolated from oral cavities. As for *C. albicans* isolated from vaginal infections, the highest percentage was 59.37 %, while the lowest inhibition percentage was 51.85 % (Table 2).

**Table 2.** Inhibition percentage of biofilm formation by levan purified from *L. mesenteroides ssp. cremoris* in different incubation time .

Candidal isolates	Inhibition of biofilm formation %		
	24 h	48 h	72 h
<i>C. albicans</i> (CO <sub>1</sub> )	43.75	50	60
<i>C. albicans</i> (CO <sub>2</sub> )	69.09	69.35	70.58
<i>C. albicans</i> (CO <sub>3</sub> )	35.71	42.10	56.66
<i>C. albicans</i> (CO <sub>4</sub> )	57.14	57.57	63.04
<i>C. albicans</i> (CO <sub>5</sub> )	33.33	44.44	55.17
<i>C. albicans</i> (CO <sub>6</sub> )	33.33	47.61	50
<i>C. albicans</i> (CO <sub>7</sub> )	62.79	63.44	66.05
<i>C. albicans</i> (CO <sub>8</sub> )	30.76	35.29	55.17
<i>C. albicans</i> (CO <sub>9</sub> )	36.84	46.42	51.28
<i>C. albicans</i> (CV <sub>1</sub> )	35.71	42.10	55.17
<i>C. albicans</i> (CV <sub>2</sub> )	52.94	54.54	59.37
<i>C. albicans</i> (CV <sub>3</sub> )	25	31.25	51.85
<i>C. albicans</i> (CV <sub>4</sub> )	33.33	45.83	55.55
<i>C. albicans</i> (CV <sub>5</sub> )	40.62	46.15	52

CO: oral isolates; CV: vaginal isolates

### 3.4.4. Inhibition in Acrylic Denture Resin Specimens

In this study, the inhibition effect of levan purified from *L. mesenteroides ssp. cremoris* on the biofilm formation of *C. albicans* isolated from oral candidiasis in acrylic denture resin specimens was studied. Purified levan had a high effect on the biofilm formation of *C. albicans* (CO<sub>2</sub>) in acrylic denture resin. Biofilm formation decreased in *C. albicans* (CO<sub>2</sub>) at different incubation time (24, 48, and 72) hours compared to the control. The results of the statistical analysis showed significant differences ( $P = 0.001$ ) between the levan treatment groups and the control (Table 3).

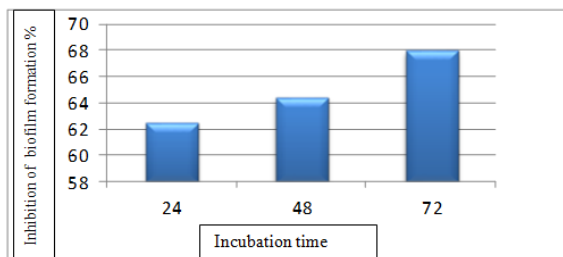


**Table 3.** Inhibition of candidal biofilm formation by levan purified from *L. mesenteroides* ssp. *cremoris* in acrylic denture resin specimens

Incubation time	O.D at (450 nm)		
	Control Mean $\pm$ SD	Treatment Mean $\pm$ SD	P value
24h	0.48 $\pm$ 0.01	0.18 $\pm$ 0.01	0.001
48h	0.59 $\pm$ 0.01	0.21 $\pm$ 0.01	0.001
72h	0.72 $\pm$ 0.01	0.23 $\pm$ 0.02	0.001

$P \leq 0.01$ : significant differences

The inhibition percentage of biofilm formation was calculated. The results showed that the highest inhibition percentage of biofilm formation was 68% at a seventy-two- hour incubation time (Figure 6). On the other hand, at a forty-eight-hour incubation time, the highest inhibition percentage for biofilm formation was 64.4%, while the lowest inhibition percentage for biofilm formation was 62.5 % at a twenty-four- hour incubation time (Figure 7).

**Figure 6.** Inhibition of *C. albicans* biofilm formation in acrylic denture resin specimens by levan purified from *L. mesenteroides* ssp. *cremoris* at a seventy-two- hour incubation time.**Figure 7.** Inhibition percentage of *C. albicans* biofilm formation in acrylic denture resin specimens by levan purified from *L. mesenteroides* ssp. *cremoris*

### 3.5. Inhibition of Hyphal Transition

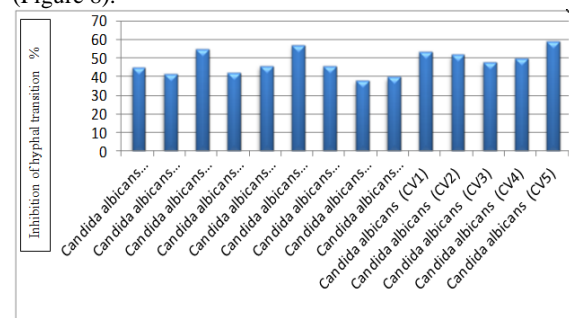
The inhibitory effect of levan purified from *L. mesenteroides* ssp. *cremoris* on the hyphal transition of *C. albicans* isolated from oral and vaginal candidiasis was recorded for this study. The hyphal transition decreased in all of the *C. albicans* isolates with significant differences ( $P = 0.001$ ) between treatment and control of all the isolates (Table 4).

**Table 4.** Inhibition of hyphal transition by levan purified from *L. mesenteroides* ssp. *cremoris*.

Candidal isolates	Treatment (Mean $\pm$ SD)	No. of hypha	
		Control (Mean $\pm$ SD)	P Value
<i>C. albicans</i> (CO <sub>1</sub> )	26.67 $\pm$ 7.64	48.33 $\pm$ 7.64	0.001
<i>C. albicans</i> (CO <sub>2</sub> )	23.33 $\pm$ 2.89	40.00 $\pm$ 5.00	0.001
<i>C. albicans</i> (CO <sub>3</sub> )	21.67 $\pm$ 7.64	48.33 $\pm$ 7.64	0.001
<i>C. albicans</i> (CO <sub>4</sub> )	25.00 $\pm$ 5.00	43.33 $\pm$ 7.64	0.001
<i>C. albicans</i> (CO <sub>5</sub> )	23.33 $\pm$ 2.89	43.33 $\pm$ 7.64	0.001
<i>C. albicans</i> (CO <sub>6</sub> )	20.00 $\pm$ 0.00	46.67 $\pm$ 7.64	0.001
<i>C. albicans</i> (CO <sub>7</sub> )	23.33 $\pm$ 5.77	43.33 $\pm$ 7.64	0.001
<i>C. albicans</i> (CO <sub>8</sub> )	26.67 $\pm$ 5.77	43.33 $\pm$ 7.64	0.001
<i>C. albicans</i> (CO <sub>9</sub> )	25.00 $\pm$ 5.00	41.67 $\pm$ 7.64	0.001
<i>C. albicans</i> (CV <sub>1</sub> )	20.00 $\pm$ 5.00	43.33 $\pm$ 7.64	0.001
<i>C. albicans</i> (CV <sub>2</sub> )	21.67 $\pm$ 2.89	45.00 $\pm$ 5.00	0.001
<i>C. albicans</i> (CV <sub>3</sub> )	23.33 $\pm$ 2.89	45.00 $\pm$ 5.00	0.001
<i>C. albicans</i> (CV <sub>4</sub> )	20.00 $\pm$ 5.00	40.00 $\pm$ 5.00	0.001
<i>C. albicans</i> (CV <sub>5</sub> )	18.33 $\pm$ 2.89	45.00 $\pm$ 5.00	0.001

CO: oral isolates; CV: vaginal isolates;  $P \leq 0.01$ : significant differences

The inhibition percentage of hyphal transition was calculated for this study, and the highest recorded inhibition percentage for hyphal transition was 59.26 %, while the lowest inhibition percentage was 38.44 % (Figure 8).

**Figure 8.** Inhibition percentage of hyphal transition of *C. albicans* by levan purified from *L. mesenteroides* ssp. *cremoris*.

## 4. Discussion

Levan is a homopolysaccharide composed of fructose units. It is a type of fructan that belongs to a group of fructose- based oligo- and polysaccharide (Fedewa and Rao, 2014). Moosavi-Nasab *et al.* (2010) reported that the  $R_f$  value of acid-hydrolyzed levan from *Microbacterium laevaniformans* was identical to that of fructose, and also found that levan was composed solely of fructose. Radhi *et al.* (2013) mentioned that levan was composed mainly of fructose residues when analyzed by thin-layer chromatography (TLC).

Mamay *et al.* (2015) mentioned that the FTIR spectra analysis of levan produced from *B. licheniformis* showed that the stretching of O- H vibrations appeared at the wavelength around 3300  $\text{cm}^{-1}$ , while the band at around 2900 represents C-H stretching, and that the peak at the wavenumber of 1660  $\text{cm}^{-1}$  is typical for C=O stretching. Also Nasir *et al.* (2015) analyzed levan secreted from *Halomonas* and *Chromobacter* by FTIR and found out that the region of typical carbohydrates at the finger prints was at the wave number range of 1000-800  $\text{cm}^{-1}$ . Levan has quite

interesting biochemical properties, and good thermostability with a melting point of 225°C (Divya and Sugumaran, 2015).

Polysaccharides exhibit activities against *C. albicans*. Tøndervik *et al.* (2014) showed that oligosaccharide. Oligo G is an alginate having the ability to reduce fungal cell growth. Martins *et al.* (2017) mentioned that polysaccharides from *Agaricus brasiliensis* can stimulate human monocytes to capture *C. albicans*.

Pritchard *et al.* (2017) found out that alginate oligosaccharides have the ability to inhibit phospholipase in *C. albicans*. Martinez *et al.* (2010) reported that chitosan, which is a polymer isolated from crustacean exoskeletons, can inhibit candidal biofilm formation *in vivo*. Salman (2018) observed the anti-biofilm effect of biosurfactant from *L. mesenteroides* against *C. albicans* in acrylic disc.

Polysaccharides have been shown to possess a broad spectrum of antimicrobial and antibiofilm activities against fungi and bacteria. Chevalier *et al.* (2012) successfully developed a day-care mouthwash specifically for the dry mouth which consisted of a healthy biofilm, including endogenous bacteria and salivary mucins with an external polysaccharide coating to protect the oral mucosa, and to create an oral environment unfavorable to *Candida* proliferation, causing inhibition of the yeast-hyphal transition and iron chelation. Pritchard *et al.* (2017) have successfully used alginate oligosaccharides to induce marked alterations in hyphal formation that result in reducing the invasion of *C. albicans* in the epithelial cell animal experiment model.

## 5. Conclusion

In conclusion, the purified levan produced from the *Leuconostoc mesenteroides* ssp. *cremoris* isolates had an inhibitory effect on the growth and virulence factors of *Candida albicans*.

## Acknowledgements

The authors would like to thank Al-Mustansiriyah University in Iraq (www.uomustansiriyah.edu.iq) for their support in the current work. The authors extend thanks to Dr. Inas A.S. Salman from the Dentistry College at Mustansiriyah University for her valuable assistance.

## References

Abou - Taleb K A , Abdel - Monem M O, Yassin M H and Draz A A. 2015. Production , purification and characterization of levan polymer from *Bacillus lentus* V8 strain. *British Microbiol Res J.*, **5**(1): 22-32.

Brunke S , Mogavero S , Kasper L and Hube B. 2016. Virulence factors in fungal pathogens of man. *Curr Opin Microbiol.*, **32**:89-95.

Chevalier M , Medioni E and Prêcheur I. 2012. Inhibition of *Candida albicans* yeast - hyphal transition and biofilm formation by *Solidago virgaurea* water extracts. *J Med Microbiol.*, **61**(7):1016-22.

Divya J M and Sugumaran K R. 2015. Fermentation parameters and condition affecting Levan production and its applications. *J Chem Pharm Res.*, **7**(2):861-865.

Fedewa A and Rao S S. 2014. Dietary fructose intolerance, fructan intolerance and FODMAPs. *Curr Gastroenterol Rep.*, **16**(1):370.

Franken J, Brandt B A, Tai S L and Bauer F F. 2013. Biosynthesis of levan, a bacterial extracellular polysaccharide, in the yeast *Saccharomyces cerevisiae*. *PLoS One.*, **8**(10): 77.

González – Garcinuño Á, Tabernero A, Sánchez-Álvarez J M, Galán M A and Martín Del Valle E M. 2017 . Effect of bacteria type and sucrose concentration on levan yield and its molecular weight . *Microb Cell Fact.*, **16** (1):91.

Hill A, Tian F and Karboune S. 2017. Synthesis of levan and fructooligosaccharides by levansucrase: catalytic, structural and substrate-specificity properties. *Cur Organic Chem.*, **21** (2) :149 – 161.

Jabra-Rizk M A, Kong E F, Tsui C, Nguyen M H, Clancy C J, Fidel PL and Noverr M. 2016 . *Candida albicans* pathogenesis: fitting within the host-microbe damage response framework. *Infect Immun.*, **84**(10):2724-39.

Jacobsen I D, Wilson D, Wächtler B, Brunke S, Naglik J R and Hube B. 2012. *Candida albicans* dimorphism as a therapeutic target. *Expert Rev Anti-infective Ther.*, **10**(1):85-93.

Kumar P, Dhiman S, Bhatt R P and Singh L. 2011 . *In-vitro* Antifungal activity of *Sapim sebiferum* against *Aspergillus niger* and aflatoxigenic *Aspergillus flavus* . *J Appl Pharm Sci.*, **1** (9): 108-110.

Lee J H, Kim Y G , Cho M H and Lee J. 2014. ZnO nanoparticles inhibit *Pseudomonas aeruginosa* biofilm formation and virulence factor production. *Microbiol Res.*, **169**(12):888-96.

Lu J, Lu L and Xiao M. 2014. Application of levansucrase in levan synthesis--a review. *Wei Sheng Wu Xue Bao.*, **54**(6):601-7.

Mamay, Wahyuningrum, D and Hertadi, R. 2015. Isolation and characterization of levan from moderate halophilic bacteria *Bacillus licheniformis* BK AG21. *Procedia Chem.*, **16**: 292-298.

Martinez LR, Mihu M R, Tar M, Cordero R J, Han G, Friedman A J, Friedman J M and Nosanchuk J D. 2010. Demonstration of antibiofilm and antifungal efficacy of chitosan against candidal biofilms, using an *in vivo* central venous catheter model. *J Infect Dis.*, **201**(9):1436-40.

Martins P R, de Campos Soares Â M V, da Silva Pinto Domeneghini A V, Golim M A and Kaneno R. 2017. *Agaricus brasiliensis* polysaccharides stimulate human monocytes to capture *Candida albicans*, express toll-like receptors 2 and 4, and produce pro-inflammatory cytokines. *J Venom Anim Toxins Incl Trop Dis.*, **23**(23):17.

Moosavi - Nasab M, Layegh B, Aminlary L and Hashemi M B. 2010. Microbial production of levan using date syrup and investigation of its properties. *Inter J Biol. Biomolec Agri Food Biotechnol Eng.*, **4**(8): 603-609.

Nasir D Q, Wahyuningrum D and Hertad R . 2015. Screening and characterization of levan secreted by halophilic bacterium of *Halomonas* and *Chromohalobacter* genres originated from Bledug Kuwu Mud Crater. *Procedia Chem.*, **16**:272-278.

Öner E T, Hernández L and Combie J. 2016. Review of Levan polysaccharide: From a century of past experiences to future prospects. *Biotechnol Adv.*, **34**(5):827-844.

Pritchard M F, Jack A A, Powell L C, Sath H, Rye P D, Hill K E and Thomas DW . 2017. Alginate oligosaccharides modify hyphal infiltration of *Candida albicans* in an *in vitro* model of invasive human candidosis. *J Appl Microbiol.*, **123**(3):625-636.

Radhi S N, Hasan SS and Alden S B. 2013. Production of Levan from *Paenibacillus polymyxa* in date syrup and analyzing of levan composition by TLC . *The First Sci Conf Collage of Sci.*, **1** :166-172.

Rehm B H A. 2009. **Microbial Production of Biopolymers and Polymer Precursors: Applications and Perspectives**. Horizon Scientific Press. pp 293.

Salman I A S. 2018. Biosurfactant as preventive agent on acrylic resin .*Mustansiria Dental J.*,**15(1)**: 83-89.

Salman J A S, Kadhim A A and Haider A J. 2018. Biosynthesis, characterization and antibacterial effect of ZnO nanoparticles synthesized by *Lactobacillus* sp. *J Global Pharma Technol.* ,**10(03)**:348-355.

Tøndervik A, Sletta H, Klinkenberg G, Emanuel C, Powell L C , Pritchard M F, Khan S, Craine K M, Onsøyen E, Rye P D, Wright C, Thomas DW and Hill KE.2014.Alginate oligosaccharides inhibit fungal cell growth and potentiate the activity of antifungals against *Candida* and *Aspergillus* sp. *PLoS One.*, **9(11)**: 11.

Zarei M A , Zarrin M and Miry S. 2010. Phospholipase activity of *Candida albicans* isolated from vagina and urine samples . *Jundishapur J Microbiol.*, **3(4)**: 169-73.

# Jordan Journal of Biological Sciences

An International Peer – Reviewed Research Journal

Published by the Deanship of Scientific Research, The Hashemite University, Zarqa, Jordan



Name: ..... الاسم:

Specialty: ..... التخصص:

Address: ..... العنوان:

P.O. Box: ..... صندوق البريد:

City & Postal Code: ..... المدينة: الرمز البريدي:

Country: ..... الدولة:

Phone: ..... رقم الهاتف:

Fax No.: ..... رقم الفاكس:

E-mail: ..... البريد الإلكتروني:

Method of payment: ..... طريقة الدفع:

Amount Enclosed: ..... المبلغ المرفق:

Signature: ..... التوقيع:

Cheque should be paid to Deanship of Research and Graduate Studies – The Hashemite University.

I would like to subscribe to the Journal

**For**

- ☐ One year
- ☐ Two years
- ☐ Three years

## One Year Subscription Rates

	Inside Jordan	Outside Jordan
Individuals	JD10	\$70
Students	JD5	\$35
Institutions	JD 20	\$90

Correspondence

**Subscriptions and sales:**

**Prof. Khaled H. Abu-Elteen**  
The Hashemite University  
P.O. Box 330127-Zarqa 13115 – Jordan  
Telephone: 00 962 5 3903333 ext. 4399  
Fax no. : 0096253903349  
E. mail: jjbs@hu.edu.jo

**المجلة الأردنية للعلوم الحياتية**  
**Jordan Journal of Biological Sciences (JJBS)**

<http://jjbs.hu.edu.jo>

المجلة الأردنية للعلوم الحياتية: مجلة علمية عالمية محكمة ومفهرسة ومصنفة، تصدر عن الجامعة الهاشمية وبدعم من صندوق البحث العلمي والابتكار – وزارة التعليم العالي والبحث العلمي.

**هيئة التحرير**

**رئيس التحرير**

الأستاذ الدكتور خالد حسين أبو التين  
الجامعة الهاشمية، الزرقاء، الأردن

**مساعد رئيس التحرير**

الدكتورة لبنى حميد تهتموني  
الجامعة الهاشمية، الزرقاء، الأردن

**الأعضاء:**

الأستاذ الدكتور جميل نمر اللحام  
جامعة اليرموك

الأستاذ الدكتورة حنان عيسى ملكاوي  
جامعة اليرموك

الأستاذ الدكتور خالد محمد خليفات  
جامعة مؤتة

الأستاذ الدكتور زهير سامي عمرو  
جامعة العلوم و التكنولوجيا الأردنية

الأستاذ الدكتور عبدالرحيم أحمد الحنيطي  
الجامعة الأردنية

الأستاذ الدكتور علي زهير الكرمي  
الجامعة الهاشمية

**فريق الدعم:**

**المحرر اللغوي**

الدكتورة هالة شريتح

**تنفيذ وإخراج**

م. مهند عقده

**ترسل البحوث الى العنوان التالي:**

رئيس تحرير المجلة الأردنية للعلوم الحياتية  
الجامعة الهاشمية

ص.ب , 330127 , الزرقاء , 13115 , الأردن

هاتف: 0096253903333 فرعي 4357

E-mail: [jjbs@hu.edu.jo](mailto:jjbs@hu.edu.jo), Website: [www.jjbs.hu.edu.jo](http://www.jjbs.hu.edu.jo)



المملكة الأردنية الهاشمية



# المجلة الأردنية



## للعلوم الحياتية

مجلة علمية عالمية محكمة

تصدر بدعم من صندوق دعم البحث العلمي والابتكار



<http://jjbs.hu.edu.jo/>